

THESIS

LINKING MORPHODYNAMIC PROCESSES AND SILVERY MINNOW HABITAT  
CONDITIONS IN THE MIDDLE RIO GRANDE- ISLETA REACH, NEW MEXICO

Submitted by

Caitlin Fogarty

Department of Civil and Environmental Engineering

In partial fulfillment of the requirements

For the degree Master of Science

Colorado State University

Fort Collins, Colorado

Fall 2020

Master's Committee:

Advisor: Pierre Julien

Ryan Morrison  
Ellen Wohl

Copyright by Caitlin Fogarty 2020

All Rights Reserved

## ABSTRACT

### LINKING MORPHODYNAMIC PROCESSES AND SILVERY MINNOW HABITAT CONDITIONS IN THE MIDDLE RIO GRANDE- ISLETA REACH, NEW MEXICO

The Middle Rio Grande, located in central New Mexico, is home to the Rio Grande Silvery Minnow (RGSM), an endangered species of fish. Much of the RGSM's historical range has been lost due to natural and human-caused alterations to the river. For this study, the availability of RGSM habitat is analyzed in the Isleta reach, a segment of the Middle Rio Grande extending approximately 42 miles from Isleta Diversion dam to the confluence of Rio Puerco. To better understand spatial and temporal trends in morphology and channel geometry, the Isleta reach is delineated into six subreaches (I1, I2, I3, I4, I5, and I6). The purpose of this study is to identify connections between hydraulics, geomorphology, and biology to better explain the changing biological conditions in the river.

To assess changes in geomorphology along the Isleta reach, the geomorphic conceptual model developed by Massong et al. (2010) was applied to representative cross-sections in each subreach. The model proposes two pathways that changes in the Middle Rio Grande can follow: aggrading (A) or migrating (M). Through inspection of aerial imagery and cross-sectional geometry data, it appears that the Isleta reach is in stage 3 and migrating stages, M4-M8, indicating high sediment transport capacity. River form was further classified using Cluer and Thorne's (2013) stream evolution model. In 2012, all subreaches were in stage 3 (i.e. degradation) of the model.

One-dimensional modeling techniques were used to assess habitat availability for the RGSM from 1962 to 2012. Using the Hydrologic Engineering Center's River Analysis System (HEC-RAS), flow distribution slices were used to compute velocity and depth along a cross-section. Hydraulically suitable RGSM habitat for larvae, juvenile, and adult stages is determined using velocity and depth criteria for the fish proposed by Mortenson et al. (2019). The results suggest that habitat availability follows three typical patterns. Earlier years (1962 and 1972) showed "rounded" habitat curves, while later years (1992, 2002, and 2012) showed "step" and "hook" habitat curves.

Detailed maps were produced in ArcMap that aid in the visualization of where RGSM habitat is located within the Isleta reach. These maps suggest that subreaches I1 to I3 contain the most habitat for all life stages. However, much of the habitat is disconnected and far away from the main channel, making it inaccessible to the fish. Through an analysis of restoration potential, it was determined that subreaches I2 to I4 may be areas of focus for river management to increase RGSM habitat.

Time-integrated habitat metrics, originally developed by Doidge et al. (2020), is a method of interpolating cumulative RGSM habitat for each year between 1992 and 2019. This method requires input of annual habitat curves and daily discharge data. These inputs are used in a summation of simple linear equations that results in habitat metrics for each of the RGSM's life stages. The results show that larval and juvenile habitat metrics are more sensitive to changes in daily discharge than adult habitat metrics. Ecological relationships were inferred based on plots created by Mortenson et al. (2020) that relate habitat metrics, discharge, occurrence probability and lognormal density. Overall, larvae proved to be strong predictors of population dynamics.

## ACKNOWLEDGEMENTS

Firstly, I would like to thank my advisor, Dr. Pierre Julien, for giving me the opportunity to work on this project and for his support. I would also like to thank the U.S. Bureau of Reclamation in Albuquerque for funding this project. I would especially like to thank Nathan Holste and Drew Baird from the Technical Service Center in Denver for extending their knowledge about the river to us and for making trips to CSU to teach us more about HEC-RAS. Also, I would like to thank everyone from ASIR and the University of New Mexico for sharing their expertise in biology and background on the Silvery Minnow. Discussions with Jake Mortenson, Steve Platania, Thomas Turner, and Robert Dudley were always super interesting.

Secondly, I would like to thank Tori Beckwith and Sydney Doidge for being so patient with me and teaching me the ropes of the project. I thoroughly enjoyed my time working with them. I would like to especially thank Tori for all her support in and out of the classroom and for making me aware of this project.

Finally, I would like to thank my family. My mom and dad have always supported me. They've pushed me through the hard times and always assured me that they had my back in whatever I chose to do. Because of them, I've found my passion and achieved my goals. Special thanks to my dad for helping me move to Fort Collins. While I dreaded the 20-hour drive from Oregon, you made it fun. Thanks to Mitch for being my rock and always being up for an adventure.

## TABLE OF CONTENTS

ABSTRACT.....	ii
ACKNOWLEDGEMENTS.....	iv
LIST OF FIGURES .....	viii
LIST OF FIGURES: APPENDIX A .....	x
LIST OF FIGURES: APPENDIX B.....	xi
LIST OF FIGURES: APPENDIX C.....	xii
LIST OF FIGURES: APPENDIX D .....	xiii
LIST OF TABLES.....	xiv
LIST OF TABLES: APPENDIX D .....	xv
Chapter 1: Introduction.....	1
Chapter 2: Literature Review.....	5
2.1 Middle Rio Grande History.....	5
2.2 Rio Grande Silvery Minnow Background.....	6
2.3 Reach Background .....	7
2.3.1 Precipitation.....	9
2.4 Previous Studies of Rio Grande Silvery Minnow Habitat .....	9
2.5 One Dimensional Numerical Modeling Using HEC-RAS.....	10
2.6 Planform Evolution Model.....	12
2.7 River Management .....	14
Chapter 3: Site Description.....	17
3.1 Subreach Delineation .....	17
3.1.1 Habitat Map Delineations.....	22
3.2 Aggradation/Degradation Lines .....	22
3.3 Geomorphic Characteristics .....	23
3.3.1 Bed Elevation .....	24
3.4 Flow Analysis.....	26
3.5 Suspended Sediment Load .....	28
3.5.1 Single Mass Curve.....	28
3.5.2 Monthly Average Histogram .....	29
Chapter 4: Geometry.....	31

Chapter 5: Hydraulic Modeling (HEC-RAS) .....	36
5.1 Bankfull Discharge.....	36
5.1.1 Methods .....	36
5.1.2 Results .....	37
5.2 Flow Distribution Slices.....	37
5.2.1 Methods .....	37
5.2.2 Results: Habitat Curves and Spatial Habitat Charts .....	39
Chapter 6: Geomorphic Conceptual Models.....	44
6.1. Geomorphic Evolution Maps .....	44
6.2 Geomorphic Classification Based on the Planform Evolution Model .....	51
6.3 Geomorphic Classification Based on the Stream Evolution Model.....	54
6.4 Primary Drivers .....	55
Chapter 7: Time-Integrated Habitat Metrics.....	58
7.1 Methods.....	58
7.1.1 Temporal Interpolation of Habitat Curves.....	61
7.2 Results .....	63
7.2.1 Ecological Relationships .....	65
Chapter 8: Habitat Mapping.....	68
8.1 Methods: RAS-Mapper .....	68
8.2 Results/Discussion .....	68
8.3 Restoration Potential .....	76
8.3.1 Disconnected Areas .....	76
8.3.2 Discussion.....	77
Chapter 9: Study Limitations .....	85
9.1 Hydraulic Modeling (HEC-RAS).....	85
9.1.1 RAS-Mapper.....	85
9.2 Data Collection.....	87
9.3 Time-Integrated Habitat Metrics .....	87
Chapter 10: Conclusions.....	88
References.....	90
Appendix A.....	94
Additional Habitat Curves and Spatial Habitat Charts.....	94

Additional Habitat Curves .....	95
Additional Spatial Habitat Charts.....	113
Appendix B .....	118
Additional Habitat Availability Maps .....	118
Appendix C .....	128
Time Integrated Habitat Metrics Program .....	128
Appendix D.....	131
Habitat Analyses Results from Previous Studies .....	131
HEC-RAS RGSM Modeling Maps in 2012 .....	132
RGSM Habitat Scoring System.....	135

## LIST OF FIGURES

Figure 1 Location map of the Isleta reach. Direction of flow is from north to south.....	8
Figure 2 Planform evolution model for the Middle Rio Grande developed by Massong et al. (2010).....	14
Figure 3 Cluer and Thorne’s (2013) stream evolution model.....	16
Figure 4 Castro and Thorne’s (2019) stream evolution triangle.....	16
Figure 5 Map of the Isleta reach showing subreach delineations and the location of USGS gages used in this study.....	18
Figure 6 Aerial view of subreaches I1 and I2 in 2012.....	19
Figure 7 Aerial view of subreaches I3 and I4 in 2012.....	20
Figure 8 Aerial view of subreaches I5 and I6 in 2012.....	21
Figure 9 Longitudinal profiles of the Isleta reach.....	25
Figure 10 Change in mean bed elevation from 1962 to 2012 in the Isleta reach (Yang et al., 2020).....	25
Figure 11 Flow duration curves.....	27
Figure 12 Single mass curves for the Albuquerque (08330000) and Bernardo (08332010) gages.....	28
Figure 13 Monthly average histogram showing seasonal trends in suspended sediment discharge.....	30
Figure 14 Monthly average histogram showing seasonal trends in suspended sediment concentration.....	30
Figure 15 Changes to cross-sectional geometry from 1962 to 2012 at agg/deg line 681 in subreach I1.....	33
Figure 16 Changes to cross-sectional geometry from 1962 to 2012 at agg/deg line 751 in subreach I2.....	33
Figure 17 Changes to cross-sectional geometry from 1962 to 2012 at agg/deg line 841 in subreach I3.....	34
Figure 18 Changes to cross-sectional geometry from 1962 to 2012 at agg/deg line 991 in subreach I4.....	34
Figure 19 Changes to cross-sectional geometry from 1962 to 2012 at agg/deg line 1026 in subreach I5.....	35
Figure 20 Changes to cross-sectional geometry from 1962 to 2012 at agg/deg line 1076 in subreach I6.....	35
Figure 21 Percent of cross-sections overtopping the top of bank points.....	37
Figure 22 Example of flow distribution slices (colored bars) in HEC-RAS for agg/deg line 690 (subreach I1).....	38
Figure 23 Larvae, juvenile, and adult habitat curves for the entire Isleta reach.....	42
Figure 24 Stacked life stage habitat charts displaying the spatial variability throughout the Isleta reach in 2012 up to 3,000 cfs.....	43
Figure 25 Geomorphic evolution in subreach I1 at agg/deg line 681.....	45

Figure 26 Geomorphic evolution in subreach I2 at agg/deg line 751 .....	46
Figure 27 Geomorphic evolution in subreach I3 at agg/deg line 841 .....	47
Figure 28 Geomorphic evolution in subreach I4 at agg/deg line 991 .....	48
Figure 29 Geomorphic evolution in subreach I5 at agg/deg line 1026 .....	49
Figure 30 Geomorphic evolution in subreach I6 at agg/deg line 1076 .....	50
Figure 31 Typical patterns seen in the Isleta reach .....	53
Figure 32 Example of SEM stage classifications applied to subreach I5 .....	55
Figure 33 Stream evolution triangle highlighting the primary drivers in the Isleta reach .....	56
Figure 34 Example hydrograph for the Bernardo gage (08332010) from 1992 to 2005. The hydrograph is colored to show representative sampling periods for each of the RGSM's life stages .....	59
Figure 35 Interpolation of daily larval habitat area between 4,000 and 4,500 cfs in 1995 .....	60
Figure 36 Single mass curve for the Albuquerque gage (08330000) from 1992 to 2002 .....	62
Figure 37 Example of temporal interpolation for the 1995 larval habitat curve .....	62
Figure 38 Cumulative habitat for larvae, juveniles, and adults over their respective sampling periods .....	64
Figure 39 RGSM occurrence probabilities from Mortenson et al. (2020) for the time period 1992 to 2019 .....	65
Figure 40 RGSM lognormal densities from Mortenson et al. (2020) for the time period 1992 to 2019 .....	66
Figure 41 Life stage habitat availability maps for subreach I1 .....	70
Figure 42 Life stage habitat availability maps for subreach I2(a) .....	71
Figure 43 Life stage habitat availability maps for subreach I2(b) .....	72
Figure 44 Life stage habitat availability maps for subreach I3(a) .....	73
Figure 45 Life stage habitat availability maps for subreach I3(b) .....	74
Figure 46 Life stage habitat availability maps for subreach I3(c) .....	75
Figure 47 Example of habitat in the floodplain that is disconnected from the main channel .....	76
Figure 48 Aerial imagery in 2016 showing an example of a low and high scoring backwater feature (Yang et al., 2020) .....	78
Figure 49 Aerial imagery in 2006 showing an example of a low and high scoring bar feature (Yang et al., 2020) .....	79
Figure 50 Aerial imagery in 2008 showing an example of a low and high scoring side channel feature (Yang et al., 2020) .....	80
Figure 51 Engineered structures used in river restoration: (a) log jam, (b) lunger, (c) J-Hook, and (d) rootwads (pictures obtained from Julien (2018) and Rosgen (2001)) .....	83
Figure 52 Evidence of RAS-Mapper limitations: (a) example of RAS-Mapper recognizing "computational levee" placement and (b) fragmented inundation at 1,000 cfs .....	86

LIST OF FIGURES: APPENDIX A

Figure A-1 Larvae, juvenile, and adult habitat curves for subreach I1..... 95

Figure A-2 Larvae, juvenile, and adult habitat curves for subreach I2..... 96

Figure A-3 Larvae, juvenile, and adult habitat curves for subreach I3..... 97

Figure A-4 Larvae, juvenile, and adult habitat curves for subreach I4..... 98

Figure A-5 Larvae, juvenile, and adult habitat curves for subreach I5..... 99

Figure A-6 Larvae, juvenile, and adult habitat curves for subreach I6..... 100

Figure A-7 RGSM life stage habitat curves for 1962, 1972, 1992, 2002, and 2012 for the  
subreach I1 ..... 102

Figure A-8 RGSM life stage habitat curves for 1962, 1972, 1992, 2002, and 2012 for subreach I2  
..... 104

Figure A-9 RGSM life stage habitat curves for 1962, 1972, 1992, 2002, and 2012 for subreach I3  
..... 106

Figure A-10 RGSM life stage habitat curves for 1962, 1972, 1992, 2002, and 2012 for subreach  
I4 ..... 108

Figure A-11 RGSM life stage habitat curves for 1962, 1972, 1992, 2002, and 2012 for subreach  
I5 ..... 110

Figure A-12 RGSM life stage habitat curves for 1962, 1972, 1992, 2002, and 2012 for subreach  
I6 ..... 112

Figure A-13 Stacked life stage habitat charts displaying the spatial variability throughout the  
Isleta reach in 1962 ..... 113

Figure A-14 Stacked life stage habitat charts displaying the spatial variability throughout the  
Isleta reach in 1972 ..... 114

Figure A-15 Stacked life stage habitat charts displaying the spatial variability throughout the  
Isleta reach in 1992 ..... 115

Figure A-16 Stacked life stage habitat charts displaying the spatial variability throughout the  
Isleta reach in 2002 ..... 116

Figure A-17 Stacked life stage habitat charts displaying the spatial variability throughout the  
Isleta reach in 2012 ..... 117

LIST OF FIGURES: APPENDIX B

Figure B-1 Life stage habitat availability maps for subreach I1. Direction of flow is from north to south..... 119

Figure B-2 Life stage habitat availability maps for subreach I2(a). Direction of flow is from north to south..... 120

Figure B-3 Life stage habitat availability maps for subreach I2(b). Direction of flow is from north to south ..... 121

Figure B-4 Life stage habitat availability maps for subreach I3(a). Direction of flow is from north to south..... 122

Figure B-5 Life stage habitat availability maps for subreach I3(b). Direction of flow is from north to south ..... 123

Figure B-6 Life stage habitat availability maps for subreach I3(c). Direction of flow is from north to south..... 124

Figure B-7 Life stage habitat availability maps for subreach I4. Direction of flow is from north to south..... 125

Figure B-8 Life stage habitat availability maps for subreach I5. Direction of flow is from north to south..... 126

Figure B-9 Life stage habitat availability maps for subreach I6. Direction of flow is from north to south..... 127

LIST OF FIGURES: APPENDIX C

Figure C-1 Example worksheet from the TIHMs program for larval habitat interpolation ..... 129  
Figure C-2 Example of worksheet results from the TIHMs program for larval habitat ..... 130

LIST OF FIGURES: APPENDIX D

Figure D-1 HEC-RAS modeling map of subreach I1 from Yang et al. (2020) ..... 132  
Figure D-2 HEC-RAS modeling map of subreach I2 from Yang et al. (2020) ..... 132  
Figure D-3 HEC-RAS modeling map of subreach I3 from Yang et al. (2020) ..... 133  
Figure D-4 HEC-RAS modeling map of subreach I4 from Yang et al. (2020) ..... 133  
Figure D-5 HEC-RAS modeling map of subreach I5 from Yang et al. (2020) ..... 134  
Figure D-6 HEC-RAS modeling map of subreach I6 from Yang et al. (2020) ..... 134  
Figure D-7 Overall habitat scores by subreach in Isleta computed by Yang et al. (2020). Score is weighted per area of subreach..... 136  
Figure D-8 Example of a habitat scoring map for subreach I1 from Yang et al. (2020)..... 137

## LIST OF TABLES

Table 1 Velocity and depth criteria for RGSM habitat (Mortensen et al., 2019) .....	7
Table 2 RGSM habitat classifications based on depth and velocity criteria proposed by Tetra Tech (2014) (Yang et al., 2020).....	10
Table 3: Subreach delineation for the Isleta reach. Subreaches were delineated based on notable geomorphic features (Yang et al., 2020).....	17
Table 4 Habitat map agg/deg line delineations by subreach.....	22
Table 5 Summary of geomorphic characteristics of the Isleta reach .....	23
Table 6 Available data for USGS gages in this study.....	26
Table 7 Exceedance probabilities from flow duration curves .....	27
Table 8 Geomorphic classification by subreach based on the planform evolution model by Massong et al. (2010).....	51
Table 9 Geomorphic stage classifications based on Cluer and Thorne's (2013) stream evolution model.....	54
Table 10 Assessment of restoration potential by subreach at 5,000 cfs .....	77
Table 11 Comparison of results from the restoration potential analysis and the habitat scoring system .....	82

LIST OF TABLES: APPENDIX D

Table D-1 Habitat types and their respective alphanumeric categories (Yang et al., 2020)..... 135  
Table D-2 Habitat scoring criteria. A higher score indicates more habitat benefits (Yang et al., 2020) ..... 135  
Table D-3 Physical features and their respective scores (Yang et al., 2020)..... 136  
Table D-4 Results from the habitat scoring system on the Isleta reach by Yang et al. (2020). Each year is given a total habitat score based on the number of habitat types that are present..... 136

## Chapter 1: Introduction

The Middle Rio Grande (MRG), located in central New Mexico, is approximately 170 miles long and is bounded by Cochiti dam to the north and Elephant Butte Reservoir to the south (Tetra Tech, 2002). The MRG basin covers approximately 3,060 mi<sup>2</sup> (Bartolino and Cole, 2002). Over the last century, the river and watershed have undergone extensive changes as a result of natural and human-caused alterations.

The river has changed geomorphically as a result of trying to reach an equilibrium state. Based on historical data, the MRG has significantly narrowed over the last 100 years due to a combination of prolonged low flow duration, decreased peak flows, decreased sediment supply, decreased floodplain connectivity, increased floodplain lateral confinement, and increased bank stability. Additionally, vegetation encroachment into the active channel has been occurring, likely due to prolonged low flow duration and decreased peak flows. Vegetative growth has caused the active channel width to decrease (Makar and Aubuchon, 2012).

Human-caused alterations to the channel have shifted the planform from wide, shallow, and braided to incised and single-threaded (Makar, 2010; Swanson et al., 2011; Klein et al., 2018). These channel modifications include the construction of levees and jetty jacks, channel-realignments, diversion dams and large dams. These modifications were implemented to control the channel and protect nearby dwellers from frequent floods (Massong 2010).

Alterations to the river and watershed have negatively impacted some aquatic species and the amount of habitat that is available to them. The Rio Grande Silvery Minnow (RGSM or Silvery Minnow), an endangered species of fish, has lost most of its historical range. Channel

narrowing and incision have decreased habitat availability in the river as water velocities and depths become too great to be considered suitable for the RGSM. Additionally, channel incision, channelization, and decreased peak flows (e.g. during spring) have reduced floodplain connectivity, which is crucial for the survival of early life stages of the RGSM (Massong et al., 2006; Mortenson et al., 2019). Flow regulating structures, like dams, cause habitat fragmentation by preventing RGSM populations from migrating upstream (Dudley and Platania, 2007; Perkin and Gido, 2011; Perkin et al., 2015). This lack of movement can decrease genetic diversity within the wild population (Osborne et al., 2012). Also, the likelihood that eggs and larvae will drift into unsuitable habitat increases (Dudley and Platania, 2007; Perkin and Gido, 2011; Perkin et al., 2015).

What remains of the wild Silvery Minnow population can be found within the MRG. The Isleta reach, a segment of the MRG, is approximately 42 miles long and is bounded by the Isleta Diversion Dam upstream and the confluence of Rio Puerco downstream. Conservation of the species will require careful restoration considerations. The goal for most river restoration projects is to improve biological conditions in the river; however, today, river management practices lack a biological component. Few studies have made connections between the disciplines of geomorphology, hydraulics, and biology. Yet all three of these disciplines are important for understanding how habitat conditions can change in rivers. Therefore, the purpose of this study is to make connections between morphodynamic processes (i.e. the interaction between geomorphology, flow field, and sediment transport) and biological-habitat conditions for the RGSM in the Isleta reach.

Specific objectives for this study include:

- Using one-dimensional (1-D) numerical modeling techniques to determine RGSM habitat availability;
- Using geomorphic conceptual models to determine how the geomorphology in the reach has changed from 1962 to 2012;
- Analyzing statistical results to determine ecological trends in RGSM occurrence and density in relation to discharge and habitat metrics;
- Developing habitat maps to aid in visualizing where RGSM habitat is located throughout the reach; and
- Assessing restoration potential by subreach to determine areas of focus for river management.

This thesis is divided into ten chapters. Chapter 1 includes a brief overview about the MRG, the Isleta reach, and the RGSM. Additionally, the purpose and objectives of this study are discussed. Chapter 2 includes a literature review of previous studies done on the MRG and the Isleta reach. This chapter also provides background information about the Isleta reach, the Rio Grande Silvery Minnow, one-dimensional numerical modeling techniques, and geomorphic conceptual models. Chapter 3 is a description of the study area including geomorphic characteristics and an analysis of flow and suspended sediment in the reach. Chapter 4 includes an analysis of the geometry used in this study. Chapter 5 includes hydraulic modeling methods for determining bankfull discharge and habitat availability using flow distribution slices in the Hydrologic Engineering Center's River Analysis System (HEC-RAS). Chapter 6 includes an analysis of geomorphic evolution throughout the Isleta reach using geomorphic conceptual models. Primary drivers of fluvial processes in the reach are also identified. Chapter 7 introduces

a method for interpolating annual cumulative habitat availability and explores ecological relationships from the results. Chapter 8 includes habitat availability maps, which show where RGSM habitat is located within the reach. Additionally, a restoration potential analysis was performed to determine which areas of the reach may be of focus for river management. Chapter 9 discusses limitations of the study, specifically involving the use of one-dimensional modeling, how data are collected, and the methodology for integrating habitat over time. Lastly, Chapter 10 provides a summary of key findings from this study.

## **Chapter 2: Literature Review**

### **2.1 Middle Rio Grande History**

For thousands of years, native people have called lands near the Rio Grande home. Their homes were often located near fertile agricultural lands that were likely to be affected by flooding because of shifts within the river's floodplain. In the 1500's, the Spanish first explored areas around the Rio Grande and wanted to establish settlements (Coonrod, 2005). For the best chance at obtaining land, the Spanish did not limit themselves to areas close to the river. Instead, they established themselves farther from the river and built irrigation canals to deliver water to meet their demands for agriculture. These irrigation canals are known as acequias and can still be found in northern New Mexico (Rivera, 1998).

From 1540 to 2000, the estimated area of land being farmed rose from 10,000 hectares to 29,200 hectares. However, at the start of the nineteenth century, there was a large decline in the number of farms as soils became waterlogged due to flooding. The Rio Grande saw increases in erosion and sediment loads due to deforestation and overgrazing, causing aggradation of the channel bed and a higher water table in the floodplain. To address flood control and drainage issues, the Middle Rio Grande Conservancy District (MRGCD) was established in 1925. Their main task was to develop an efficient irrigation system for the Middle Rio Grande Valley. Prior to the formation of the MRGCD, dams had already been built on the upstream and downstream ends of the Middle Rio Grande. The MRGCD built 180 miles of river levees, 248 miles of irrigation ditches, 345 miles of drainage canals, and rehabilitated approximately 400 miles of old irrigation ditches by 1936. Additionally, El Vado Dam was constructed on the Rio Chama, and diversion dams were constructed in the Rio Grande (Coonrod, 2005). Examples of these

diversion dams include San Acacia, Isleta, and Angostura, built in 1934. Lastly, Cochiti dam was built in 1974-1975 by the Army Corps of Engineers to act as a flood control structure (Bureau of Reclamation, n.d.).

Further channelization efforts were done after a large flood (discharge recorded at 30,000 cfs) overtopped levees in 1941 (Coonrod, 2005; Makar and Aubuchon, 2012). To protect levees and stabilize the banks, jetty jacks were installed in the river and on the floodplain, which create resistance to flow and cause sedimentation. Initially, the river channel underwent rapid narrowing (approximately 25 feet per year) as a result of the jetty jacks (Grassel, 2002; Swanson et al. 2011). More recently, the MRG experiences channel narrowing from vegetation encroachment during long periods of low flows (Makar, 2010).

## **2.2 Rio Grande Silvery Minnow Background**

The Rio Grande Silvery Minnow was listed as an endangered species in 1994 under the Endangered Species Act (U.S. Office of the Federal Register, 1994). Historically, RGSM populated 2,400 miles of the Rio Grande, ranging from Española, NM to the Gulf of Mexico. Today, the last of the wild RGSM only populate 7% of its historical range, or 174 miles of the MRG (U.S. Fish and Wildlife, 2010). Loss of RGSM habitat is mostly due to consequences from geomorphic changes of the Rio Grande and river management practices (Mortensen et al., 2019).

A thorough study of the biology of the RGSM and their habitat conditions was performed by Mortensen et al. (2019). Habitat for fish species is typically determined using water velocity and depth criteria. RGSM favor low velocity and shallow depth conditions, which are often found in the floodplains. Access to floodplain habitat is particularly important for larval fish, which need near-zero velocities and shallow depths to maintain their location and find food to grow. Additionally, floodplain habitat provides warmer temperatures for eggs so that they hatch

slower and grow faster (Platania, 2000; Tockner et al., 2000). Lastly, the floodplains promote egg retention, which is important because RGSM produce eggs that are semi-buoyant and susceptible to “drifting” downstream (Dudley and Platania, 2007). Peak flows during spring are of importance because the floodplain becomes inundated, thus increasing habitat for the RGSM (Gonzales et al., 2014). Whether RGSM inhabit the main channel versus the floodplain depends on availability, and access to the floodplains is spatially and temporally variable (U.S. Army Corps of Engineers, 2010; Stone et al., 2017).

Physical habitat criteria for each of the Silvery Minnow’s life stages (i.e. larvae, juveniles, and adults) was proposed by Mortensen et al. (2019). Experimental swimming performance studies and long-term population/habitat monitoring were used to determine the velocity and depth criteria for juveniles and adults. Larval criteria are determined using a regression model that relates total fish length to critical swimming speed. Table 1 summarizes the velocity and depth criteria findings from the study.

*Table 1 Velocity and depth criteria for RGSM habitat (Mortensen et al., 2019)*

Life Stage	Velocity		Depth	
	cm/s	ft/s	cm	ft
Larvae	<5	<0.2	<15	<0.5
Juveniles	<30	<1.0	>1 and <50	>0.03 and <1.6
Adults	<40	<1.3	>5 and <60	>0.2 and <2.0

### 2.3 Reach Background

This study will focus primarily on the Isleta reach, located just south of Albuquerque. The Isleta reach is approximately 42 miles long, beginning at the Isleta Diversion Dam and ending at the confluence of Rio Puerco. Figure 1 shows the location of the study reach. In 1934, the Isleta Diversion Dam was built to divert water for irrigation. During operation, the Isleta Diversion Dam reduces the river’s downstream discharge. Channelization efforts have stabilized

the reach. Jetty jack lines were installed between levees to narrow and confine the river so that water and sediment were more efficiently transported downstream and to protect the levees from floods that cause erosion. Sediment, along with vegetation, has now filled these jetty jack lines, thus stabilizing the banks (Varyu, 2016).

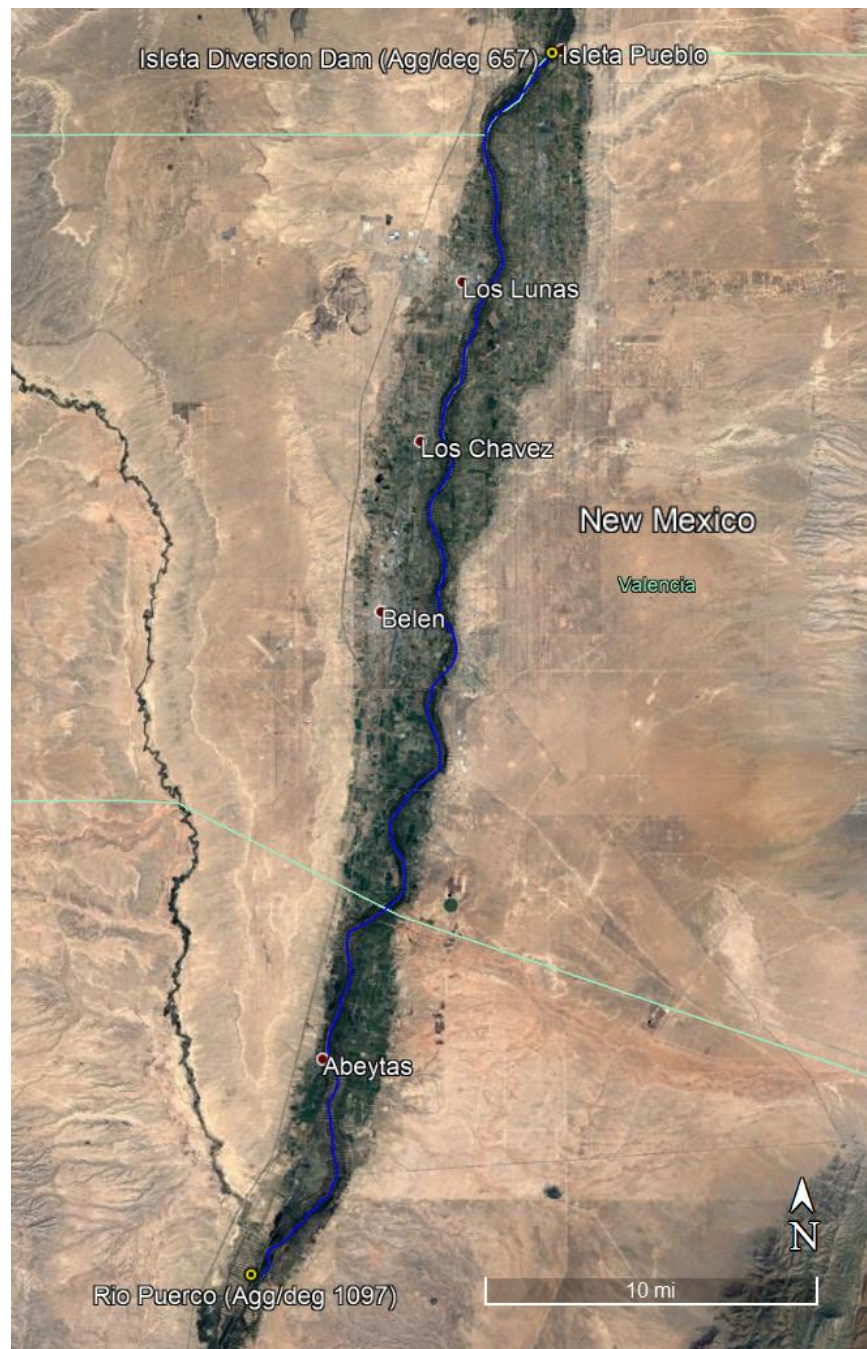


*Figure 1 Location map of the Isleta reach. Direction of flow is from north to south*

### **2.3.1 Precipitation**

Yang et al. (2020) used annual precipitation data compiled by the Bosque Ecosystem Monitoring Program (BEMP) at the University of New Mexico to determine monthly average trends seen in the Isleta reach. The data were collected between Los Lunas, near the start of the Isleta reach, and Sevilleta, near the confluence of Rio Puerco. The period of record extends from 1998 to 2017. Results from this analysis showed that “the highest rainfall events tend to happen in late summer or early fall.” Rainfall associated with monsoonal events in late summer or early fall has increased since 2005. This is most likely attributed to large storms that occurred in 2006 and 2013. Prior to 2005, monthly average rainfall peaked in March and April.

### **2.4 Previous Studies of Rio Grande Silvery Minnow Habitat**

Yang et al. (2020) performed an analysis of Rio Grande Silvery Minnow Habitat in the Isleta reach using HEC-RAS version 5.0.3 (U.S. Army Corps of Engineers, 2016) and ArcMap (Environmental Systems Research Institute, Inc., 2020). HEC-RAS was used to analyze flow depth and velocity at varying flow conditions. Three flow profiles were used in the analysis: 600, 1,400, and 3,500 cfs, which relate to low, medium, and high spring runoff flows within the last decade. Cross-sectional geometry data provided by the Technical Service Center for 1992, 2002, and 2012 were used because they overlapped with available fish population density data. Flow depth and velocity values were exported to ArcMap using a geo-referencing program to spatially analyze RGSM habitat based on criteria developed by Tetra Tech (2014). Table 2 summarizes the RGSM habitat classifications used in the work of Yang et al. (2020).

*Table 2 RGSM habitat classifications based on depth and velocity criteria proposed by Tetra Tech (2014) (Yang et al., 2020)*

Depth (ft)	Velocity (ft/s)			
	0 – 0.05	0.05 – 0.5	0.5 – 1.5	> 1.5
0 - 1.5	Spawning	Feeding/rearing	Good	Inadequate
1.5 – 1.6	Adequate	Adequate	Adequate	Inadequate
>1.6	Inadequate	Inadequate	Inadequate	Inadequate

Additionally, aerial imagery in ArcMap was used to identify river features that provide suitable habitat for the RGSM. LaForge et al. (2020) developed a scoring system that would help determine which subreaches would contain the most habitat availability depending on the presence of different types of river features. Ten years of aerial imagery data, ranging from 1992 to 2016, at varying months and flows were studied. Each habitat feature was assigned a point in ArcMap and a score. Examples of physical features include main channel and bankline complexity, side channels, bars, confluences, islands, and backwaters. Features of interest were based on literature and those that were easily identified or measured using ArcMap. Features of importance to the RGSM that provide “good” habitat are backwaters, debris piles, and secondary channels that create areas of shallow depths and low velocities (LaForge et al., 2020). Yang et al. (2020) implemented this same scoring system for the Isleta reach.

## **2.5 One Dimensional Numerical Modeling Using HEC-RAS**

The challenges of modeling perched channels in one-dimensional programs like HEC-RAS were analyzed by Baird and Holste (2020). Perched channels are characterized by a lower floodplain elevation than the main channel elevation. Perched channels induce difficulties in 1-D modeling techniques, as flow in the channel is not accurately represented when the proper method is not followed. Therefore, Baird and Holste (2020) describe the appropriate approach to modeling these types of channels.

For the purposes of this study, it is important to accurately represent flow at a range of discharges to determine hydraulically suitable habitat for all life stages of the RGSM. Depth and velocity results are very sensitive to how the HEC-RAS geometry is set up. In a cross-section that is considered perched, HEC-RAS will fill the channel from the lowest elevation up. This poses a problem because HEC-RAS will fill the floodplain before overbanking has occurred. To prevent this issue, “computational levees” must be placed at bankfull or top of bank (TOB) points. Note that “computational levees” does not refer to an actual flood control structure. Without the addition of “computational levees,” HEC-RAS will tend to overestimate floodplain depth and water surface elevation (WSE) and underestimate main channel depth and WSE. This directly relates to the overestimation or underestimation of RGSM habitat. Baird and Holste (2020) found that the elevation and width of the floodplain in relation to the main channel will influence the extent of overestimation or underestimation.

Adding “computational levees” to TOB points creates instabilities in the model at discharges greater than or equal to bankfull as the flow area becomes larger. These instabilities can be seen in the water surface profile within HEC-RAS. Water surface profiles will cross one another and appear out of order. Without “computational levees” the model remains stable. Therefore, it is important to perform a sensitivity analysis on overbanking to determine when these “computational levees” should be removed to ensure stability of the model.

The following steps were used for setting up a 1-D model for perched channels in HEC-RAS:

1. Ensure Manning’s  $n$  values are appropriate for the reach. The United States Bureau of Reclamation (USBR) suggests certain Manning’s  $n$  values based on floodplain vegetation and main channel bed material.
2. Set bank station and elevation data as levee points.

3. Run a steady flow analysis for a range of discharges.
4. Use HEC-RAS' "Graphical Cross-section Editor" alongside aerial imagery (when available) to set levee points at bankfull. Ensure that levee points are not set on top of "spikes" of high elevation. These are likely errors in LiDAR data or some tall feature (e.g. a tree).
5. Place "blocked obstructions" in low-flow conveyance channels.
6. Re-run a steady flow analysis and check that water surface profiles are reasonable.
7. Define "L. Levee Frbrd" and "R. Levee Frbrd" in HEC-RAS' output table. Freeboard is a measure of difference between the TOB point and the WSE. Overtopping of the levee is indicated by a negative freeboard value. Using a spreadsheet, identify the largest discharge contained by the levees before overtopping occurs.
8. An additional method for higher discharges without "computational levees" involves placing a "blocked obstruction" in the main channel. This forces HEC-RAS to only model overtopping flows. This method allows the user to check if HEC-RAS is assigning the proper amount of discharge in the floodplains and the main channel. The total discharge should equal the main channel discharge plus the modeled floodplain discharge.

## **2.6 Planform Evolution Model**

Massong et al. (2010) developed a planform evolution model (PEM) to describe geomorphic changes in the MRG. It was determined that changes in the MRG follow two paths: aggrading (A) or migrating (M). The aggrading path includes channels that have high sediment load and low sediment transport capacity, while the migrating path includes channels that have

low sediment load and high sediment transport capacity resulting in the erosion of the channel's bed and banks.

Stage 1 includes wide channels free of vegetation. Sand and some gravel material form dunes. These channels can maintain this stage as they typically see large floods and have high sediment loads. Stages 2 and 3 encompass the development of islands and bars through stabilization of dunes by vegetation. In stage A4, the main channel begins filling with sediment, forcing it to be at a higher elevation than the floodplain. Stage A5 is the result of sediment reaching the top of the banks creating a plug. Water is then forced to flow onto the lower elevation floodplain, where a new channel eventually forms in stage A6. Stage M4 is the opposite of A4, where channel incision occurs, forming a dominant channel. Stage M5 can be considered an equilibrium state, where sediment transport is roughly equal to sediment supply, and can often be a final stage. Stages M6 to M8 represent lateral migration patterns and the formation of bends. The planform evolution model for the MRG can be seen in Figure 2.

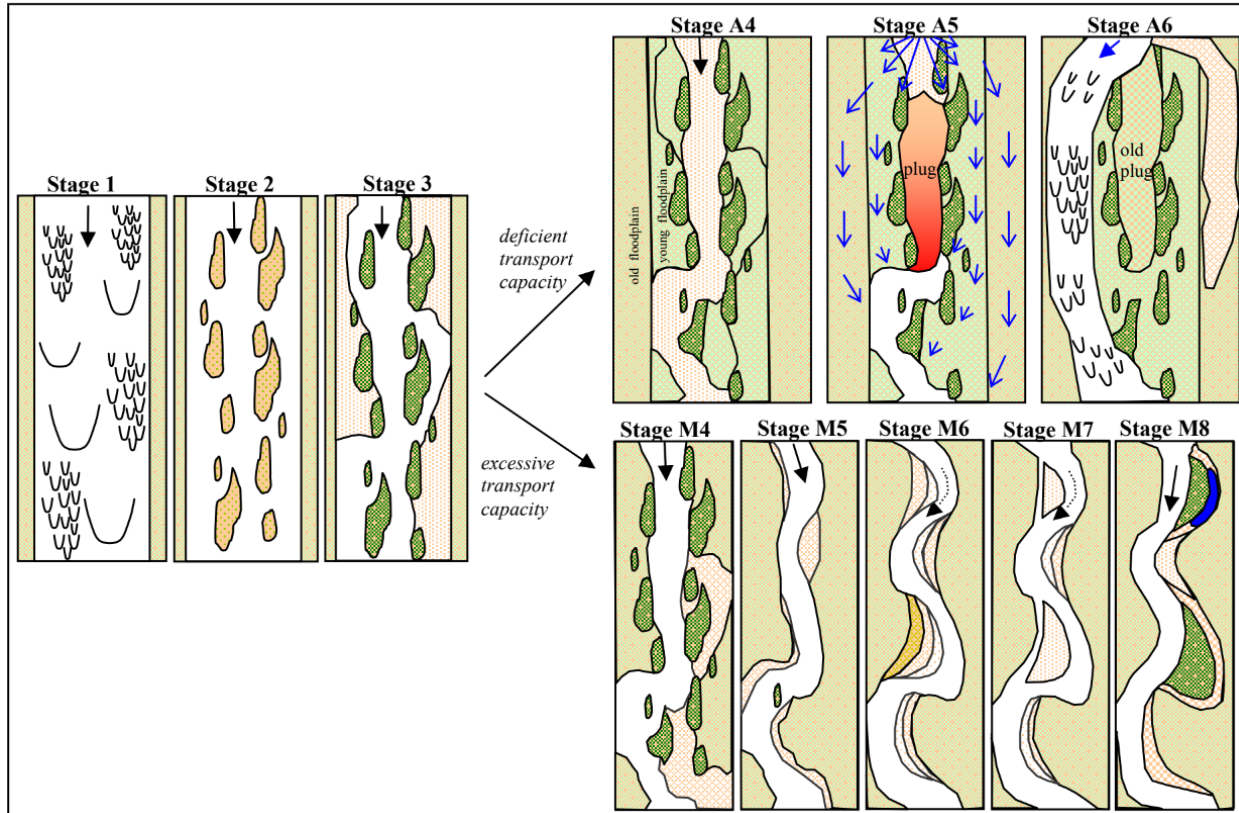


Figure 2 Planform evolution model for the Middle Rio Grande developed by Massong et al. (2010)

## 2.7 River Management

River management practices are typically rooted in engineering, hydrology, and geology. However, the goal for most river restoration projects is to improve biological conditions. Stream classification systems, which are often used in river restoration design, lack a biological component. Cluer and Thorne (2013) investigated implementing biology into their own stream classification system, known as the stream evolution model (SEM). The SEM, as seen in Figure 3, is a cyclical model rather than a linear model. One criticism of older, linear models is that rivers don't often go through every stage, as this would require at least a decade of undisturbed evolution (Zheng et al., 2017), and don't often follow a specific sequence. For example, a river may experience a stage more than once or revert to an earlier stage. Therefore, Cluer and Thorne (2013) represent these responses as "short-circuits" (i.e. the dashed arrows in the model). The

SEM also includes “dead-end” stages or final stages (i.e. stages 2 and 3s), which can be seen outside of the main circle.

Alongside the SEM, Castro and Thorne (2019) developed a stream evolution triangle (SET), which is a tool that relates primary drivers like biology, hydrology, and geology to fluvial geomorphology. Biology is a primary driver because organisms have been shown to influence bio-geomorphic and fluvial processes. Hydrology is another primary driver because fluvial processes rely on flowing water to provide energy to the environment. Lastly, geology is a primary driver because boundary materials that are highly resistant to erosion limit the stream’s ability to adjust its geometry over time. The SET (see Figure 4) is used for plotting stages in the SEM, capturing temporal variability by providing insight into how long an evolving stream will stay in a particular morphological stage. The degree of change is dependent on whether the stage of the stream falls in the center or corner of the triangle. Resistance to change tends to be greatest in the corners of the triangle where there is one primary driver controlling the system.

Johnson et al. (2019) also investigated the current river management system. They claim that the current approach, based on physical science, doesn’t often solve the problem at hand. In addition, the current approach causes long-term damage to river ecosystems, thus reducing their ability to meet societal demands. Therefore, they proposed a new approach called “biomic river restoration,” which focuses on using “biological power” to influence river processes rather than stable channel design. This entails reconnecting streams to healthy, balanced habitat. They make use of Castro and Thorne’s (2013) SET to determine how changes in river morphology affect the ability of aquatic, riparian, and floodplain organisms to build, maintain, and manage habitat.

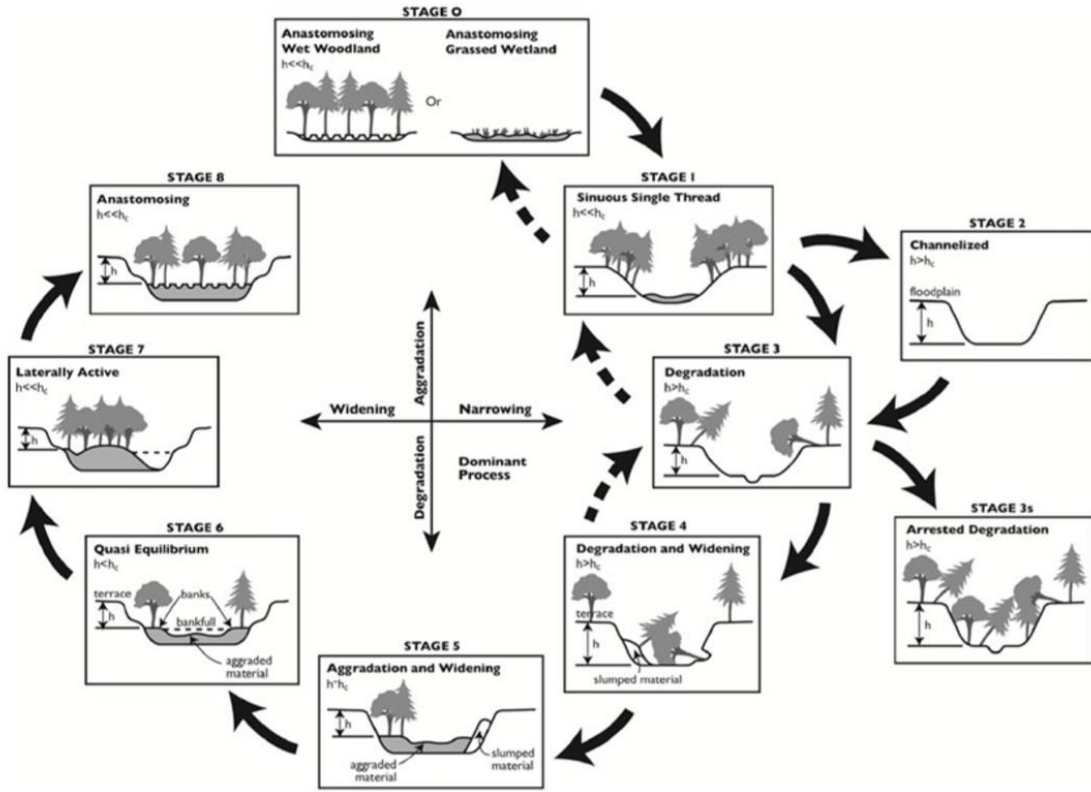


Figure 3 Cluer and Thorne's (2013) stream evolution model

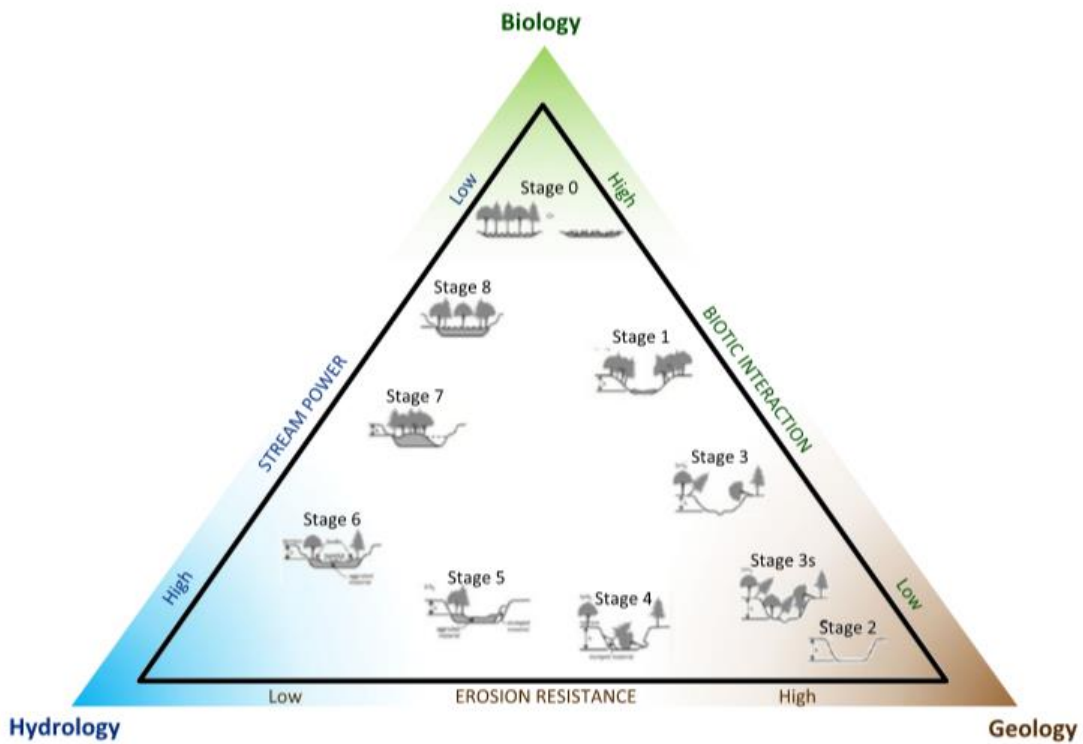


Figure 4 Castro and Thorne's (2019) stream evolution triangle

## Chapter 3: Site Description

### 3.1 Subreach Delineation

A subreach delineation analysis for the Isleta reach was performed by Yang et al. (2020). The subreach was broken up into six subreaches to better analyze habitat and hydraulic variables associated with the reach. Subreaches are identified by aggradation/degradation lines (agg/deg lines) and were delineated based on notable features. Table 3 summarizes the length of each subreach and its respective agg/deg lines. Figure 5 shows an aerial map of the Isleta reach delineated by subreach. Figure 6 through Figure 8 shows subreach specific aerial maps in 2012 noting the location of USGS gages used in this study and any RGSM population monitoring sites within the reach.

*Table 3: Subreach delineation for the Isleta reach. Subreaches were delineated based on notable geomorphic features (Yang et al., 2020)*

<b>Subreach</b>	<b>Agg/Deg lines</b>	<b>Length (mi)</b>	<b>Notable Features</b>
I1	657-700	4.2	Isleta Diversion Dam, right bank drain outfall
I2	700-815	11.0	Bend
I3	815-964	14.0	Straight reach, Abo Arroyo Confluence
I4	964-1015	4.8	No visible geomorphic control
I5	1015-1053	3.7	HWY60 Bridge
I6	1053-1097	4.2	Rio Puerco

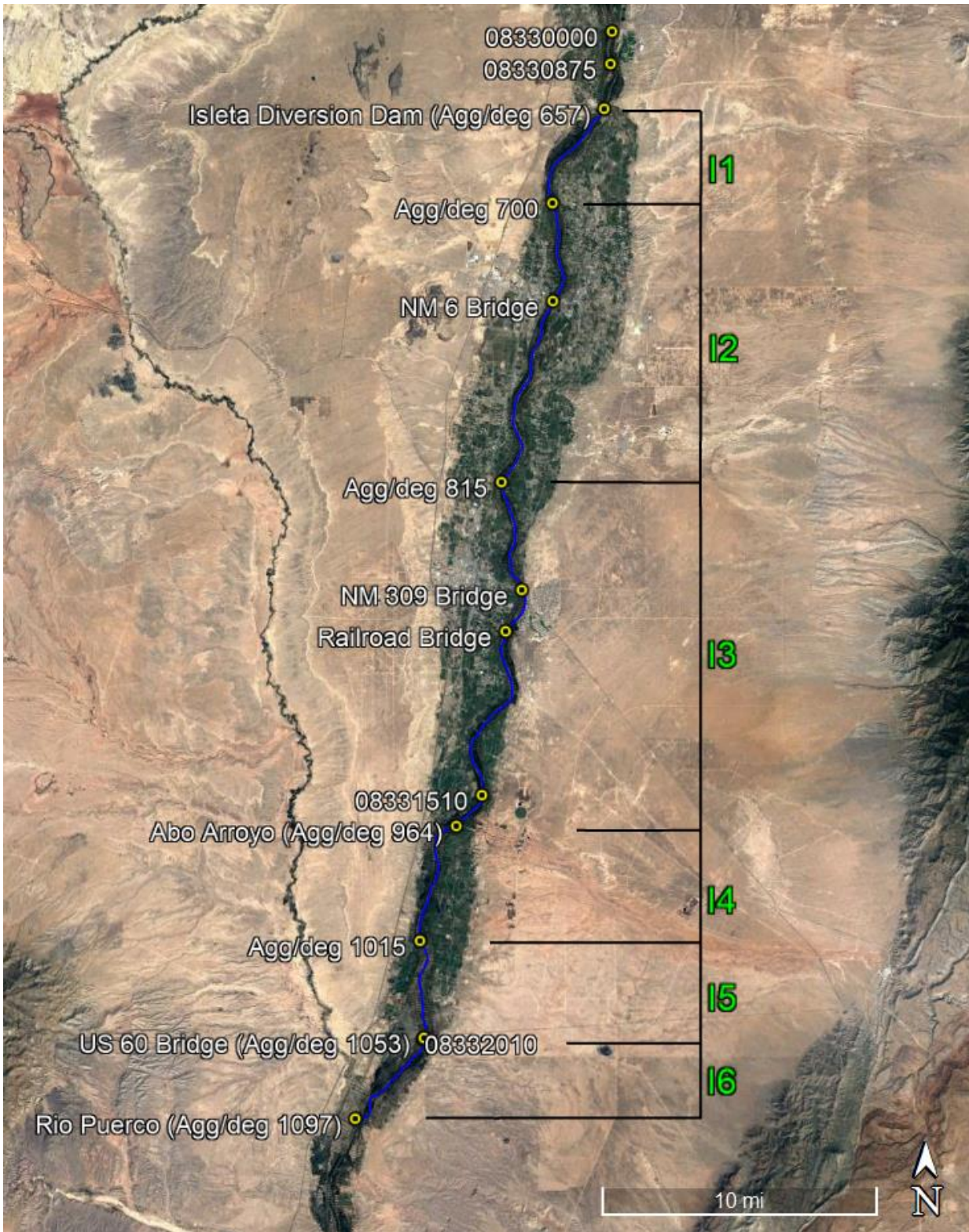


Figure 5 Map of the Isleta reach showing subreach delineations and the location of USGS gages used in this study

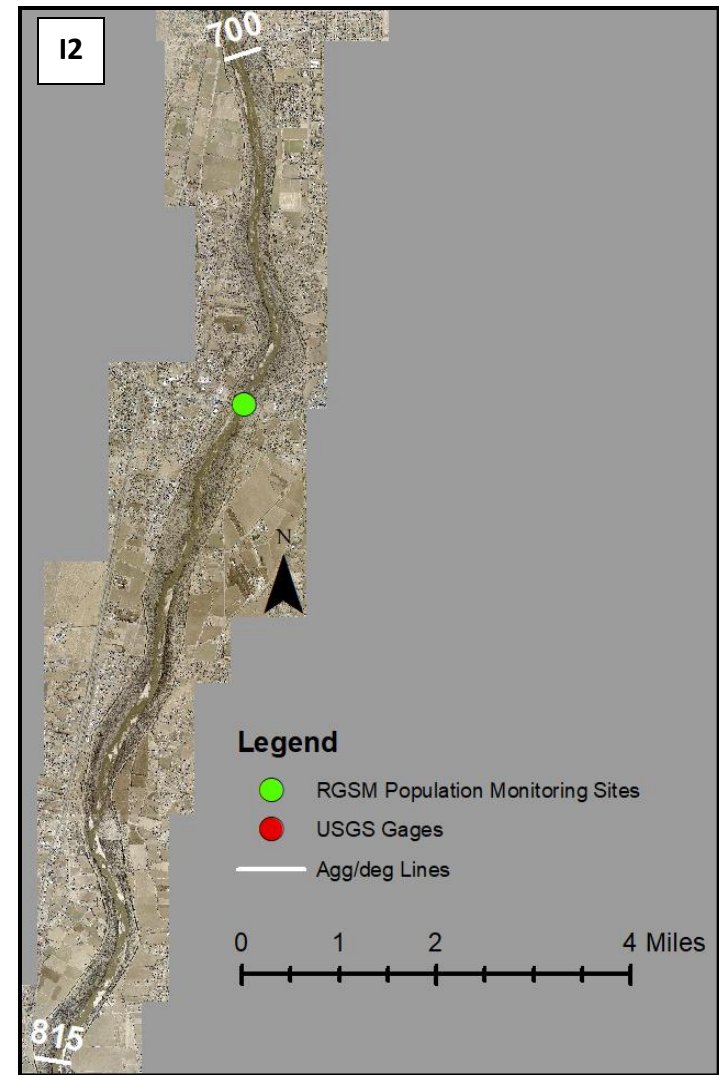
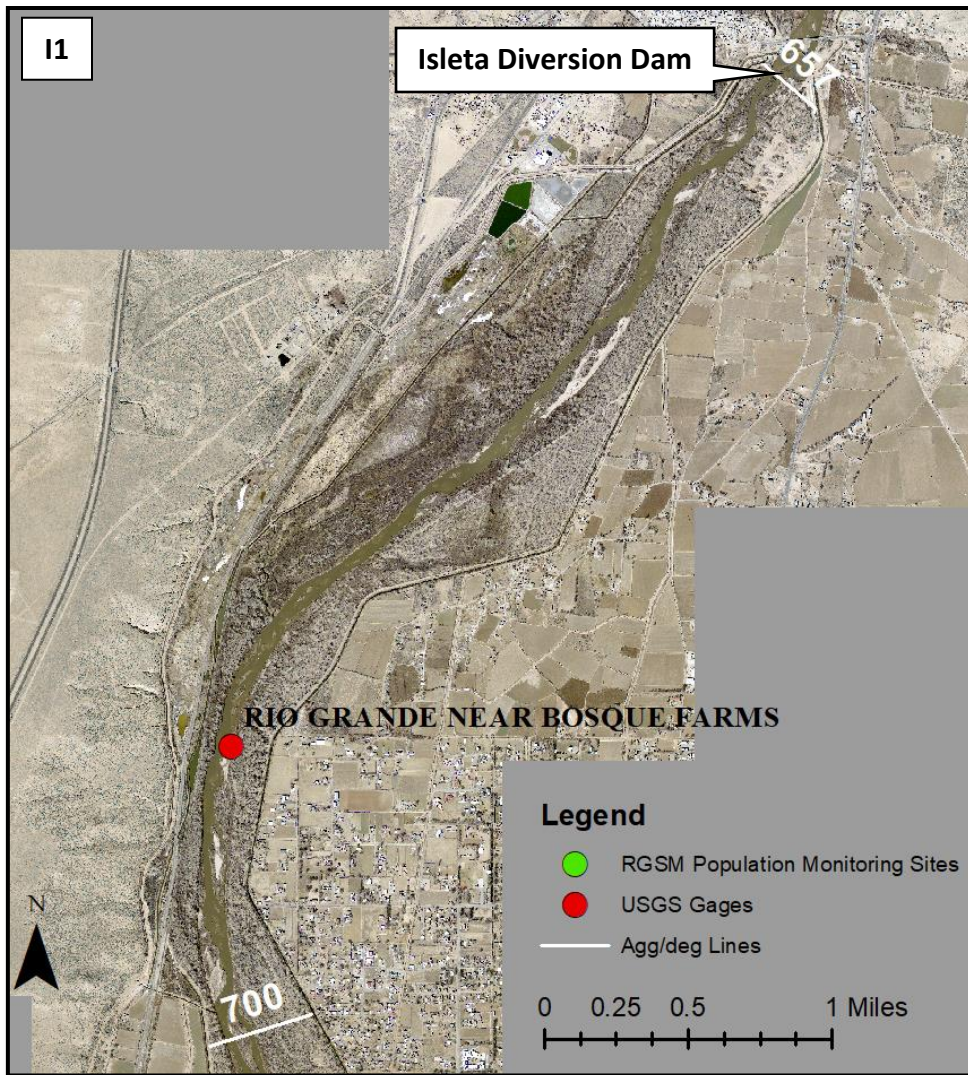


Figure 6 Aerial view of subreaches I1 and I2 in 2012

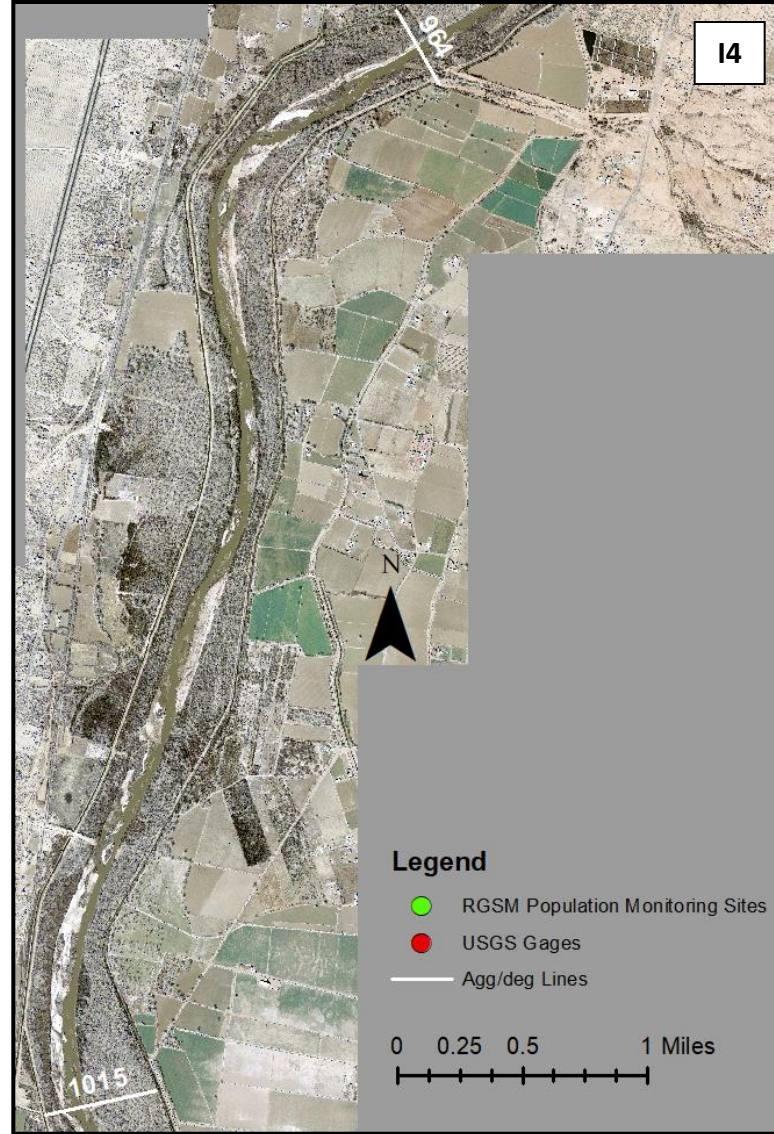
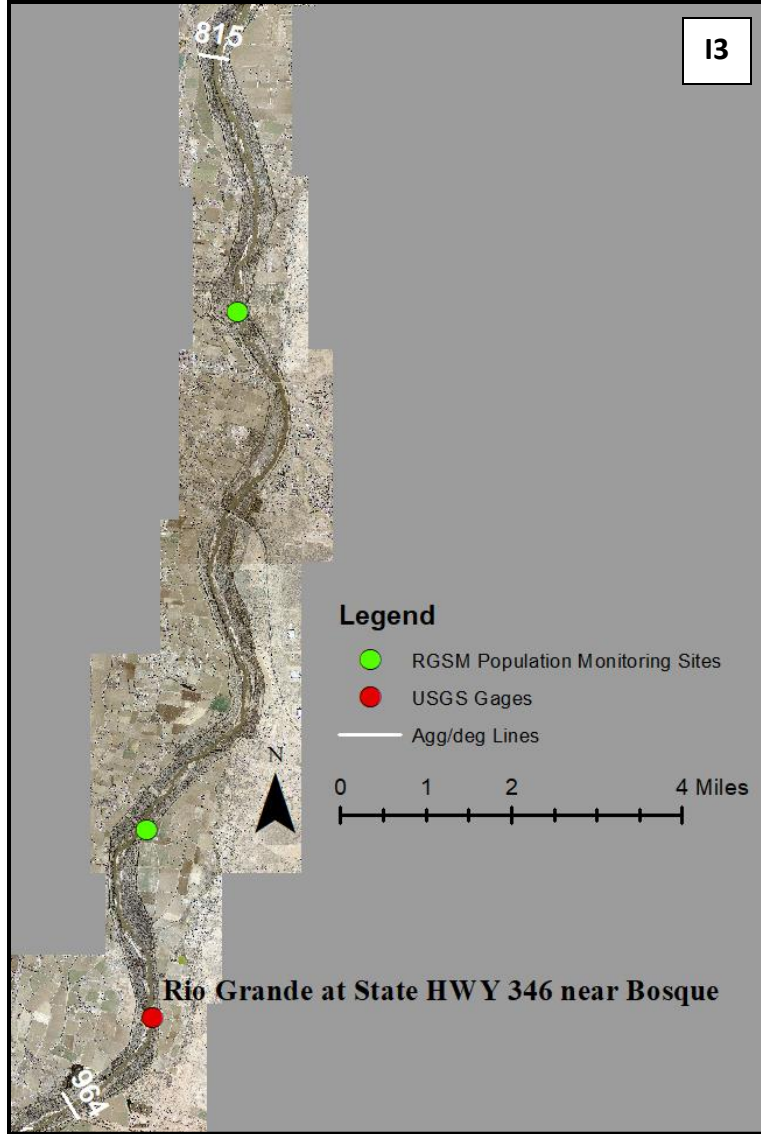


Figure 7 Aerial view of subreaches I3 and I4 in 2012

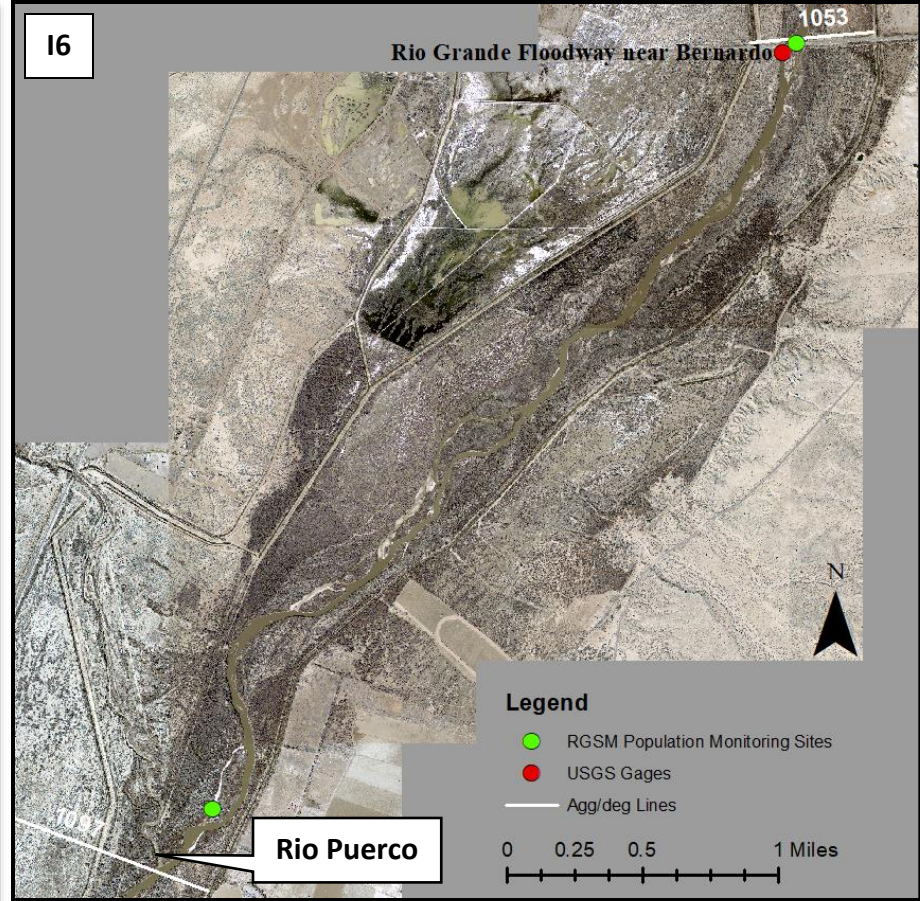
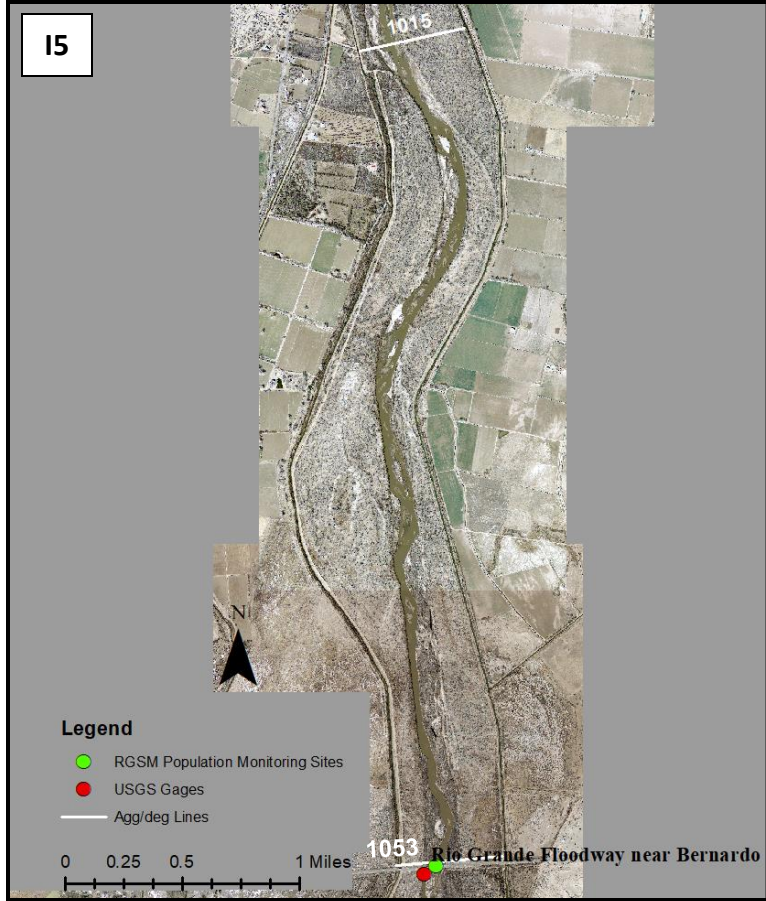


Figure 8 Aerial view of subreaches I5 and I6 in 2012

### 3.1.1 Habitat Map Delineations

For habitat mapping purposes, certain subreaches needed to be broken down into smaller segments to obtain the best resolution possible. The longest subreaches, I2 and I3, were delineated into smaller segments as seen in Table 4. These delineations will be referenced in Chapter 8: Habitat Mapping.

*Table 4 Habitat map agg/deg line delineations by subreach*

<b>Subreach</b>	<b>Agg/deg Lines</b>
I1	657-700
I2(a)	700-760
I2(b)	760-815
I3(a)	815-875
I3(b)	875-920
I3(c)	920-964
I4	964-1015
I5	1015-1053
I6	1053-1097

### 3.2 Aggradation/Degradation Lines

Aggradation/degradation lines are “spaced approximately 500-feet apart and are used to estimate sedimentation and morphological changes in the river channel and floodplain for the entire MRG” (Posner 2017). Each agg/deg line is surveyed approximately every 10 years, when the USBR performs monitoring and is established as a cross-section in the Rio Grande HEC-RAS models. The most recent entire MRG survey was performed in 2012. Cross-sectional geometry at each agg/deg line is available from models developed by the Technical Service Center (TSC) in Denver, CO. Models are available for 1962, 1972, 1992, 2002 and 2012. The 2012 model was developed from LiDAR data, while models prior to 2012 used photogrammetry techniques. All models use the NAVD88 vertical datum.

### 3.3 Geomorphic Characteristics

Anthropogenic impacts to the MRG, as well as changes to sediment and flow regimes, have forced the river to adjust. Yang et al. (2020) analyzed the temporal change of geomorphic characteristics in the Isleta reach by looking at aerial photographs, cross-sectional geometry data, and performing HEC-RAS simulations. The findings from this study are summarized in Table 5. Values for width, depth, velocity, and bed slope were computed using HEC-RAS at 3,000 cfs and averaged over the length of each subreach. Sinuosity values are for 2016 and mean grain size ( $D_{50}$ ) was determined from samples collected in 2012, 2014, and 2016.

*Table 5 Summary of geomorphic characteristics of the Isleta reach*

<b>Subreach</b>	<b>Width (ft)</b>	<b>Depth (ft)</b>	<b>Velocity (ft/s)</b>	<b>Bed Slope</b>	<b>Sinuosity</b>	<b><math>D_{50}</math> (mm)</b>
I1	325	2.50	3.90	$8.25 \times 10^{-4}$	1.10	0.40
I2	400	2.20	3.60	$8.20 \times 10^{-4}$	1.10	0.54
I3	350	2.50	3.70	$7.50 \times 10^{-4}$	1.17	0.42
I4	350	2.50	3.70	$7.20 \times 10^{-4}$	1.12	0.44
I5	350	2.50	3.70	$8.20 \times 10^{-4}$	1.11	0.44
I6	340	2.60	3.70	$7.70 \times 10^{-4}$	1.14	0.40

Channel width has decreased over time for all subreaches due to river management efforts like the construction of dams, levees and jetty jacks, as well as vegetation encroachment. This has caused peak flows and upstream sediment supply to be reduced (Culbertson and Dawdy 1964; Crawford et al. 1993; Berry and Lewis 1997; Bauer 2000; MEI 2002; Bauer and Hilldale 2006; Tashjian and Massong 2006; Parametrix 2008; Bauer 2009; Makar 2010; Makar and AuBuchon 2012; Baird 2014). I1 and I2 show the greatest reductions in width since 1972, with

I2 containing the widest channel in 2012. Depth and velocity have both increased over time for all subreaches, reaching values outside of the acceptable bounds for RGSM habitat. Overall, there is little change in depth and velocity between subreaches. Bed slope is mild and more variable between subreaches. Sinuosity has fluctuated over time, with the greatest decrease occurring after 1949. Sinuosity remained low between 1962 and 1992, where it then increased until 2016. Sinuosity is greatest in subreach I3, with all subreaches nearing one, suggesting that the main channel is relatively straight. Lastly, grain size downstream of the Isleta Diversion Dam can be classified as medium sand ( $D_{50} < 0.5$  mm).

### **3.3.1 Bed Elevation**

Mean bed elevation in the Isleta reach was obtained from HEC-RAS for each cross-section using 1962, 1972, 1992, 2002, and 2012 geometry datasets. Figure 9 shows longitudinal profiles that were created for each year. From the longitudinal profiles, little change is seen in bed elevation from 1962 to 2012 for subreaches I1 and I2. Subreaches I3 to I6 show indications of channel degradation. Yang et al. (2020) performed an aggradation/degradation analysis for each subreach and time period, which can be seen in Figure 10. This plot shows that aggradation occurred in all subreaches except I6 in 1962, with degradation occurring in all subreaches in subsequent years. The shift from aggradation to degradation is likely due to the installation of Cochiti dam in 1974 to 1975. The highest degradation, of approximately 3.7 feet, occurs in I6 from 1972 to 1992. From 1992 to 2002, degradation lessened in all subreaches, but increased again from 2002 to 2012. Degradation could be due to sediment transport capacity being higher than sediment supply in the reach. Cochiti dam likely causes the reduction in sediment supply, while narrow channels tend to increase shear stresses along the bed, thus increasing sediment transport capacity (Yang et al., 2020).

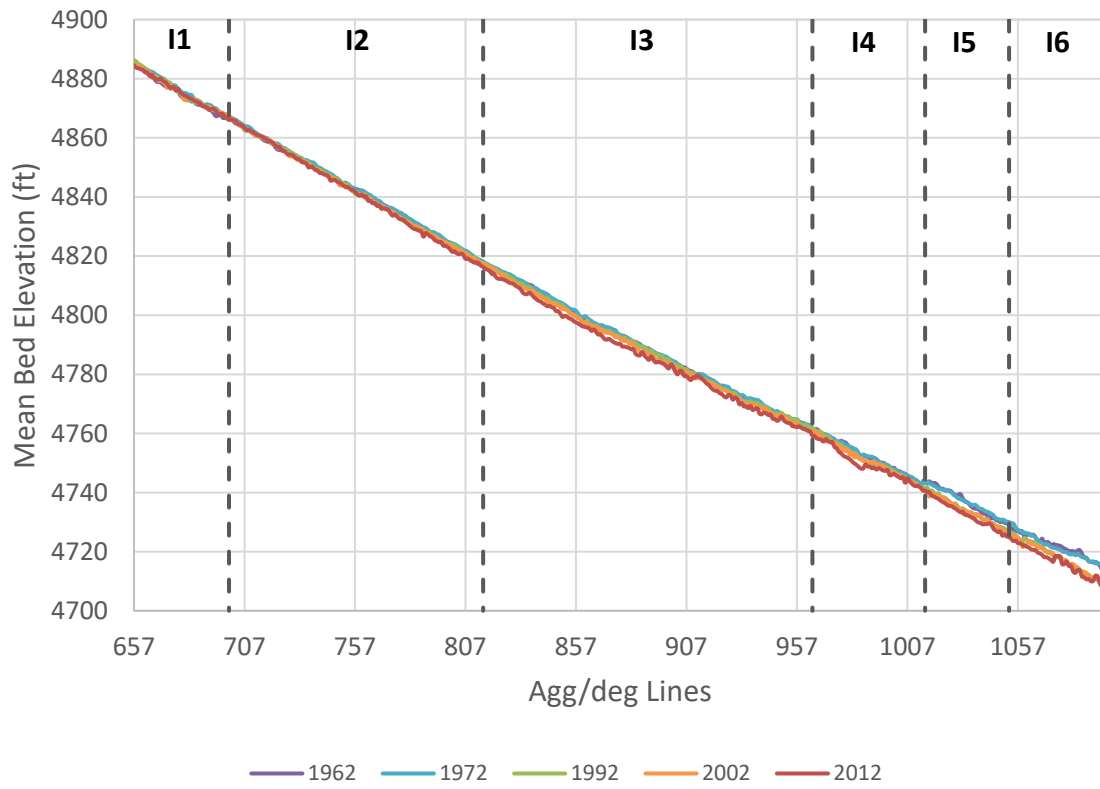


Figure 9 Longitudinal profiles of the Isleta reach

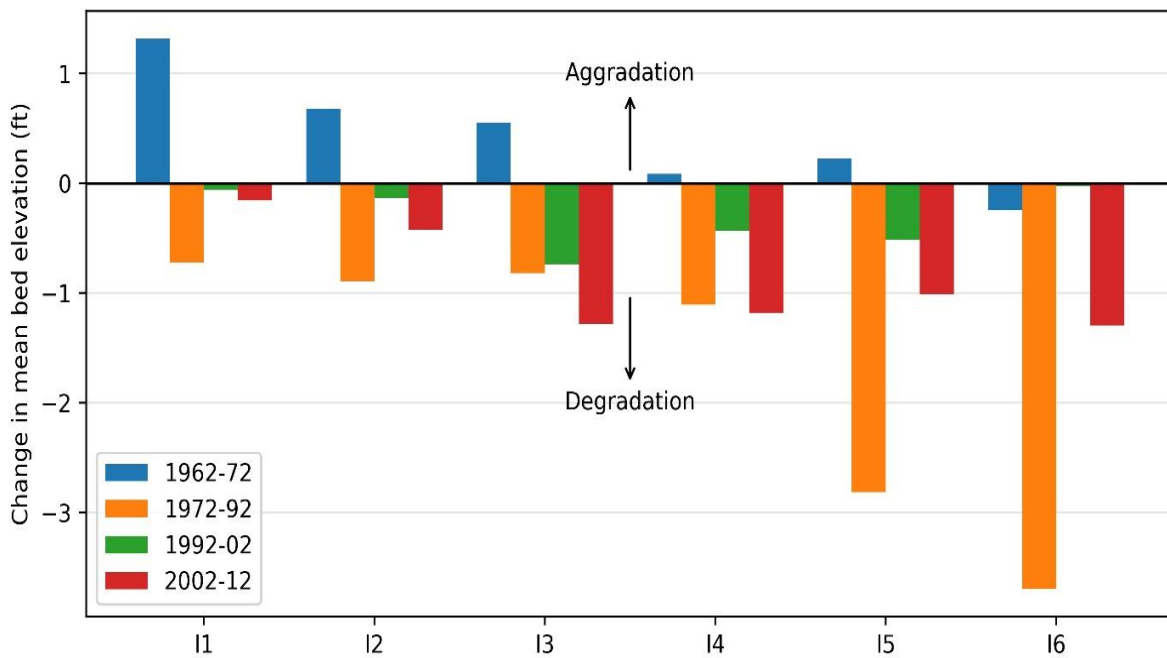


Figure 10 Change in mean bed elevation from 1962 to 2012 in the Isleta reach (Yang et al., 2020)

### 3.4 Flow Analysis

For flow analysis, gage data were obtained from the United States Geological Survey (USGS). Mean daily discharge and suspended sediment data were obtained and used throughout this study. Table 6 summarizes the USGS gages that were used in this study and the available periods of record. Refer to Figure 5 for their relative locations in the Isleta reach.

*Table 6 Available data for USGS gages in this study*

<b>Station</b>	<b>Station Number</b>	<b>Mean Daily Discharge</b>	<b>Suspended Sediment</b>
Rio Grande at Albuquerque, NM	08330000	October 1, 1965 – Present	October 1, 1969 – September 30, 2018
Rio Grande at Isleta Lakes Nr Isleta, NM	08330875	October 1, 2002 - Present	No data
Rio Grande at State HWY 346 Near Bosque, NM	08331510	October 1, 2005 - Present	No data
Rio Grande Floodway Near Bernardo, NM	08332010	October 1, 1957 - Present	October 1, 1964 – September 30, 2019

Flow duration curves were created for the Albuquerque, Isleta Lakes, and HWY 346 gages for their entire periods of record, and the Bernardo gage for the time period 1976 to 2004 (due to sporadic data before 1976 and missing data after 2004). These curves are presented in Figure 11. Table 7 summarizes the exceedance probability values taken from the flow duration curves and their respective recurrence intervals for each USGS gage. It is apparent that flows exceeding 3,000 cfs are rarely seen in the Isleta reach. Also, notice that the 75 and 90 percent exceedance probabilities (approximately 1-year recurrence intervals) are much lower for the highway 346 and Bernardo gages versus the Albuquerque and Isleta Lakes gages. This is likely

due to the influence of the Isleta Diversion Dam, which reduces the river’s downstream discharge when in use (Varyu, 2016).

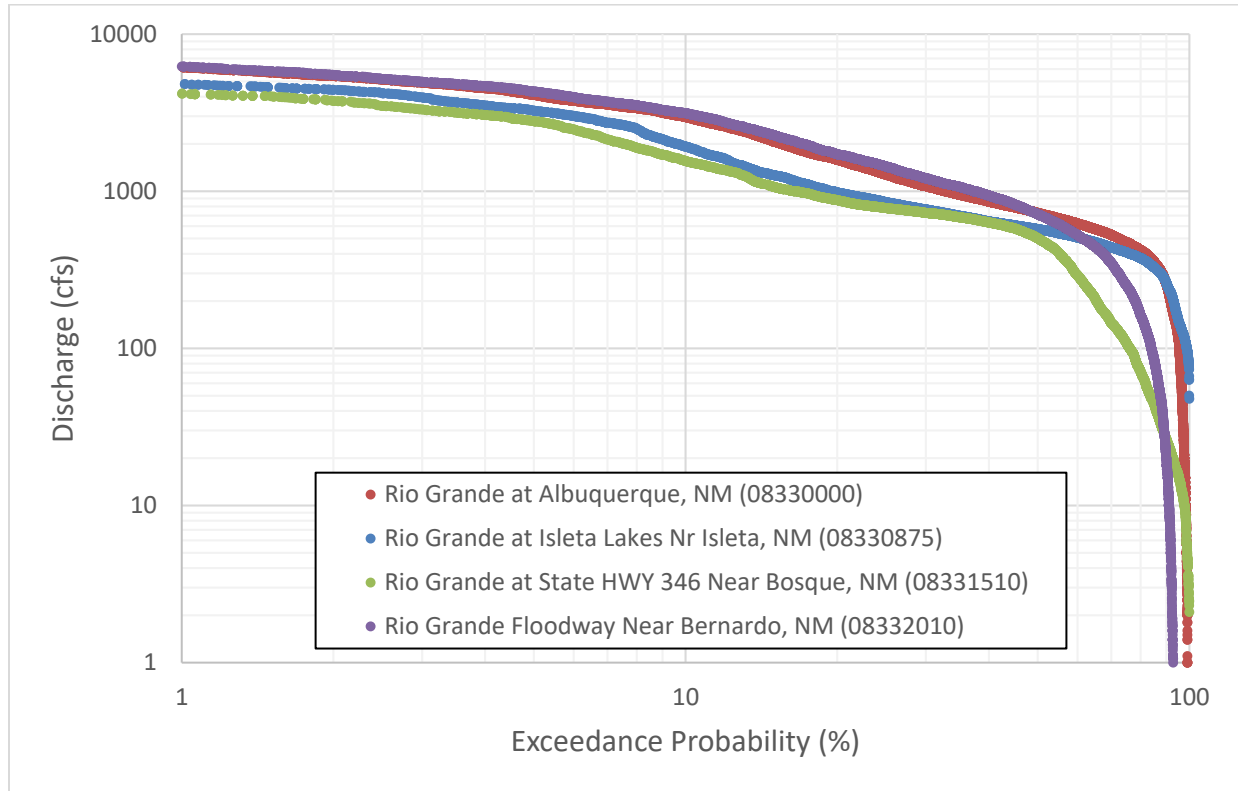


Figure 11 Flow duration curves

Table 7 Exceedance probabilities from flow duration curves

Exceedance Probability (%)	Recurrence Interval (years)	Rio Grande at Albuquerque, NM	Rio Grande at Isleta Lakes Nr Isleta, NM	Rio Grande at State HWY 346 Near Bosque, NM	Rio Grande Floodway Near Bernardo, NM
		Flow (cfs)			
1	100	6,120	4,810	4,180	6,230
10	10	2,960	1,920	1,550	3,140
25	4	1,280	851	781	1,440
50	2	727	575	503	714
75	1	474	409	109	252
90	1	258	261	26.5	20

### 3.5 Suspended Sediment Load

#### 3.5.1 Single Mass Curve

Mass curves show changes in cumulative sediment discharge over time and aid in the identification of major flows. Figure 12 shows the single mass curves for the Albuquerque and Bernardo gages from 1970 to 2018. Mass curves were discretized into three time periods to observe large scale trends in mean annual sediment. Mean annual sediment load is determined by finding the slope of the line.

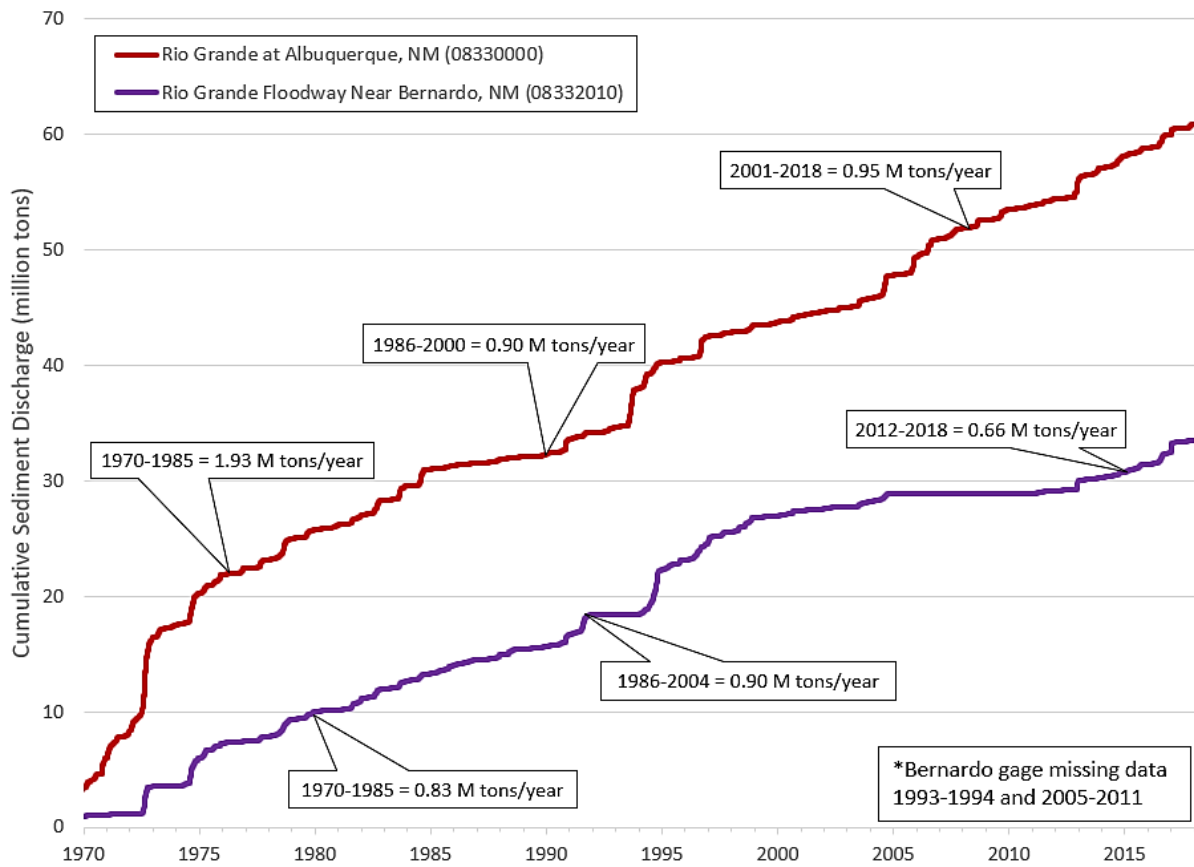


Figure 12 Single mass curves for the Albuquerque (08330000) and Bernardo (08332010) gages

Significant sediment loss (~ 15- 20 million tons from 1975 to 2005) can be seen between gages. Sediment is most likely lost to the Isleta Diversion Dam irrigation canals. Just south of the Bernardo gage is the confluence of Rio Puerco where a massive amount of sediment is

reintroduced into the river. At the Albuquerque gage, the largest mean annual sediment load, ~ 1.93 million tons/year, occurred from 1970 to 1985. Past 1974, the single mass curve becomes more linear and less steep. This is likely due to the influence of Cochiti dam which has decreased the sediment supply in the reach. The Bernardo gage sees similar trends, with the largest mean annual sediment load, ~ 0.90 million tons/year, occurring between 1986 and 2004. Both the Albuquerque and Bernardo gages experienced a significant increase in sediment discharge from 1994 to 1995. This is most likely the result of high spring runoff flows (recorded at 5,000 to 6,000 cfs) from May through June during this time period. These high spring flows are attributed to snow melt.

### **3.5.2 Monthly Average Histogram**

Monthly average histograms comparing suspended sediment discharge and concentration to mean flow discharge were created for the Albuquerque gage from 2012 to 2018. These histograms are helpful for visualizing seasonal trends in the reach. Figure 13 shows that spring months tend to have increased suspended sediment discharge due to snowmelt. However, suspended sediment discharge is also high in late summer and early fall, when rainfall peaks due to monsoon events (Yang et al., 2020). September 2013 was a major monsoon that occurred in the MRG and is the highest peak in both graphs. In addition, Figure 14 shows that suspended sediment concentration is highest in late summer and early autumn. This is likely the result of a combination of spring runoff flows and monsoons. Overall, these two plots suggest that monsoons and spring flows are the main drivers of sediment transport throughout the reach.

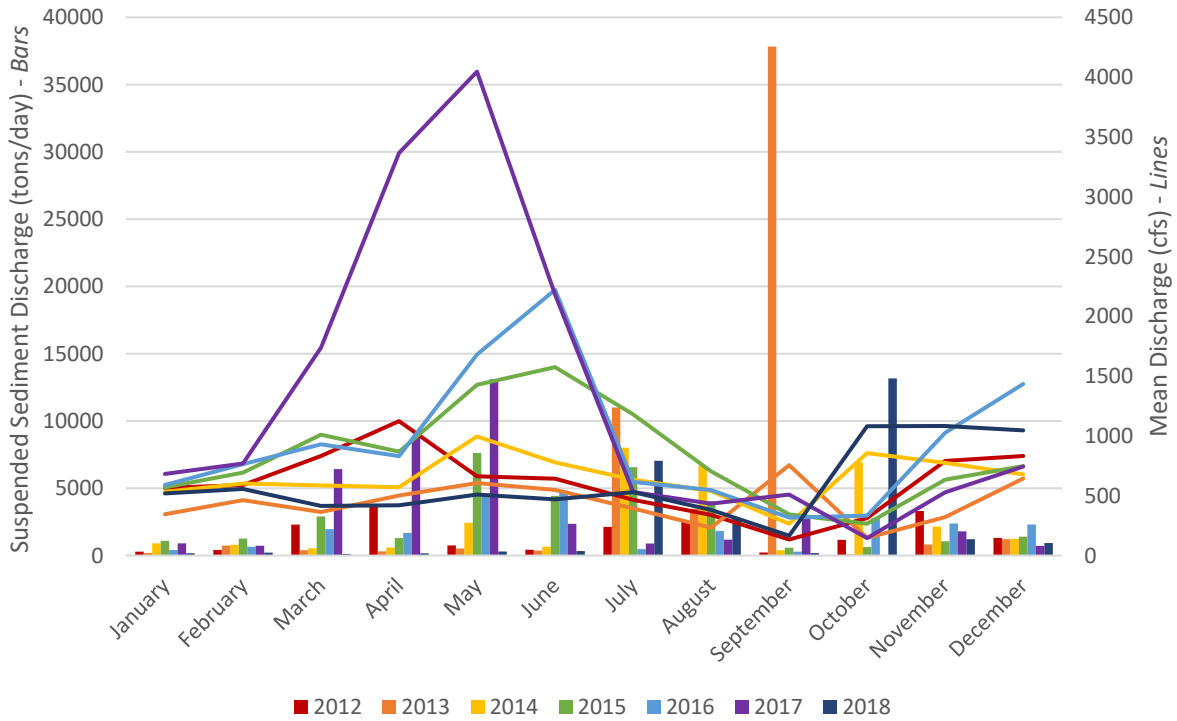


Figure 13 Monthly average histogram showing seasonal trends in suspended sediment discharge

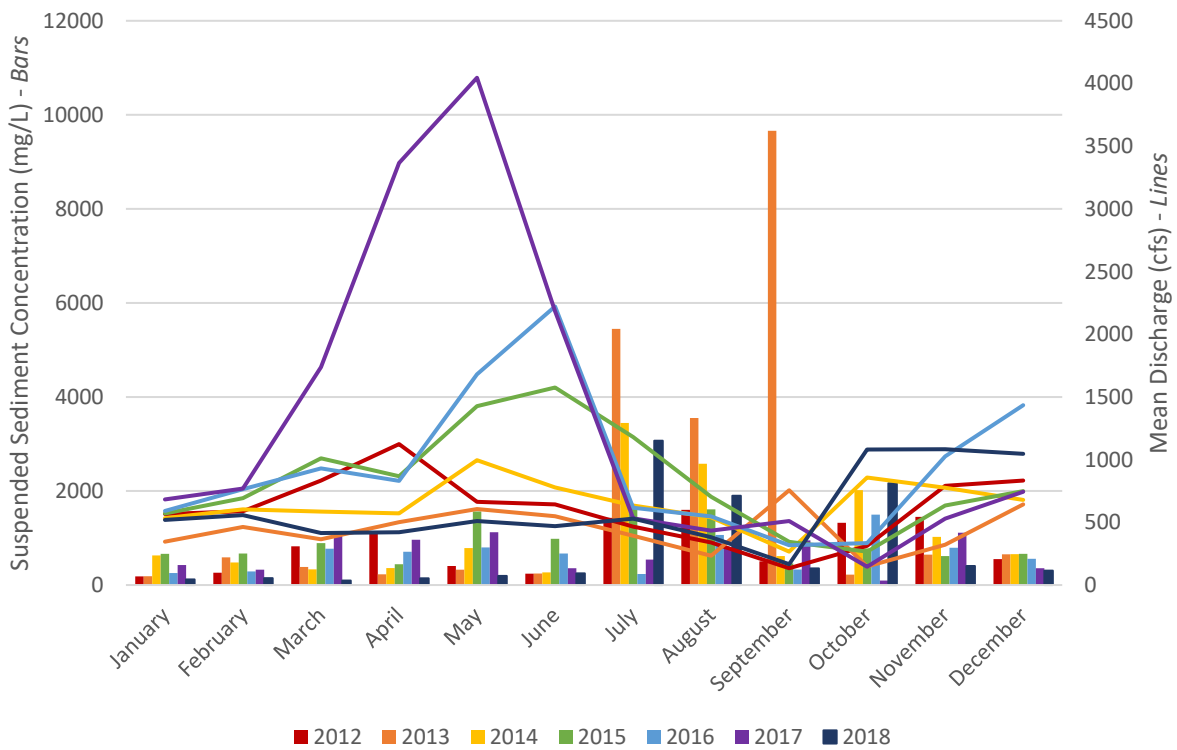


Figure 14 Monthly average histogram showing seasonal trends in suspended sediment concentration

## Chapter 4: Geometry

For the purpose of showing how the geomorphology in the reach has changed over time, cross-sections were chosen to represent each subreach. Representative cross-sections were chosen as the median cross-section in each subreach to eliminate bias. Elevation and station data for 1962, 1972, 1992, 2002, and 2012 were obtained from HEC-RAS and plotted. Changes to cross-sectional geometry throughout time can be seen in Figure 15 through Figure 20.

Subreach I1 shows signs of degradation and aggradation over time. Significant aggradation occurred from 1962 to 1972 (~ 2 feet) and from 1992 to 2012 (~ 1.5 feet), while significant degradation occurred from 1972 to 1992 (~ 2 feet). This shift between aggradation and degradation may be due to the channel trying to reach an equilibrium state. Since 1962, the width of the main channel has slightly increased and the small left side channel has eroded away.

Subreach I2 is one of the few subreaches that shows significant widening of the main channel. From 1972 to 1992 the channel gains an additional 200 feet of width, where it then remains constant until 2012. This subreach has also experienced 3.5 feet of degradation. Widening and degradation are likely due to an excess in sediment transport capacity, where sediment supply is restored through erosion of the bed and banks (Massong et al., 2010). From 1992 to 2012, a mid-channel bar formed, forcing the flow to split.

Subreach I3 shows evidence of lateral migration as the main channel has shifted towards the left. From 2002 to 2012, the mid-channel bar connected with the banks most likely from sediment filling the side channel, thus forming a more dominant channel (Massong et al., 2010).

Additionally, this subreach has gone from being wide and shallow in 1972 to more incised in 2012. From 1972 to 2012, the main channel bed degraded by approximately three feet.

Subreach I4 is characteristic of main channel degradation and slight widening. Again, this is likely due to an excess of sediment transport capacity in the reach. Since 1972, the main channel has degraded by four feet. Some aggradation occurred from 1962 to 1972 with the loss of the mid-channel feature. From 2002 to 2012, bar/island formation on the left side of the channel forced the main channel to migrate to the right side.

Subreach I5 has seen significant channel incision from 1962 to 2012, with erosion occurring mostly on the right bank. Since 1962, bed elevation has decreased by approximately 5 feet. Additionally, the floodplain on the right side degraded by approximately 2 feet from 1962 to 1972. The formation of more prominent features along the banks has forced the flow to follow a narrower path. Note that the narrow feature on the far-right side of the plot is a low-flow conveyance channel. The same conveyance channel is present in subreach I6.

Subreach I6 experienced the most channel degradation and widening within the reach. From 1962 to 2012, the channel has degraded approximately 5.5 feet. The channel has also significantly widened since 1972, gaining approximately 800 feet. From 1992 to 2012, more prominent islands/bars have formed, splitting the flow into two very incised channels.

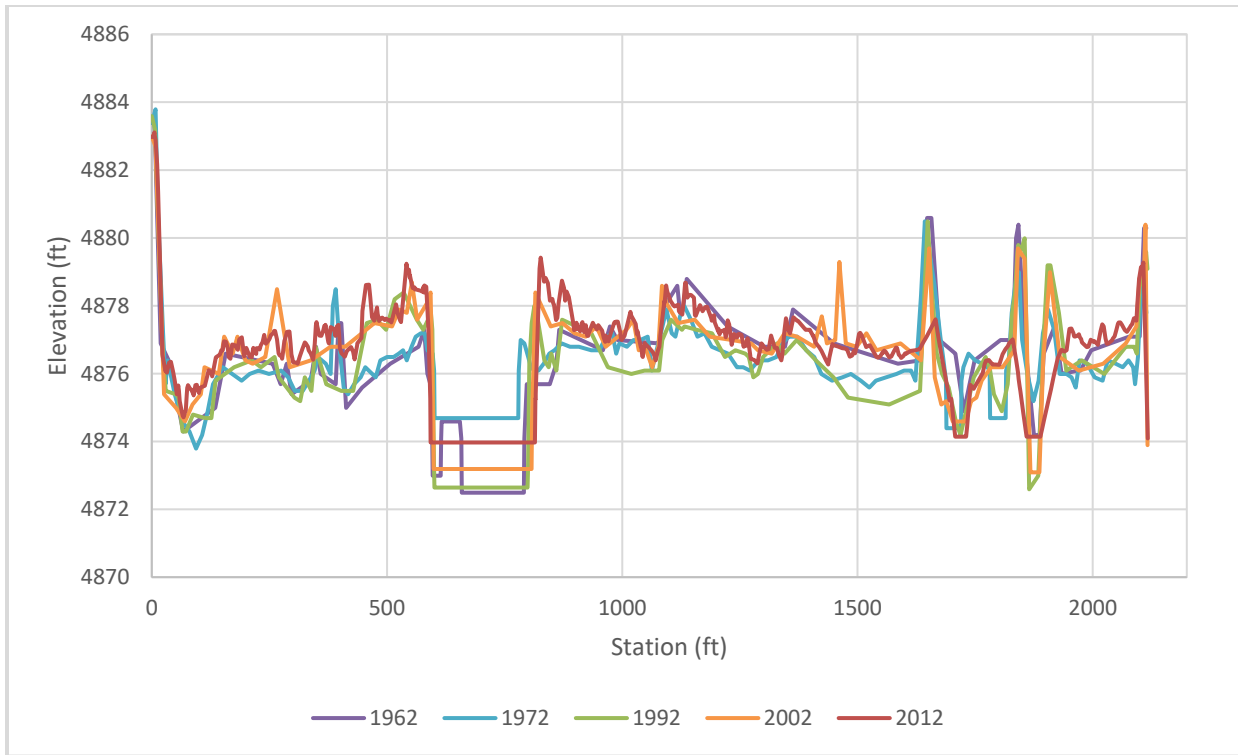


Figure 15 Changes to cross-sectional geometry from 1962 to 2012 at agg/deg line 681 in subreach I1

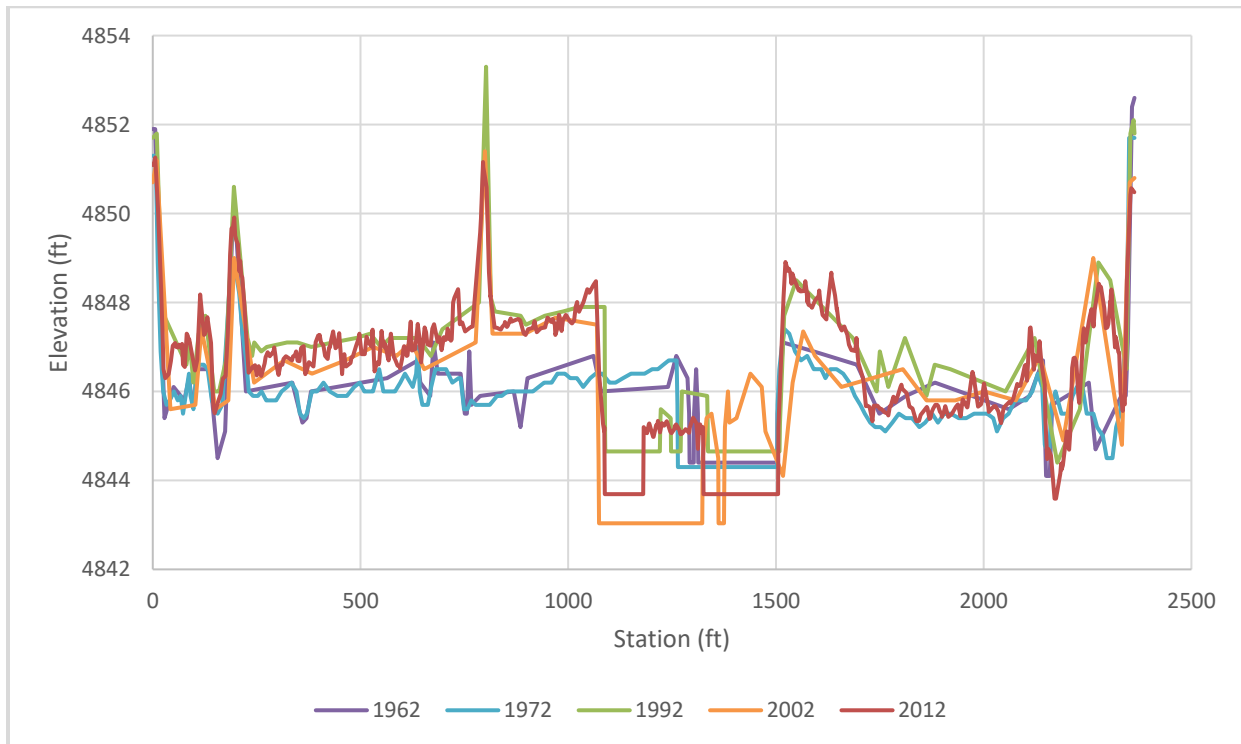


Figure 16 Changes to cross-sectional geometry from 1962 to 2012 at agg/deg line 751 in subreach I2

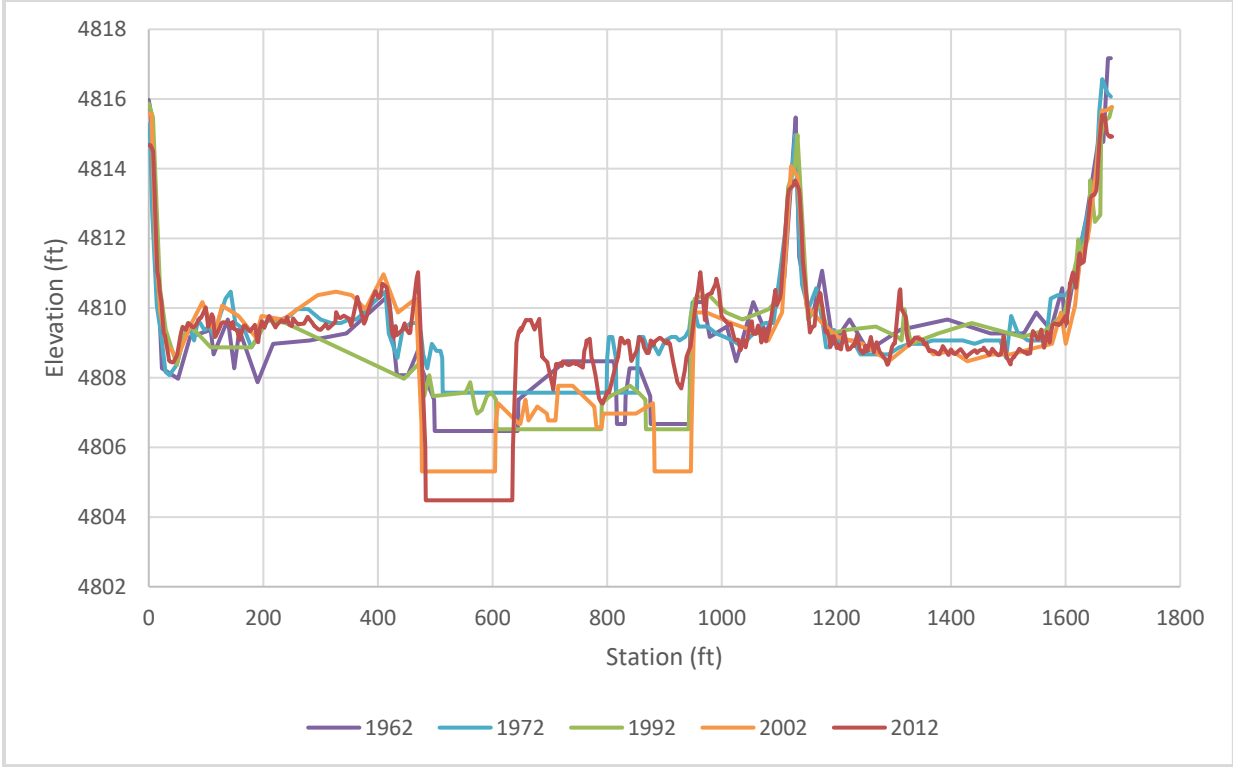


Figure 17 Changes to cross-sectional geometry from 1962 to 2012 at agg/deg line 841 in subreach I3

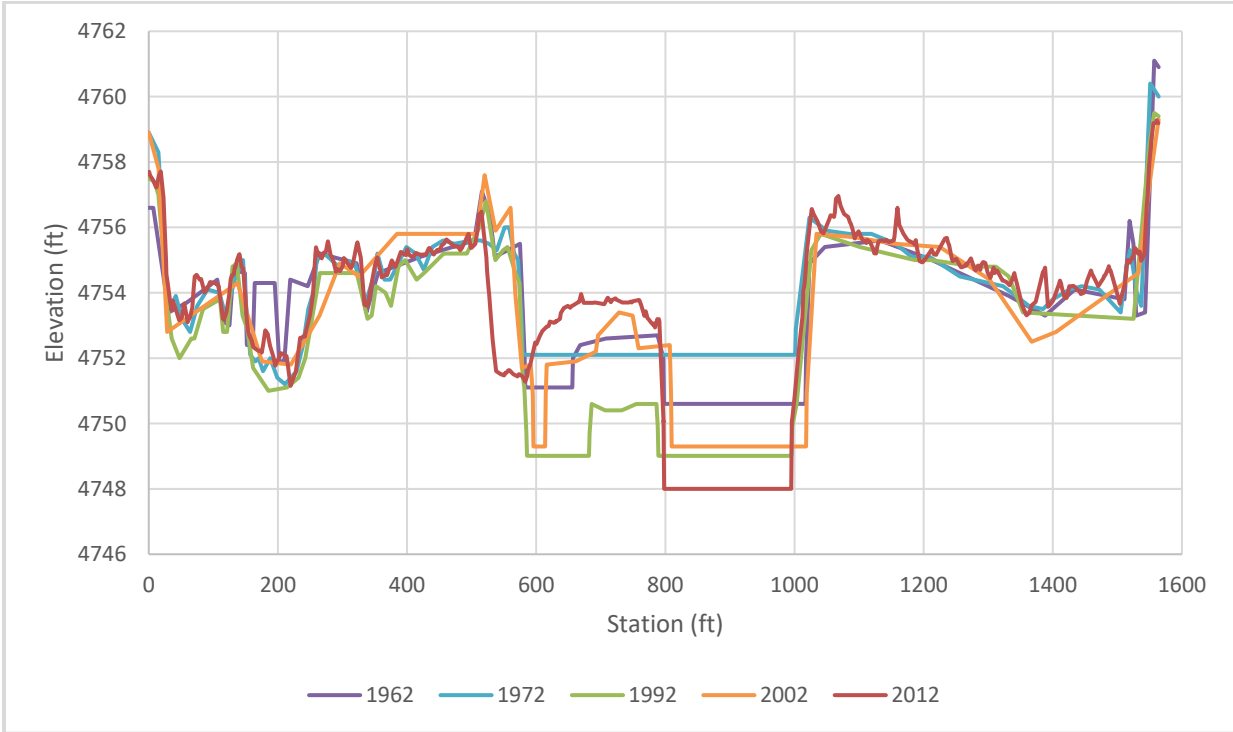


Figure 18 Changes to cross-sectional geometry from 1962 to 2012 at agg/deg line 991 in subreach I4

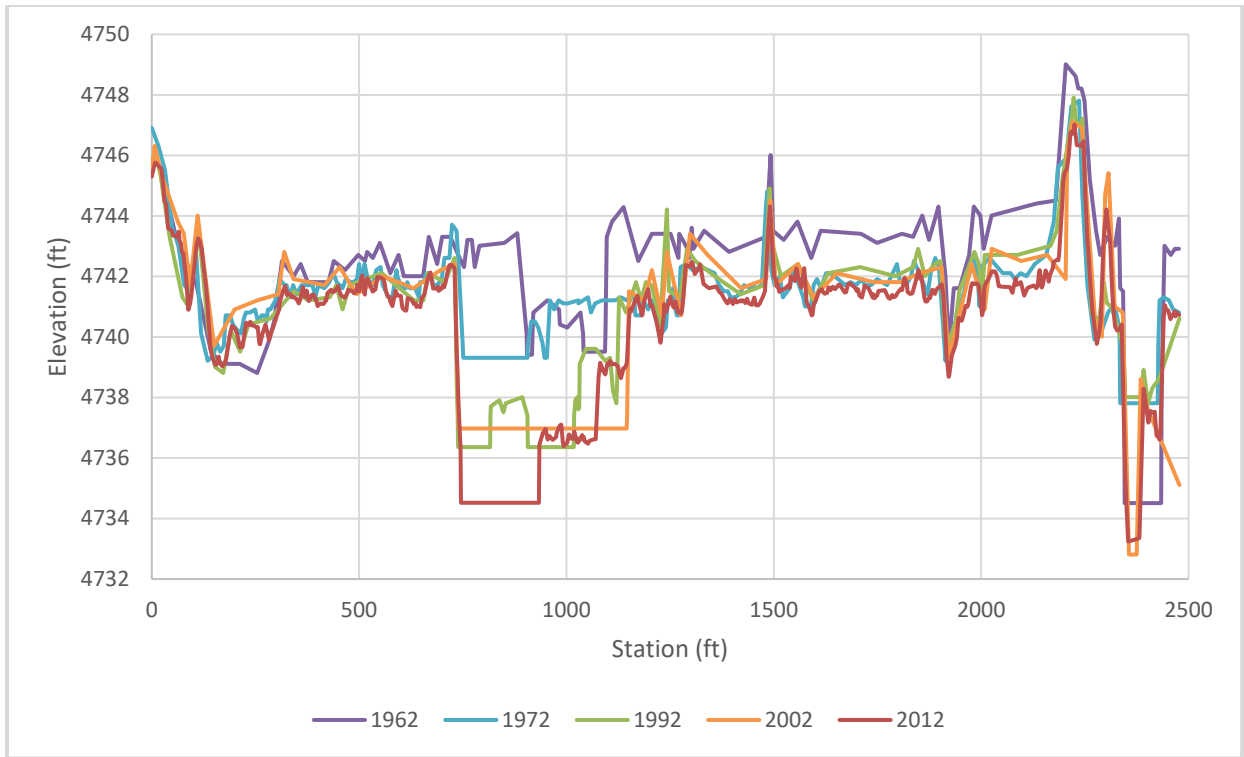


Figure 19 Changes to cross-sectional geometry from 1962 to 2012 at agg/deg line 1026 in subreach I5

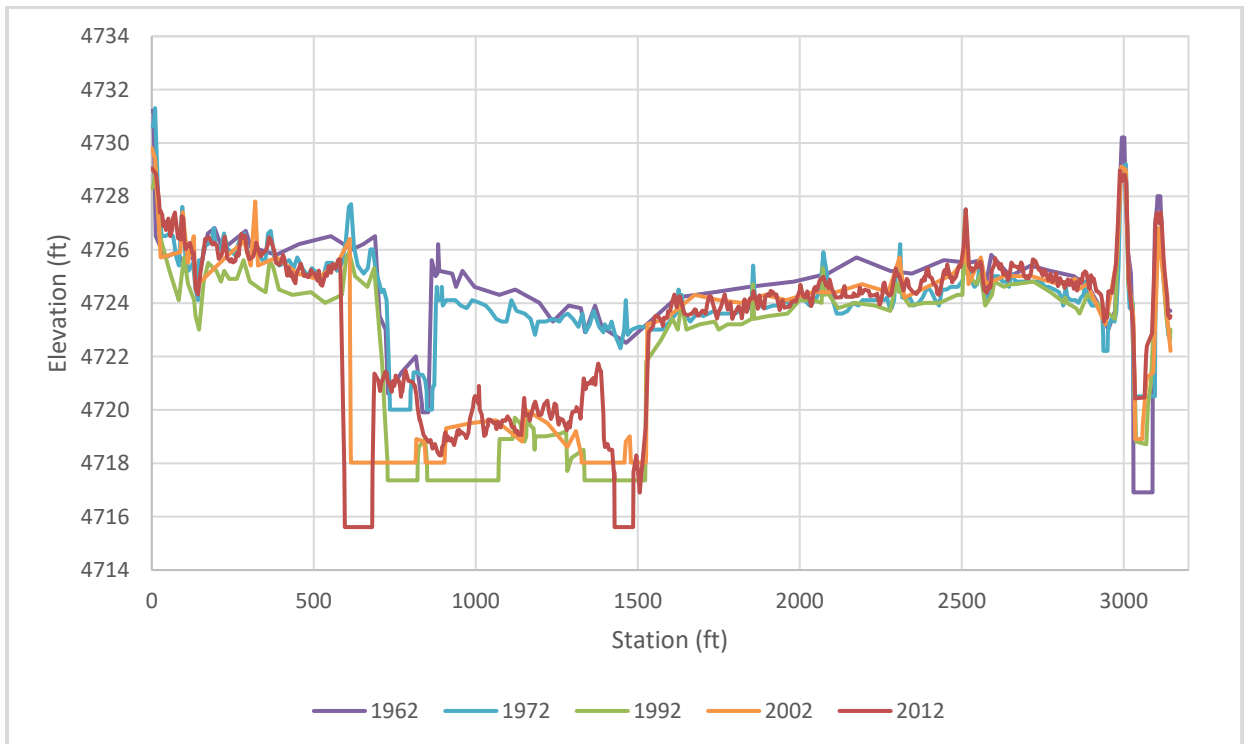


Figure 20 Changes to cross-sectional geometry from 1962 to 2012 at agg/deg line 1076 in subreach I6

## **Chapter 5: Hydraulic Modeling (HEC-RAS)**

### **5.1 Bankfull Discharge**

#### **5.1.1 Methods**

Bankfull discharge throughout the reach was determined using the method developed by Baird and Holste (2020). One issue with HEC-RAS one-dimensional modeling is the prediction of the water distribution as discharge increases. HEC-RAS distributes the water from the lowest elevation up. Because much of the MRG is perched, a problem arises in which HEC-RAS assumes water is in the floodplains at a much lower discharge than what would occur. To correct this issue, “computational levees” were assigned to TOB points to prevent the floodplains from filling before expected. Further background on this method was provided in section 2.5 One Dimensional Numerical Modeling Using HEC-RAS.

First, “computational levees” were placed at the locations that best represent the TOB point on each side of the channel. The water is contained within the main channel (between the TOB points) until there is a discharge large enough to overtop these points. HEC-RAS is capable of calculating left and right levee freeboard, which is the difference between water surface elevation and “computational levee” elevation. A negative value indicates an overtopping discharge. A sensitivity analysis was completed to determine the percentage of cross-sections that should be overtopped before removing the “computational levees” in HEC-RAS. Resulting bankfull discharge values were verified by engineers from the TSC based on field observations of the MRG.

### 5.1.2 Results

For this study, when 25% of the cross-sections in the Isleta reach experienced overtopping, signifying 25% had reached bankfull discharge, the TOB points were removed, allowing water to inundate the floodplains. Figure 21 shows the percent of cross-sections overtopping the TOB points for 1962, 1972, 1992, 2002, and 2012 and the resulting bankfull discharges. The gray dashed line in this figure indicates the 25% cutoff for computational levees.

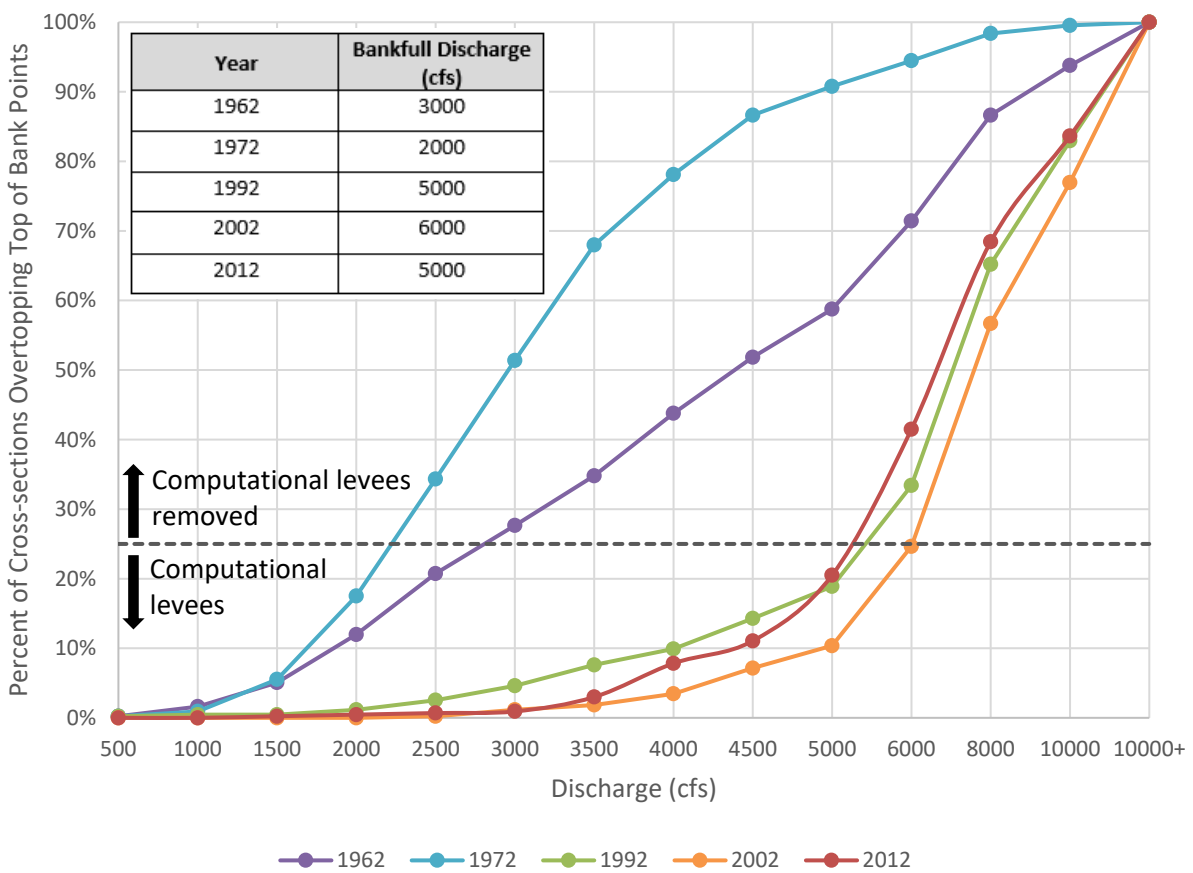


Figure 21 Percent of cross-sections overtopping the top of bank points

## 5.2 Flow Distribution Slices

### 5.2.1 Methods

Flow distribution slices can be used to estimate the available RGSM habitat throughout the Isleta reach by compiling depth and velocity data for each cross-section. HEC-RAS can

analyze the lateral flow distribution throughout a cross-section as described in chapter 4 of the HEC-RAS Hydraulic Reference Manual (U.S. Army Corps of Engineers, 2016). A cross-section can be divided into a maximum of 45 vertical slices. Since the RGSM relies heavily on the floodplain for habitat, it is important to capture greater detail in the floodplain than in the main channel. Therefore, 20 slices were assigned to the floodplain and 5 slices were assigned to the main channel. A steady flow analysis was run in HEC-RAS version 5.0.6 for the years 1962, 1972, 1992, 2002, and 2012 at thirteen discharges ranging between 500 and 10,000 cfs. Flows in the Middle Rio Grande tend to be below 5,000 cfs; therefore, to better represent these flows, increments of 500 cfs were used up to a discharge of 5,000 cfs. Figure 22 shows an example of the computed flow distribution at 10,000 cfs using the 2012 cross-section geometry dataset.

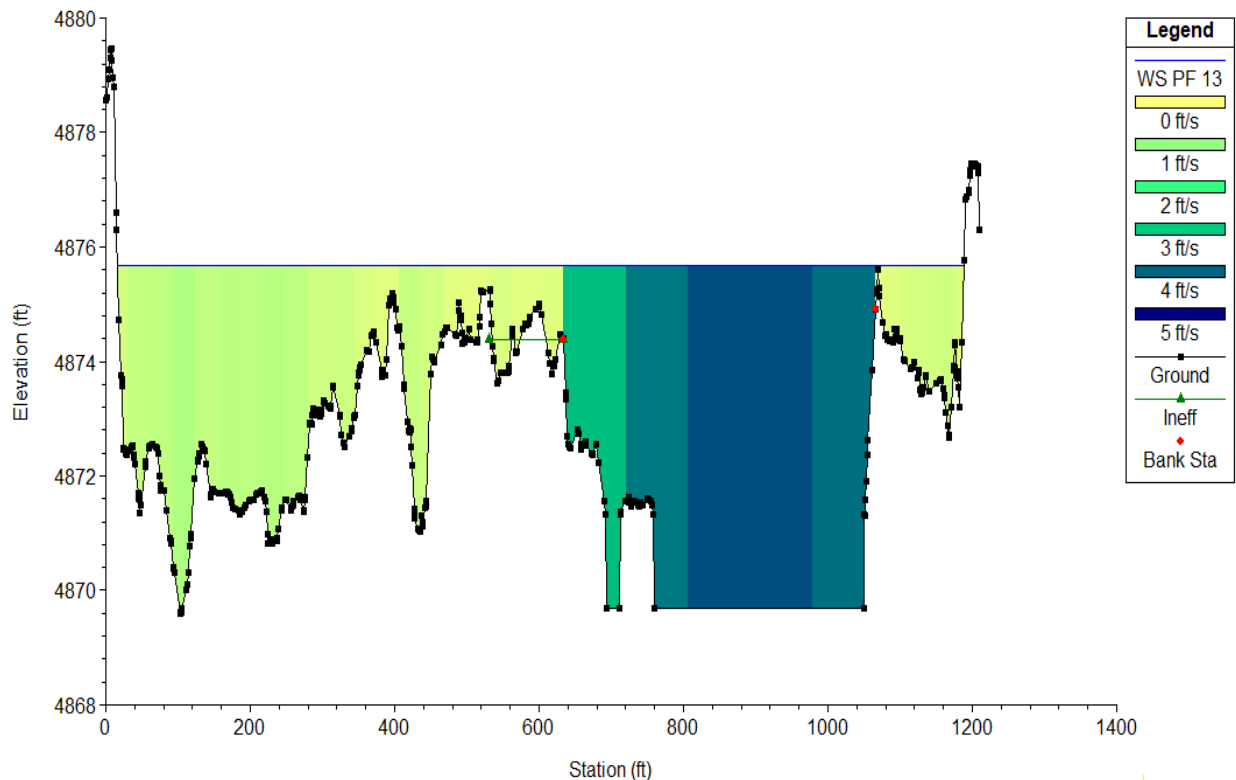


Figure 22 Example of flow distribution slices (colored bars) in HEC-RAS for agg/deg line 690 (subreach II)

After running a steady flow analysis, the flow distribution data were exported to Excel for further analysis. For each cross-section, the data were analyzed to determine how many of the vertical slices meet the RGSM depth and velocity criteria for each life stage. From these data, a width of suitable habitat can be obtained for each cross-section. This width is then multiplied by 500 feet (the distance between each agg/deg line) and normalized based on the length of the reach or subreach, resulting in units of square feet of potential habitat per mile of river.

### **5.2.2 Results: Habitat Curves and Spatial Habitat Charts**

Figure 23 shows the resulting habitat curves for the entire Isleta reach from the flow distribution slices for larvae, juveniles, and adults. Overall, larvae have the least amount of habitat availability, while juveniles and adults are rather similar and have the most habitat availability. This is to be expected as larvae have more strict velocity and depth criteria than juveniles and adults. For larvae, peak habitat availability of approximately 1.5 million ft<sup>2</sup>/mi occurred in 1972 at a discharge of 2,000 to 2,500 cfs. Subsequent years (1992, 2002, and 2012) have a lower peak habitat availability of approximately 1 million ft<sup>2</sup>/mi at a much higher discharge of 6,000 to 8,000 cfs. Habitat availability nears zero at lower, more frequent discharges. Juveniles and adults also see peak habitat availability occurring in 1972, nearing 5 million ft<sup>2</sup>/mi at a discharge of 4,000 to 4,500 cfs. Again, habitat availability drops in subsequent years, showing little habitat at lower discharges. For all subsequent years, peak habitat availability of approximately 4 million ft<sup>2</sup>/mi occurs at a discharge of 10,000 cfs. Habitat availability is higher in 1962 and 1972 than in 2012 because the main channel bed elevation was much higher, allowing water to spill over into the floodplains at lower discharges. Habitat curves by subreach can be found in Appendix A: Additional Habitat Curves.

In 2012, subreaches I2 and I4 show the most available larval habitat at discharges less than 3,500 cfs. For juveniles and adults, subreaches I4 and I6 show the greatest amount of habitat. At higher discharges, larval habitat is greatest in subreaches I2 and I3, while juvenile and adult habitat is greatest in I1 and I2. The results from this study were compared with a previous study of habitat availability performed by Yang et al. (2020), as described in section 2.4 Previous Studies of Rio Grande Silvery Minnow Habitat. HEC-RAS simulations at 3,500 cfs produced the best “spawning” and “feeding/rearing” habitat (i.e. larval habitat) in subreaches I1 to I3. At 600 cfs, subreaches I1 to I4 showed the most available “good” habitat (i.e. juvenile and adult habitat). Overall, both studies agree that at low flows, subreach I2 has the most larval habitat availability while subreach I4 has the most juvenile and adult habitat availability. Discrepancies between studies are likely attributed to a difference in modeling techniques (i.e. the use of “computational levees” to contain flow in this study).

A trend can be seen in the shape of the habitat curves across all subreaches. This change in shape from year to year may be attributed to changes in geomorphology. Incision has played a large role in the Isleta reach since 1962, increasing bankfull discharge and thus making it more difficult for water to reach the floodplains. In all subreaches, earlier years (1962 and 1972) showed “rounded” habitat curves, where habitat availability rapidly increases at discharges of 2,000 to 3,000 cfs followed by a rounding down of habitat availability at higher discharges. In more recent years (1992, 2002, and 2012), subreaches I1 and I2 showed “step” habitat curves. These “step” habitat curves show a pattern of rapid increase in habitat availability occurring around 5,000 cfs, beyond which the curve flattens out and remains constant above bankfull discharge. Subreaches I3 to I6 showed “hook” habitat curves in more recent years. “Hook”

habitat curves show a pattern of constant, low habitat availability at discharges less than 5,000 cfs, followed by a gradual, continuous increase in habitat availability above bankfull discharge.

Figure 24 shows stacked habitat charts representing spatial variability in habitat area throughout the Isleta reach for the year 2012. Note that the scale differs between charts and that they only extend to 3,000 cfs for better resolution. Stacked habitat charts for 1962, 1972, 1992, and 2002, as well as the stacked habitat chart for 2012 extending to 10,000 cfs, can be found in Appendix A: Additional Spatial Habitat Charts. Discharge seems to influence which subreach has the most habitat area. In other words, subreach I4 has the most larval habitat area at 1,500 cfs, but subreach I3 has the most larval habitat area at 3,000 cfs. Which subreach tends to dominate habitat area also changes between life stages. For example, at 1,500 cfs, juvenile and adult habitat area is greatest in subreach I2, while larval habitat area is greatest in subreach I4.

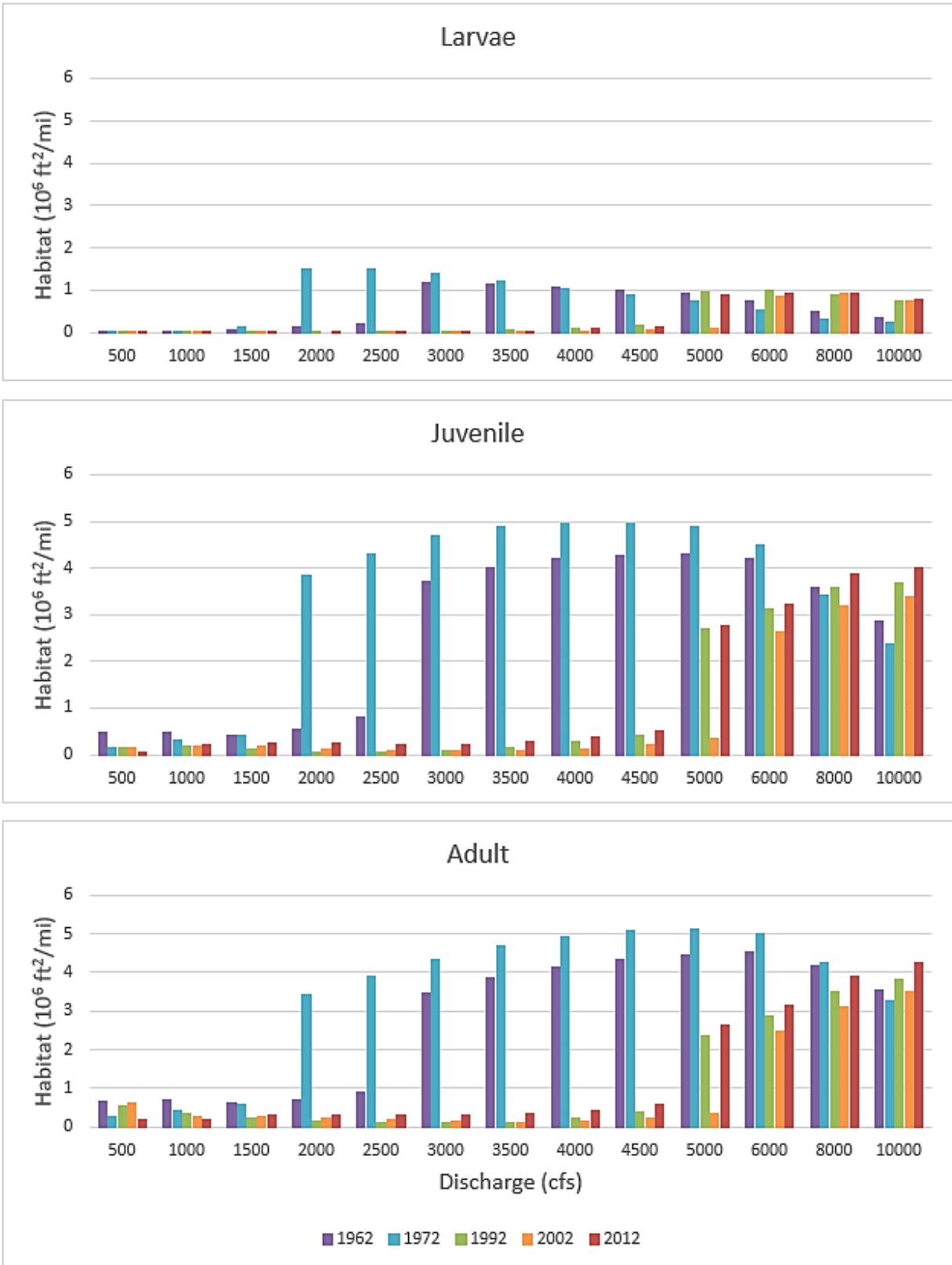


Figure 23 Larvae, juvenile, and adult habitat curves for the entire Isleta reach

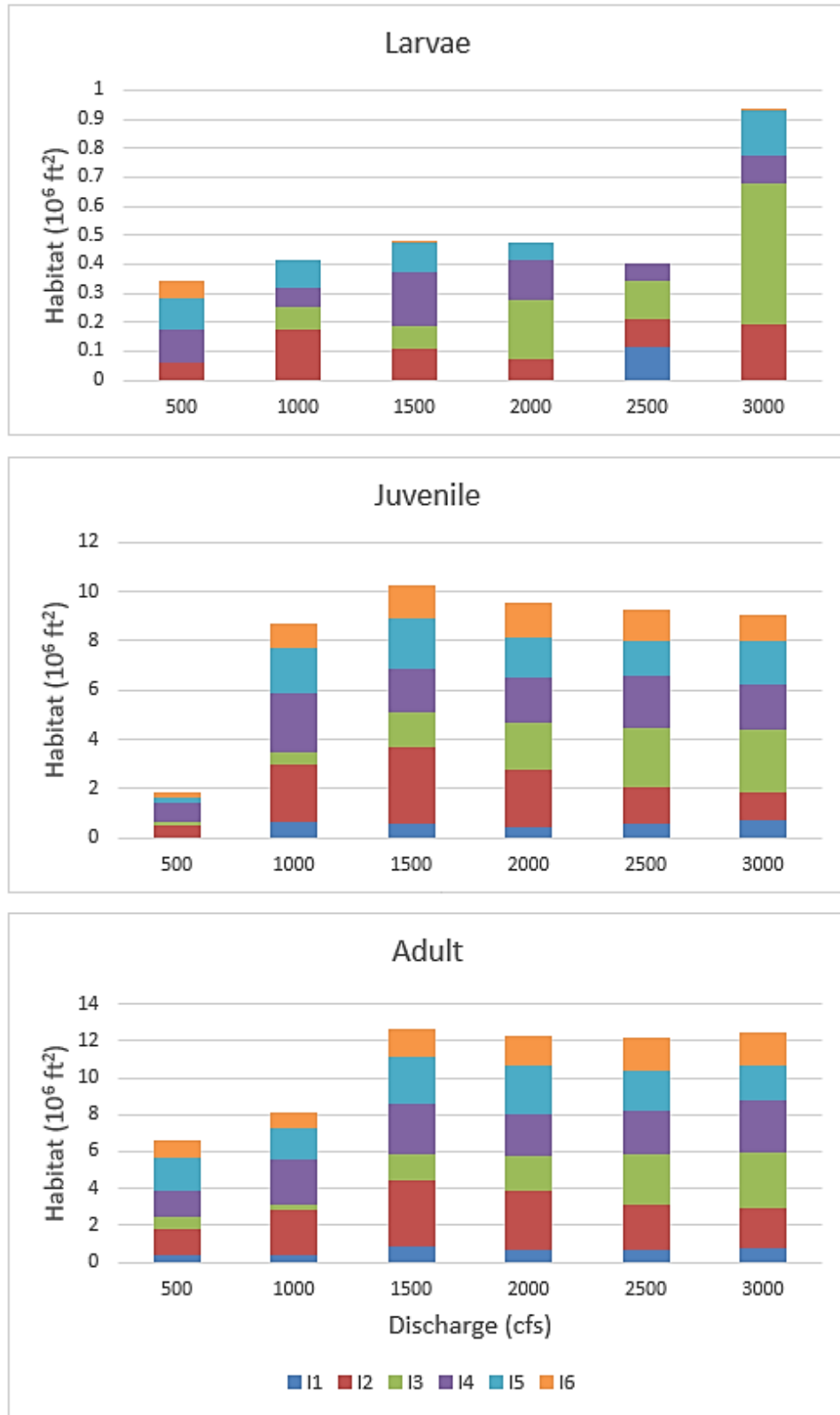


Figure 24 Stacked life stage habitat charts displaying the spatial variability throughout the Isleta reach in 2012 up to 3,000 cfs

## Chapter 6: Geomorphic Conceptual Models

### 6.1. Geomorphic Evolution Maps

Geomorphic evolution maps for each subreach were created to show changes in geomorphology from 1962 to 2012. These maps include cross-sectional geometry plots, aerial imagery, habitat curves, and an assigned stage from the PEM developed by Massong et al. (2010). The direction of flow in the aerial photographs is from top to bottom and discharge is unknown at the time of the photograph. The purpose of these maps is to draw connections between changing geomorphology and habitat availability in the reach. These maps can be seen in Figure 25 through Figure 30.

Looking at the aerial imagery in earlier years (1962 to 1992), all subreaches show the presence of sand dune fields. During the year, these fields could be frequently found moving downstream throughout the active channel. However, these large sand dune fields were lost during a drought in 1999-2004. The drought stopped the downstream movement of dunes, allowing vegetation encroachment onto these bars. Woody vegetation stabilized these surfaces before flows returned to normal in 2004 (Massong et al., 2010). This can be seen in the aerial imagery for all subreaches from 1992 to 2012 but is most clearly seen in subreach I6. In 2005, a spring flood with a 2-year recurrence interval forced many mid-channel bars to grow vertically. In 2006, high peak flows from summer rainstorms caused side channels to fill with sediment (Massong et al., 2010). Examples of this can be seen in the aerial imagery from 2002 to 2012 in subreaches I3 and I4.

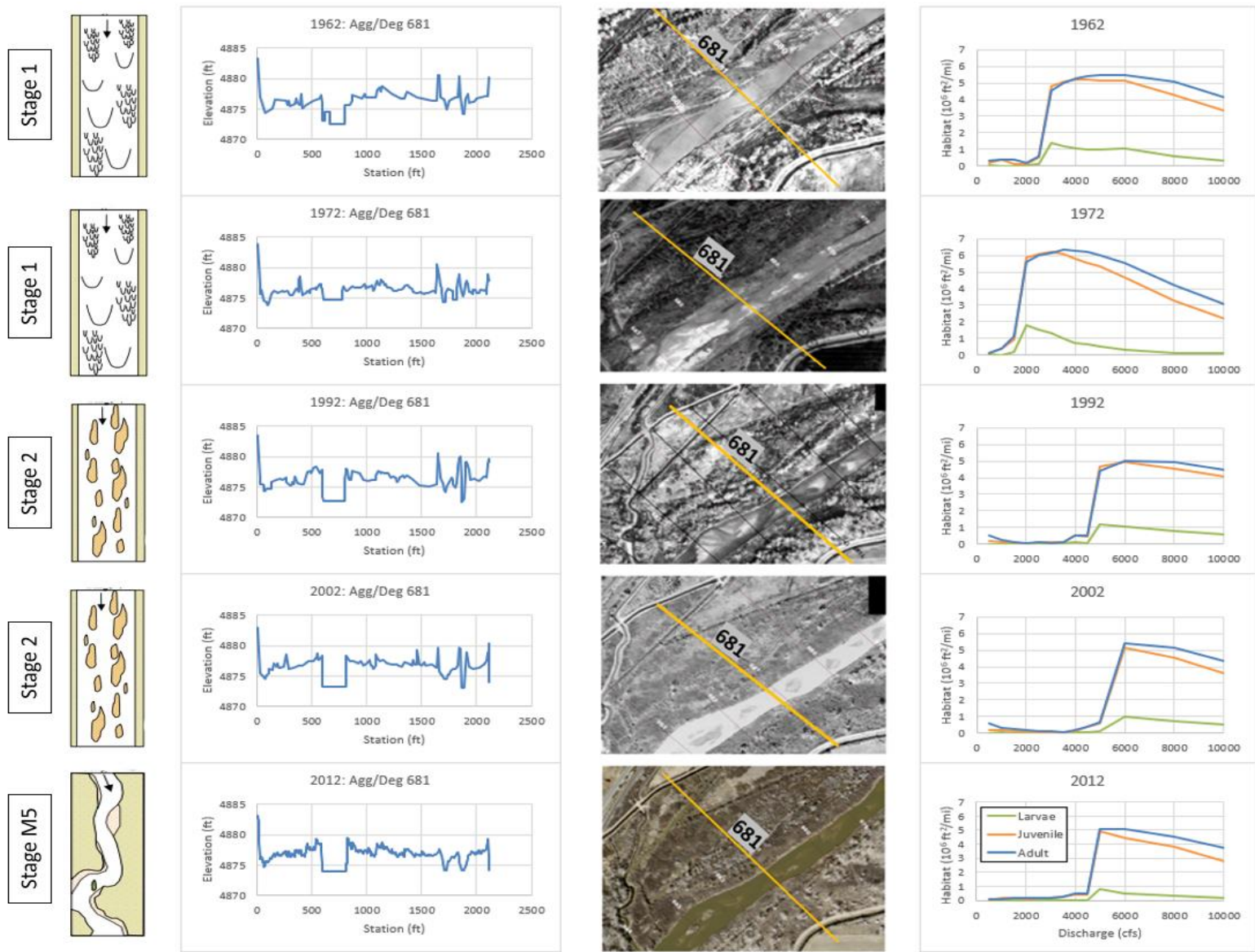


Figure 25 Geomorphic evolution in subreach II at agg/deg line 681

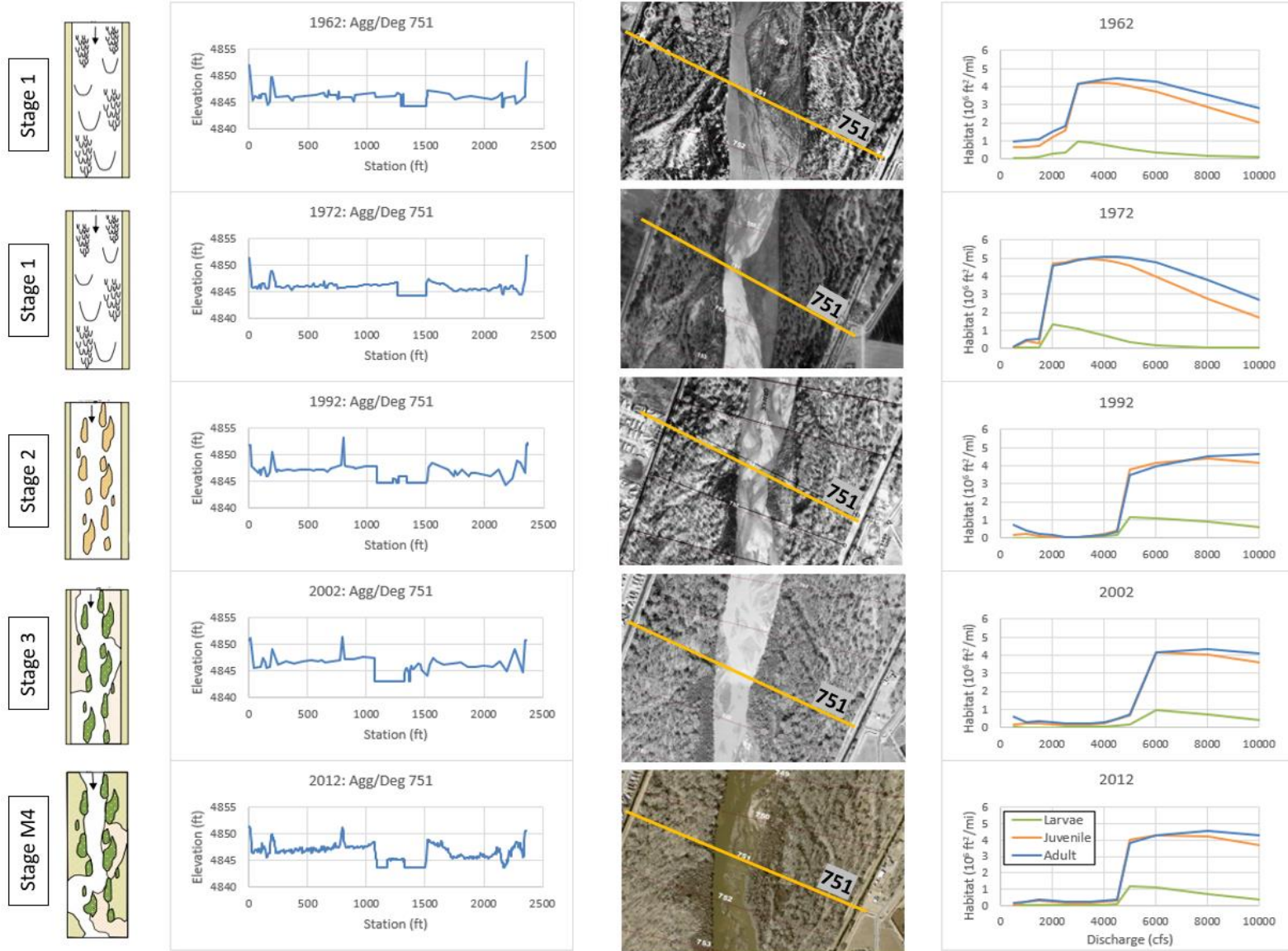


Figure 26 Geomorphic evolution in subreach I2 at agg/deg line 751

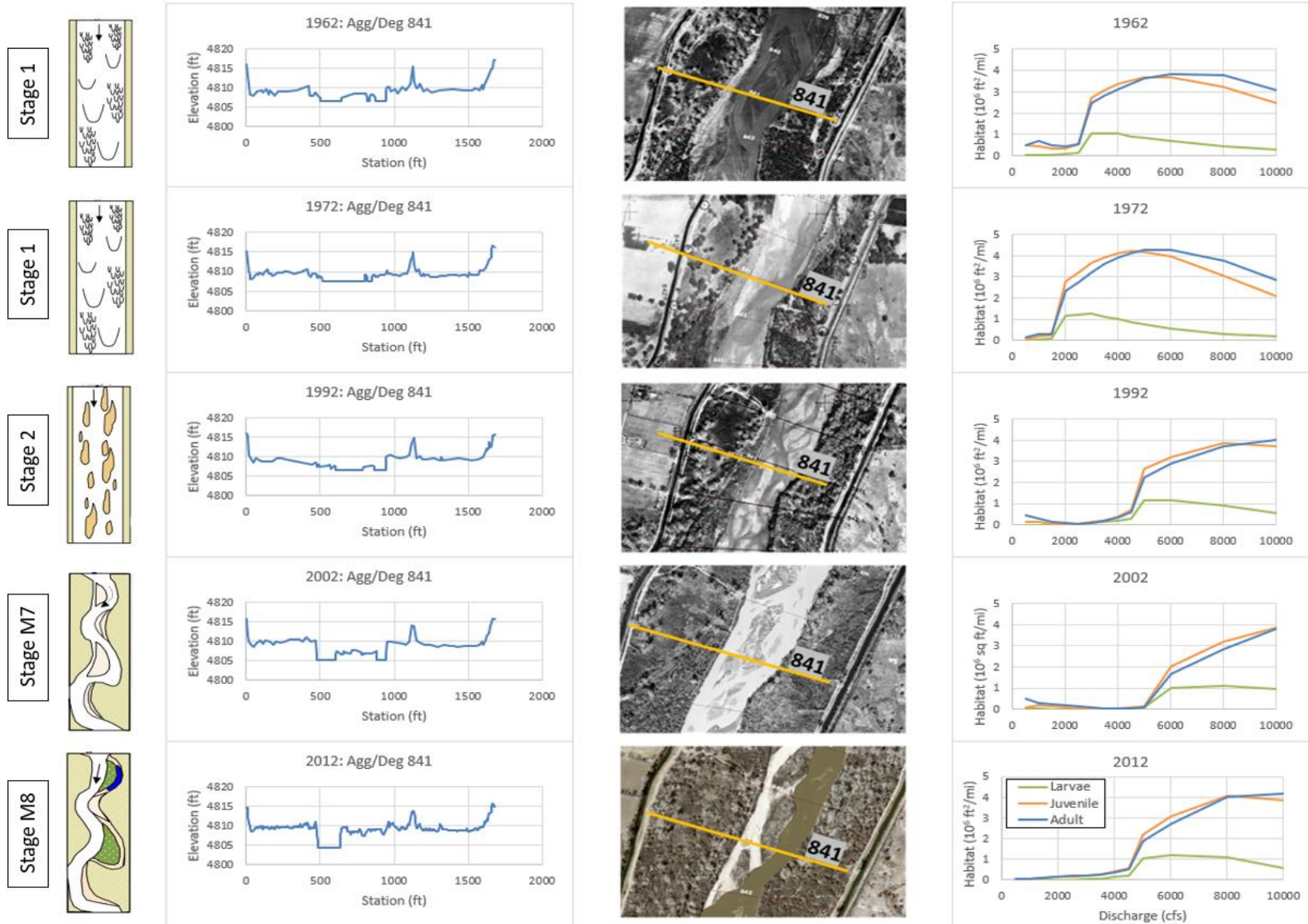


Figure 27 Geomorphic evolution in subreach I3 at agg/deg line 841.

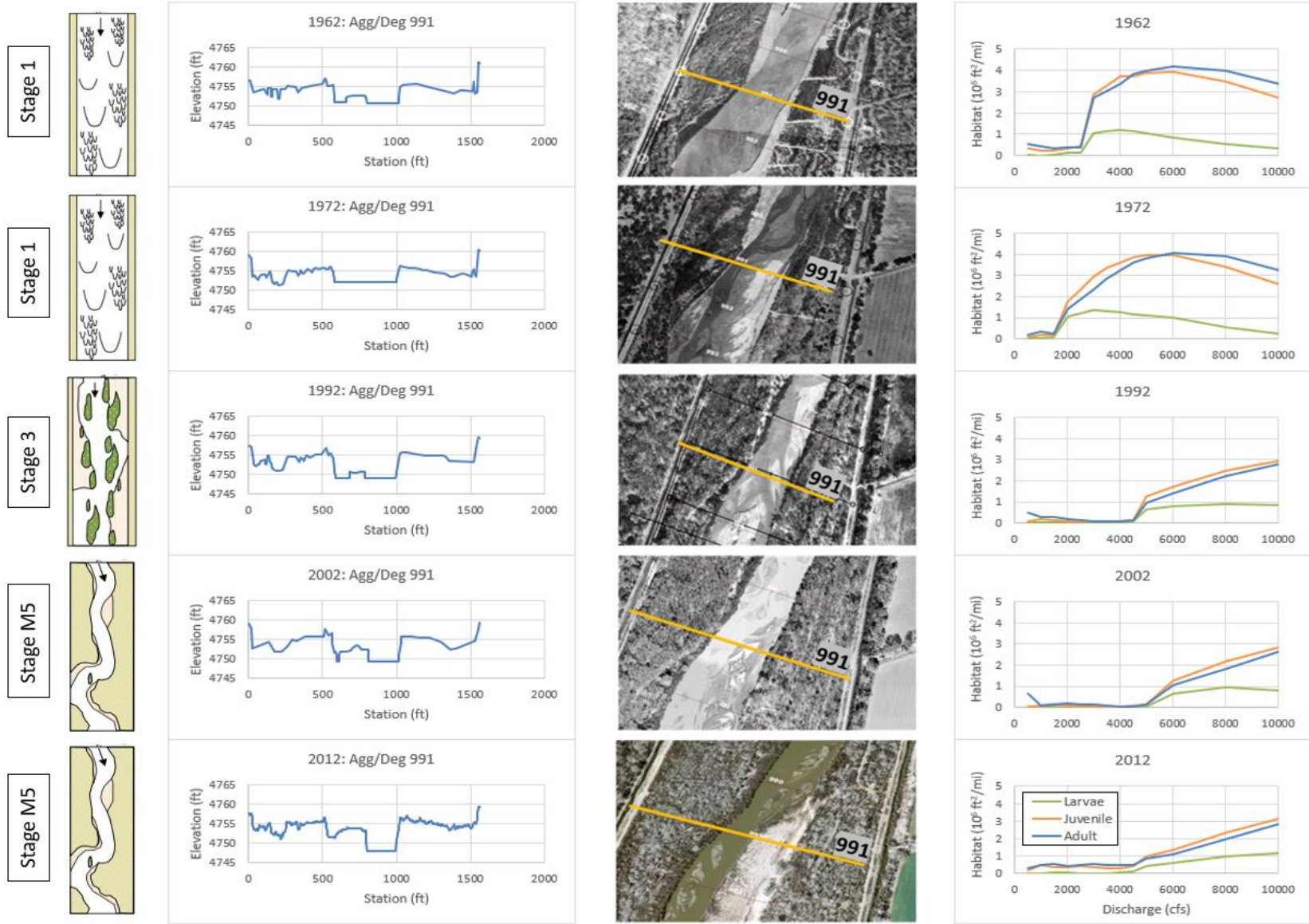


Figure 28 Geomorphic evolution in subreach I4 at agg/deg line 991

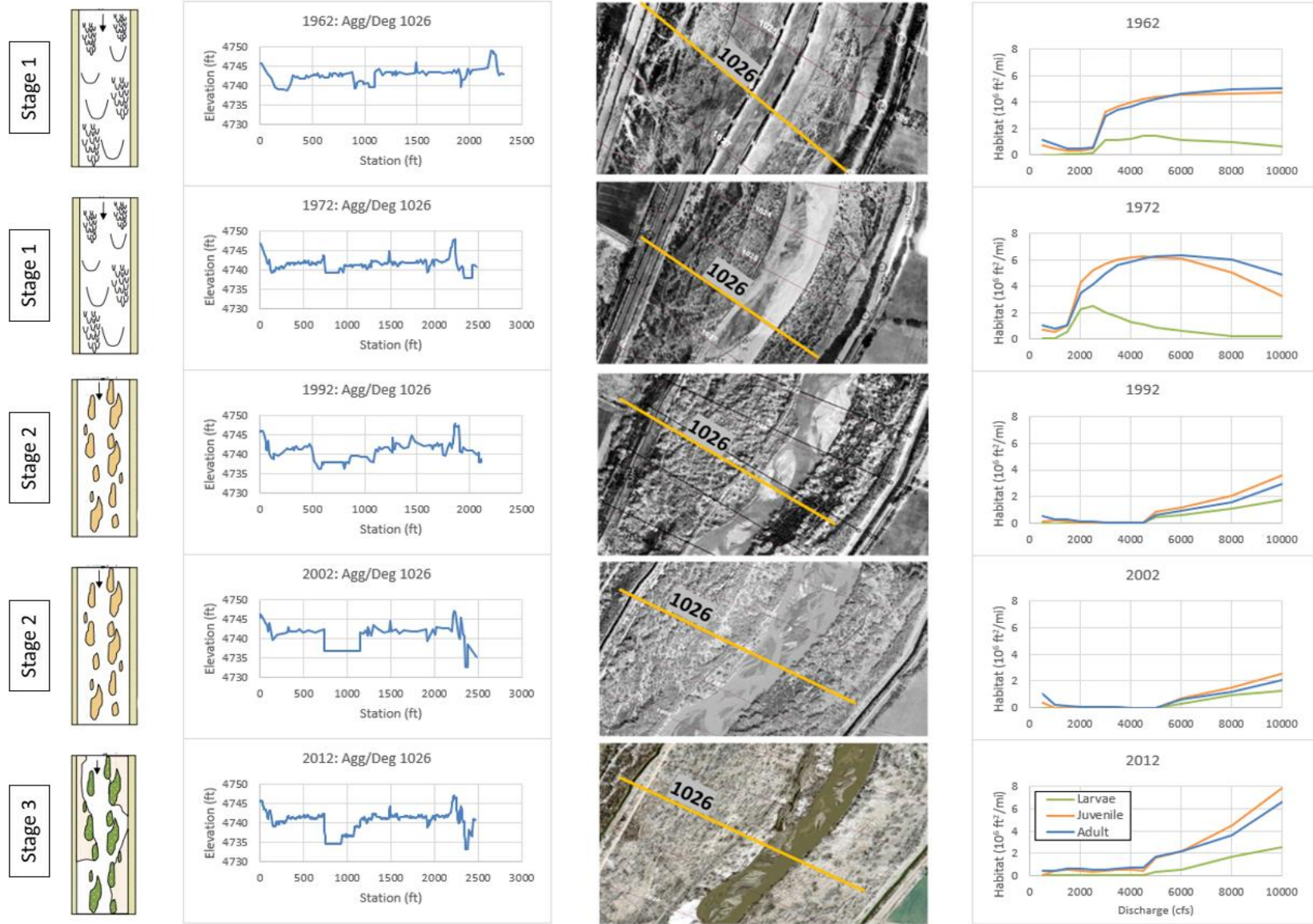


Figure 29 Geomorphic evolution in subreach I5 at agg/deg line 1026

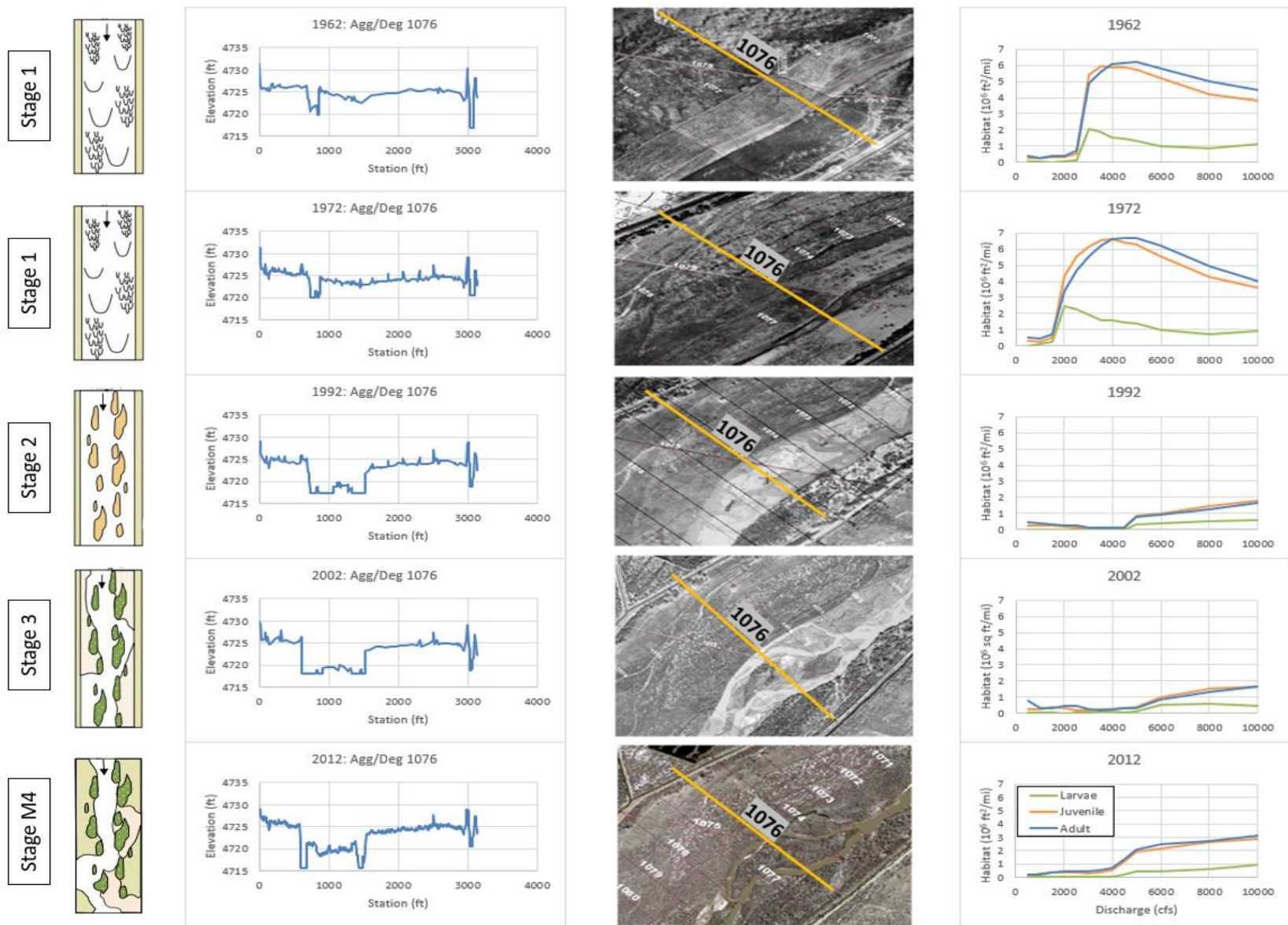


Figure 30 Geomorphic evolution in subreach I6 at agg/deg line 1076

## 6.2 Geomorphic Classification Based on the Planform Evolution Model

Each subreach in Isleta was assigned a geomorphic stage classification from 1962 to 2012, as seen in Table 8, using the PEM developed by Massong et al. (2010). Earlier years (1962, 1972, and 1992) showed stage 1 and 2 patterns. More recent years (2002 and 2012) showed a shift towards stage 3 and migrating stages, M4-M8.

*Table 8 Geomorphic classification by subreach based on the planform evolution model by Massong et al. (2010)*

Subreach	PEM Stage Classification				
	1962	1972	1992	2002	2012
I1	1	1	2	2	M5
I2	1	1	2	3	M4
I3	1	1	2	M7	M8
I4	1	1	3	M5	M5
I5	1	1	2	2	3
I6	1	1	2	3	M4

Typical patterns seen in the Isleta reach are shown in Figure 31. Stages 1 and 2 tend to have “rounded” habitat curves, while other stages tend to have “step” or “hook” habitat curves. Stage 1 patterns, seen in subreach I3 in 1972, tend to be wide, shallow, and braided. The shallow channel allowed water to overtop the banks and fill the floodplains at much lower discharges (~ 2,000-3,000 cfs). Recently, much of Isleta has shown a trend toward channel incision, causing the bankfull discharge to greatly increase (~ 5,000 cfs in 2012). This explains why habitat availability spiked much sooner in the earlier years than in more recent years. At a certain point, habitat availability will begin to “round down” as velocity and depth exceed the criteria for each of the RGSM’s life stages.

Stage 3 patterns, seen in subreach I2 in 2002, tend to be rather incised with evidence of vegetation encroachment onto islands and bars. Because the channel is incised, little habitat is

seen at lower discharges. At higher discharges, habitat availability does not rapidly decrease as in stage 1 patterns. It's possible that the presence of more vegetation on the floodplain reduces the flow velocity enough to maintain more area of suitable habitat for the RGSM.

Stage M5 patterns, seen in subreach I4 in 2012, can be a final stage and often show signs of channel incision and narrowing. Again, bankfull discharge is higher in the migrating stages, which is why little habitat availability is seen at low discharges. The “hook” in habitat availability at higher discharges is likely attributed to flow depth and velocity remaining shallow or slow enough on the floodplain for all life stages. Further explanation of the habitat curve patterns was discussed in section 5.2.2 Results: Habitat Curves and Spatial Habitat Charts.

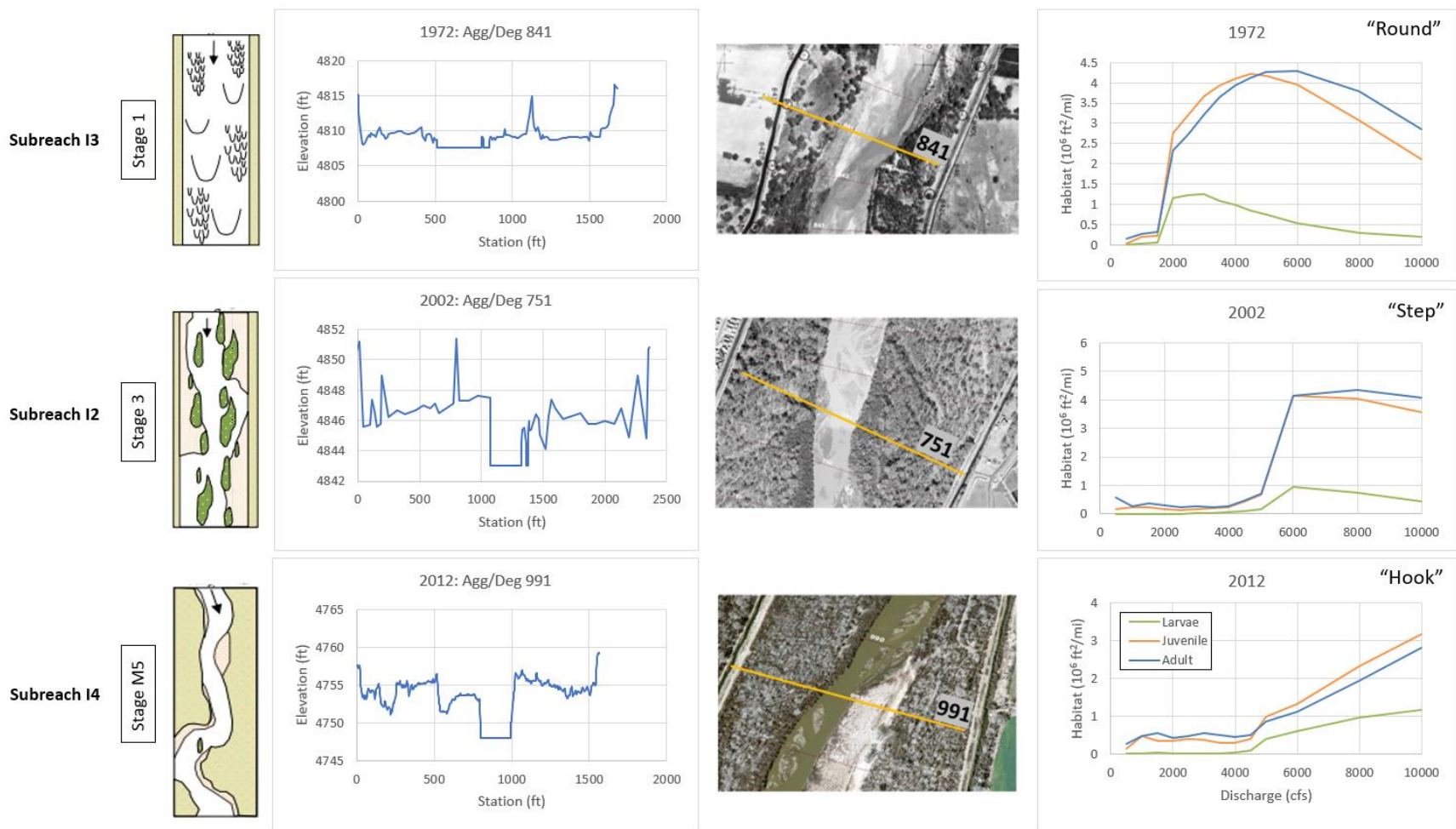


Figure 31 Typical patterns seen in the Isleta reach

### 6.3 Geomorphic Classification Based on the Stream Evolution Model

River form from 1962 to 2012 was further classified using the SEM developed by Cluer and Thorne (2013). A summary of these classifications can be found in Table 9. The SEM was also related to the PEM by Massong et al. (2010).

*Table 9 Geomorphic stage classifications based on Cluer and Thorne’s (2013) stream evolution model*

Subreach	SEM Stage Classification				
	1962	1972	1992	2002	2012
I1	1	1	2	2	3
I2	1	1	2	2	3
I3	1	1	2	3	3
I4	1	1	2	3	3
I5	1	1	2	2	3
I6	1	1	2	2	3

Earlier years (1962 and 1972) showed stage 1 patterns. A stage 1 pattern refers to a stable, single-thread channel with evidence of bedforms and bars (Cluer and Thorne, 2013). This stage most likely corresponds to stage 1 of the PEM. More recent years (1992, 2002, and 2012) showed stage 2 and 3 patterns. Stage 2 represents the effects of channelization efforts. Some bedforms and bars remain, while functionality and connectivity of the floodplain and riparian zone are diminished. Additionally, stage 2 channels have a “high in-channel discharge capacity” (Cluer and Thorne, 2013). This agrees well with the results found in section 5.1 Bankfull Discharge. This stage of the SEM most closely resembles stages 2 and 3 of the PEM. Stage 3 patterns indicate incision and a disconnect with the floodplain. Functionality of the riparian zone is reduced due to a disconnect from the main channel (Cluer and Thorne, 2013). This stage is most like the migrating stages of the PEM.

While difficult to determine visually, some stage 3 classifications could be in stage 3s. Stage 3s refers to a channel that has an erosion-resistant layer that stabilizes and maintains the

incised channel banks. Rivers in this stage typically get stuck and do not progress to other stages (Cluer and Thorne, 2013). Figure 32 shows an example of cross-sectional geometry and aerial photographs associated with the SEM stage classifications in subreach I5.

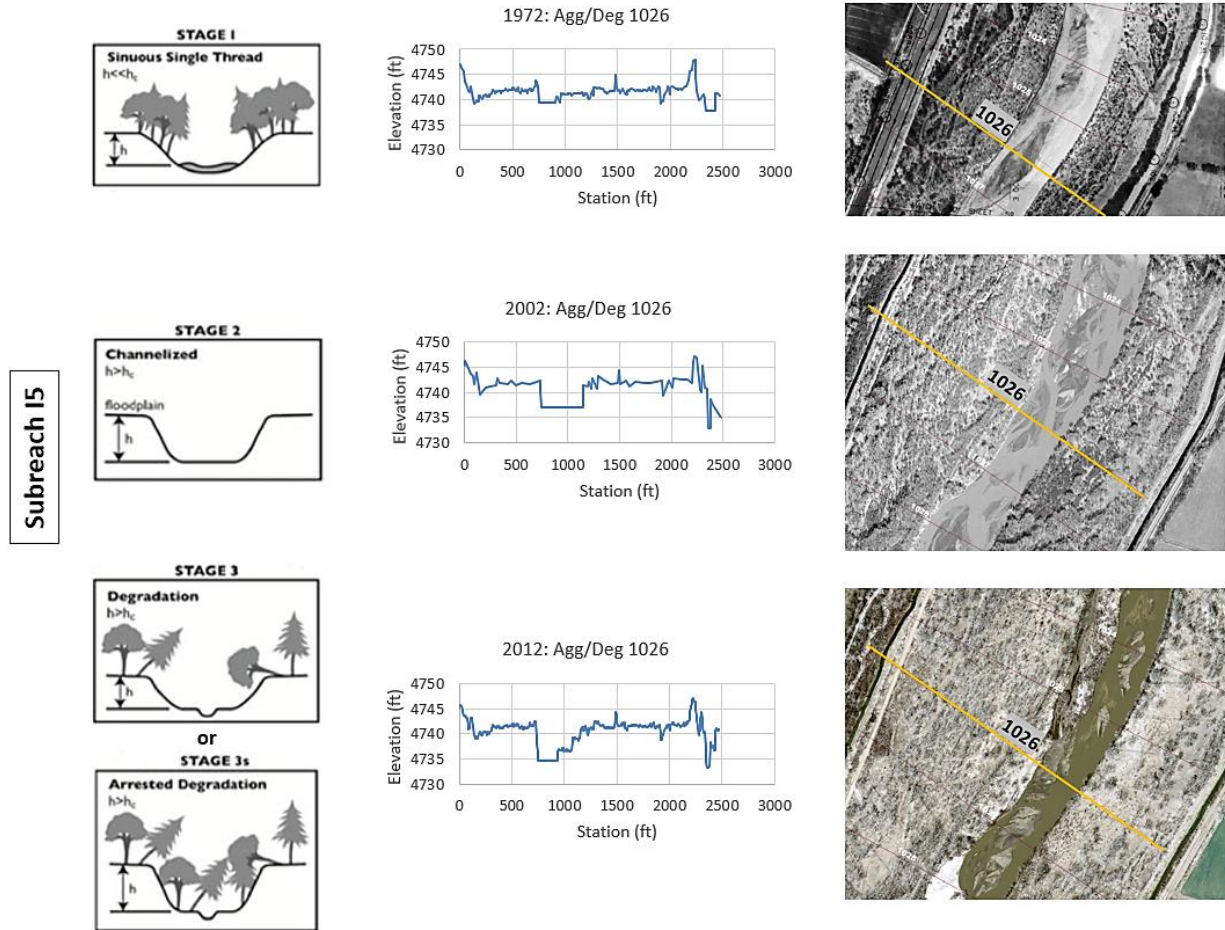
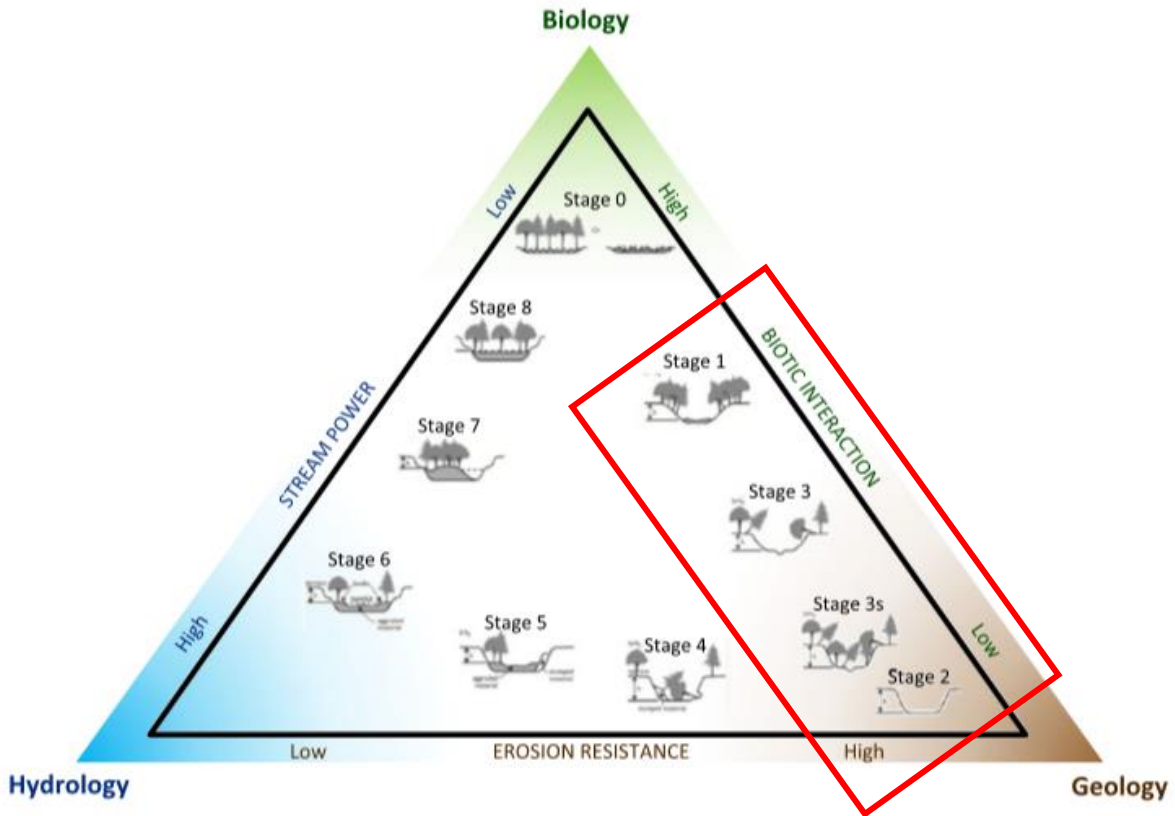


Figure 32 Example of SEM stage classifications applied to subreach I5

### 6.4 Primary Drivers

The primary drivers in the Isleta reach were determined using the SEM stage classifications for each subreach and plotting them on Castro and Thorne’s (2019) SET. All subreaches plot on the right side of the triangle, seen in Figure 33, suggesting that the primary drivers present from 1962 to 2012 were biology and geology. The use of dams and diversion

channels in the Isleta reach likely shifted the primary drivers away from the hydrology corner of the triangle (Castro and Thorne, 2019).



*Figure 33 Stream evolution triangle highlighting the primary drivers in the Isleta reach*

In 1962 and 1972, biotic interaction was higher than geologic influence. A stage 1 classification provides a good amount of habitat and is connected to the floodplain (Thorp et al., 2010). This finding pairs well with the habitat curves for 1962 and 1972, which show a large amount of habitat availability and the ability for water to reach the floodplains at lower discharges.

In 1992 and 2002, except for subreach I3 and I4, the primary driver shifted to the geology corner of the triangle, indicating high erosive resistance. The high erosive resistance comes from

channelization efforts, forcing the river to act as though it were in “geological confinement.” Geologically controlled rivers are often resilient to morphological change, even when a large flood occurs. Because of the disturbance created by channelization efforts, native species are not given adequate time to adapt, resulting in decreases to diversity. Additionally, channel uniformity eliminates most habitat (Cluer and Thorne, 2013). This agrees with the habitat curves in 1992 and 2002 for subreaches I4 to I6, which show low habitat availability for all discharges. Stage 2 channels are likely to aggrade, degrade or shift laterally (Cluer and Thorne, 2013), which may explain why there was a shift away from the geology corner in 2012.

In 2012, the primary drivers were biology and geology, with geologic influence being slightly higher than biologic interaction. Degradation in stage 3 channels results in loss of features in the main channel that provide habitat and causes a disconnect between the floodplain and the main channel. Additionally, any remaining habitat and ecosystem benefits are easily affected by disturbances resulting from changes to flow and sediment regimes (Cluer and Thorne, 2013). Since stage 3 channels are influenced by multiple drivers, it is likely that in 2012 and beyond, the river’s morphology will constantly adjust to changes in influences or after a major disturbance (Castro and Thorne, 2019).

## Chapter 7: Time-Integrated Habitat Metrics

### 7.1 Methods

Time-Integrated Habitat Metrics (TIHMs), developed by Doidge et al. (2020), is an interpolation method that determines cumulative habitat between 1992 and 2019 based on known habitat curves (1992, 2002, and 2012) and daily discharge data for the reach. Discharge data were obtained for each water year, typically from October 1 to September 30, from the Rio Grande at Isleta Lakes Nr Isleta, NM (08330875), Rio Grande at State HWY 346 Near Bosque, NM (08331510) and the Rio Grande Floodway Near Bernardo (08332010) gages. Discharge data were obtained for the Isleta Lakes gage from 2005 to 2006, for the HWY 346 gage from 2007 to 2011, and for the Bernardo gage from 1992 to 2004 and 2012 to 2019. Discharge data from multiple gages were necessary to form a complete record from 1992 to 2019.

Figure 34 shows an example hydrograph created for the Bernardo gage separated by representative sampling months for each of the RGSM's life stages. The representative sampling period is May to June for the larval stage, July to September for the juvenile stage, and October to April for the adult stage. Results were separated by sampling periods to allow correlations to be made with fish population monitoring data. Fish population density was estimated using October sampling data when fish are in the adult stage. Habitat curves for each year are determined and imported to the program along with the gage discharge data.

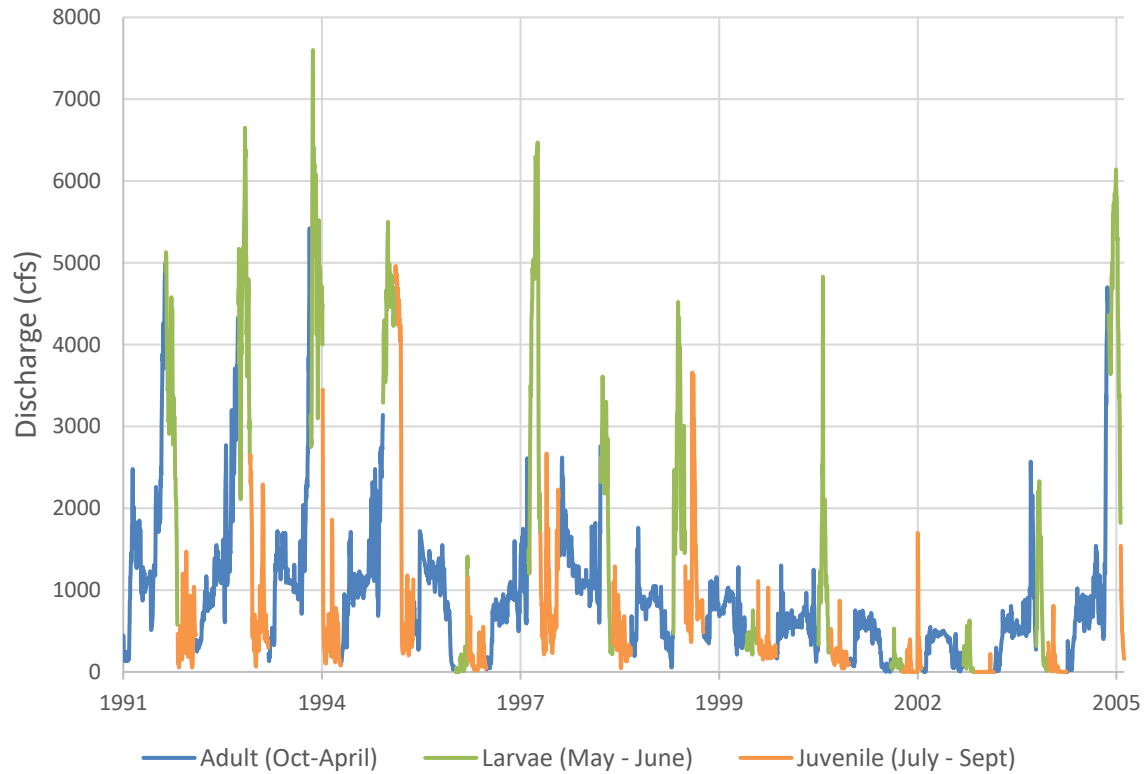


*Figure 34 Example hydrograph for the Bernardo gage (08332010) from 1992 to 2005. The hydrograph is colored to show representative sampling periods for each of the RGSM's life stages*

The following equation was used to compute the cumulative habitat metrics for each year:

$$TIHM = \sum_{i=1}^t A_i \Delta t \quad (1)$$

Where  $t$  is the total number of days over the sampling period for each of the RGSM's life stages in a given water year,  $\Delta t$  is the daily time step, and  $A_i$  is the daily habitat area per mile of river for larvae, juveniles, and adults. A simple linear equation was determined for each flow profile and used to compute  $A_i$ . The general linear equation is as follows:

$$A_i = mQ_i + b \quad (2)$$

Where  $m$  is the slope between adjacent flow profiles,  $Q_i$  is the daily discharge, and  $b$  is the intercept of the line.  $m$  is calculated as habitat area (from the input habitat curves) divided by the discharge between two points and  $b$  is solved for algebraically. This results in different  $m$  and  $b$  values for each flow profile. Daily habitat area is then calculated using the linear equation for the flow profile that most closely matches the input discharge data for that day. Figure 35 shows an example of interpolated daily larval habitat values for discharges between 4,000 and 4,500 cfs. Notice that many of the daily habitat values fall close to the line (i.e. the input habitat curve) and fall between the known habitat values at 4,000 and 4,500 cfs. Using equation (1), daily habitat was summed over the respective sampling period, resulting in habitat metrics with units of ft<sup>2</sup> day/mile. For further insight into the TIHMs program refer to Appendix C: Time Integrated Habitat Metrics Program.

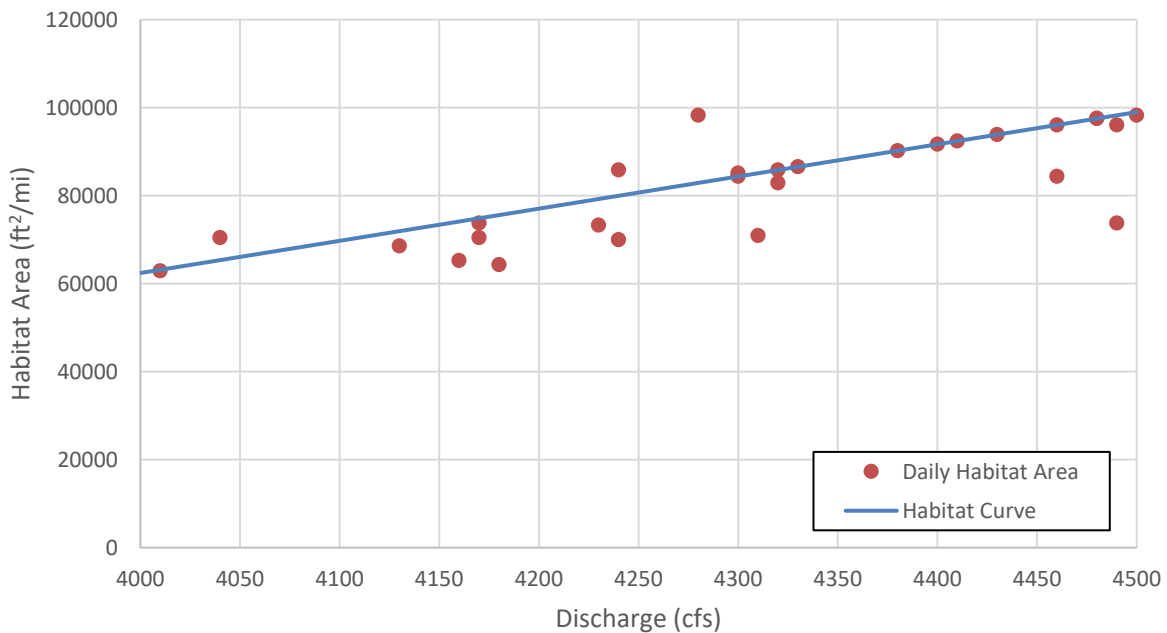


Figure 35 Interpolation of daily larval habitat area between 4,000 and 4,500 cfs in 1995

### 7.1.1 Temporal Interpolation of Habitat Curves

The annual RGSM habitat curves were developed using a temporal interpolation method, which allowed for interpolation between the known years to get a habitat curve for every year between 1992 and 2019. Cross-sectional geometry data, which are necessary for generating habitat curves, were available for 1962, 1972, 1992, 2002, and 2012. However, fish sampling data began in 1993 so the temporal interpolation starts with the 1992 data. To estimate the habitat for the unknown years, the habitat curves were interpolated temporally using a single mass curve, which helps to identify major changes in sediment transport, thus indicating greater changes to the cross-section geometry. Figure 36 shows the single mass curve from 1992 to 2002 that was created using sediment discharge data from the Rio Grande at Albuquerque gage (08330000). This gage was chosen because it has a complete sediment discharge record from 1992 to 2012.

The interpolation method uses a variable " $\alpha$ " which represents the fraction of cumulative sediment transport at a given year relative to the cumulative sediment transport of the time interval. The single mass curve was divided into decadal time periods determined by the available cross-section data (1992-2002, 2002-2012). The cumulative sediment at the end of the time period marks the max cumulative amount of sediment in that time period. The sediment discharge at any point can be divided by the max, which results in the term ( $\alpha$ ). The habitat curves for the years in between were interpolated by taking a fraction of the habitat from the earlier year ( $1-\alpha$ ) plus a fraction of the habitat curve from the later year ( $\alpha$ ). An example of this method for larval habitat in 1995 can be seen in Figure 37.

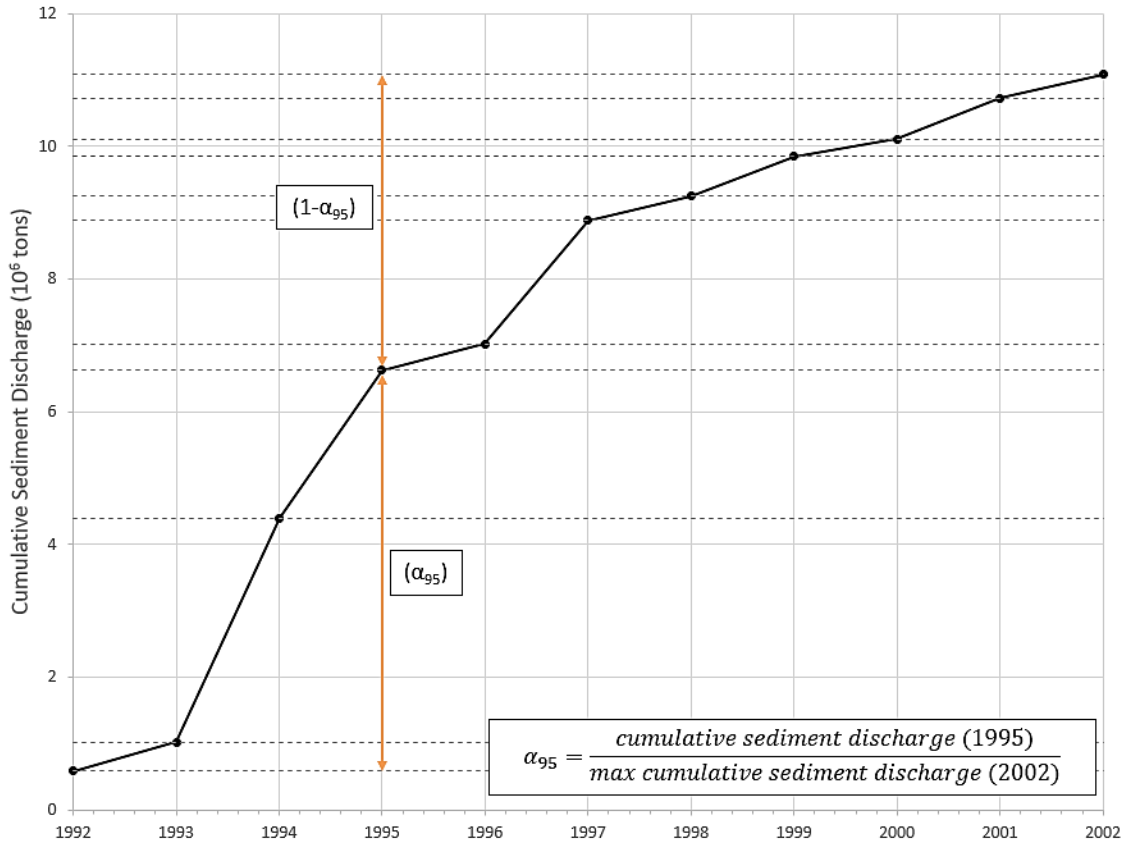


Figure 36 Single mass curve for the Albuquerque gage (08330000) from 1992 to 2002

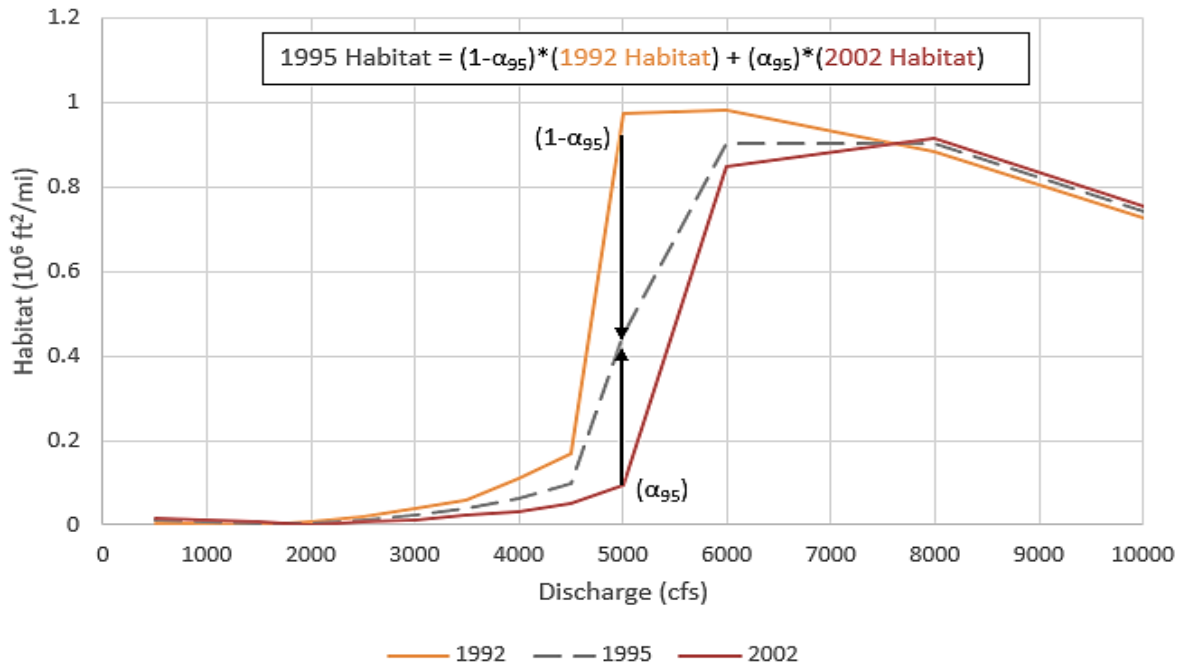


Figure 37 Example of temporal interpolation for the 1995 larval habitat curve

## 7.2 Results

Figure 38 shows the cumulative habitat results from the TIHMs for larvae, juveniles, and adults over their representative sampling months for each water year. Overall, adult habitat metrics remain fairly constant from 1992 to 2019, ranging from 18 to 132 million ft<sup>2</sup> day/mi. Larvae and juvenile habitat metrics are more sensitive to changes in discharge, evident by the fluctuations seen from year to year. This is likely because spring and summer months tend to have more variable discharges than in fall and winter. Juvenile habitat metrics range from approximately 0.016 to 24 million ft<sup>2</sup> day/mi, while larval habitat metrics range from 0.012 to 30 million ft<sup>2</sup> day/mi. Note that cumulative habitat in 2005 and 2006 may be overestimated as the USGS gage used for these years is located behind the Isleta Diversion dam where discharges can be higher. Lastly, even though the fish population density data are for the adult stage, it appears that the larvae and juvenile habitat metrics follow the trend in the population data best.

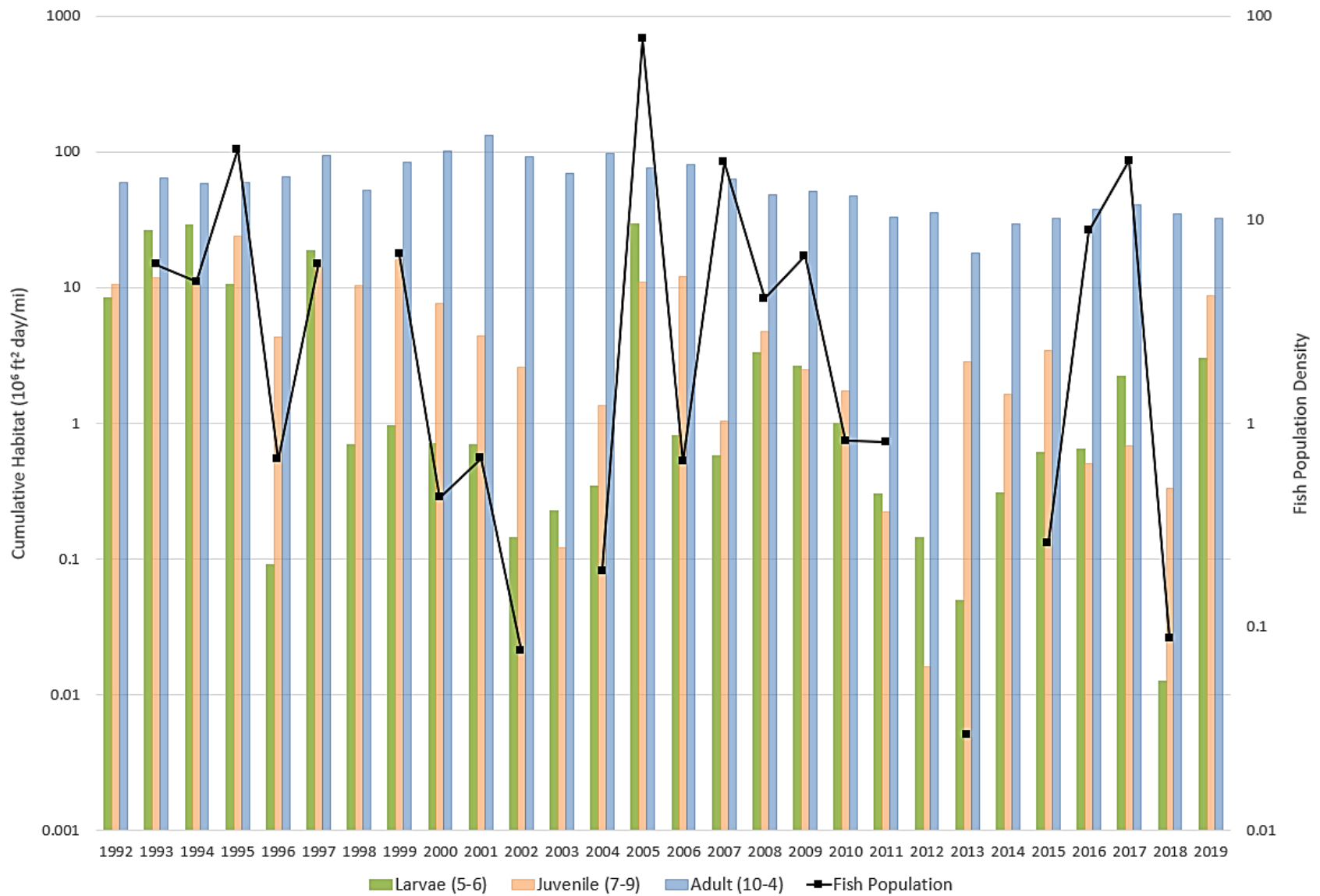


Figure 38 Cumulative habitat for larvae, juveniles, and adults over their respective sampling periods

### 7.2.1 Ecological Relationships

Correlations between the habitat metrics, mean daily discharge, and the RGSM population monitoring data were performed by Mortenson et al. (2020) using vigorous statistical techniques. This involved the computation of occurrence probability ( $\delta$ ) and simulated lognormal density ( $\mu$ ). Occurrence probabilities typically range from zero to one with zero indicating an absence of fish and one indicating the presence of fish at a monitoring site. Both the habitat metrics and mean discharge were based on the representative sampling period for each of the RGSM's life stages. Figure 39 and Figure 40 show the results of this analysis, with the red dot indicating the most recent water year (2019).

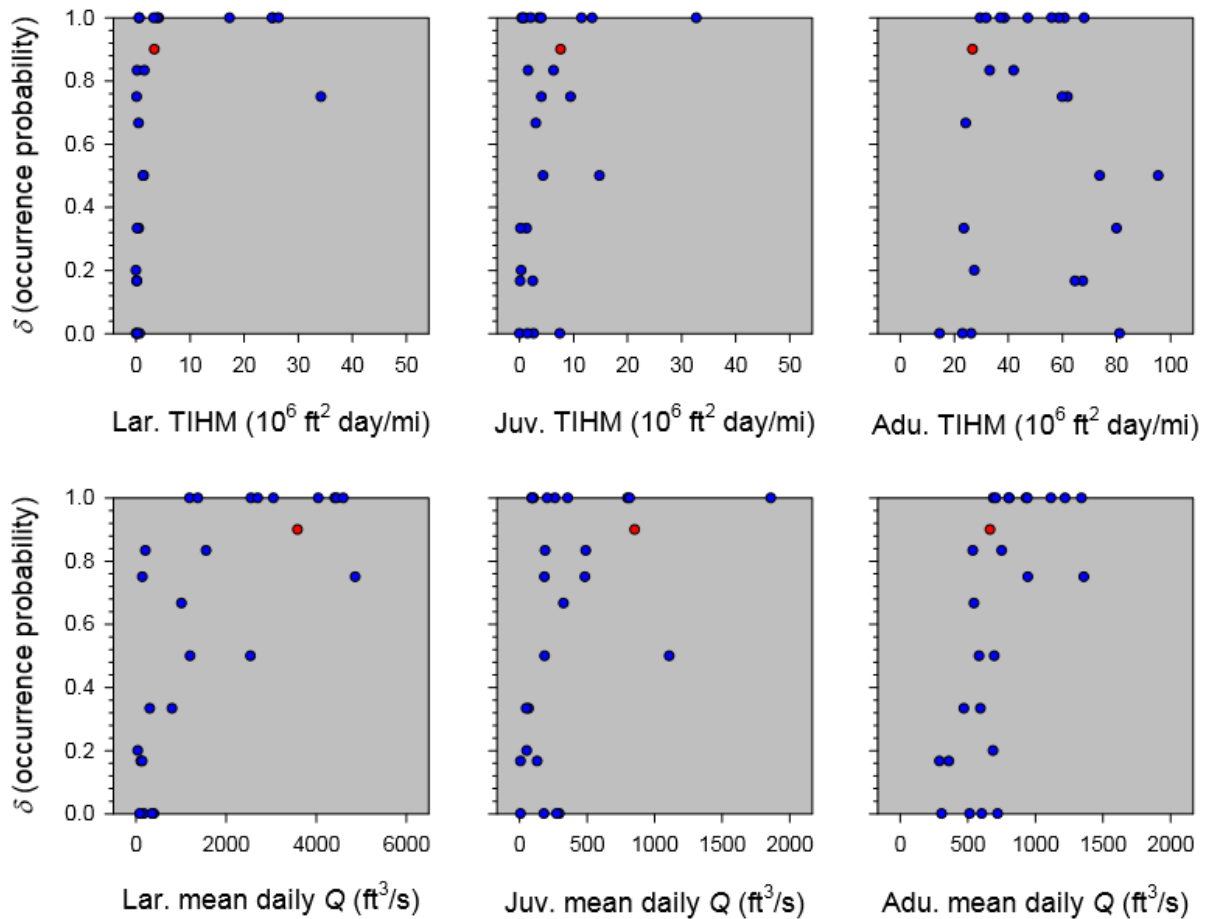


Figure 39 RGSM occurrence probabilities from Mortenson et al. (2020) for the time period 1992 to 2019

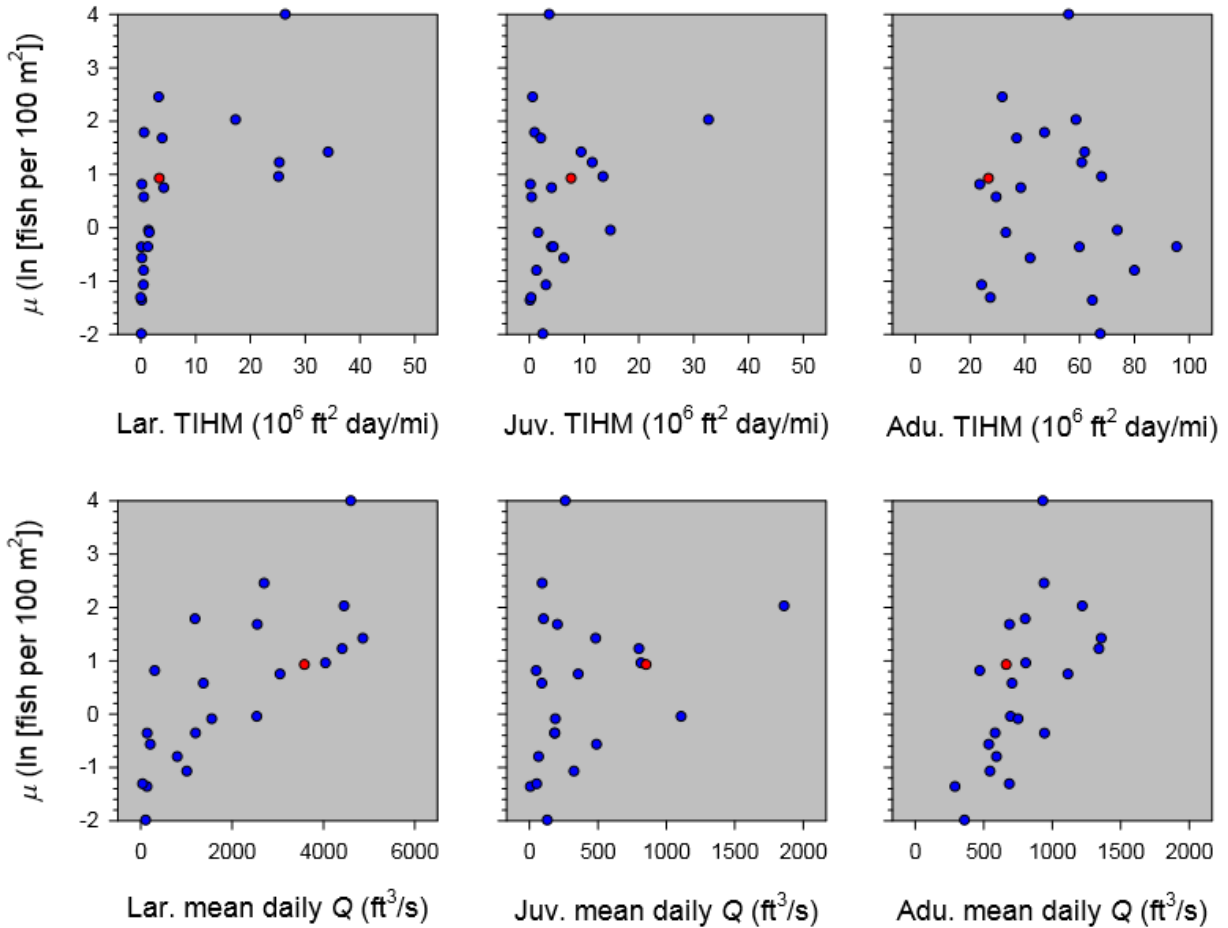


Figure 40 RGSM lognormal densities from Mortenson et al. (2020) for the time period 1992 to 2019

The main finding from Figure 39 and Figure 40 is that larvae are strong predictors of population dynamics. Larval occurrence and density increase with an increase in mean daily discharge. This finding agrees with what biologists at the University of New Mexico have observed over the past couple of decades: that more RGSM are present during spring flows (i.e. when more frequent higher flows occur) (Dudley et al., 2020). In addition, higher habitat metrics correspond with a higher occurrence probability of larval fish. This finding makes sense because more fish should be present in an area with more available habitat. Lastly, we see this same relationship with population density. An increase in habitat metrics is related to an increase in larval fish density. However, note that many of the data points in the top left plot of Figure 40

are clustered to the left side, near very low habitat metrics. This may be a result of the TIHMs not being able to properly capture spatial and temporal changes in floodplain inundation (Mortenson et al., 2020). In contrast, juvenile and adult correlations with the habitat metrics and mean daily discharge were not as predictive of increases in density and occurrence over the reach. This finding further emphasizes the importance of elevated spring flows for larval fish. Overall, the discharge relationships prove to be stronger, capturing more variance around the population monitoring data than the habitat metrics.

## **Chapter 8: Habitat Mapping**

### **8.1 Methods: RAS-Mapper**

RAS-Mapper is a function of HEC-RAS that can be used to overlay one-dimensional results onto an imported terrain, thus creating pseudo two-dimensional (2-D) results as a map. A terrain for the Isleta reach was made using LiDAR mass points data obtained in 2012 to create a digital elevation model. Importing the terrain into RAS-Mapper allows HEC-RAS to determine how water will be distributed over the terrain and the Isleta reach.

Using the steady flow data from HEC-RAS, RAS-Mapper was used to calculate depth and velocity over the Isleta terrain for thirteen flow profiles (same as those used in the Flow Distribution method). As a result, rasters are generated that can be used to map habitat availability for each of the RGSM's life stages throughout the reach. Version 10.6 of ArcMap (Environmental Systems Research Institute, Inc., 2020) has a function called ModelBuilder, which allowed for the creation of a model that uses the depth and velocity rasters from RAS-Mapper to assign values to thousands of small polygons over the entire reach. This results in a 10-foot resolution grid for which attributes can be filtered to display cells of hydraulically suitable habitat. This is accomplished by specifying the velocity and depth criteria for each of the Silvery Minnow's life stages. Discharges of 1,500, 3,000, and 5,000 cfs were selected for mapping. Aerial imagery aids in showing where RGSM habitat conditions are met.

### **8.2 Results/Discussion**

Maps showing hydraulically suitable habitat for larvae, juveniles, and adults in subreaches I1 to I3 are seen in Figure 41 through Figure 46. Note that the direction of flow is from north to south and inundated area refers to habitat that is unsuitable for all life stages. In

addition, maps at 1,500 and 3,000 cfs display water on the floodplain that shouldn't exist. This is likely an error in RAS-Mapper and will be further discussed in Chapter 9.

Subreaches I1 to I3 showed the most available habitat for all life stages at all three discharges. Focusing on the main channel in the 1,500 and 3,000 cfs maps, juvenile and adult habitat appears to be more abundant than larvae habitat. This result is expected as larvae require shallow, low velocity areas that are most often found on the floodplain. At 5,000 cfs, habitat availability for all life stages greatly increases as the floodplains become inundated. Notice that juvenile and adult habitat that was present in the main channel at lower discharges has disappeared because depth and velocity has exceeded the suitable criteria. While these subreaches show the most amount of habitat, much of the available habitat at 5,000 cfs is disconnected and far away from the main channel. Overall, higher discharges (i.e. 5,000 cfs) provide the most habitat for all life stages. Maps for the remaining subreaches can be found in Appendix A: Additional Habitat Availability Maps.

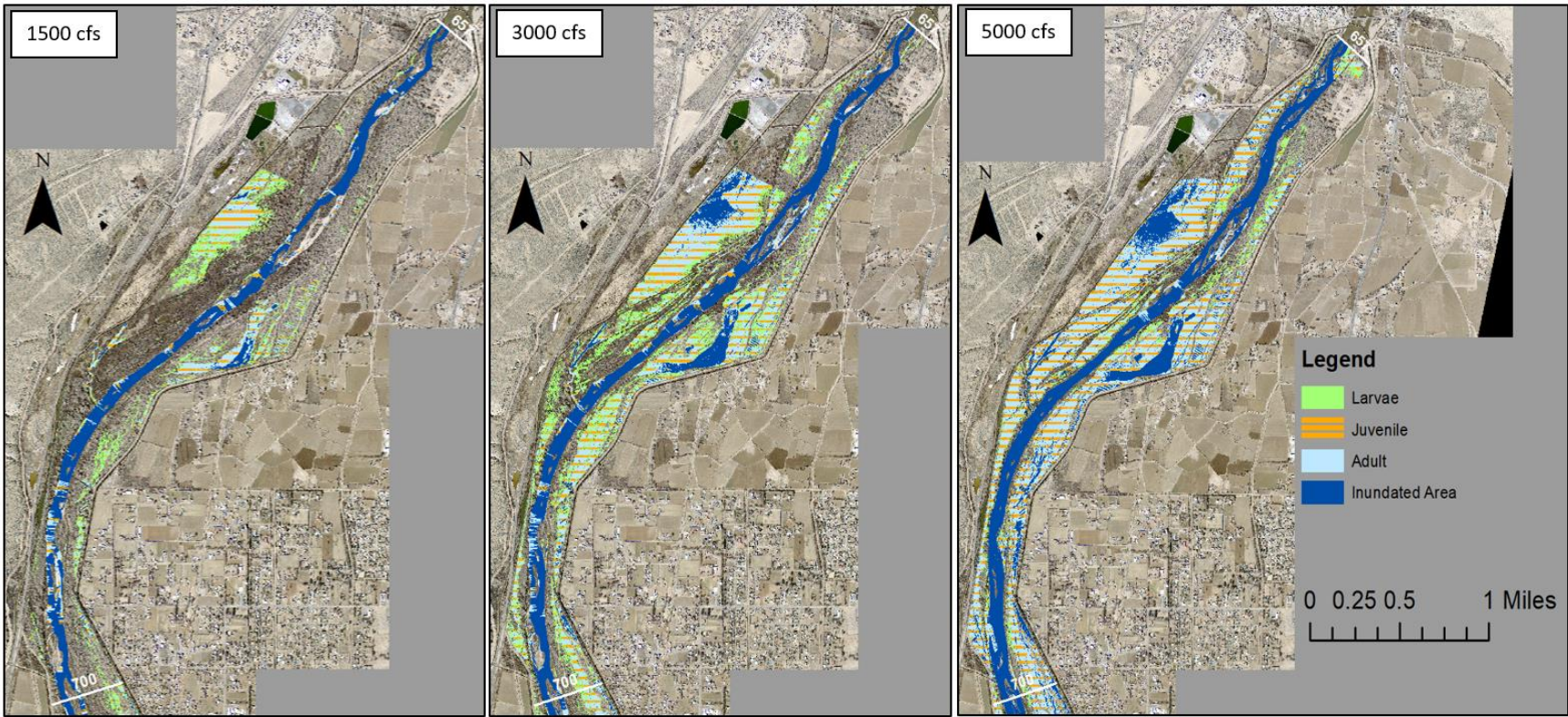


Figure 41 Life stage habitat availability maps for subreach II

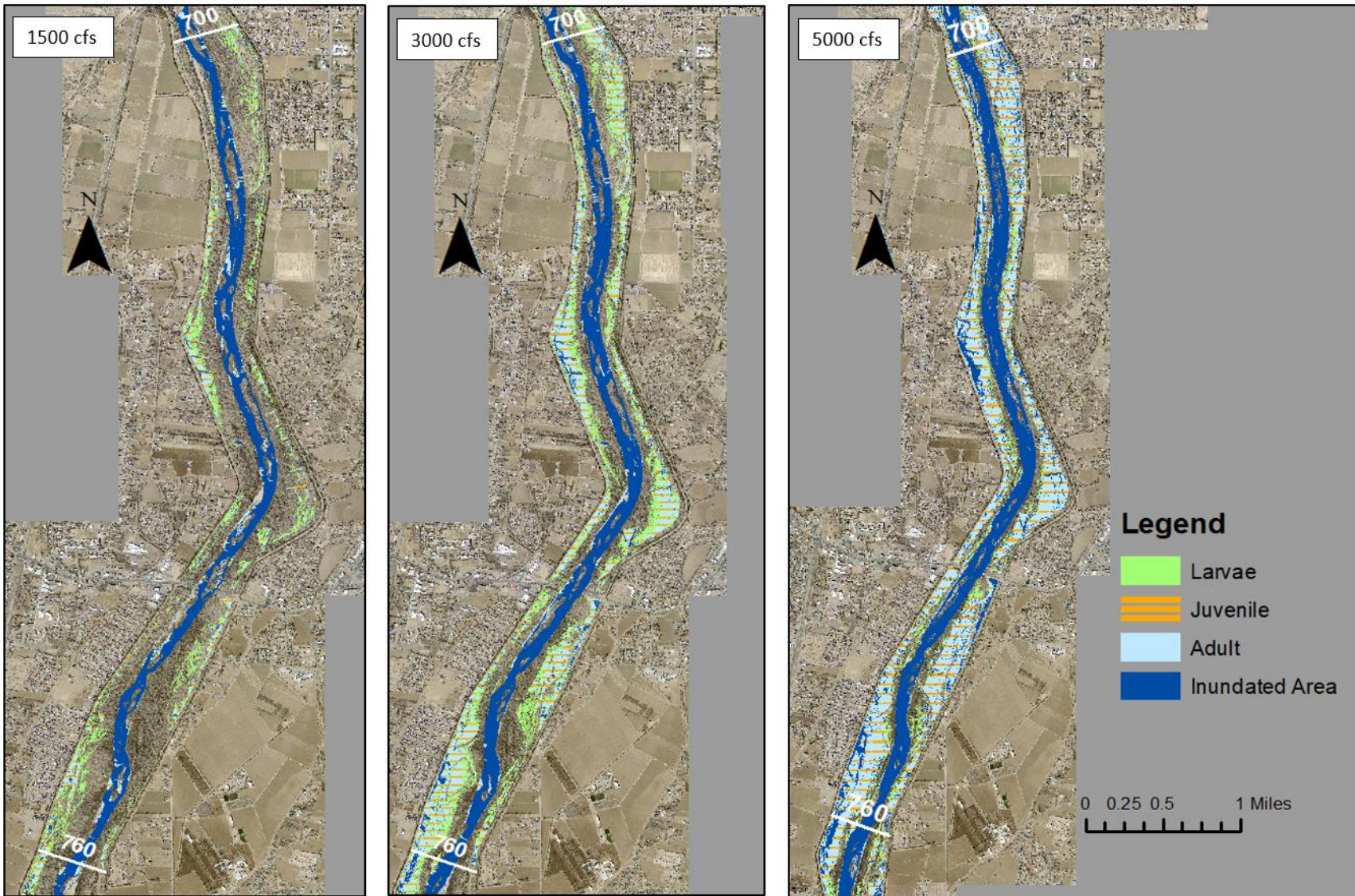


Figure 42 Life stage habitat availability maps for subreach I2(a)

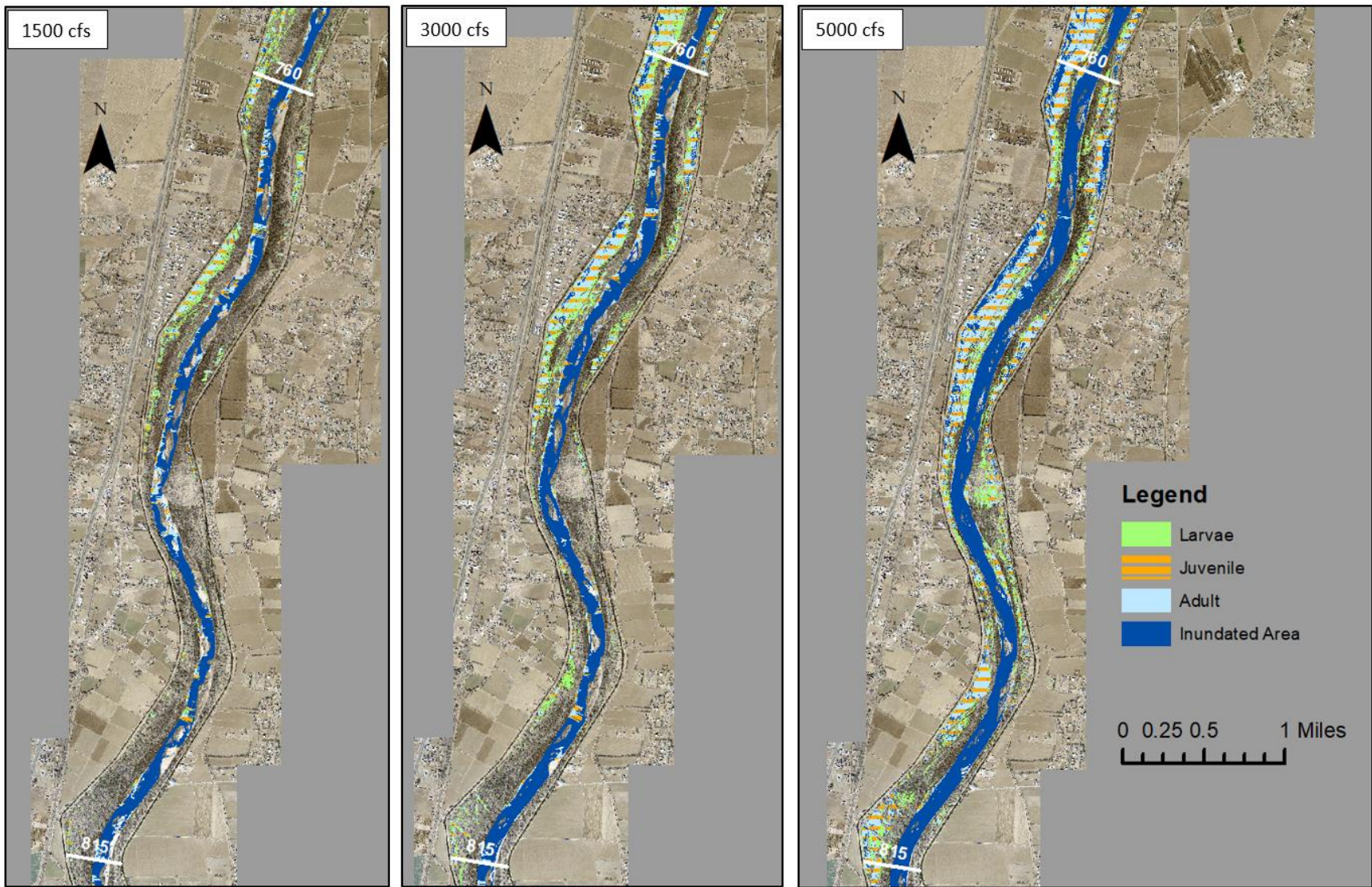


Figure 43 Life stage habitat availability maps for subreach I2(b)

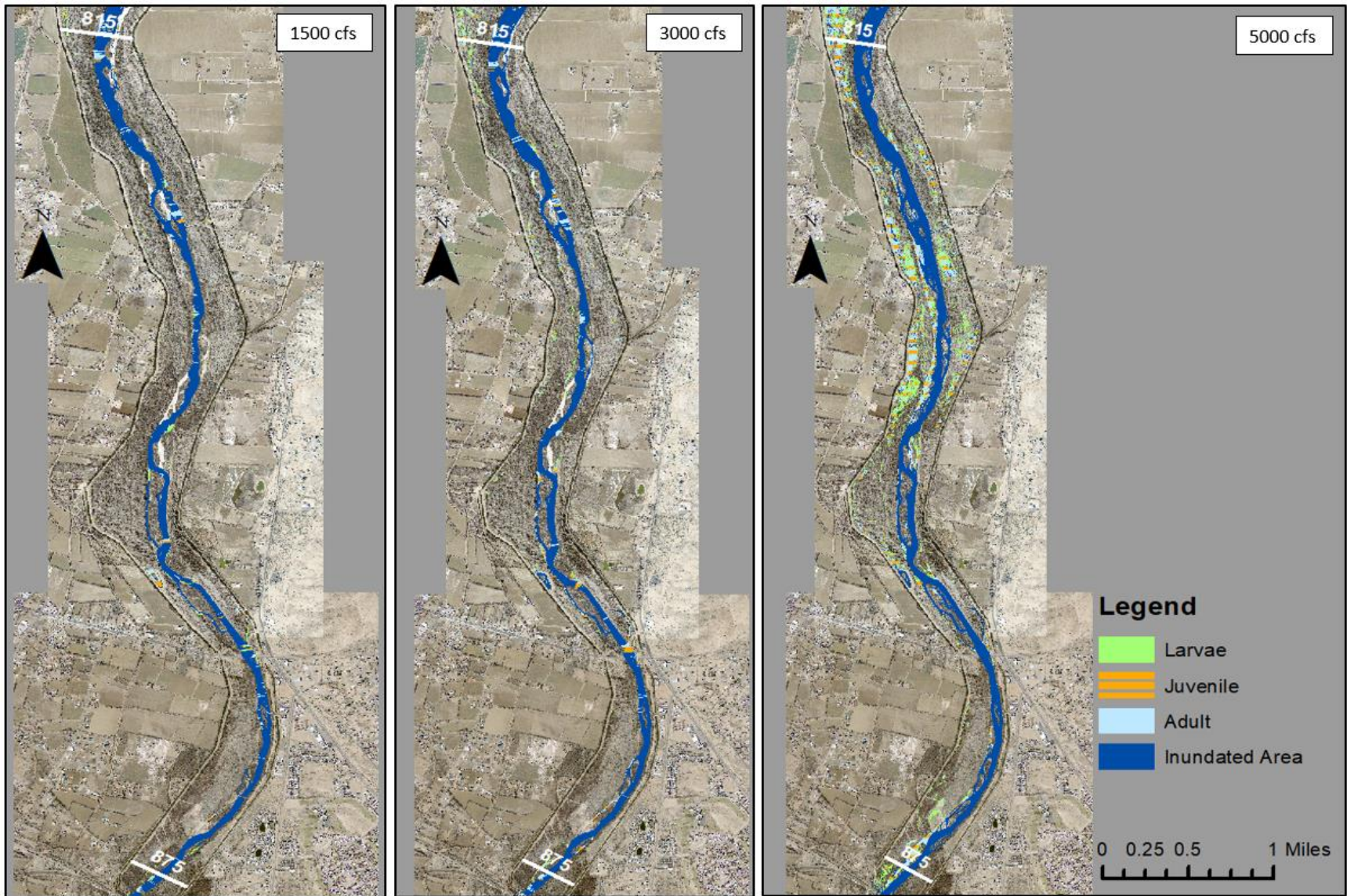


Figure 44 Life stage habitat availability maps for subreach I3(a)

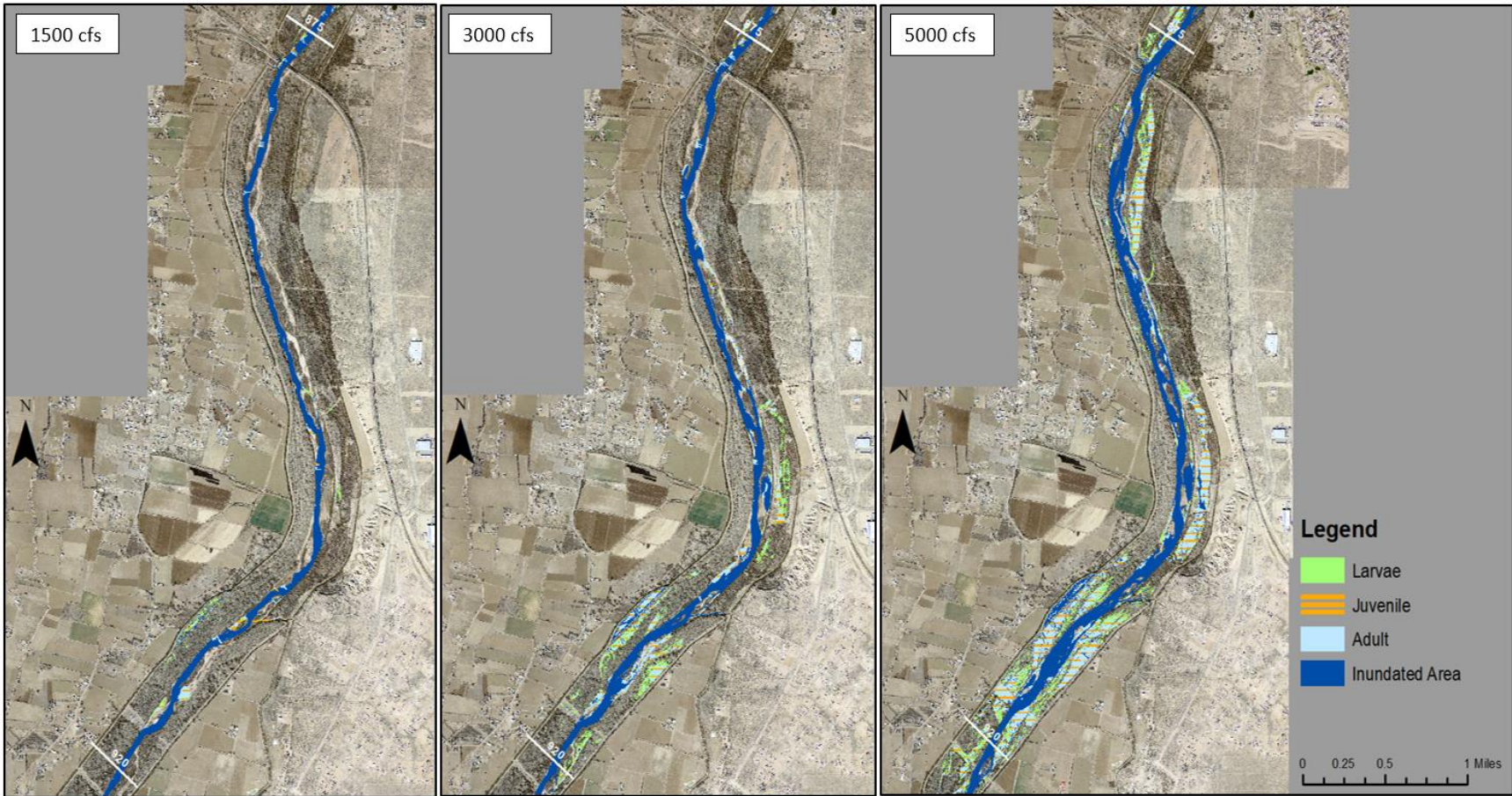


Figure 45 Life stage habitat availability maps for subreach I3(b)

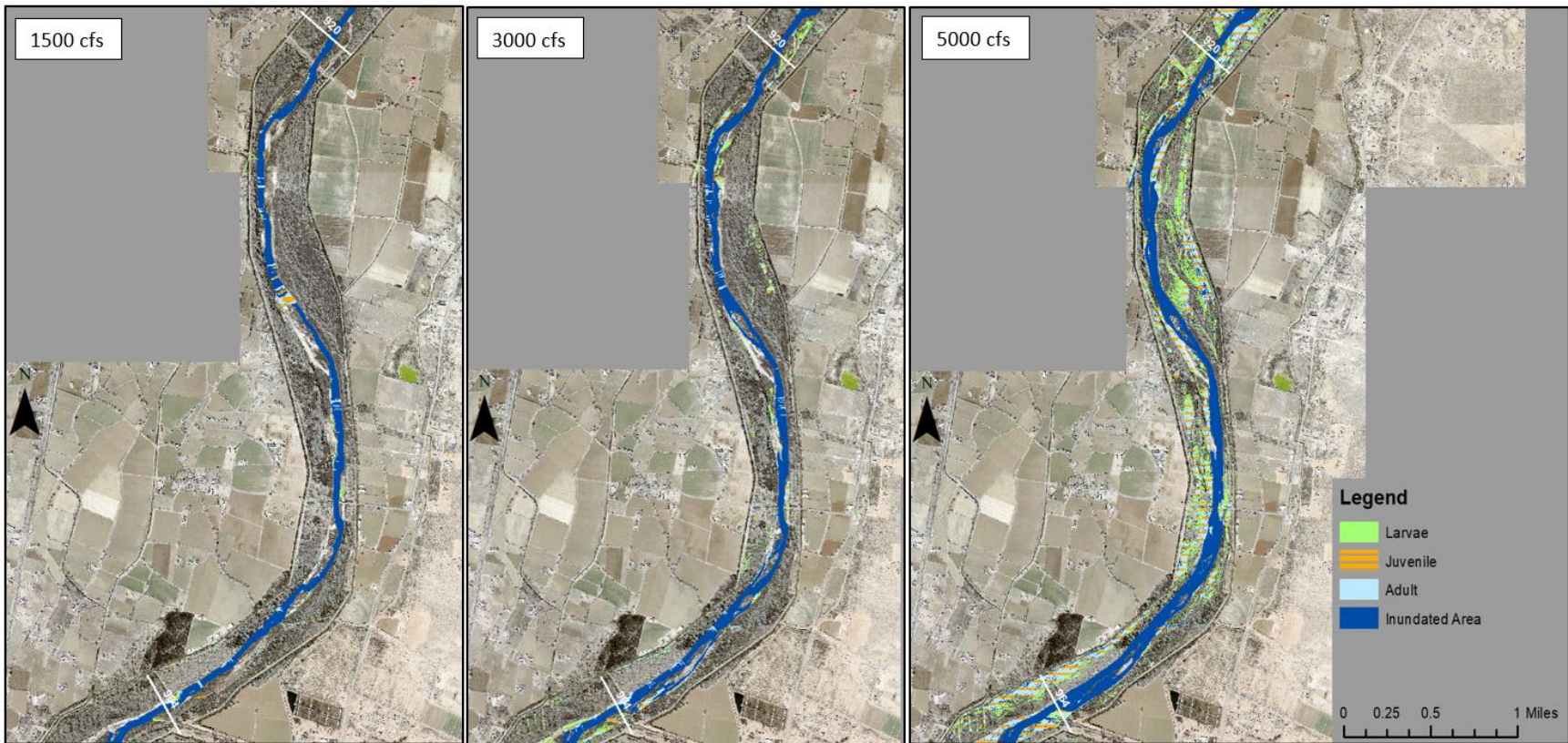
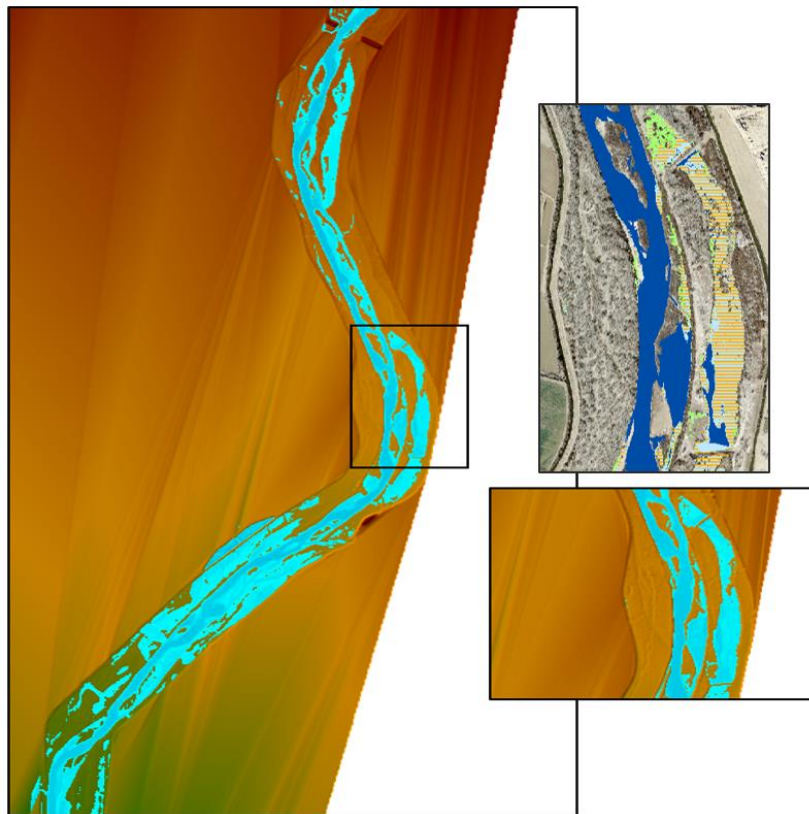


Figure 46 Life stage habitat availability maps for subreach I3(c)

## 8.3 Restoration Potential

### 8.3.1 Disconnected Areas

RAS-Mapper can also be used to identify disconnected areas, or areas that meet suitable criteria for the RGSM but remain detached from the main channel and inaccessible to the fish. These areas can be dangerous for the RGSM when large floods occur that allow them to occupy these spaces during inundation but cause fish to become stranded when flows decrease. Figure 47 highlights an example of a disconnected area in subreach I3(b). While these areas are typically easier to find in RAS-Mapper, the habitat maps are also useful in visualizing just how much habitat these areas contain. Therefore, these areas may be of importance to the USBR and future restoration projects as they could be reconnected to the main channel to create more habitat for the RGSM.



*Figure 47 Example of habitat in the floodplain that is disconnected from the main channel*

To determine which subreaches in Isleta may be of focus for river management, a qualitative assessment of restoration potential by subreach was performed. Along with RAS- Mapper, the habitat availability maps were used to assign each subreach a low, medium, or high score for restoration potential. Scores of restoration potential are based on the presence of disconnected areas that are close to the main channel and habitat availability. In addition, the analysis was based on the 5,000 cfs maps since that is the discharge for which water can inundate the floodplains. Table 10 summarizes the scores for restoration potential by subreach. Overall, subreach I3 was found to have the most restoration potential.

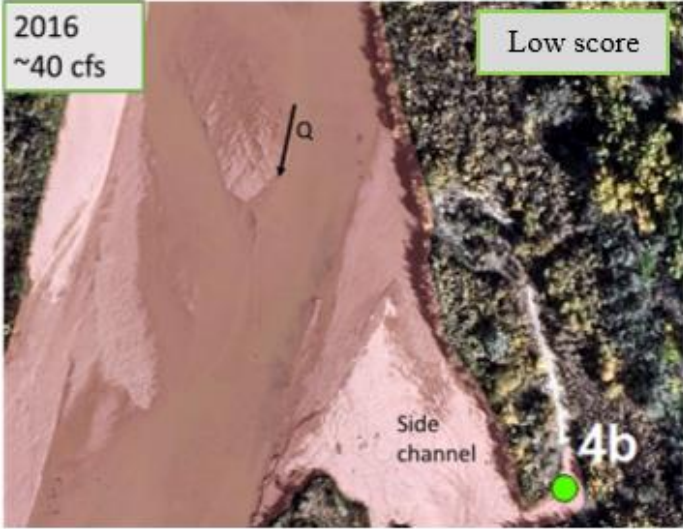
*Table 10 Assessment of restoration potential by subreach at 5,000 cfs*

<b>Subreach</b>	<b>Restoration Potential</b>
I1	Low
I2(a)	Low
I2(b)	Low
I3(a)	Low
I3(b)	Medium
I3(c)	Low-Medium
I4	Low
I5	Low
I6	Low

### **8.3.2 Discussion**

Physical features in the Isleta reach that provide suitable Silvery Minnow habitat were investigated by Yang et al. (2020), as discussed in section 2.4 Previous Studies of Rio Grande Silvery Minnow Habitat. Physical features with the highest scores, indicating more habitat benefits, are hydraulic backwaters, bank-attached bars, and side channels. Figure 48 through Figure 50 shows aerial imagery from varying years of these features. Examples of low and high scoring features are shown, and descriptions of the scoring criteria are given. Refer to Appendix D: RGSM Habitat Scoring System for further insight about the habitat types and scoring criteria.

4b) Backwater extending back < 100 ft; Not as accessible or wide



4a) Backwater extending back > 100 ft; Wide and appear accessible



Figure 48 Aerial imagery in 2016 showing an example of a low and high scoring backwater feature (Yang et al., 2020)

5c) Non-vegetated bar with little geomorphic variability



5a) Bar is large and provides shallow channels and complex habitat

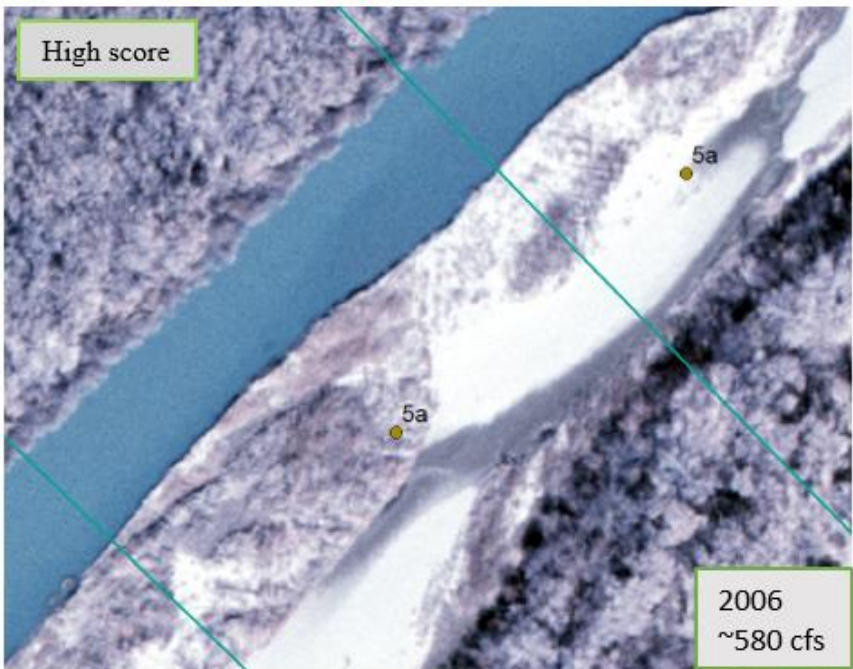


Figure 49 Aerial imagery in 2006 showing an example of a low and high scoring bar feature (Yang et al., 2020)

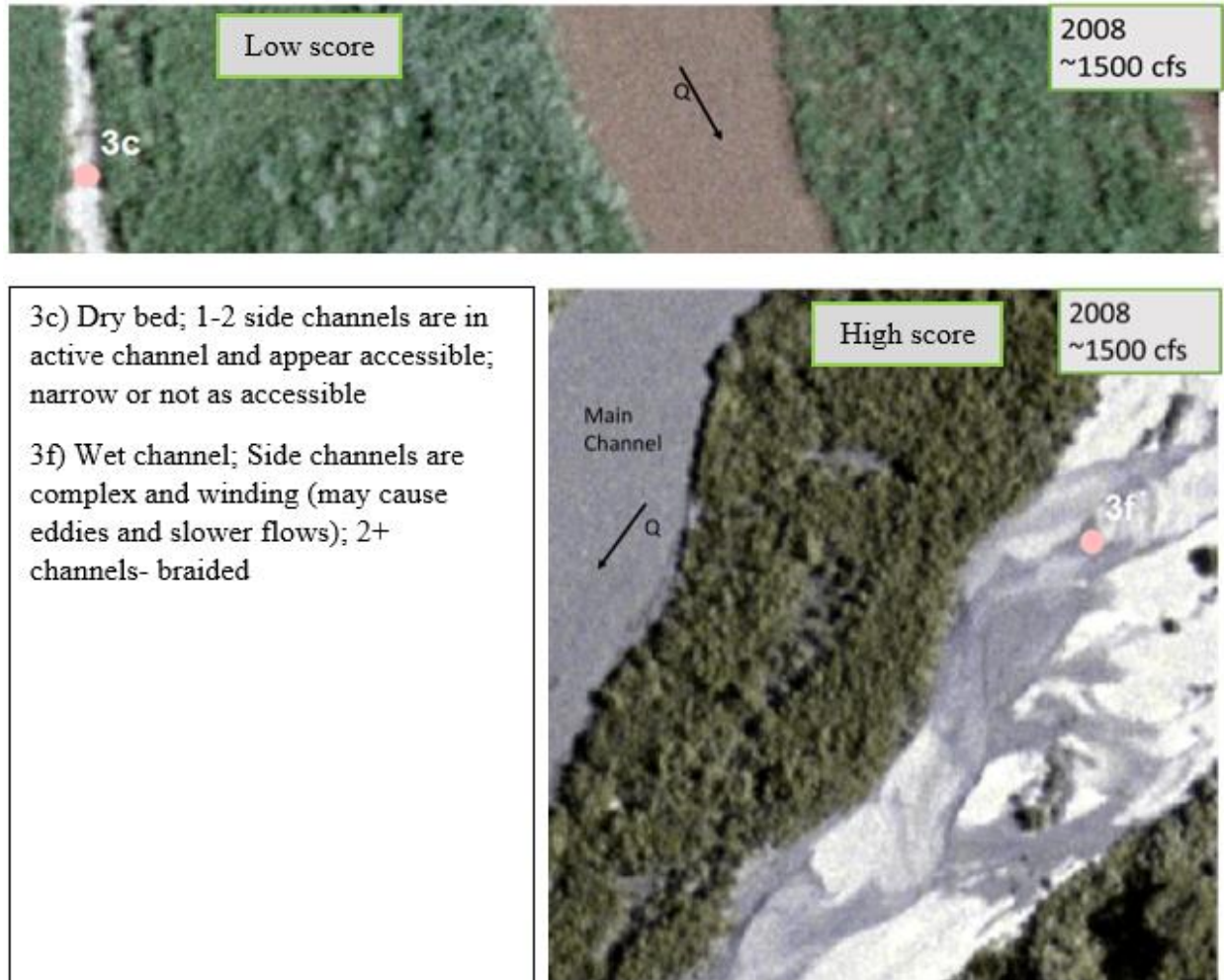


Figure 50 Aerial imagery in 2008 showing an example of a low and high scoring side channel feature (Yang et al., 2020)

Hydraulic backwaters are given a high score because they provide areas of low to near-zero velocities, which is particularly important for larvae and juveniles so that they can grow and find food (Mortenson et al., 2019). Notice that in Figure 48, a high scoring backwater feature (i.e. 4a) has a larger area than a low scoring feature (i.e. 4b), thus providing more suitable habitat (Yang et al., 2020). Bank-attached bars are given a high score because they provide shallow habitat at high flows if the main channel becomes inundated. Complex topography and large structural features are key to providing in-channel habitat. However, complex topography may not provide optimum spawning habitat and may be more important for adult habitat (Tetra Tech,

2014). Figure 49 shows that a high scoring bar (i.e. 5a) has more complex geomorphic features, vegetation, or small side channels that provide the Silvery Minnow with protection from predators and high velocities (Cluer and Thorne, 2014). In contrast, a low scoring bar (i.e. 5c) has less topographic complexity, but still provides an area of shallow habitat at high flows.

Lastly, side channels are given a high score because during high flows they provide the Silvery Minnow with access to diverse habitat with lower velocities. Side channel complexity and accessibility are directly related to more RGSM habitat. Figure 50 shows that a high scoring side channel (i.e. 3f) is wide and has braided features that induce eddies which dissipate energy and reduce flow velocity. In addition, high scoring side channels are inundated and accessible to the fish. A low scoring side channel (i.e. 3c) is narrow due to vegetation encroachment and is less likely to become inundated and provide suitable habitat (Yang et al., 2020).

Scores were computed by Yang et al. (2020) for each subreach based on the presence of habitat features for the RGSM. An overall habitat score was computed for the years 1992, 2001, 2002, 2005, 2006, 2008, 2012, and 2016. Scores for these years were done at discharges ranging between 40 and 5,980 cfs. Daily average discharge data were obtained from the following gages: Rio Grande at Isleta Lakes Near Isleta (08330875), Rio Grande Floodway at San Acacia (08354900), and Rio Grande at Albuquerque (08330000). In 2012, subreaches I2 and I4 showed the highest scores, while subreaches I5 and I6 showed the lowest scores. Table 11 shows a comparison of results from the restoration potential analysis and the overall habitat scores from Yang et al. (2020) for each subreach.

*Table 11 Comparison of results from the restoration potential analysis and the habitat scoring system*

<b>Subreach</b>	<b>Restoration Potential</b>	<b>Habitat Score</b>
I1	Low	Medium
I2	Low	High
I3	Low-Medium	Medium
I4	Low	Medium-High
I5	Low	Low-Medium
I6	Low	Low

Combining the results from the restoration potential analysis and the habitat scoring system suggests that subreaches I2 to I4 may be areas of focus for river management. Physical features that create suitable RGSM habitat, like backwaters and debris piles, found in these subreaches could be mimicked in small areas of other subreaches to increase the amount of suitable habitat for the RGSM. Engineered fish-friendly structures like lunkers provide shade, protection, shelter from high velocities, and good spawning habitat for fish. Other engineered structures like J-Hooks and root wads help to improve channel-floodplain connectivity and dissipate energy. These structures create scour holes that fish can use for protection (Julien, 2018). These pools may also be useful during low flow periods when parts of the river are dry. Lastly, engineered log jams can be used to reverse channel incision, create areas with backwater conditions, and protect channel banks (Abbe et al., 2018). Figure 51 depicts each of these engineered structures. In addition to building structures, disconnected areas in subreach I3 could be made into side channels to increase RGSM habitat. As mentioned previously, river management may focus on creating more complex side channels as complexity directly relates to more habitat.

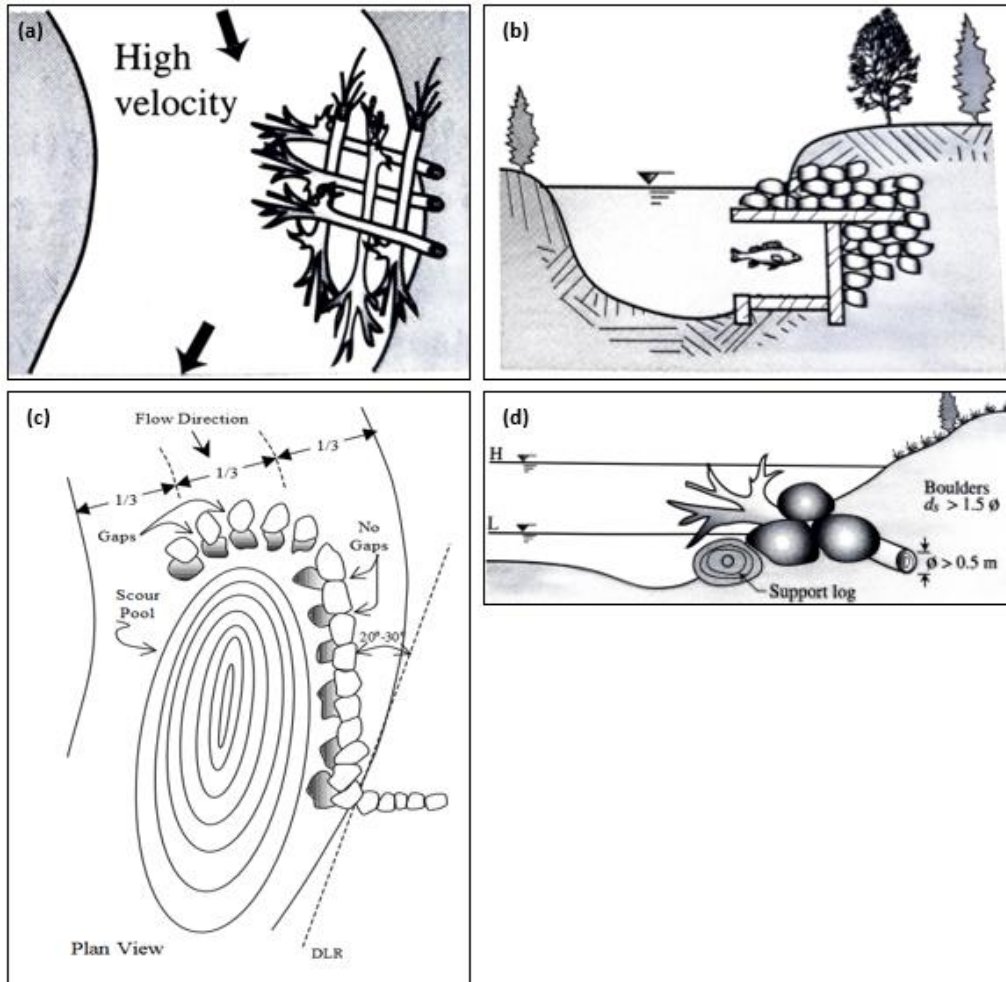


Figure 51 Engineered structures used in river restoration: (a) log jam, (b) lunker, (c) J-Hook, and (d) rootwads (pictures obtained from Julien (2018) and Rosgen (2001)).

### 8.3.2.1 Further Recommendations

The SET has aided in classifying the primary drivers influencing the MRG's geomorphology for various time periods. This is important for determining how the river will respond to disturbances and how it can recover. Recovery in the Isleta reach may involve restoring the system to a stage that resembles a pre-disturbed state or allowing the river to reach an equilibrium state with little disturbance. Restoring the river to a stage that resembles a pre-disturbed state would involve resetting the floodplain and channel network. This is achieved by

filling the main channel until the floodplain is reconnected. This method of restoration has been executed in incised channels like Whychus Creek in Oregon (Castro and Thorne, 2019).

Additionally, river restoration design may consider the “biomic restoration” approach, which looks to empower organisms to drive and manage biogeomorphology. “Biological power” may be maximized in rivers that feature a multithreaded planform where floodplains are inundated frequently. To meet the velocity and depth requirements of the Silvery Minnow, there must be enough width to accommodate floods and allow for sediment to deposit and erode (Johnson et al., 2019).

## **Chapter 9: Study Limitations**

### **9.1 Hydraulic Modeling (HEC-RAS)**

Cross-sectional geometry data are obtained at agg/deg lines, which are spaced approximately 500 feet apart. The lateral flow distribution can only be obtained at these agg/deg lines (i.e. every 500 feet) because 1-D models, like HEC-RAS, do not account for flow distributions between cross-sections (Baird and Holste, 2020). Therefore, the assumption was made that the width of habitat in a cross-section will remain the same until the next cross-section. If the river is fairly straight, like Isleta, this assumption is acceptable. However, if the river is sinuous, habitat estimates can be overestimated. For example, habitat is overestimated if the computed habitat falls on the inside of a large bend (i.e. stretching over several cross-sections), where the space between the agg/deg lines may be less than 500 feet. While a two-dimensional (2-D) model would capture more detail, insufficient data for the MRG may make using a 1-D model more appropriate even though the results are limited (Varyu, 2013).

#### **9.1.1 RAS-Mapper**

As mentioned previously in Chapter 8: Habitat Mapping, RAS-Mapper appears to compute depth values in areas where water should not be present. This is particularly apparent in maps for discharges lower than bankfull. As discussed in section 5.1 Bankfull Discharge, “computational levees” were assigned at each cross-section to ensure water could not escape the main channel until bankfull discharge (i.e. 5,000 cfs in 2012) had been reached. Inspection of HEC-RAS water surface profiles at each cross-section show water properly contained in the main channel. RAS-Mapper appears to recognize these “computational levees” at most cross-sections throughout the reach, but not all. An example of this is shown in Figure 52(a) and

highlighted in the red box. The straight edges on the bodies of water represent where “computational levees” have contained the water in the main channel between cross-sections. This error appears to be most severe in subreaches I1 and I2.

Further evidence that RAS-Mapper is not properly computing water surface elevation is shown in Figure 52(b). Depth rasters at low discharges (i.e. 500 and 1,000 cfs) show fragmented inundation along the main channel. One possible reasoning for this could be that the elevation of the terrain in RAS-Mapper is higher than the water surface elevation, thus showing that no water is present in the main channel at certain cross-sections. Ultimately, both errors may be a consequence of placing 1-D results onto a 2-D terrain. Since errors in computing water surface elevation have been identified, it’s possible that the disconnected areas seen throughout the reach could be artifacts. These areas may not be truly disconnected from the main channel and could instead be a result of RAS-Mapper filling areas of low elevation with water.

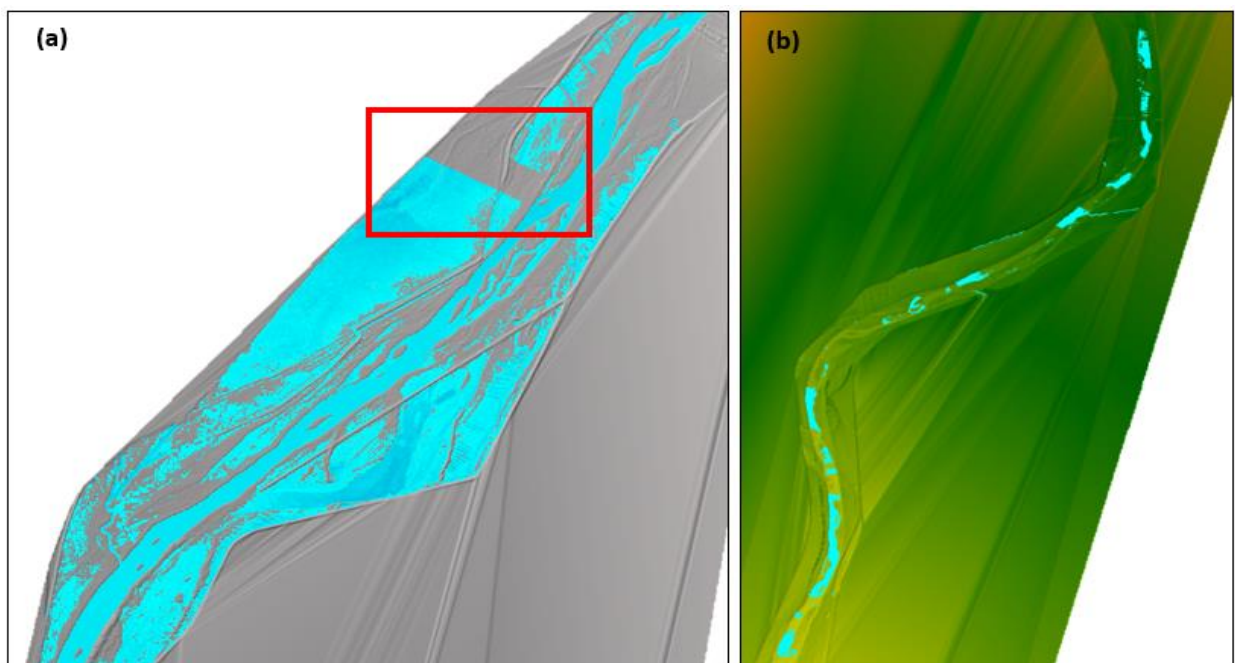


*Figure 52 Evidence of RAS-Mapper limitations: (a) example of RAS-Mapper recognizing "computational levee" placement and (b) fragmented inundation at 1,000 cfs*

## **9.2 Data Collection**

For this study, cross-section data were collected on a decadal time scale between 1962 and 2012, minus the year 1982. The Rio Grande is a dynamic river, meaning cross-sections are likely to change between surveys, reducing the ability to accurately model habitat availability throughout a reach from year to year. While the Isleta reach is incising and narrowing, it appears that no significant changes have occurred in recent years (1992 to 2012) that would severely impact the habitat modeling results. Therefore, the decadal time scale for collecting cross-sectional geometry data seems sufficient for the Isleta reach. However, this may not hold true for other reaches in the MRG. Additionally, habitat mapping was limited by the availability of LiDAR data. For this study, the only available LiDAR mass points data were for 2012. It would be beneficial to create these maps more often to gain a better understanding of where habitat availability is the greatest and locate sites for possible restoration.

## **9.3 Time-Integrated Habitat Metrics**

To compute the TIHMs, yearly habitat curves and daily discharge data are needed. Some USGS gages along the Isleta reach are missing multiple years of discharge data for the time period analyzed. The program is unable to compute habitat where discharge data are missing. Therefore, it was necessary to use multiple gages to get a complete record from 1992 to 2019. This may be problematic in other reaches in the MRG, where fewer gages are present, and could limit our understanding of RGSM habitat for a wide range of years. However, it may be possible to perform a regression analysis on the discharge data to obtain an equation that can be used to estimate missing data. Lastly, the results from the TIHMs may be limited as habitat was interpolated based on three years of known data (1992, 2002, and 2012).

## Chapter 10: Conclusions

This study focused on the Isleta reach, a segment of the Middle Rio Grande expanding 42 miles from the Isleta Diversion Dam to the confluence of Rio Puerco, which is considered critical habitat for the Rio Grande Silvery Minnow (RGSM). Links between morphodynamic processes and RGSM habitat conditions were investigated using the following methods: (1) 1-D modeling techniques were used to quantitatively determine RGSM habitat availability by subreach and infer relationships between discharge and habitat; (2) geomorphic evolution maps were used to visualize how the Isleta reach has changed over time and how this has affected the biological conditions in the river; (3) time-integrated habitat metrics were developed to provide yearly estimates of cumulative RGSM habitat based on daily discharge data and ecological relationships were identified; and (4) habitat availability maps were created, showing where critical habitat for the RGSM is located within the reach. Restoration potential was assessed qualitatively throughout the reach based on these maps and recommendations were made.

The major findings from this study include:

- HEC-RAS modeling results suggest that habitat availability follows three typical patterns in the Isleta reach. Earlier years (1962 and 1972) had “rounded” habitat curves, while later years (1992, 2002, and 2012) had “step” and “hook” habitat curves. Channel incision has caused habitat availability to spike at much higher discharges than earlier years.
- Using the planform evolution model developed by Massong et al. (2010), aerial imagery, and cross-sectional geometry data, it was determined that the Isleta reach has transformed from being wide, shallow and braided to narrow and incised. Most

subreaches appear to be following the migrating path indicating high sediment transport capacity. The stream evolution model developed by Cluer and Thorne (2013) suggests that in 2012 all subreaches were in the degradation stage which causes a reduction in features that create habitat in the main channel and a disconnect with the floodplain.

- The time-integrated habitat metrics show that larval and juvenile habitat metrics are more sensitive to changes in daily discharge from 1992 to 2019. Correlations between the habitat metrics, discharge, and RGSM population monitoring data from Mortenson et al. (2020) suggest larvae are strong predictors of population dynamics.
- From the habitat availability maps, subreaches I1 to I3 show the most hydraulically suitable habitat for all life stages. However, much of the habitat on the floodplain is inaccessible to the fish because it is disconnected from the main channel. Most importantly, the habitat maps demonstrate that larval habitat is limited by access to the floodplain.
- Subreaches I2 to I4 may be key areas for river management to increase RGSM habitat based on the presence of disconnected areas close to the main channel and features that provide suitable habitat.

## References

- Abbe, T., M. Hrachovec, and S. Winter. (2018). *Engineered Log Jams: Recent Developments in Their Design and Placement, With Examples from the Pacific Northwest, U.S.A.* Natural Systems Design. Seattle, WA.
- Baird, D. (2014). *Historical Rio Grande Channel Width Design Literature Review Summary*, U.S. Department of the Interior, Bureau of Reclamation, Technical Services Center, Sedimentation and River Hydraulics Group. Denver, CO, 42 p.
- Baird, D. and N. Holste. (2020). *One-Dimensional Numerical Modeling of Perched Channels*. U.S. Bureau of Reclamation. Denver, Colorado.
- Bartolino, J. and J. Cole. (2002). *Ground-Water Resources of the Middle Rio Grande Basin*. U.S. Geological Survey. Reston, Virginia.
- Bauer, T.R. (2000). *Morphology of the Middle Rio Grande from Bernalillo Bridge to San Acacia Diversion Dam*, New Mexico, Colorado State University, Fort Collins, CO.
- Bauer, T.R. (2009). *Sediment Evolution on the Middle Rio Grande, New Mexico*, U.S. Department of the Interior, Bureau of Reclamation, Technical Services Center, Sedimentation and River Hydraulics Group. Denver, CO. 36 p.
- Bauer, T.R. and Hildale, R. (2006). *Sediment Model for the Middle Rio Grande – Phase 2: Isleta Diversion Dam to San Acacia Diversion Dam*. U.S. Department of the Interior, Bureau of Reclamation, Technical Services Center, Sedimentation and River Hydraulics Group. Denver, CO, 295 p.
- Berry, K. L. and Lewis, K. (1997). *Historical Documentation of Middle Rio Grande Flood Protection Projects, Corrales to San Marcial*. Office of Contract Archeology, University of New Mexico, Albuquerque, NM
- Bureau of Reclamation. *Projects and Facilities*. Retrieved July 16, 2020 from <https://www.usbr.gov/projects/index.php?id=50>
- Castro, J. and Thorne, C. (2019). *The Stream Evolution Triangle: Integrating Geology, Hydrology, and Biology*. River Research and Applications, 35: 315– 326.
- Cluer, B. and C. Thorne. (2013). *A Stream Evolution Model Integrating Habitat and Ecosystem Benefits*. River Research and Applications, 30(2), 135-154.
- Coonrod, J. (2005). *The Middle Rio Grande: History and Restoration*. Managing Watersheds for Human and Natural Impacts: Engineering, Ecological, and Economic Challenges. University of New Mexico, Albuquerque, New Mexico.

- Crawford, C. S., Cully, A. C., Leutheuser, R., Sifuentes, M. S., White, L. H., and Wilber, J. P. (1993). *Middle Rio Grande Ecosystem: Bosque Biological Management Plan*, Middle Rio Grande Biological Interagency team, Albuquerque, NM, 320p.
- Culbertson, J. K., and Dawdy, D. R. (1964). *A Study of Fluvial Characteristics and Hydraulic Variables, Middle Rio Grande, New Mexico*, U.S. Geological Survey, Professional Paper 1498-F, Washington, D.C., 82 p
- Doidge, S., C. Fogarty, T. Beckwith, and P. Julien. (2020). *San Acacia Reach: Morphodynamic Processes and Silvery Minnow Habitat from San Acacia Diversion Dam to Escondida Bridge 1918-2018*. Report to U.S. Bureau of Reclamation, Albuquerque, New Mexico.
- Dudley, R., and S. Platania. (2007). *Flow Regulation and Fragmentation Imperil Pelagic-Spawning Riverine Fishes*. *Ecological Applications* 17(7):2074–2086.
- Dudley, R., S. Platania, and G. White. (2020). *Rio Grande Silvery Minnow Population Monitoring During 2019*. Submitted to the U.S. Bureau of Reclamation, Albuquerque, New Mexico.
- Environmental Systems Research Institute, Inc (ESRI). (2020). ArcMap [Computer Software]. <https://desktop.arcgis.com/en/arcmap/>.
- Gonzales, E., D. Tave, and G. Haggerty. (2014). *Endangered Rio Grande Silvery Minnow Use Constructed Floodplain Habitat*. *Ecohydrology* 7(4):1087–1093.
- Grassel, K. (2002). *Taking Out the Jacks: Issues of Jetty Jack Removal in Bosque and River Restoration Planning*. Master's Thesis, University of New Mexico, Albuquerque, New Mexico.
- Julien, P. (2018). Stream Restoration. In *River Mechanics* (pp. 348-378). Cambridge: Cambridge University Press. doi:10.1017/9781316107072.014
- Klein, M., C. Herrington, J. Aubuchon, and T. Lampert. (2018). *Isleta to San Acacia Geomorphic Analysis*. U.S. Bureau of Reclamation, River Analysis Group, Technical Services Division, Albuquerque, New Mexico.
- Laforge, K., C. Yang, S. Doidge, T. Beckwith, C. Fogarty, and P. Julien. (2020). *Rio Puerco Reach: Morphodynamic Processes and Silvery Minnow Habitat*. Report to U.S. Bureau of Reclamation, Albuquerque, New Mexico.
- Makar, P. (2010). *Channel Characteristics of the Middle Rio Grande, NM*. U.S. Bureau of Reclamation, SRH-2011-05, Albuquerque, New Mexico.
- Makar, P., and J. AuBuchon. (2012). *Channel Changes on the Middle Rio Grande*. World Environmental and Water Resources Congress 2012: Crossing Boundaries. American Society of Civil Engineers, Albuquerque, New Mexico.
- Massong, T., P. Makar, and T. Bauer. (2010). *Planform Evolution Model for the Middle Rio Grande, NM*. Page 2nd Joint Federal Interagency Conference. Las Vegas, Nevada.

- Mortensen, J., R. Dudley, S. Platania, and T. Turner. (2019). *Rio Grande Silvery Minnow Biology and Habitat Syntheses*. Report to U.S. Bureau of Reclamation, Albuquerque, New Mexico.
- Mortenson, J., R. Dudley, S. Platania, G. White, T. Turner, P. Julien, S. Doidge, T. Beckwith, and C. Fogarty. (2020). *Linking Morpho-Dynamics and Bio-Habitat Conditions on the Middle Rio Grande: Linkage Report I – Isleta Reach Analyses*. Draft Final Report. Prepared for the U.S. Bureau of Reclamation, Albuquerque, New Mexico.
- MEI. (2002). *Geomorphic and Sedimentologic Investigations of the Middle Rio Grande between Cochiti Dam and Elephant Butte Reservoir*, Mussetter Engineering, Inc., Fort Collins, CO, 220 p.
- Osborne, M., E. Carson, and T. Turner. (2012). *Genetic Monitoring and Complex Population Dynamics: Insights From a 12-Year Study of the Rio Grande Silvery Minnow*. *Evolutionary Applications* 5(6):553–574.
- Parametrix. (2008). *Restoration Analysis and Recommendations for the Isleta Reach of the Middle Rio Grande, NM*, Parametrix, Inc., Albuquerque, NM, 292 p.
- Perkin, J., and K. Gido. (2011). *Stream Fragmentation Thresholds for a Reproductive Guild of Great Plains Fishes*. *Fisheries* 36(8):371–383.
- Perkin, J., K. Gido, A. Cooper, T. Turner, M. Osborne, E. Johnson, and K. Mayes. (2015). *Fragmentation and Dewatering Transform Great Plains Stream Fish Communities*. *Ecological Monographs* 85(1):73–92.
- Platania, S. (2000). *Effects of Four Water Temperature Treatments on Survival, Growth, and Developmental Rates of Rio Grande Silvery Minnow, Hybognathus amarus, Eggs and Larvae*. Report to the U.S. Fish and Wildlife Service, Albuquerque, New Mexico.
- Posner, A. J. 2017. *Channel Conditions and Dynamics of the Middle Rio Grande*. Draft Report. River Analysis Group, Technical Services Division, U.S. Bureau of Reclamation, Albuquerque, New Mexico.
- Rivera, J. (1998). *Acequia Culture, Water, Land, and Community in the Southwest*. University of New Mexico Press.
- Rosgen, D. (2001) *The Cross-Vane, W-Weir and J-Hook Vane Structures... Their Description, Design and Application for Stream Stabilization and River Restoration*. Wetlands Engineering and River Restoration Conference.
- Stone, M., C. Byrne, and R. Morrison. (2017). *Evaluating the Impacts of Hydrologic and Geomorphic Alterations on Floodplain Connectivity*. *Ecohydrology* 10(5):e1833.
- Swanson, B., G. Meyer, and J. Coonrod. (2011). *Historical Channel Narrowing Along the Rio Grande Near Albuquerque, New Mexico in Response to Peak Discharge Reductions and Engineering: Magnitude and Uncertainty of Change from Air Photo Measurements*. *Earth Surface Processes and Landforms* 36(7):885–900.

- Tashjian, P. and T. Massong. (2006). *The Implications of Recent Floodplain Evolution on Habitat within the Middle Rio Grande, NM*, 2006 Federal interagency Sedimentation Conference, 9 p.
- Tetra Tech. (2002). *Development of the Middle Rio Grande FLO-2D Flood Routing Model Cochiti Dam to Elephant Butte Reservoir*, Tetra Tech, Inc. 48 p.
- Tetra Tech. (2014). *Ecohydrological Relationships along the Middle Rio Grande of New Mexico for the Endangered Rio Grande Silvery Minnow*. US Army Corps of Engineers, Albuquerque District, Albuquerque, New Mexico, 109 p.
- Thorp, J., J. Flotemersch, M. Delong, A. Casper, M. Thoms, F. Ballantyne, B. Williams, B. O'Neill, C. Haase. (2010). *Linking Ecosystem Services, Rehabilitation, and River Hydrogeomorphology*. *BioScience*. 60(1): 67–74
- Tockner, K., F. Malard, and J. Ward. (2000). *An Extension of the Flood Pulse Concept*. *Hydrological Processes* 14(16–17):2861–2883.
- U.S. Army Corps of Engineers (USACE). (2010). *Historic Inundation Analysis Along the Middle Rio Grande for the Period 1990 to 2009*. Albuquerque, New Mexico.
- U.S. Army Corps of Engineers (USACE). (2016). *HEC-RAS River Analysis System Hydraulic Reference Manual*. Institute for Water Resources, Hydrologic Engineering Center. Davis, California.
- U.S. Fish and Wildlife Service (USFWS). (2010). *Rio Grande Silvery Minnow (*Hybognathus amarus*) Recovery Plan, First Revision*. U.S. Fish and Wildlife Service, Albuquerque, New Mexico.
- U.S. Office of the Federal Register (USOFR). (1994). *Endangered and Threatened Wildlife; Final Rule to List the Rio Grande Silvery Minnow as an Endangered Species*. Final Rule. *Federal Register* 59:138 (20 July 1994): 36988–36995.
- Varyu, D. (2016). *SRH-1D Numerical Model for the Middle Rio Grande: Isleta Diversion Dam to San Acacia Diversion Dam*. U.S. Department of the Interior, Bureau of Reclamation, Technical Services Center, Sedimentation and River Hydraulics Group. Denver, CO.
- Yang, C., K. LaForge, P. Julien, and S. Doidge. (2020). *Isleta Reach: Hydraulic modeling and Silvery Minnow habitat analysis*. Report to U.S. Bureau of Reclamation, Albuquerque, New Mexico.
- Zheng, S., C. Thorne, B. Wu, and S. Han. (2017). *Application of the Stream Evolution Model to a Volcanically Disturbed River: The North Fork Toutle River, Washington State, USA*. *River Research and Applications*, 33(6), 937-948

**Appendix A**  
**Additional Habitat Curves and Spatial Habitat Charts**

### Additional Habitat Curves

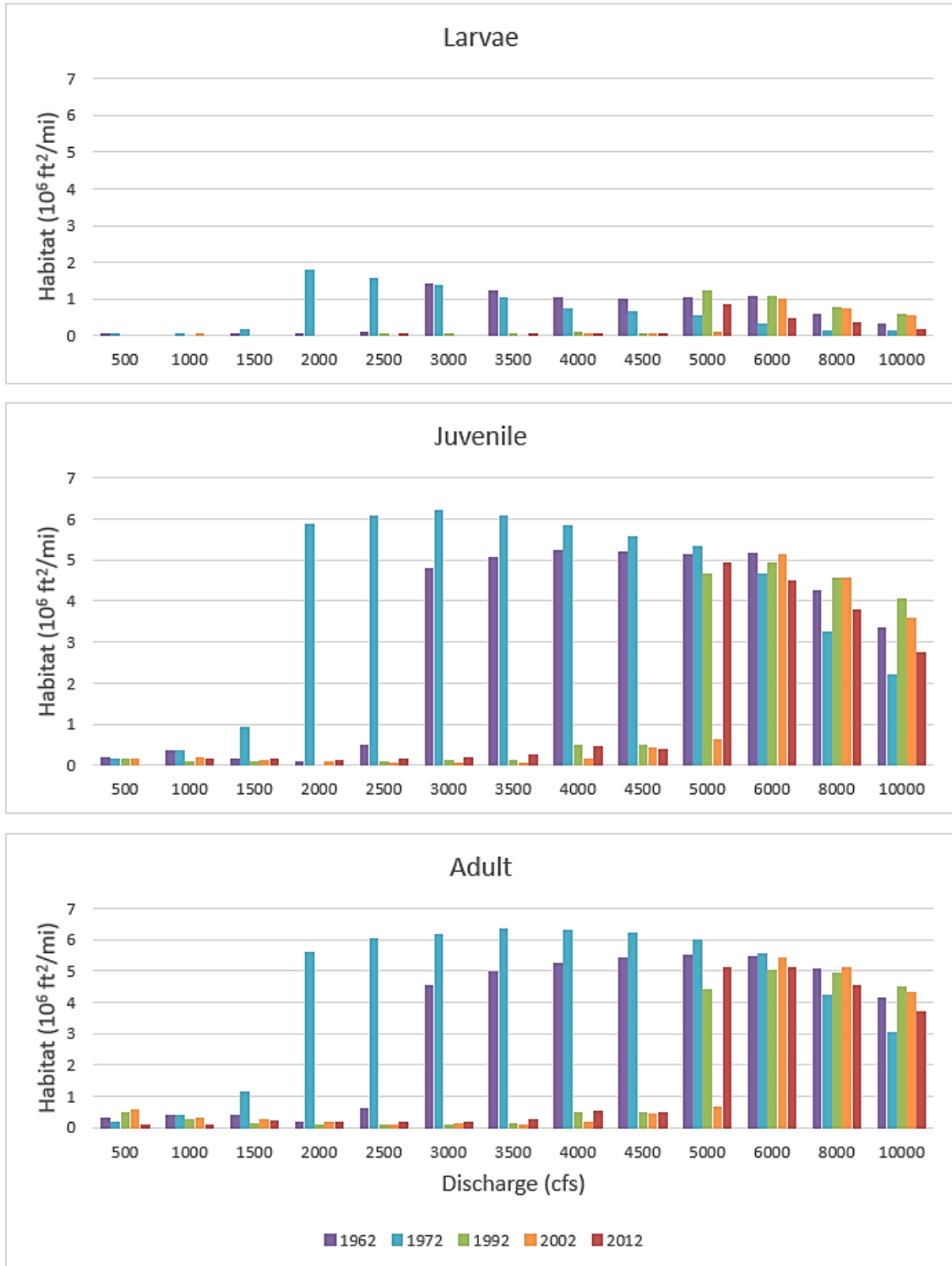


Figure A-1 Larvae, juvenile, and adult habitat curves for subreach II

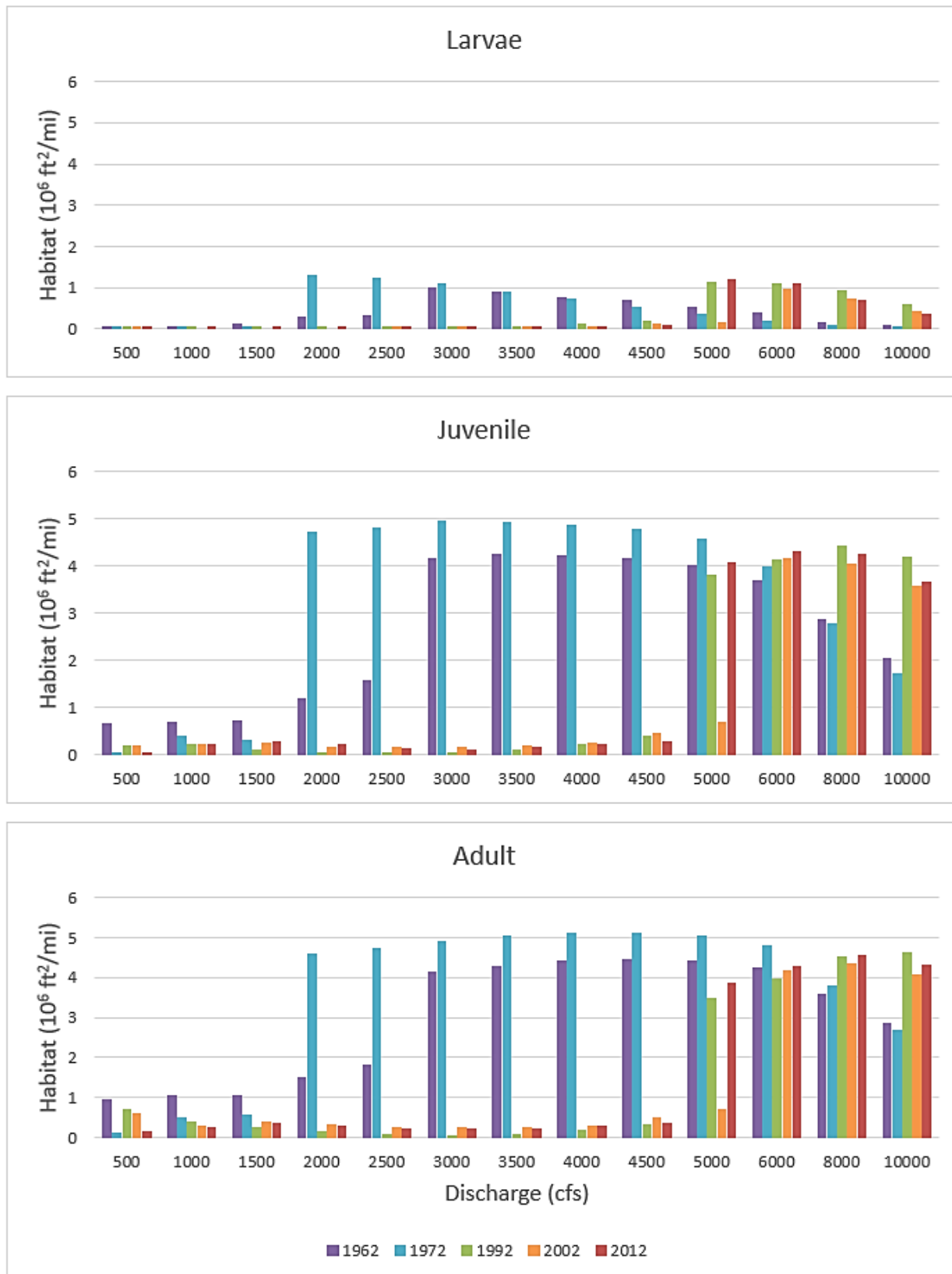


Figure A-2 Larvae, juvenile, and adult habitat curves for subreach I2

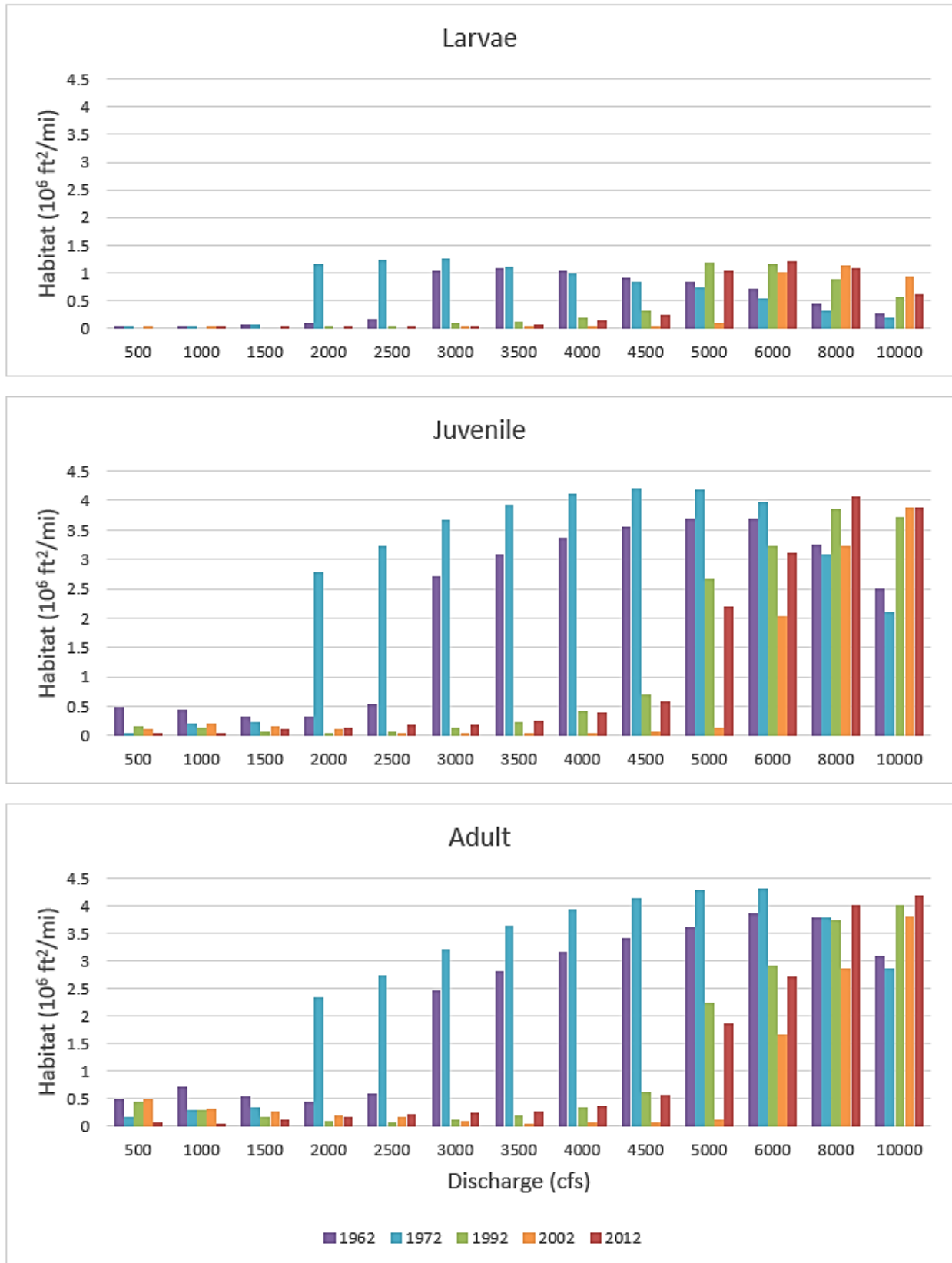


Figure A-3 Larvae, juvenile, and adult habitat curves for subreach I3

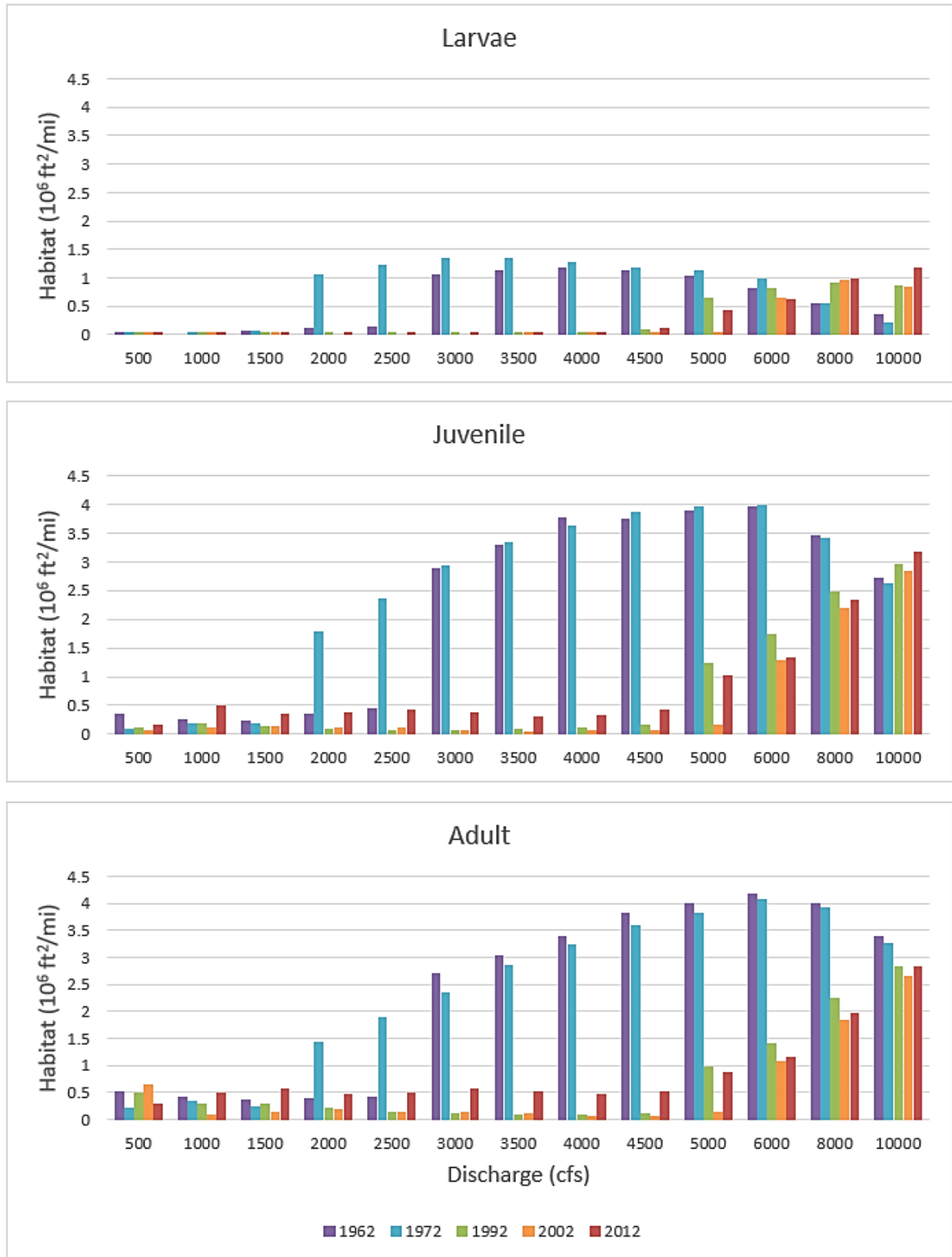


Figure A-4 Larvae, juvenile, and adult habitat curves for subreach I4

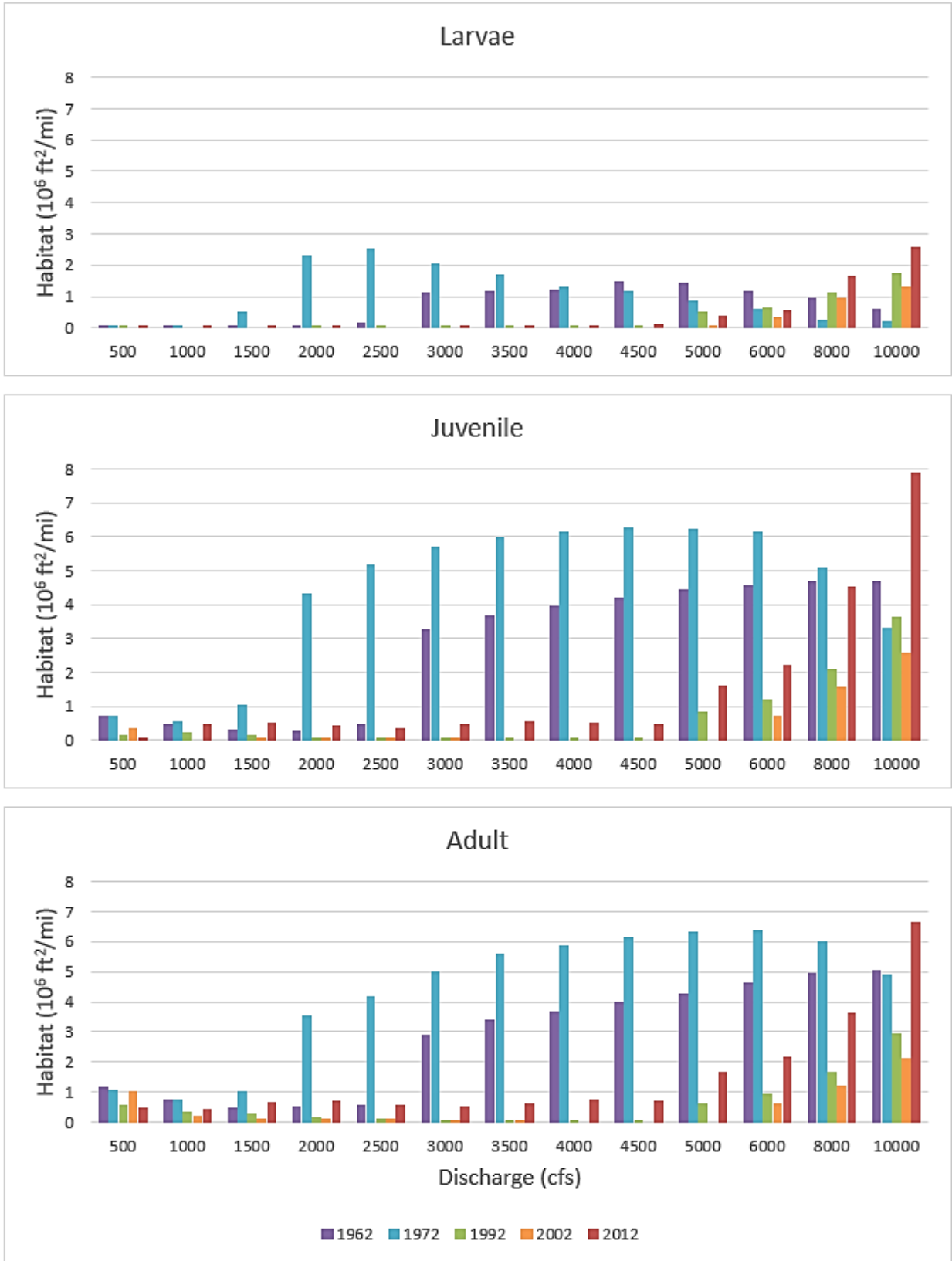


Figure A-5 Larvae, juvenile, and adult habitat curves for subreach I5

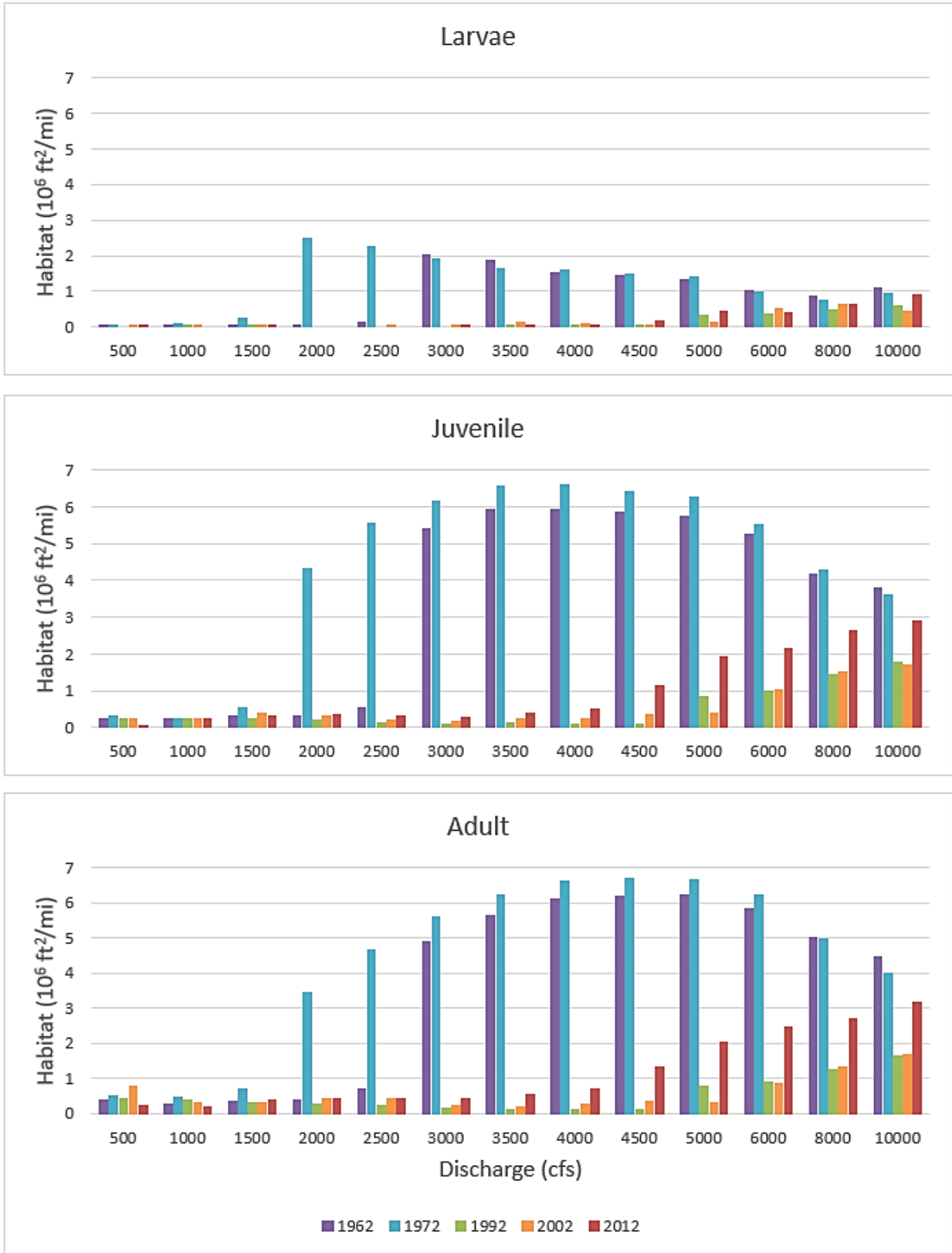
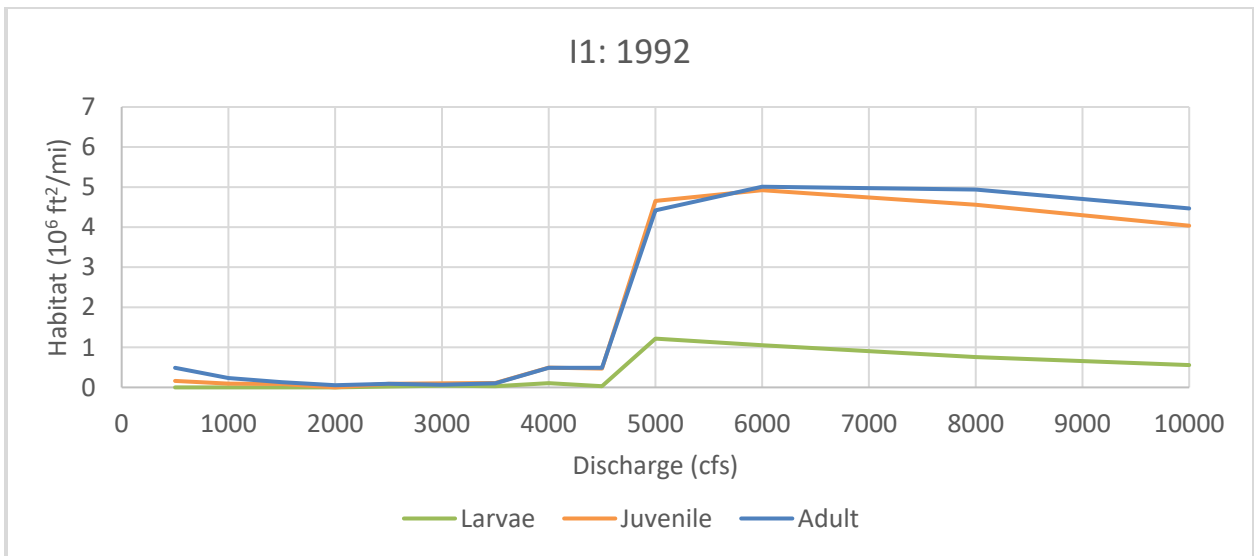
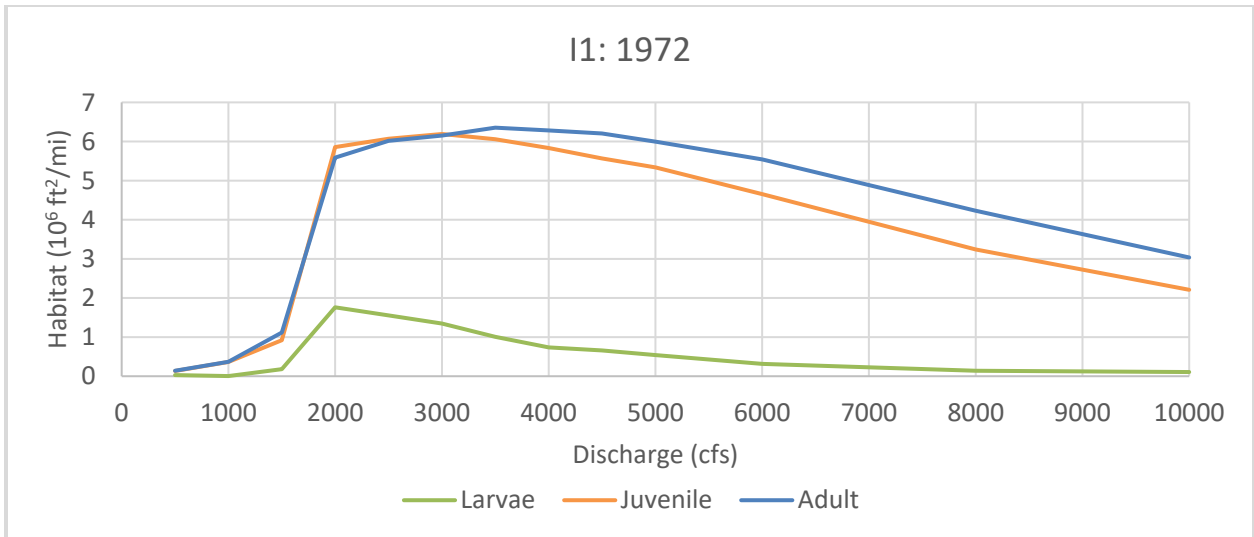
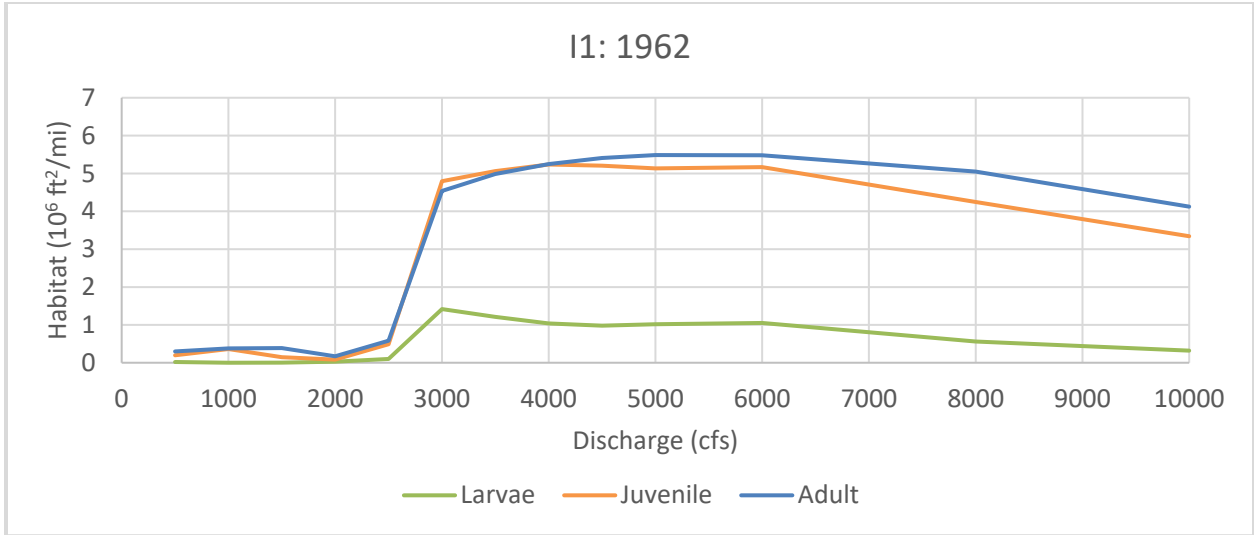
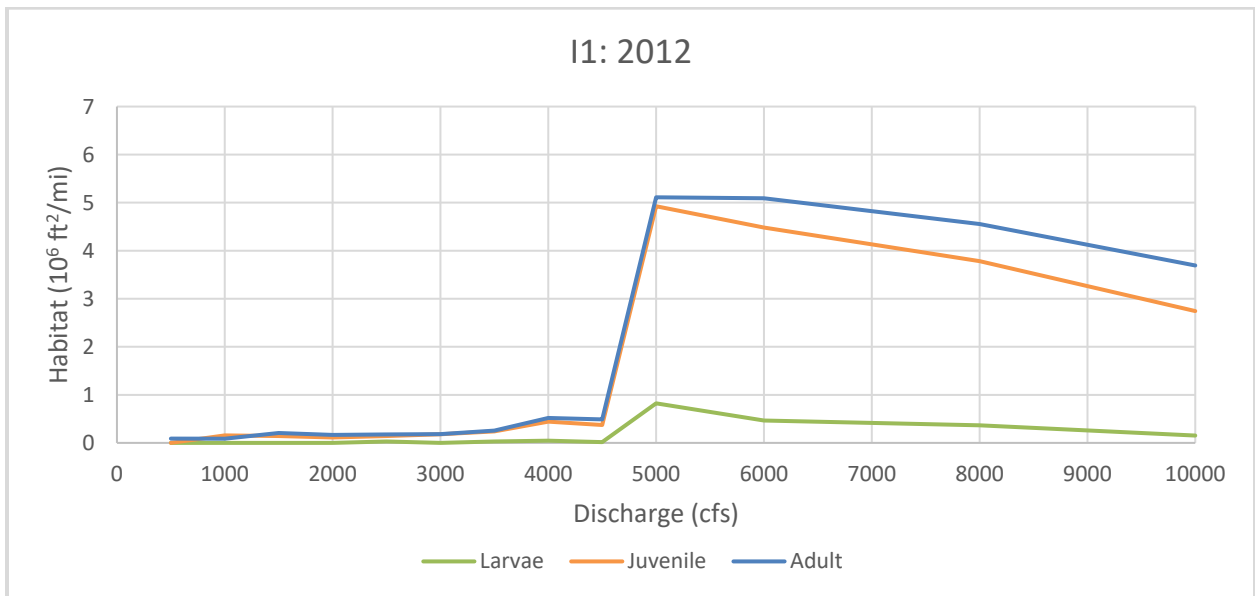
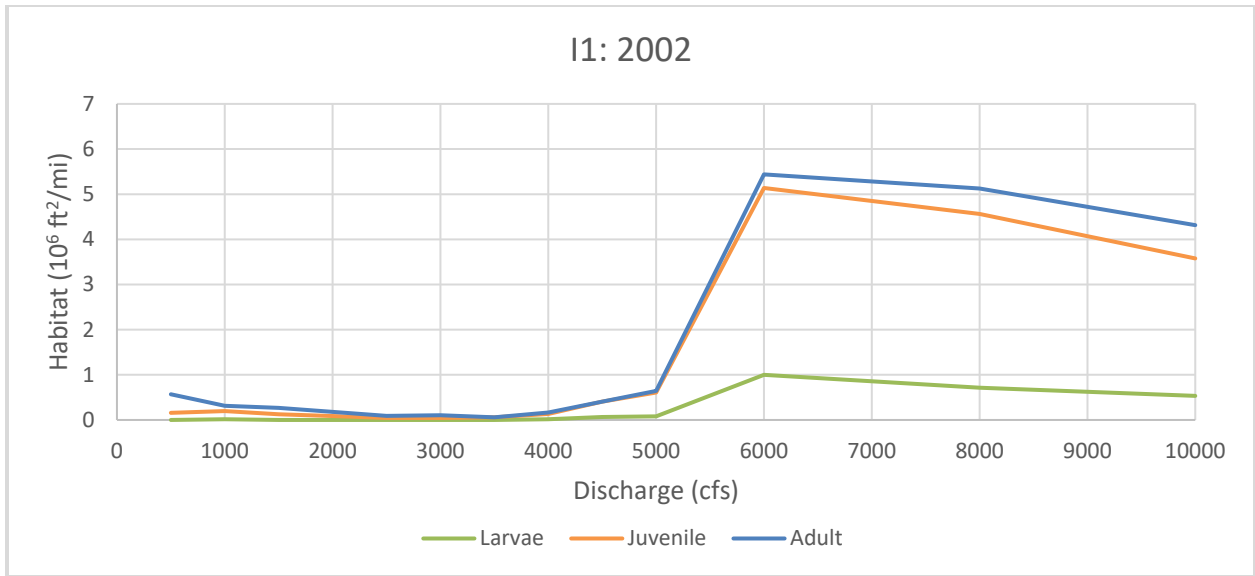
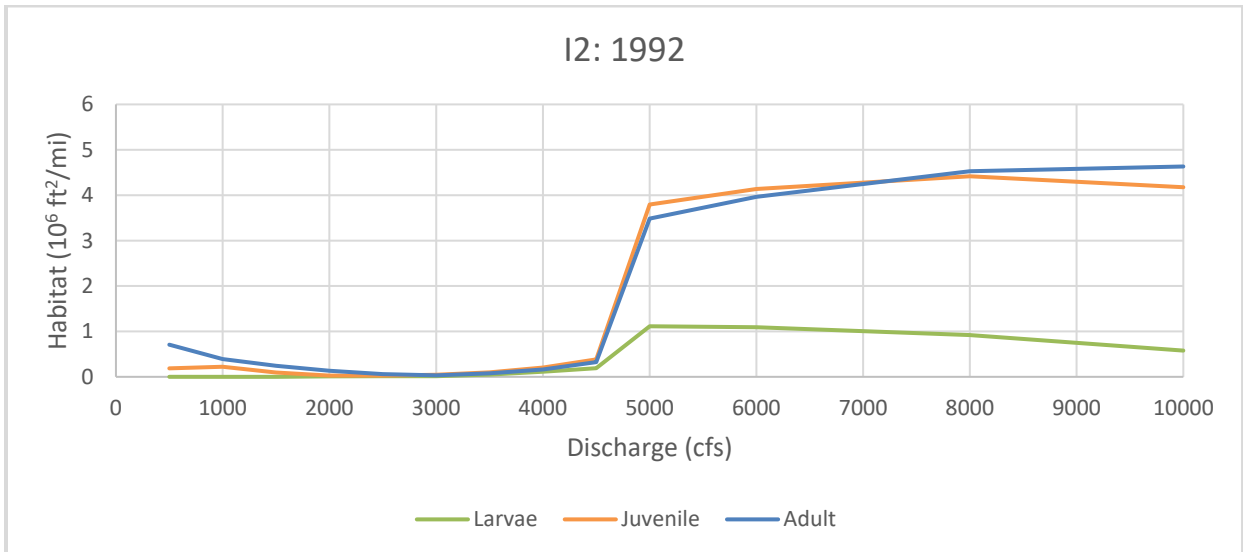
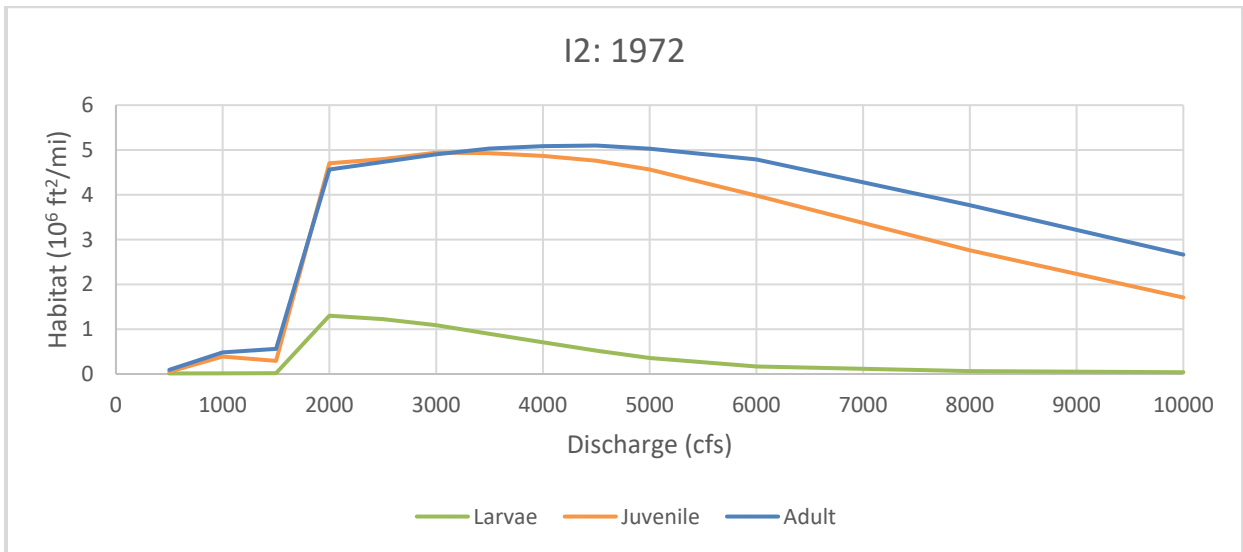
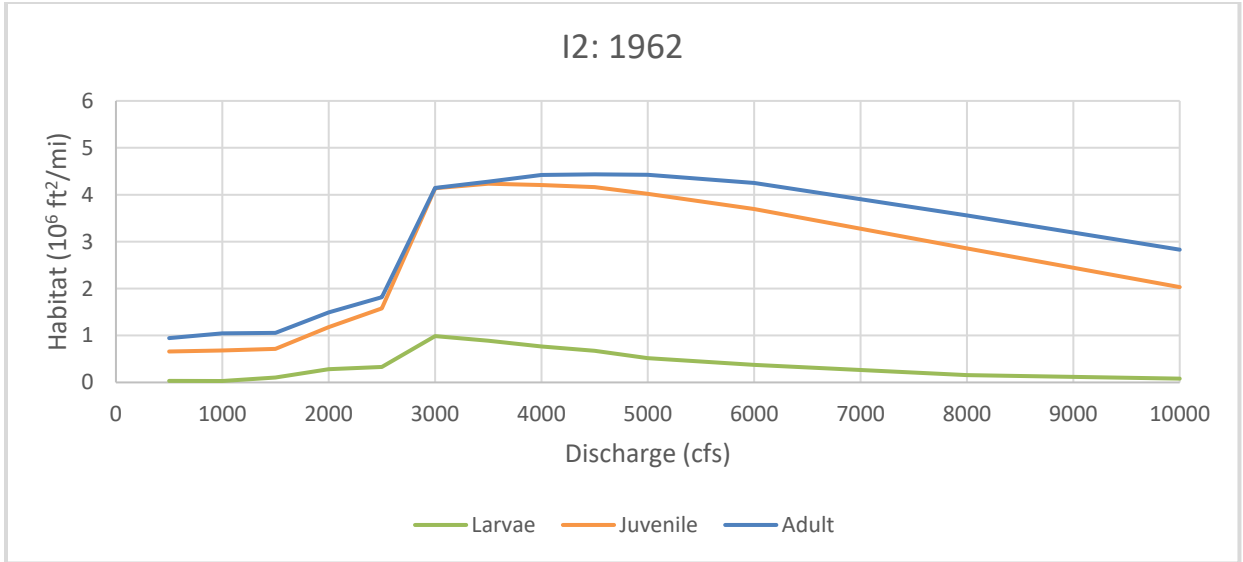


Figure A-6 Larvae, juvenile, and adult habitat curves for subreach I6





*Figure A-7 RGSM life stage habitat curves for 1962, 1972, 1992, 2002, and 2012 for the subreach I1*



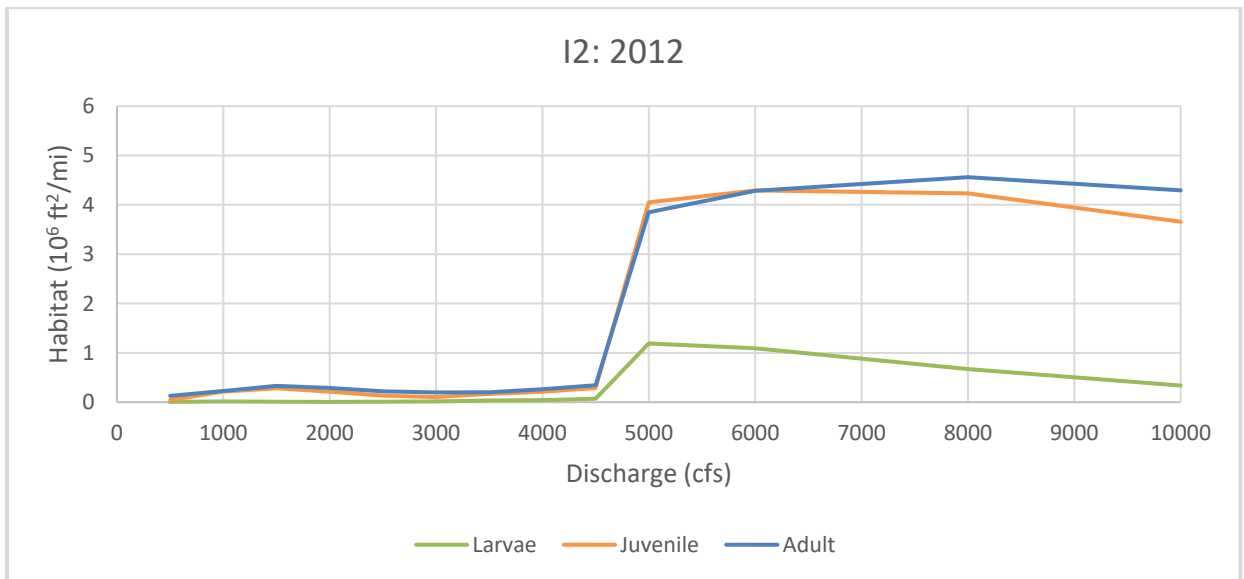
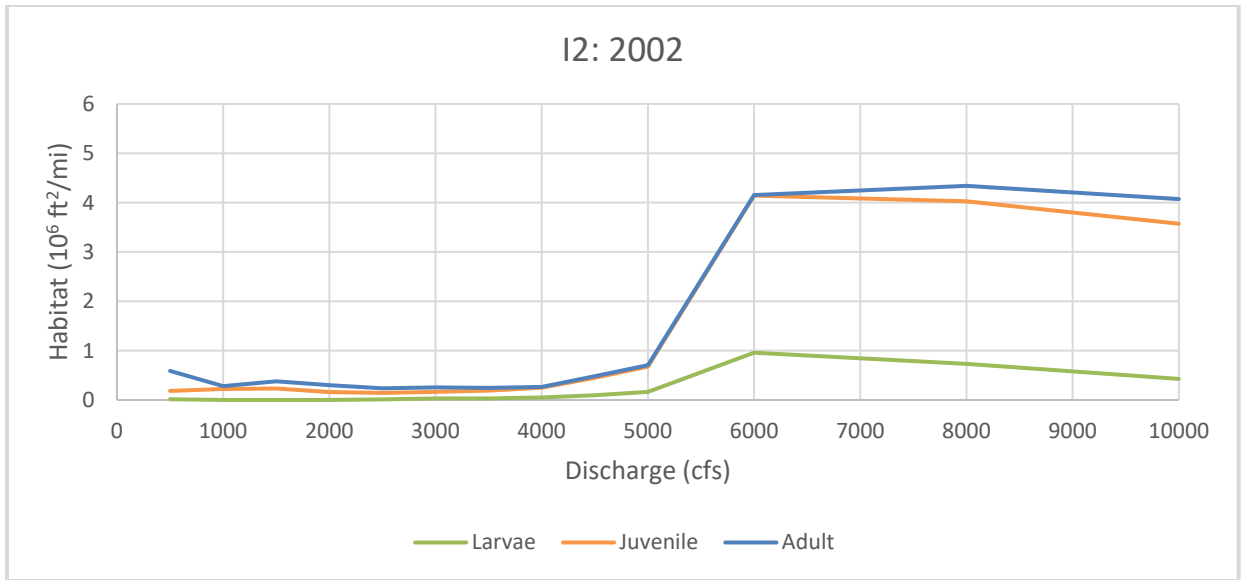
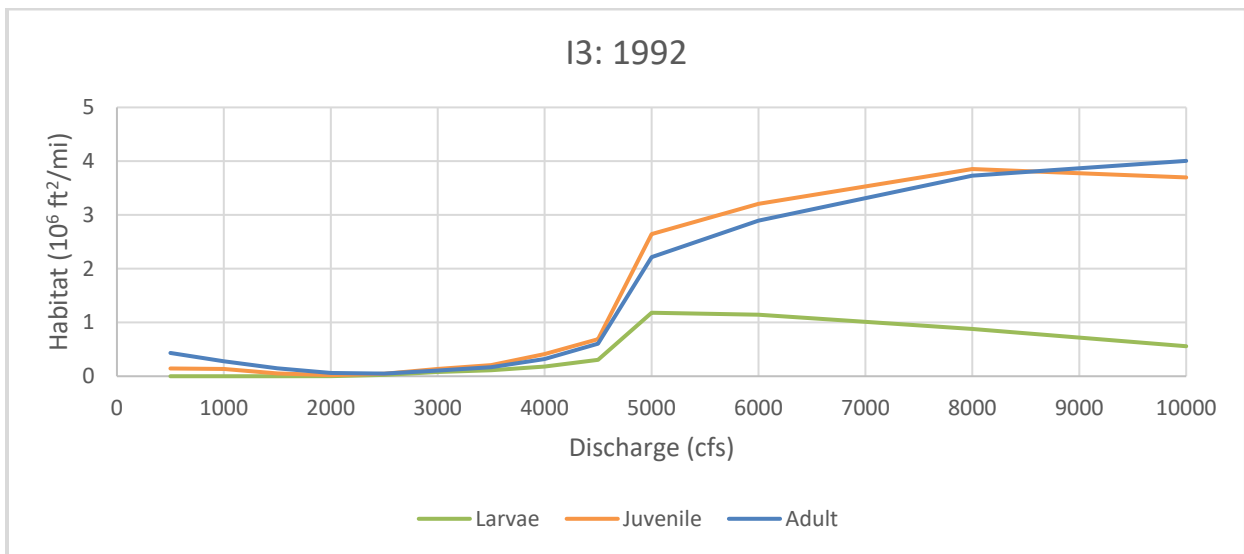
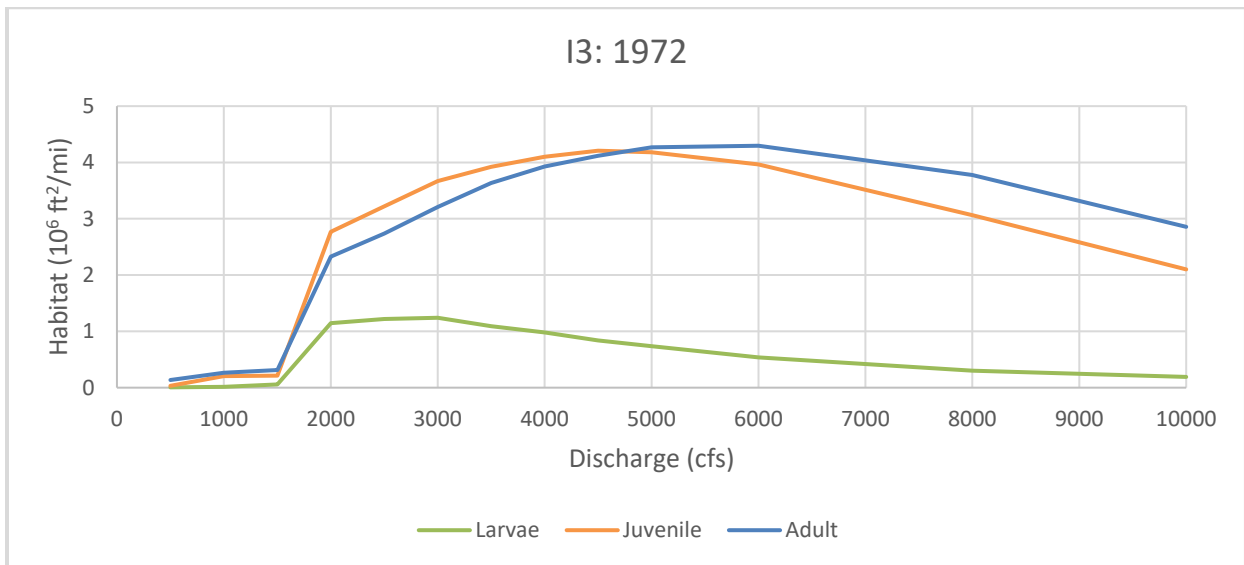
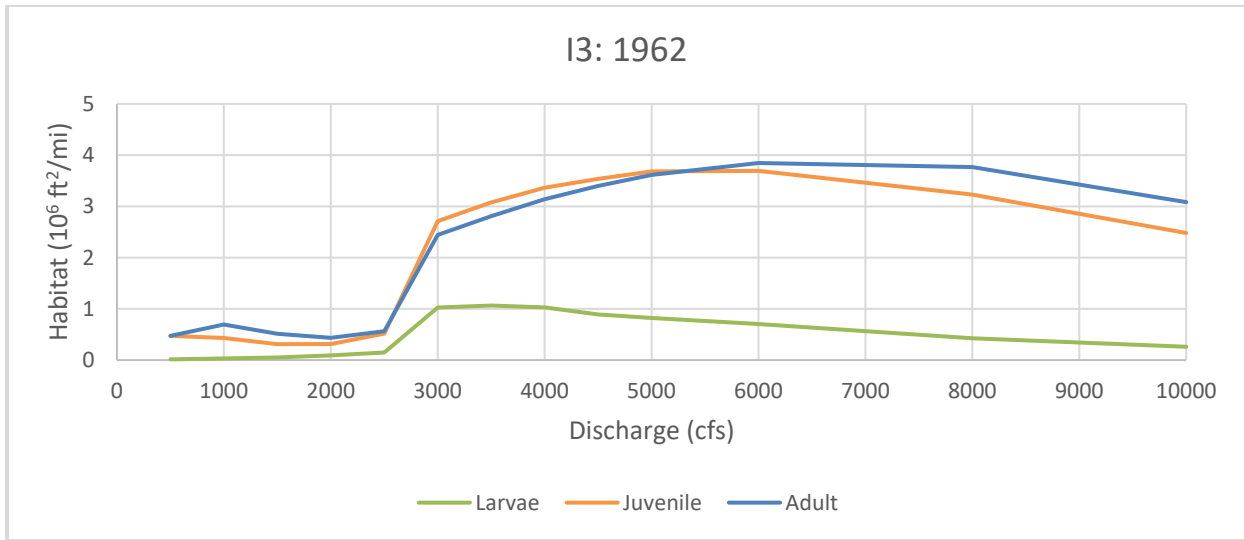


Figure A-8 RGSM life stage habitat curves for 1962, 1972, 1992, 2002, and 2012 for subreach I2



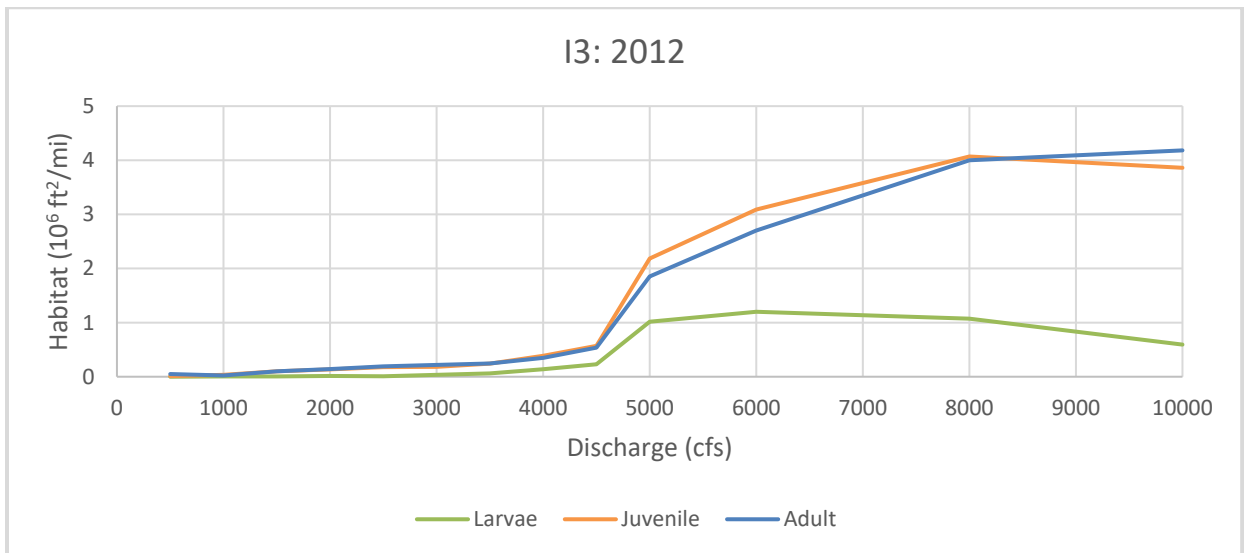
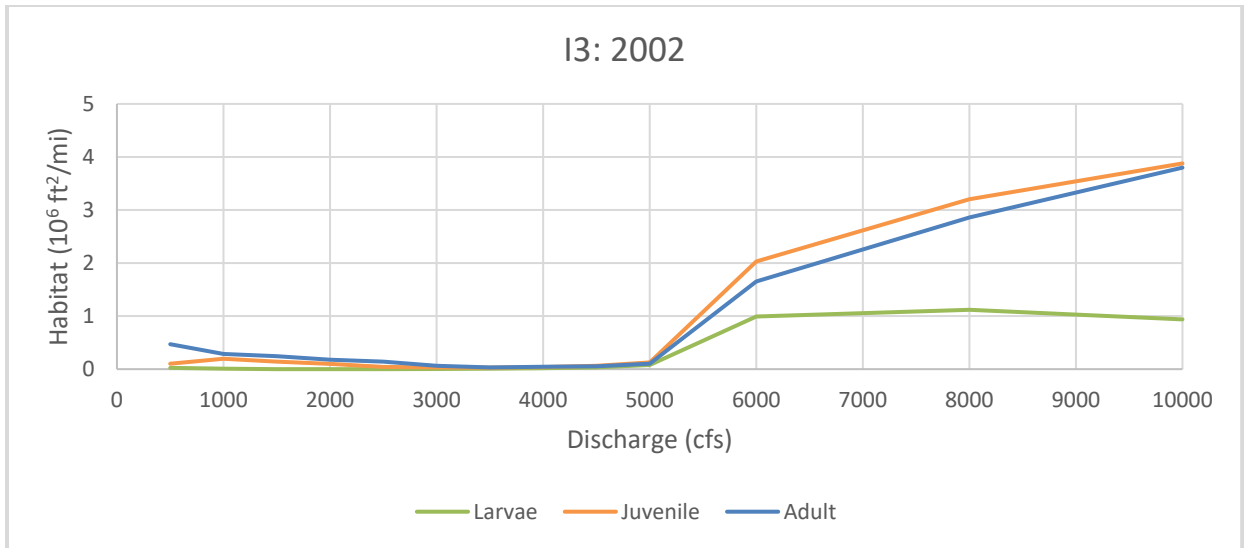
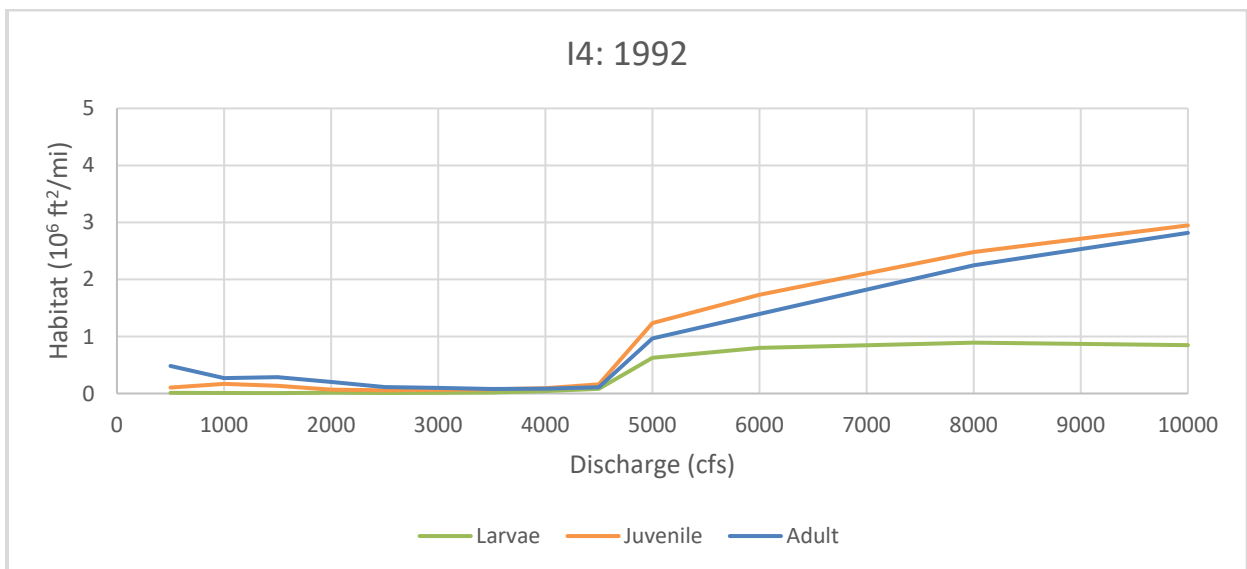
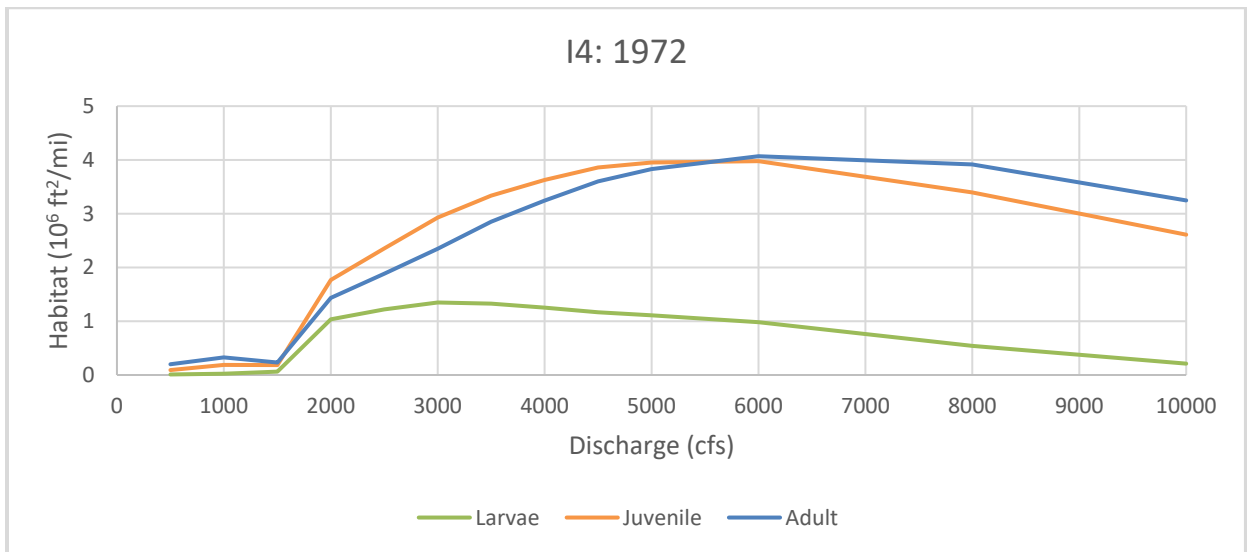
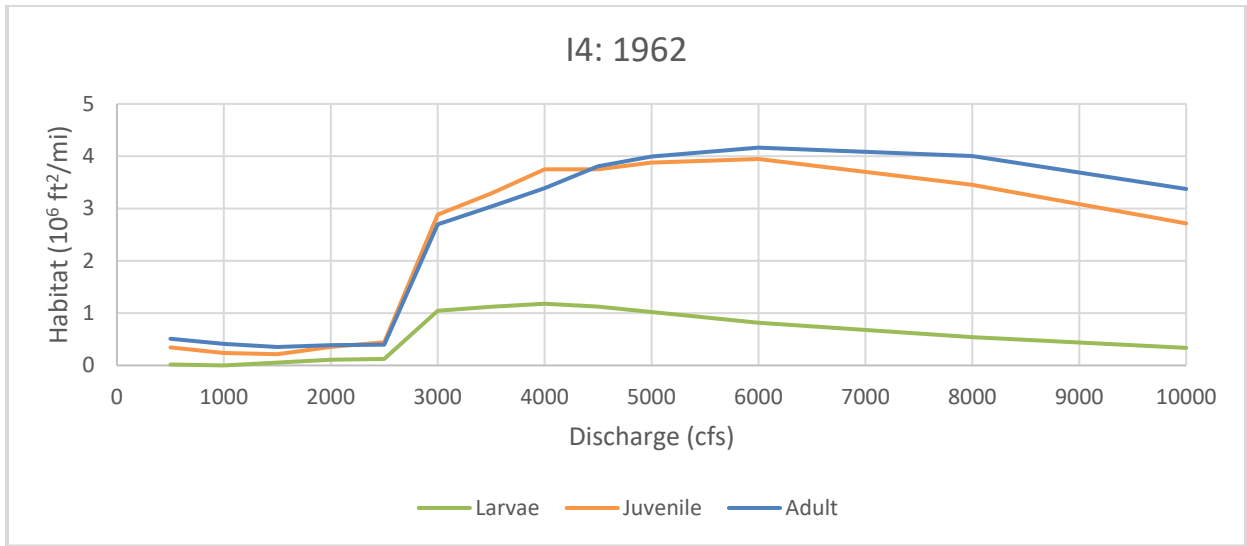


Figure A-9 RGSM life stage habitat curves for 1962, 1972, 1992, 2002, and 2012 for subreach I3



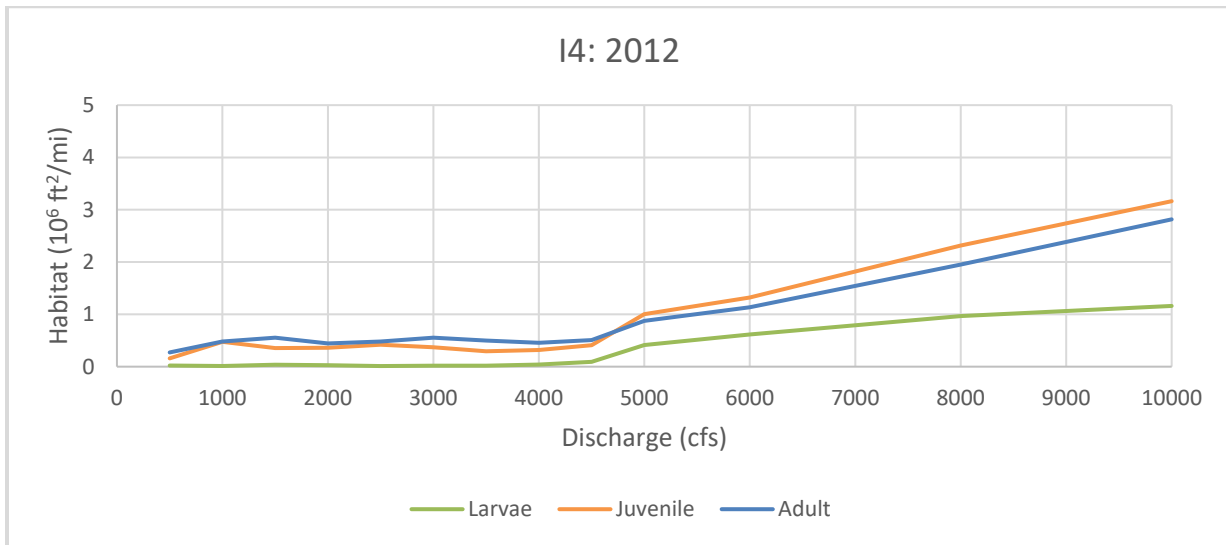
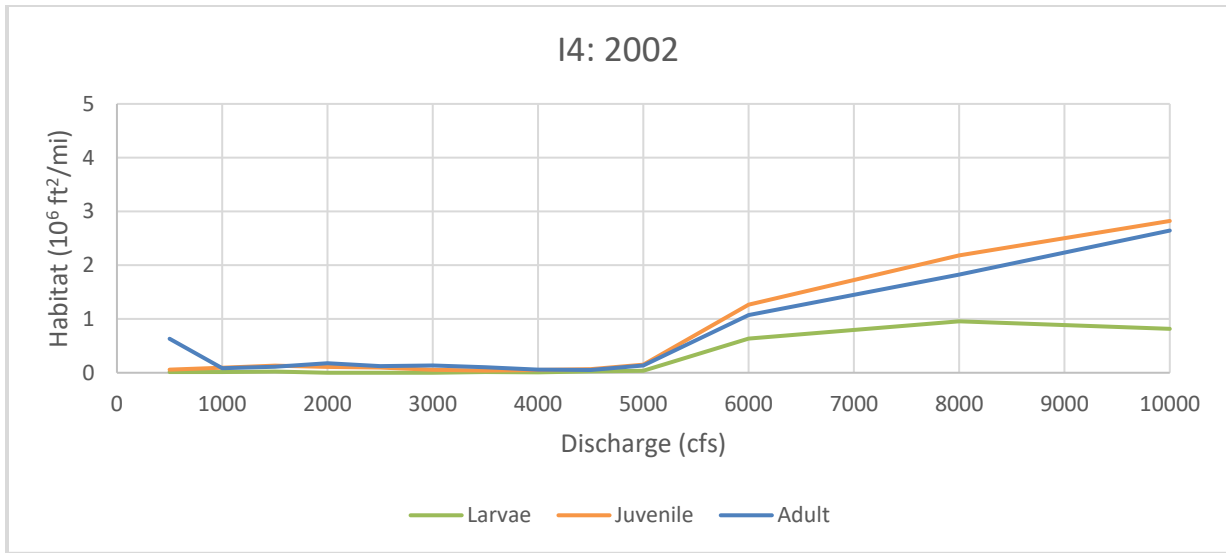
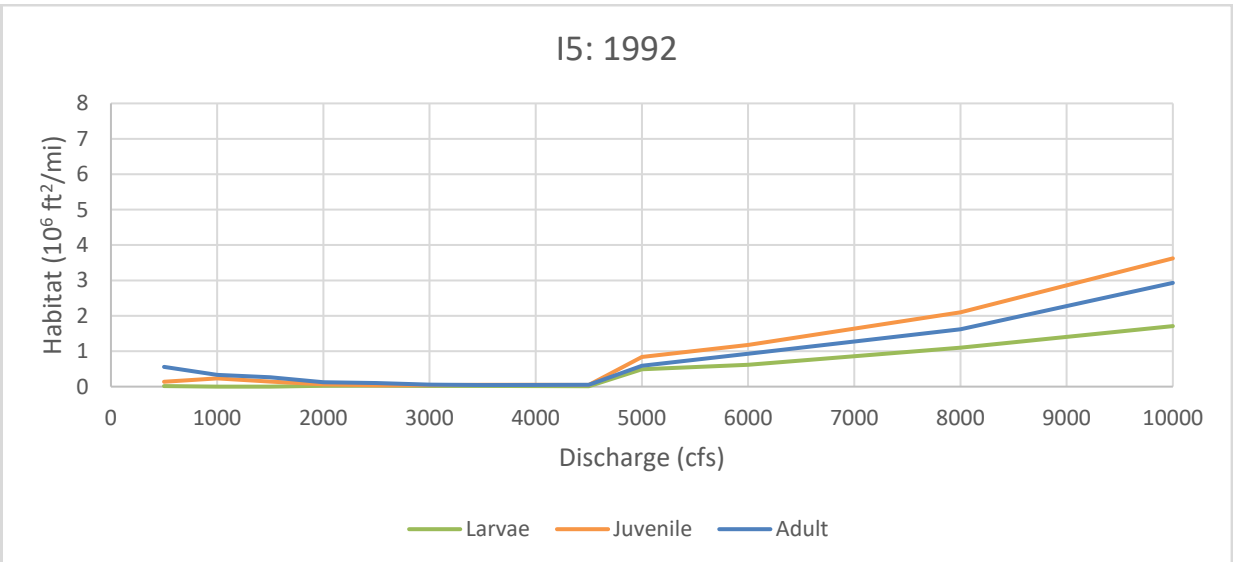
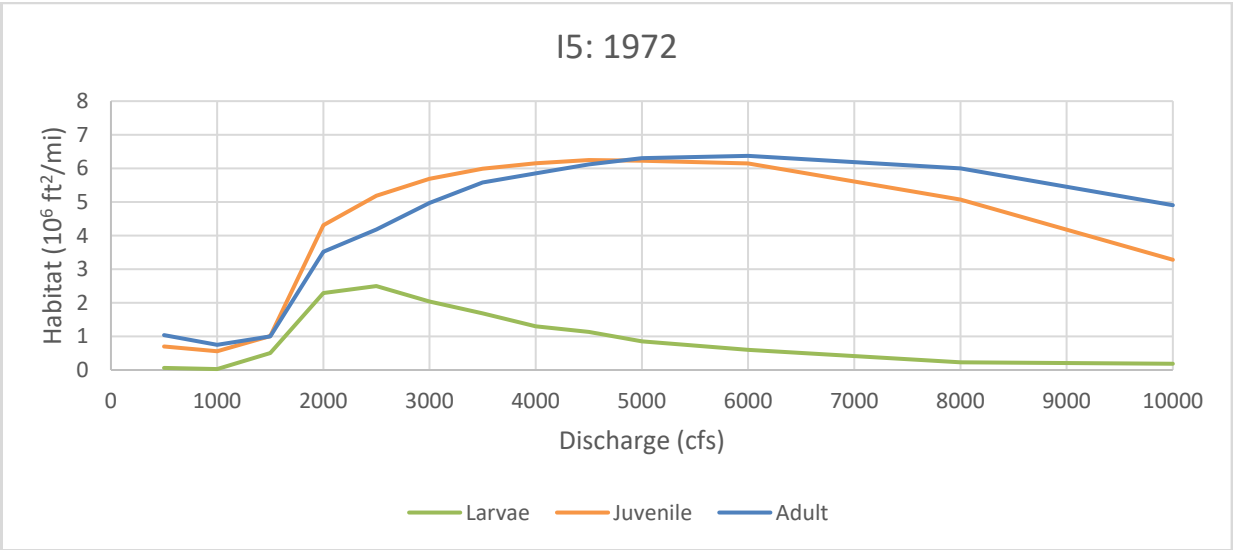
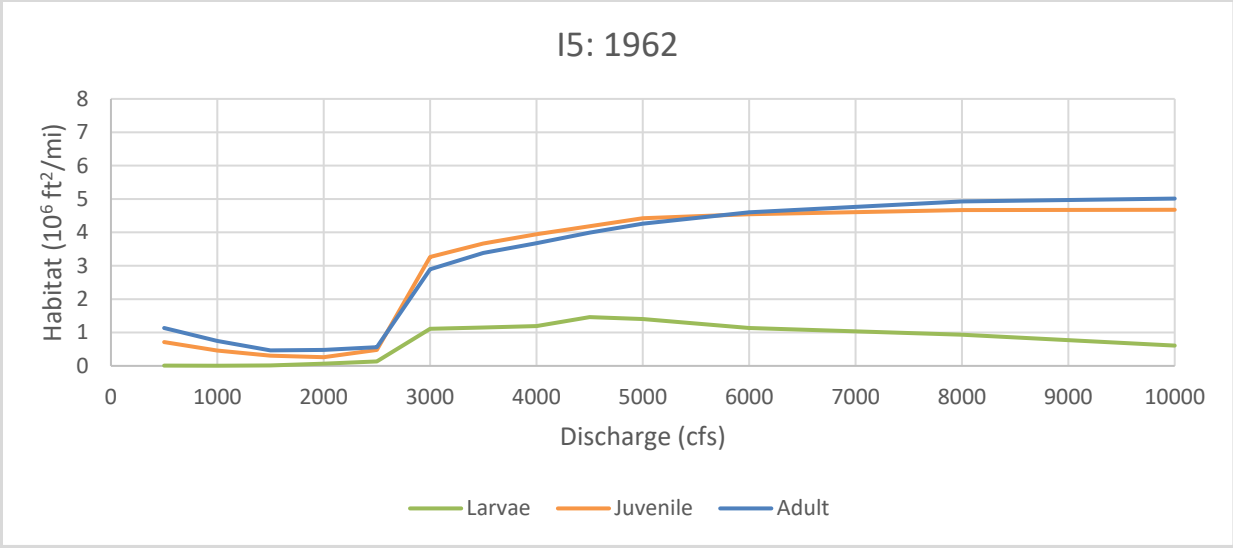


Figure A-10 RGSM life stage habitat curves for 1962, 1972, 1992, 2002, and 2012 for subreach I4



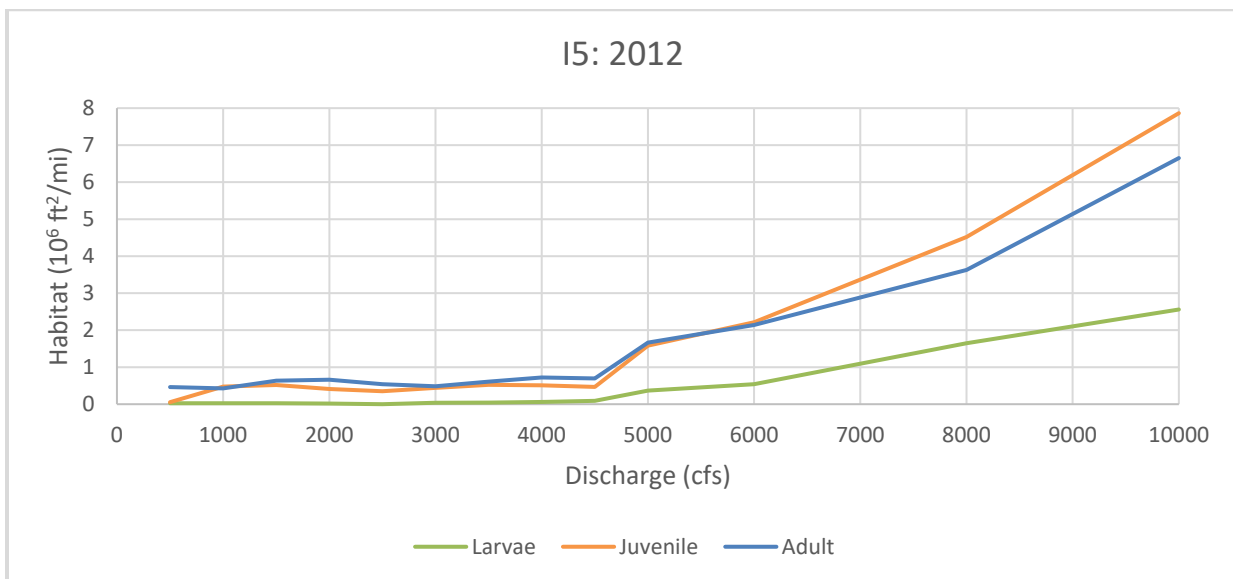
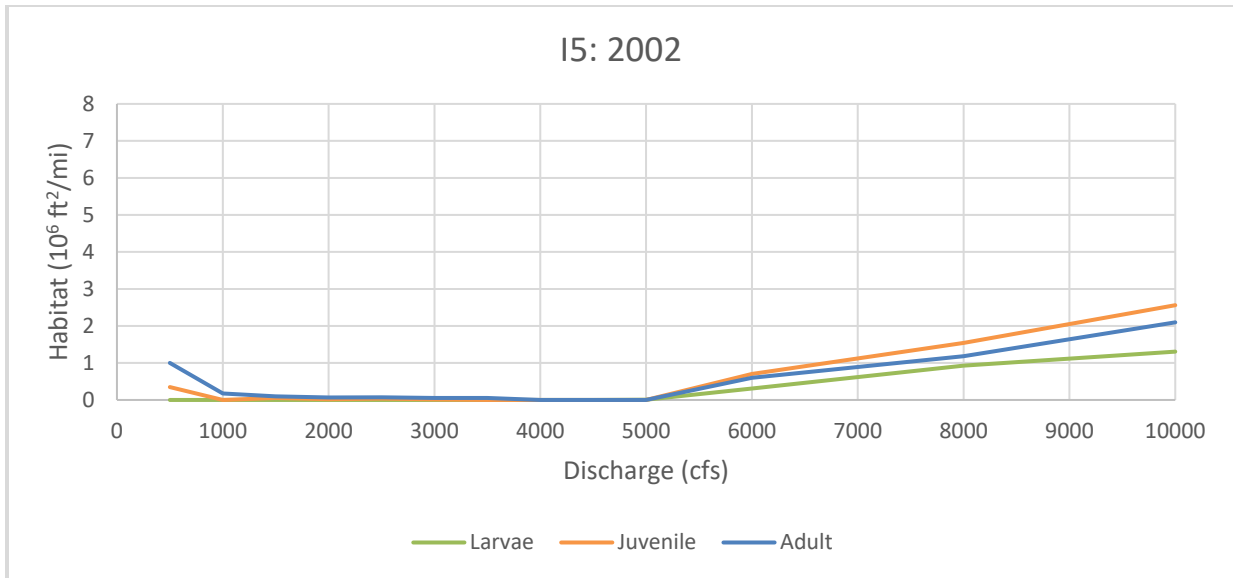
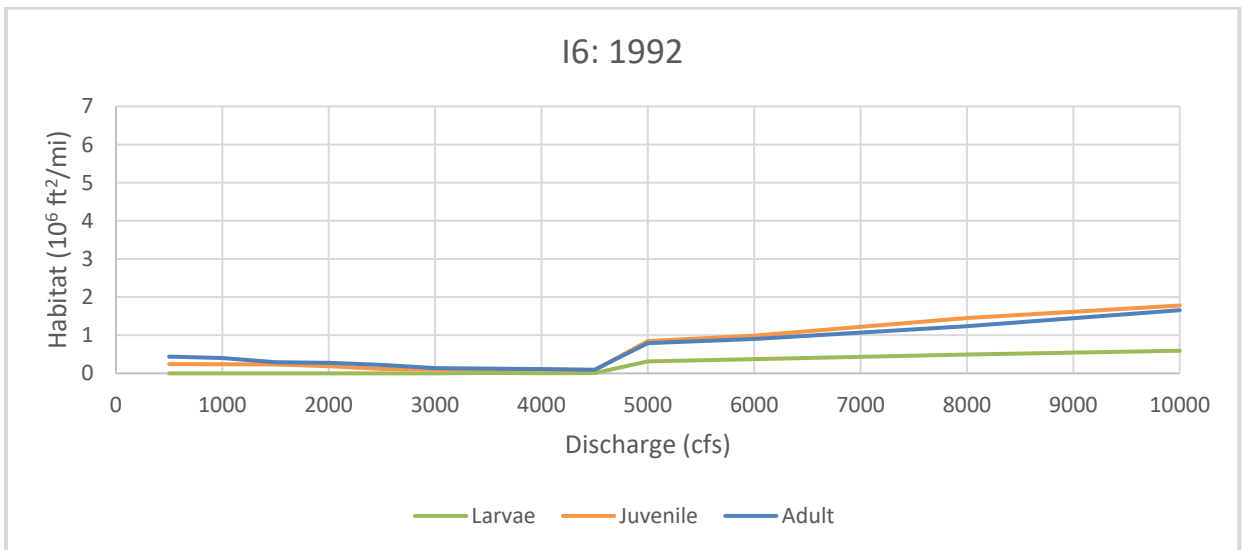
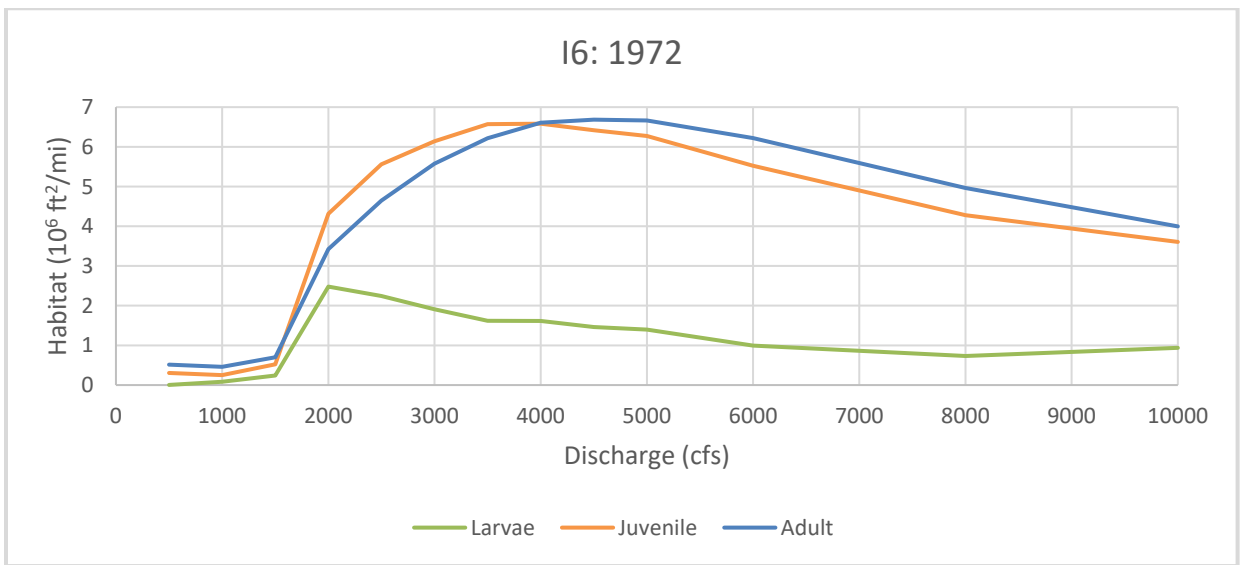
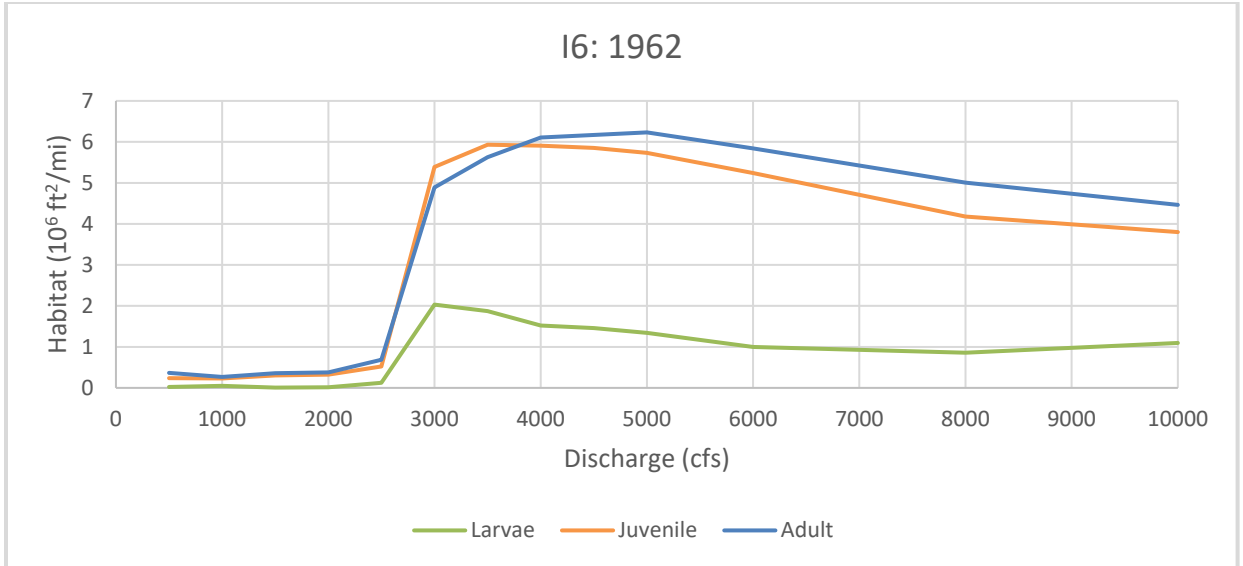


Figure A-11 RGSM life stage habitat curves for 1962, 1972, 1992, 2002, and 2012 for subreach I5



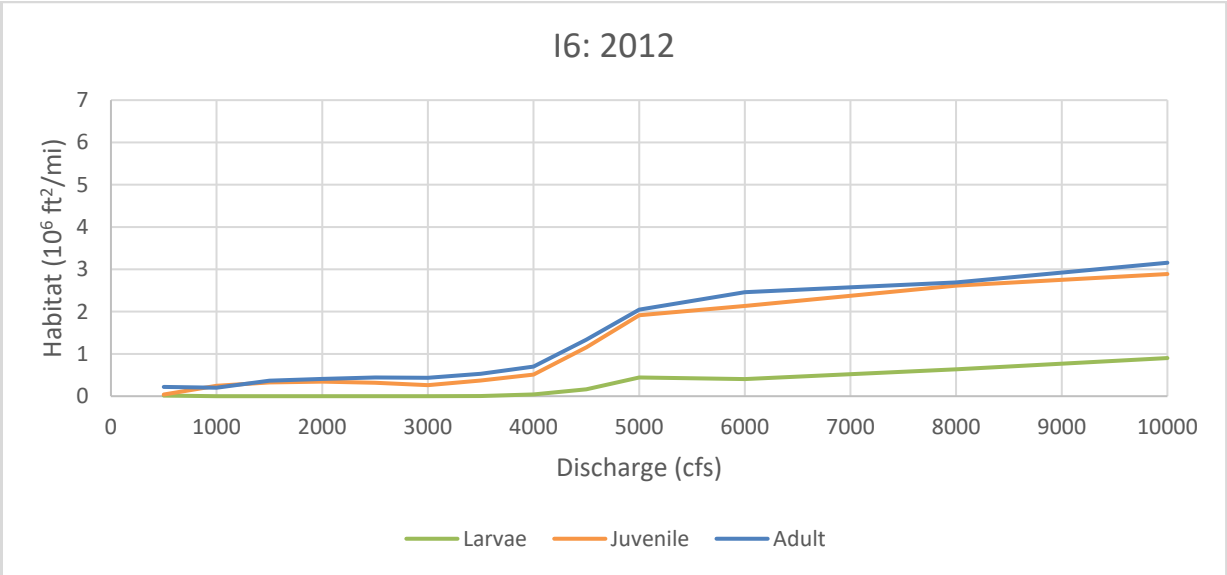
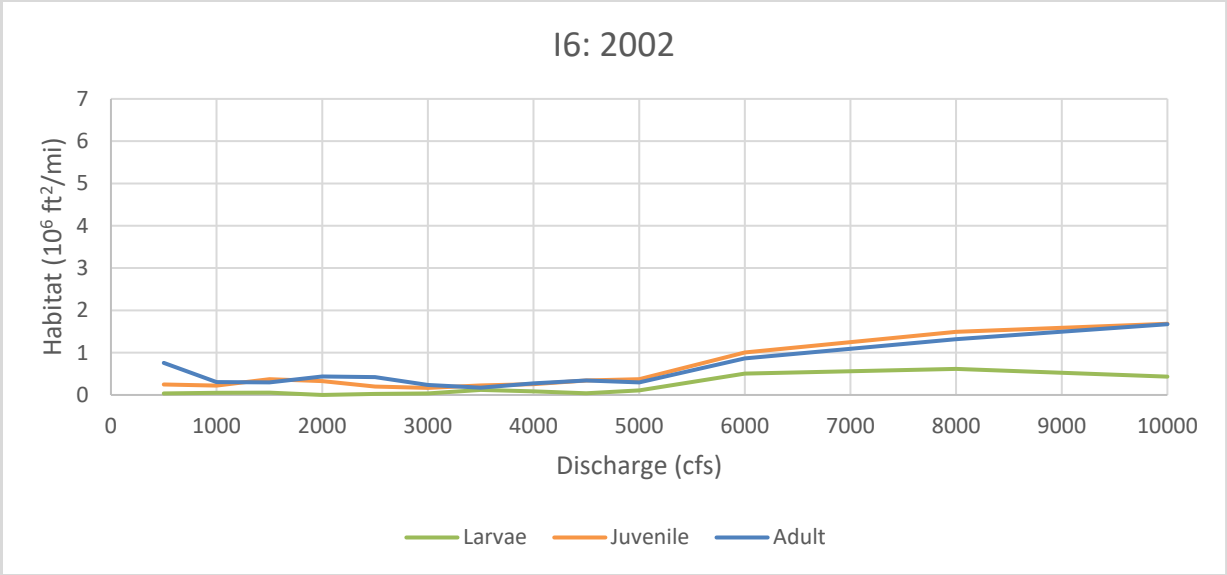


Figure A-12 RGSM life stage habitat curves for 1962, 1972, 1992, 2002, and 2012 for subreach I6

### Additional Spatial Habitat Charts

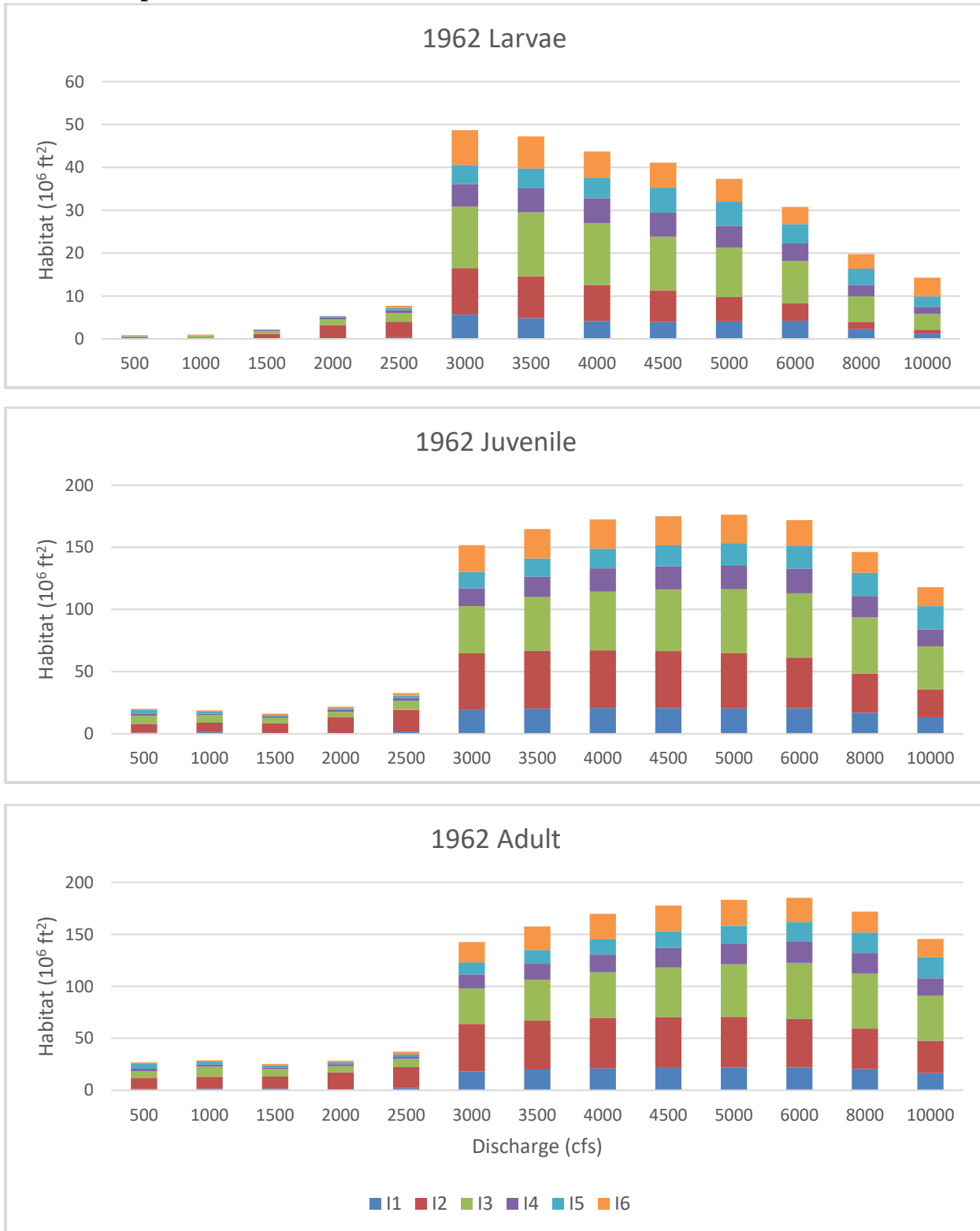


Figure A-13 Stacked life stage habitat charts displaying the spatial variability throughout the Isleta reach in 1962

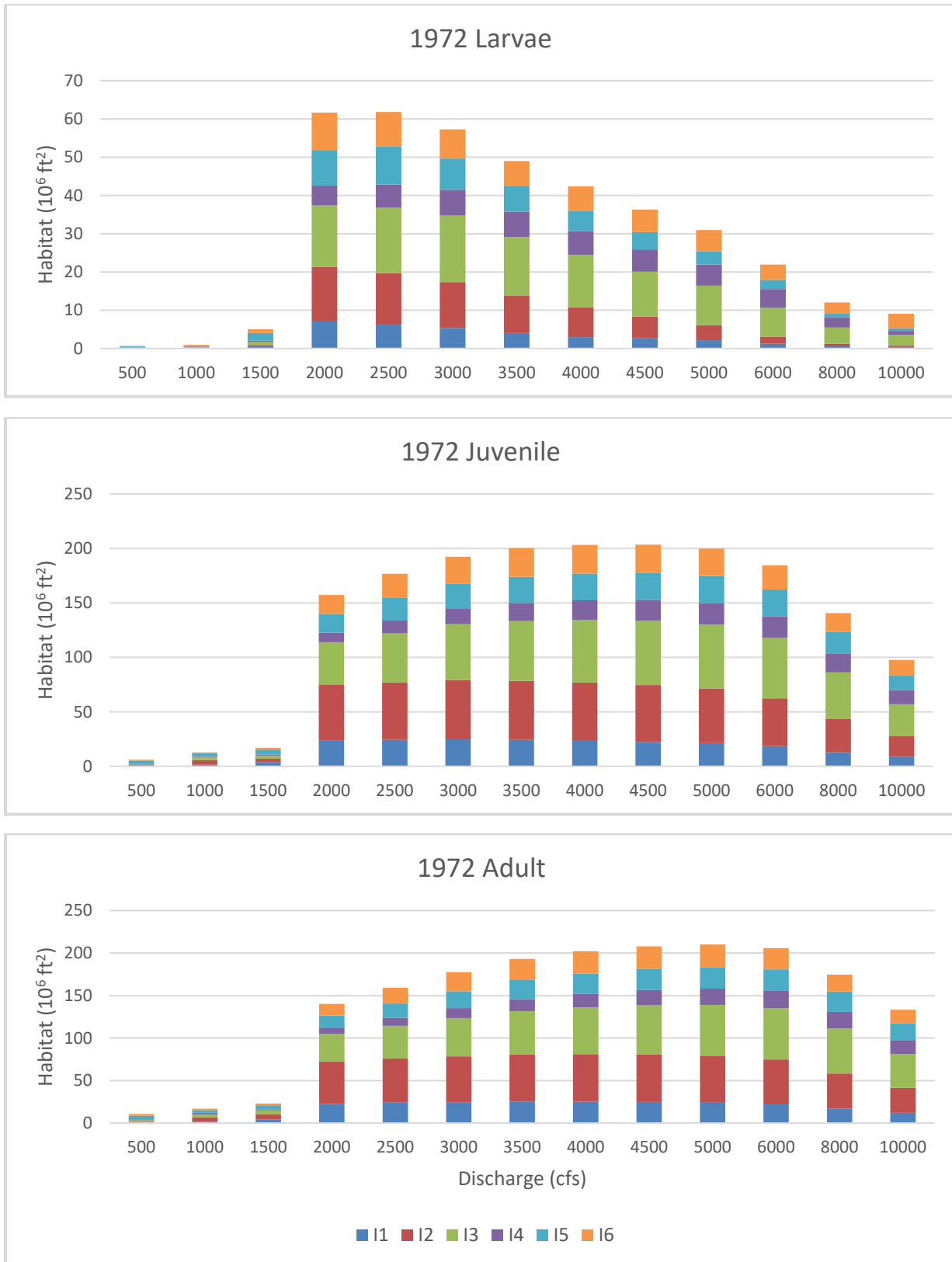
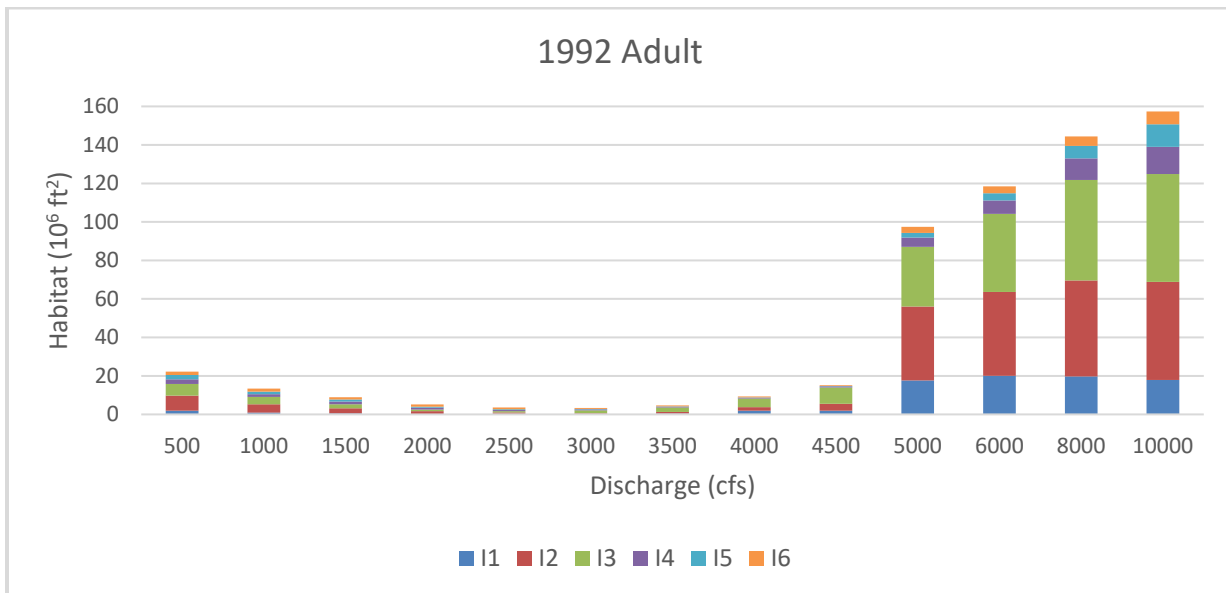
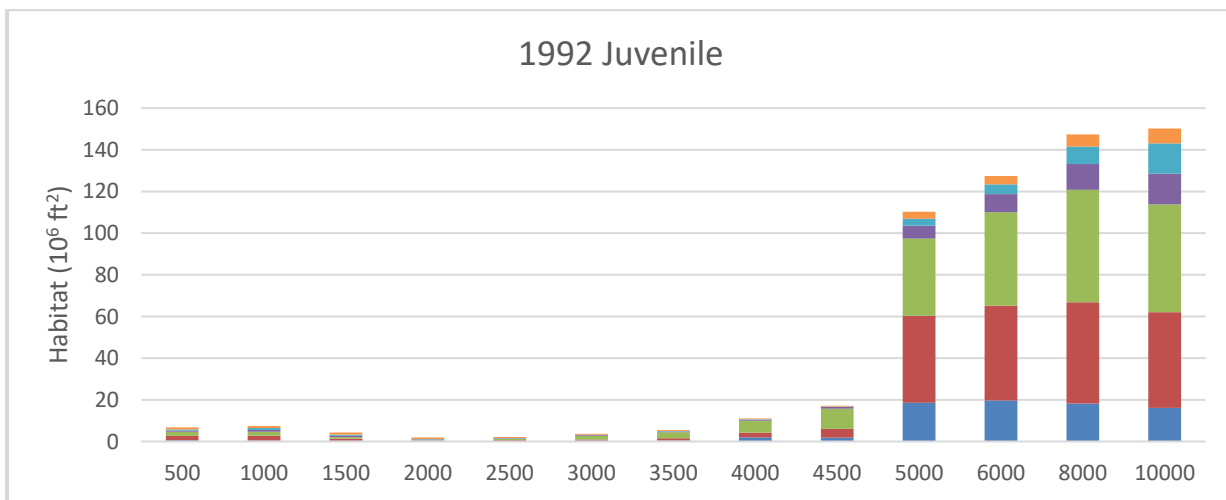
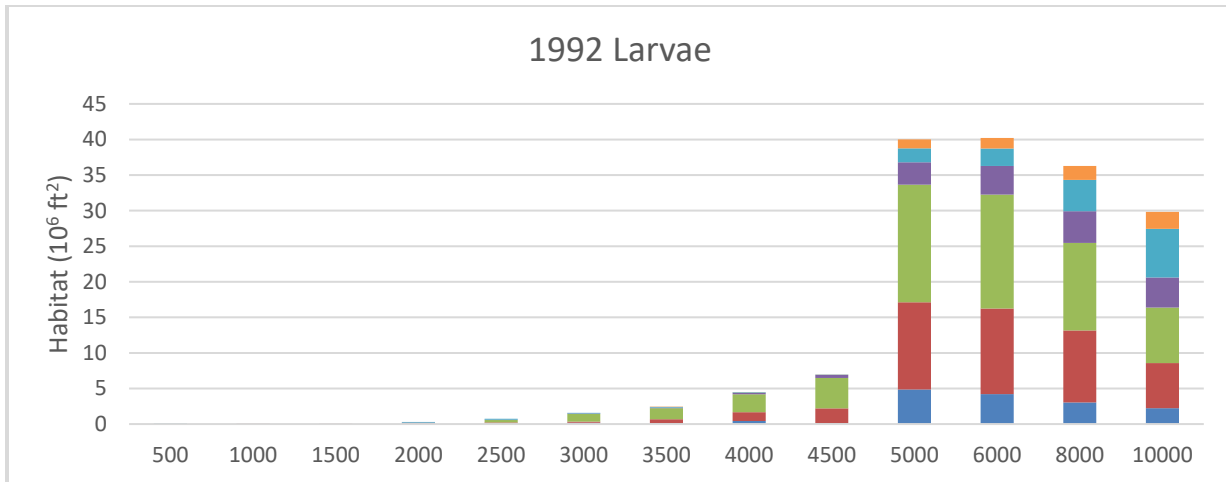


Figure A-14 Stacked life stage habitat charts displaying the spatial variability throughout the Isleta reach in 1972



*Figure A-15 Stacked life stage habitat charts displaying the spatial variability throughout the Isleta reach in 1992*

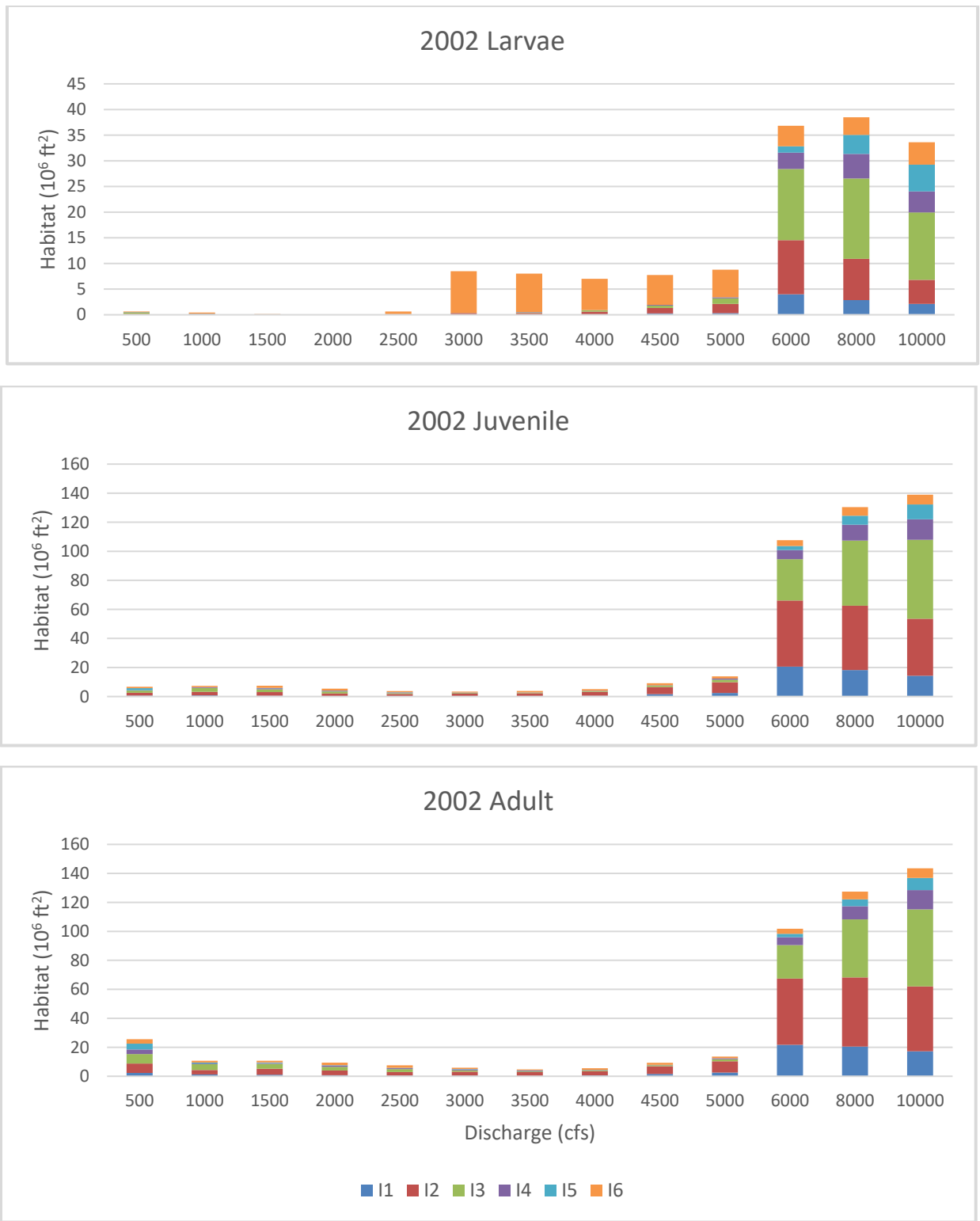


Figure A-16 Stacked life stage habitat charts displaying the spatial variability throughout the Isleta reach in 2002

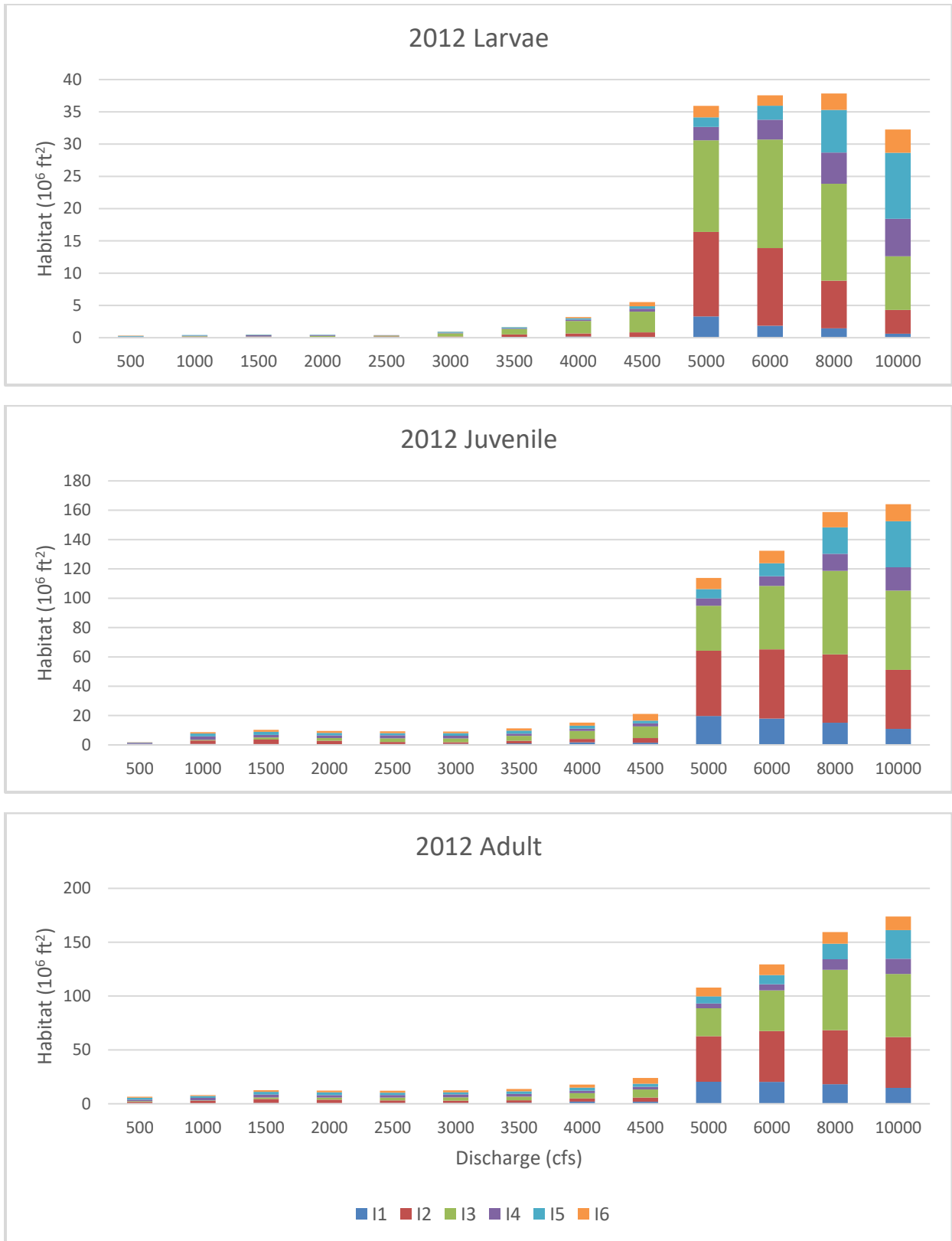


Figure A-17 Stacked life stage habitat charts displaying the spatial variability throughout the Isleta reach in 2012

**Appendix B**  
**Additional Habitat Availability Maps**

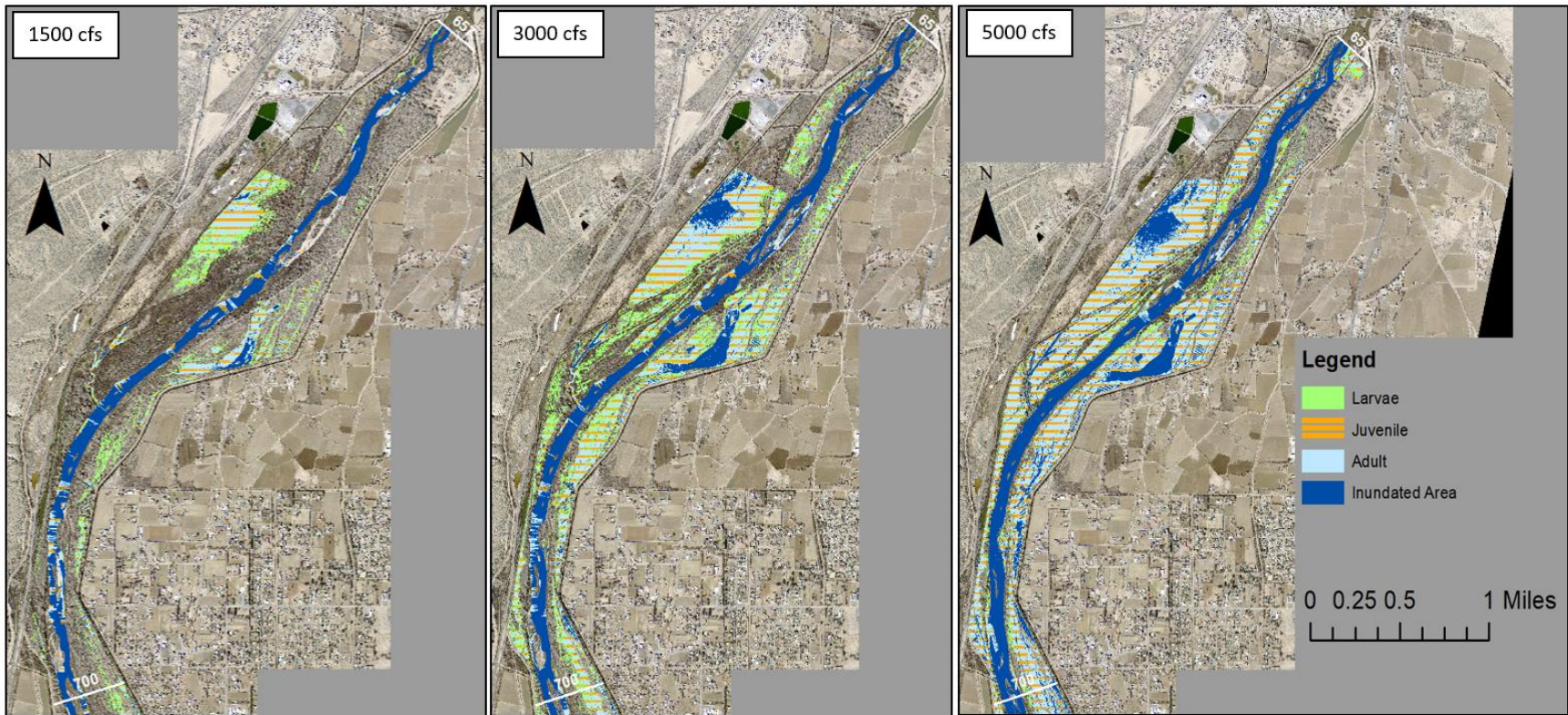


Figure B-1 Life stage habitat availability maps for subreach II. Direction of flow is from north to south

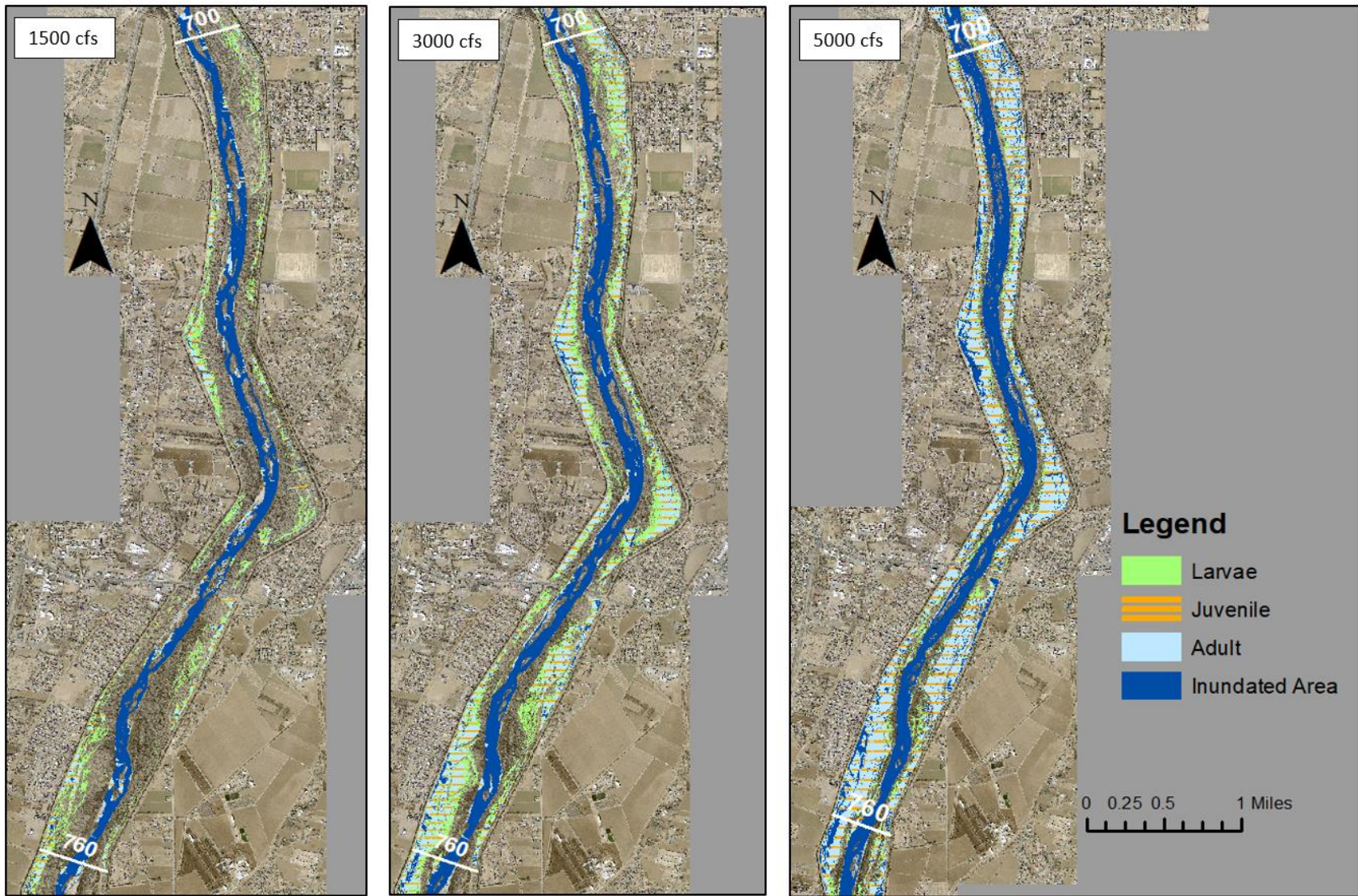


Figure B-2 Life stage habitat availability maps for subreach I2(a). Direction of flow is from north to south

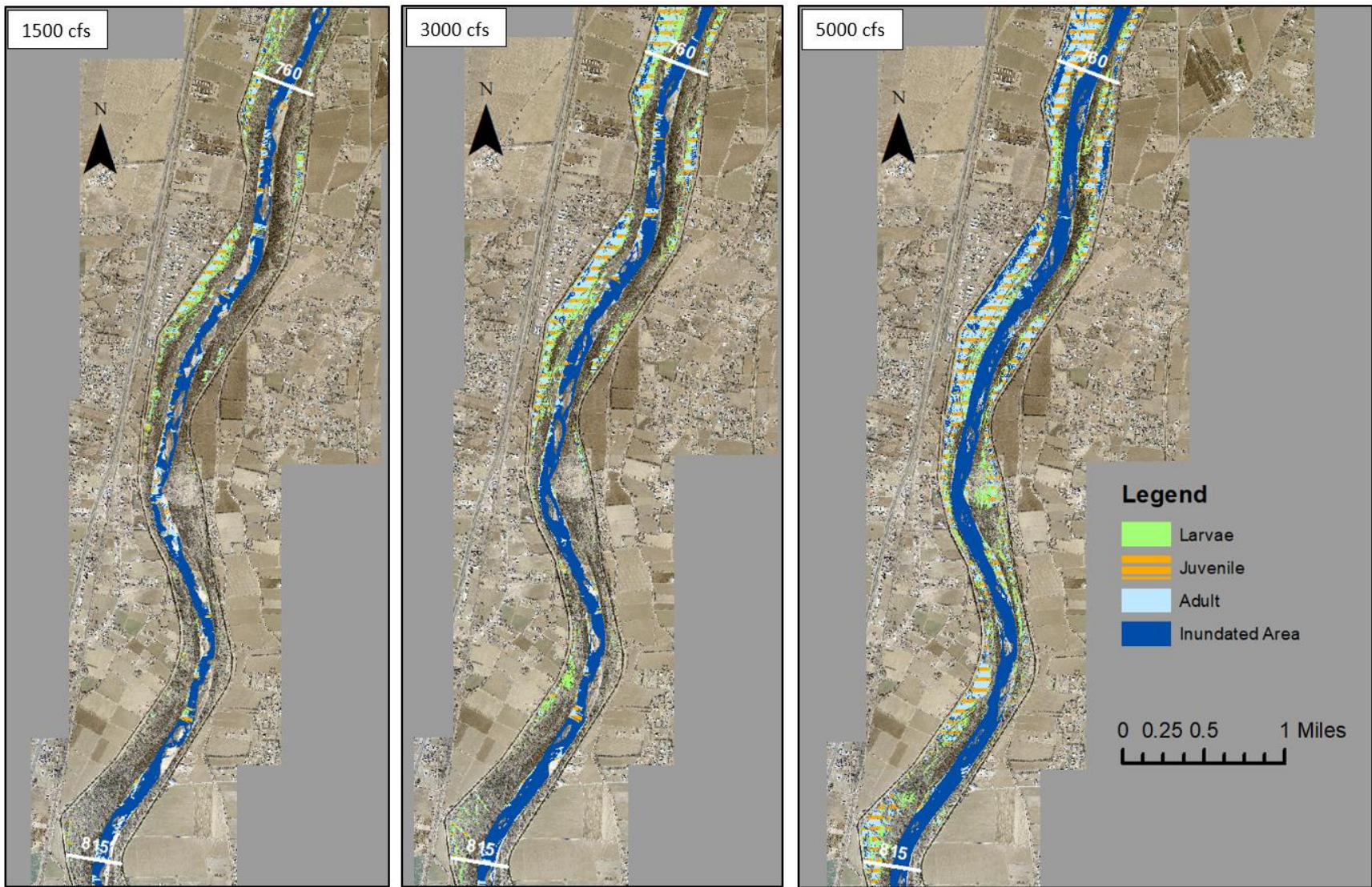


Figure B-3 Life stage habitat availability maps for subreach I2(b). Direction of flow is from north to south

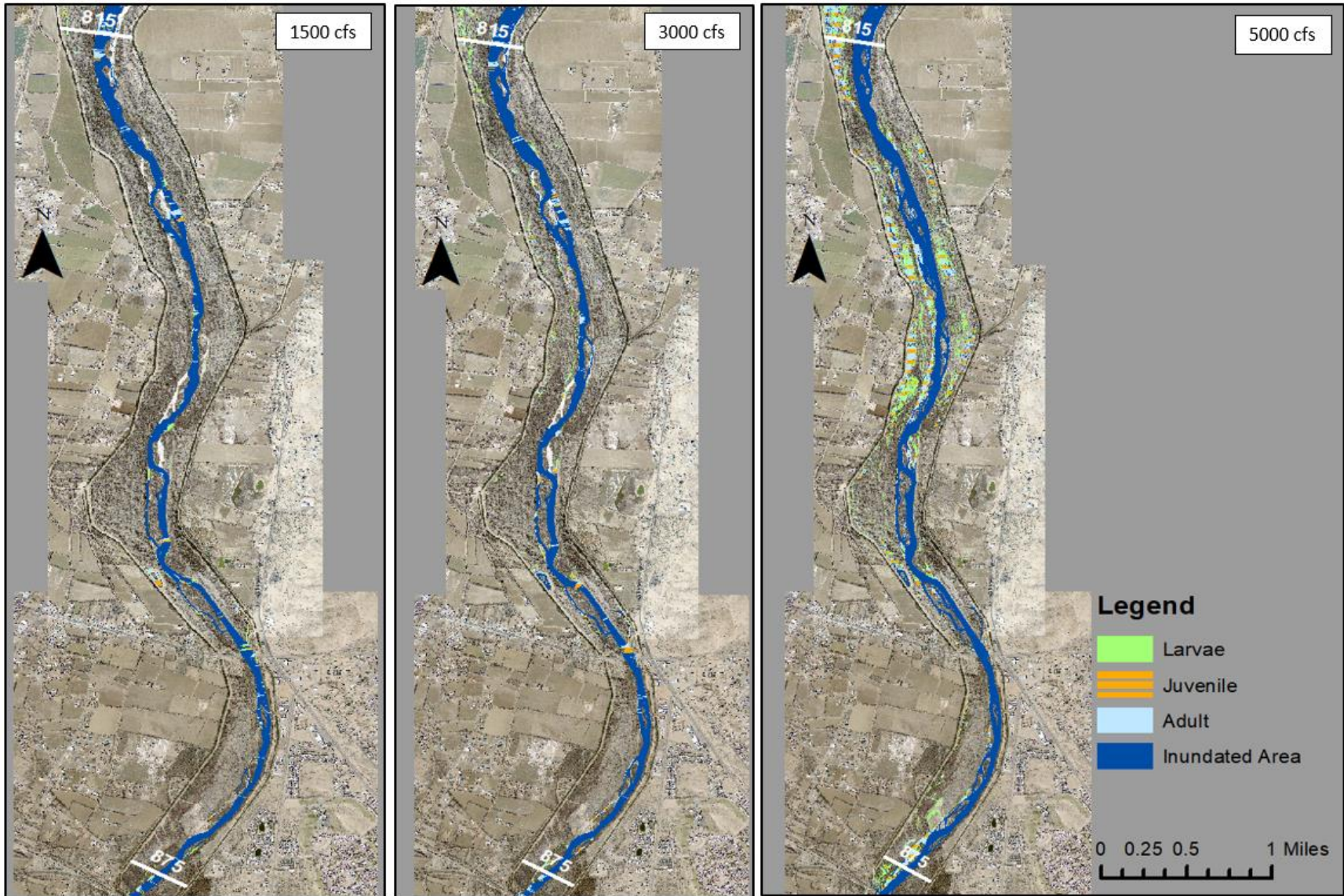


Figure B-4 Life stage habitat availability maps for subreach I3(a). Direction of flow is from north to south

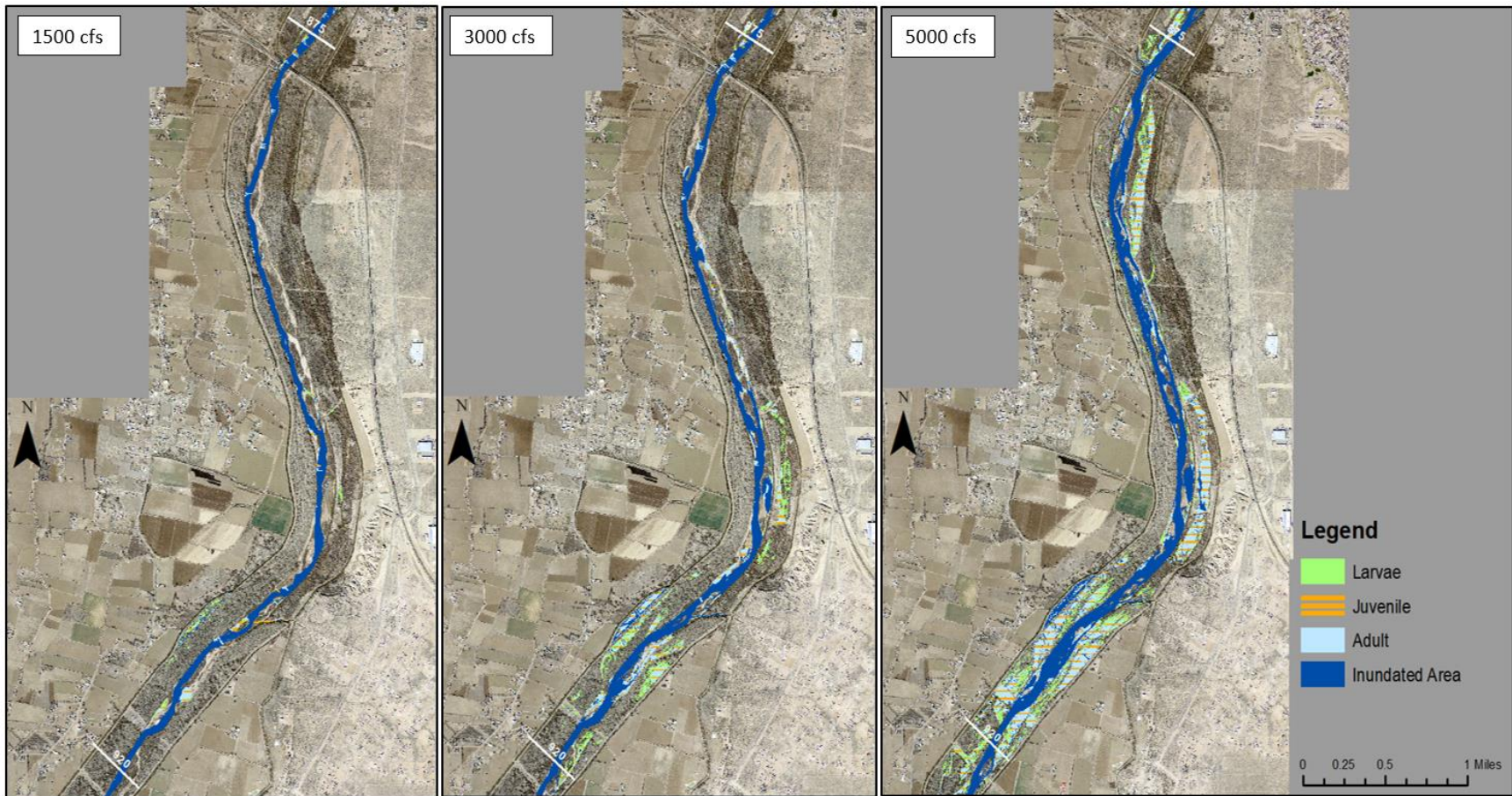


Figure B-5 Life stage habitat availability maps for subreach I3(b). Direction of flow is from north to south

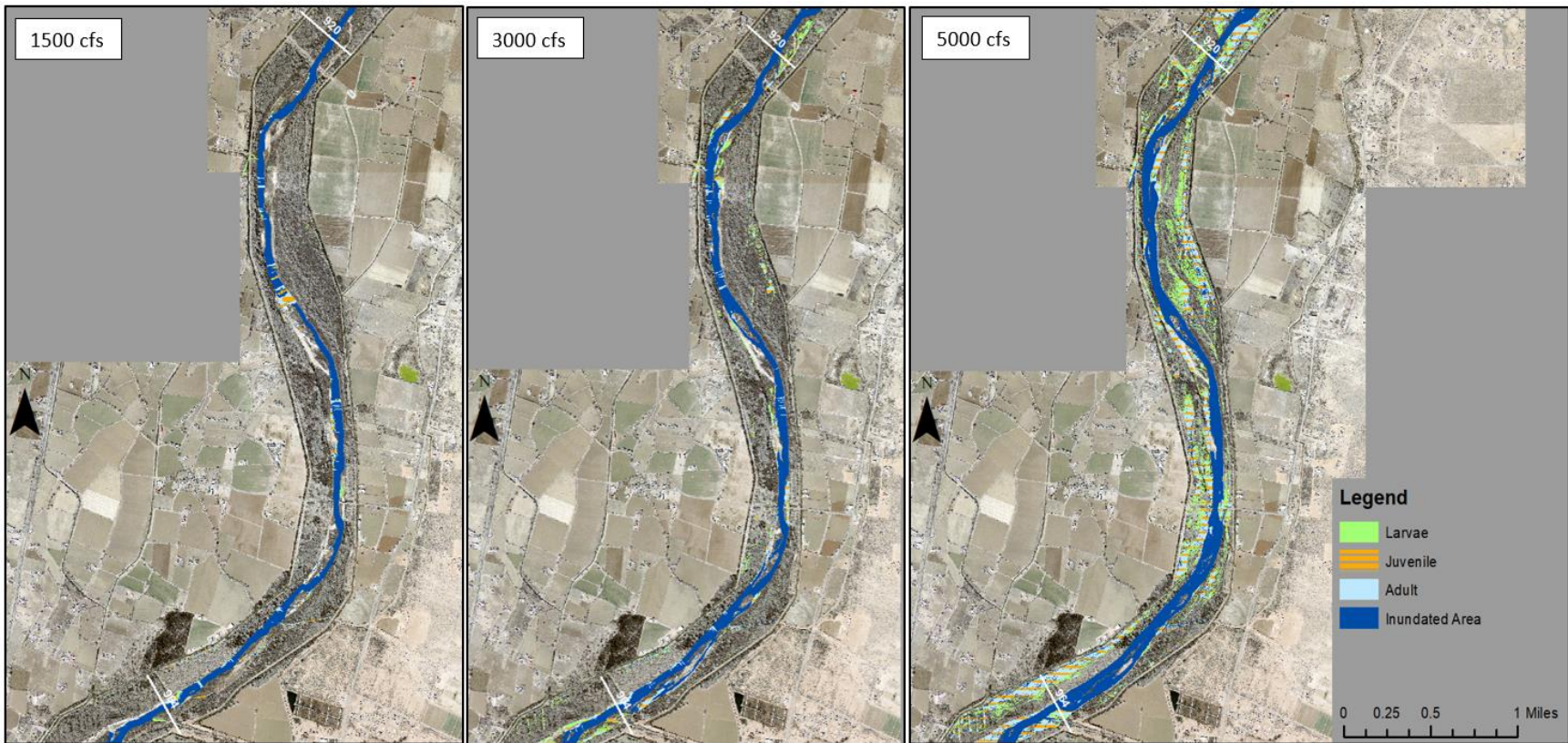


Figure B-6 Life stage habitat availability maps for subreach I3(c). Direction of flow is from north to south

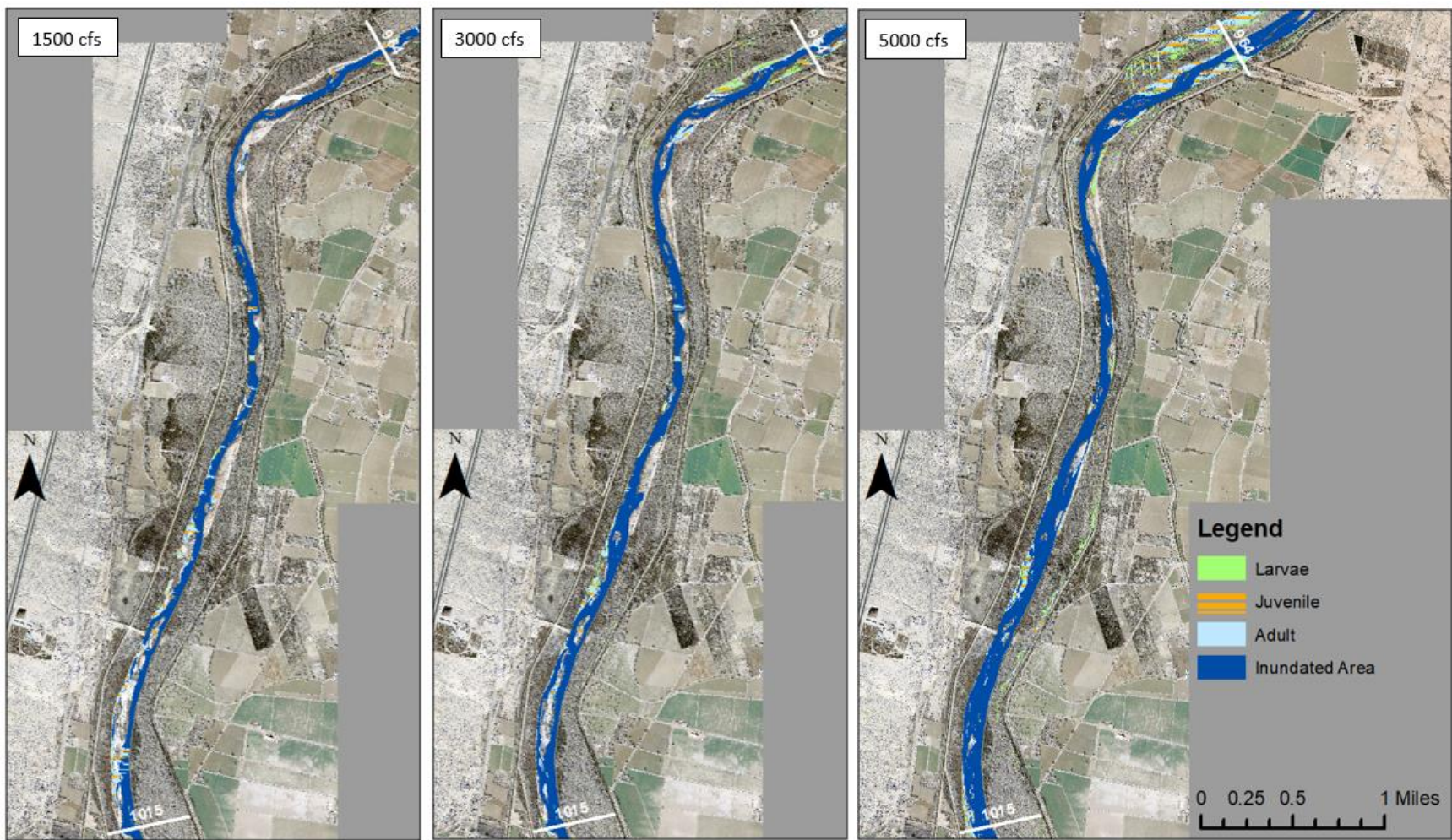


Figure B-7 Life stage habitat availability maps for subreach I4. Direction of flow is from north to south

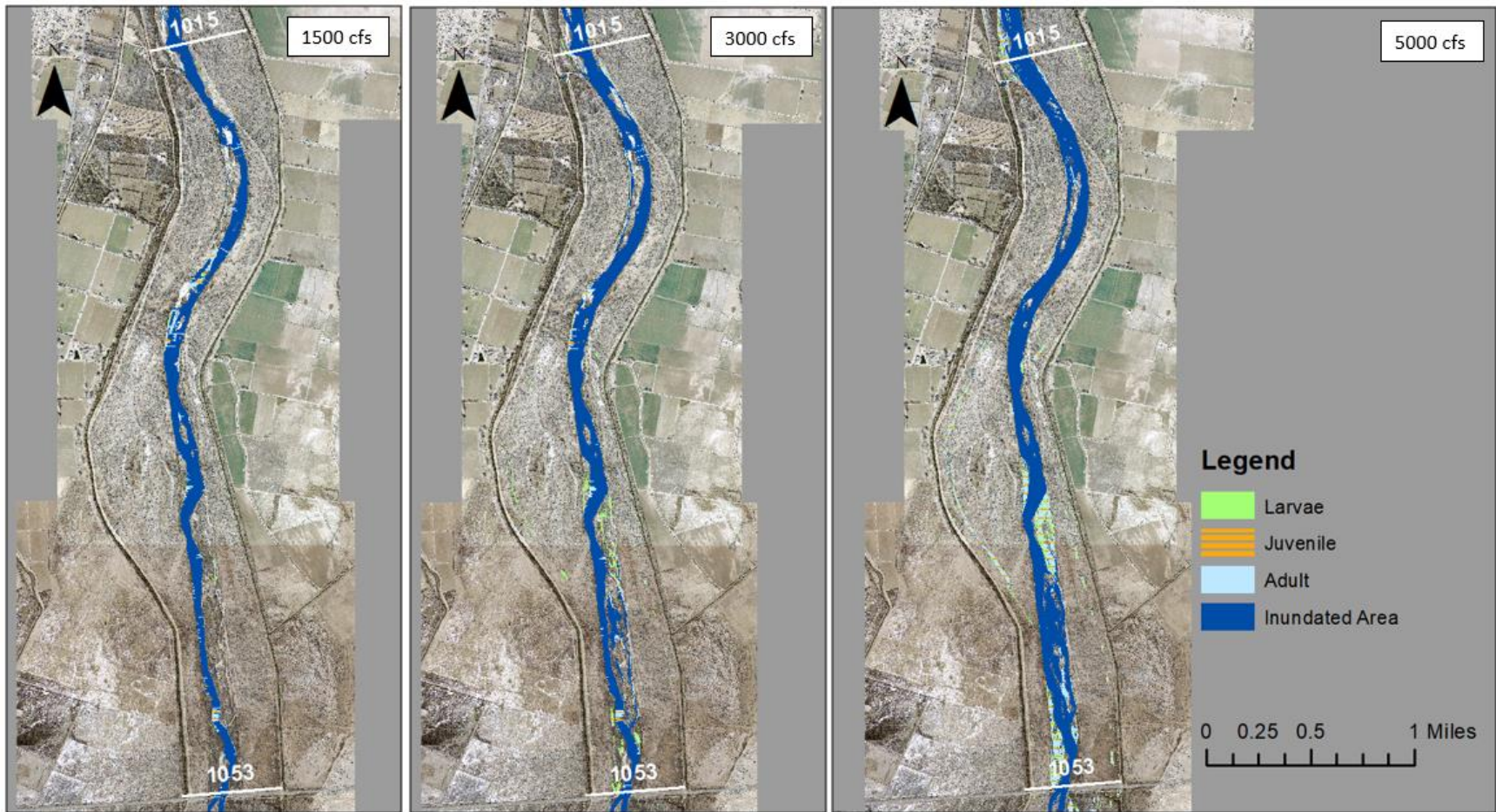


Figure B-8 Life stage habitat availability maps for subreach 15. Direction of flow is from north to south

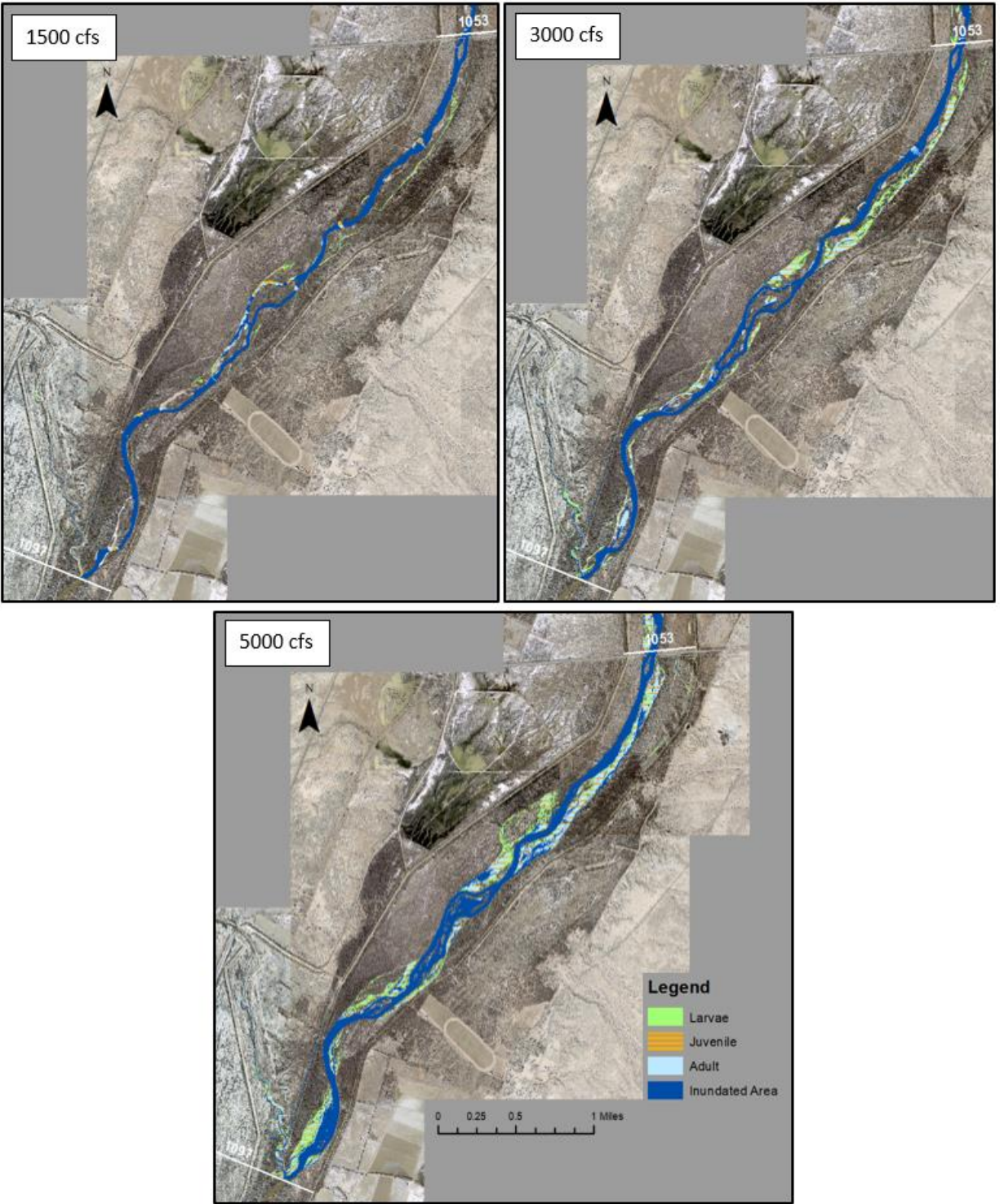


Figure B-9 Life stage habitat availability maps for subreach I6. Direction of flow is from north to south

**Appendix C**  
**Time Integrated Habitat Metrics Program**

Input		Calculation					Calculate Habitat Lengths	
Larvae Habitat Curve (Isleta Reach)		Interpolation		USGS Gage Data				
Discharge (cfs)	Habitat Area (ft <sup>2</sup> /mile)	m	b	Month	Date	Discharge (cfs)	Habitat Area (ft <sup>2</sup> /mile)	
0	0	-	-	10	10/1/2015	12.1	0	
50	0	0.00	0.00	10	10/2/2015	8.09	0	
500	8362	18.58	-928.98	10	10/3/2015	6.85	0	
1000	10169	3.61	6555.00	10	10/4/2015	12	0	
1500	11542	2.75	7421.59	10	10/5/2015	36	0	
2000	11634	0.18	11266.34	10	10/6/2015	56.2	115	
2500	9834	-3.60	18833.17	10	10/7/2015	44.8	0	
3000	22771	25.87	-54847.32	10	10/8/2015	21.4	0	
3500	40415	35.29	-83091.95	10	10/9/2015	14.5	0	
4000	78044	75.26	-222993.78	10	10/10/2015	14	0	
4500	134464	112.84	-373314.76	10	10/11/2015	24.6	0	
5000	875937	1482.95	-6538795.49	10	10/12/2015	14	0	
6000	915908.41	39.97	676082.56	10	10/13/2015	11.5	0	
8000	922837.32	3.46	895121.71	10	10/14/2015	11.5	0	
10000	787050.00	-67.89	1465986.59	10	10/15/2015	30.6	0	
				10	10/16/2015	18.4	0	
				10	10/17/2015	17.4	0	
				10	10/18/2015	18.3	0	
				10	10/19/2015	46	0	
				10	10/20/2015	40.4	0	
				10	10/21/2015	70.5	381	
				10	10/22/2015	246	3642	
				10	10/23/2015	713	12320	
				10	10/24/2015	524	8808	
				10	10/25/2015	554	9365	
				10	10/26/2015	558	9440	
				10	10/27/2015	424	6950	
				10	10/28/2015	391	6336	
				10	10/29/2015	271	4107	
				10	10/30/2015	350	5575	
				10	10/31/2015	450	7433	
				11	11/1/2015	467	7749	
				11	11/2/2015	438	7210	
				11	11/3/2015	444	7321	
				11	11/4/2015	391	6336	
				11	11/5/2015	414	6764	
				11	11/6/2015	389	6299	
				11	11/7/2015	469	7786	
				11	11/8/2015	441	7266	
				11	11/9/2015	524	8808	
				11	11/10/2015	528	8882	
				11	11/11/2015	713	12320	
				11	11/12/2015	901	9811	
				11	11/13/2015	932	9923	
				11	11/14/2015	954	10002	
				11	11/15/2015	980	10096	
				11	11/16/2015	1010	10205	
				11	11/17/2015	1110	10566	
				11	11/18/2015	1250	11072	

Cut-off discharge

Linear interpolation between discharges

Figure C-1 Example worksheet from the TIHMs program for larval habitat interpolation

Month	Total Habitat (ft <sup>2</sup> /mile)	avg
10	74471.6	2402.3
11	290220.7	9674
12	348720.7	11249
1	334342.2	10785
2	305219.0	10525
3	299269.4	9653.9
4	199216.6	6640.6
5	313798.8	10123
6	328620.8	10954
7	36341.1	1172.3
8	59653.5	1924.3
9	0.9	0.0293

Lifestage Time Period	Total Habitat (ft <sup>2</sup> /mile)
Larvae (5-6)	642419.7
Larvae Entire Year	2589875.2

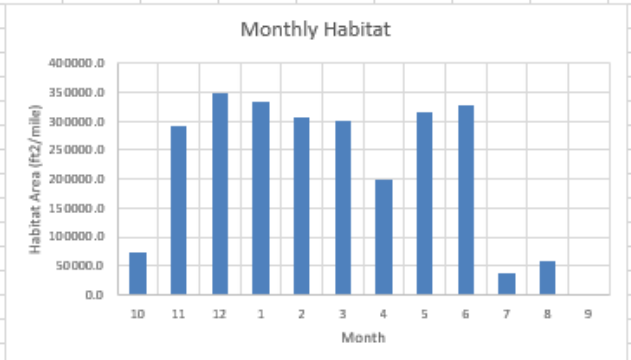
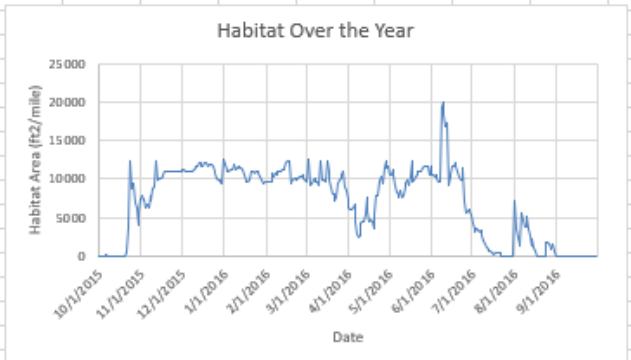
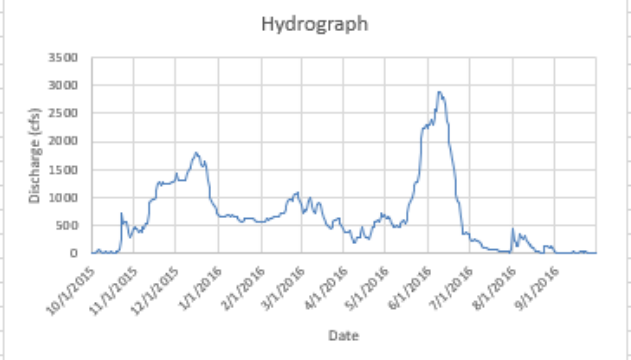
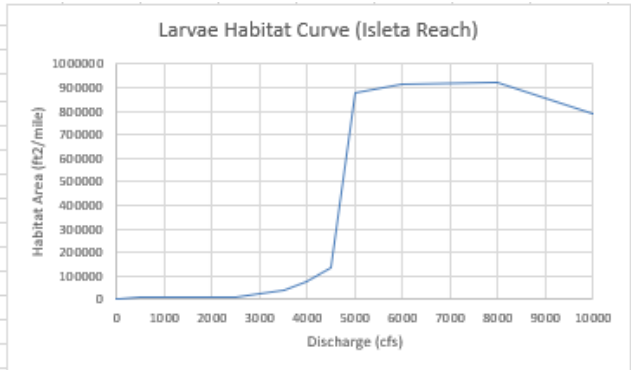


Figure C-2 Example of worksheet results from the TIHMs program for larval habitat

**Appendix D**  
**Habitat Analyses Results from Previous Studies**

### HEC-RAS RGSM Modeling Maps in 2012

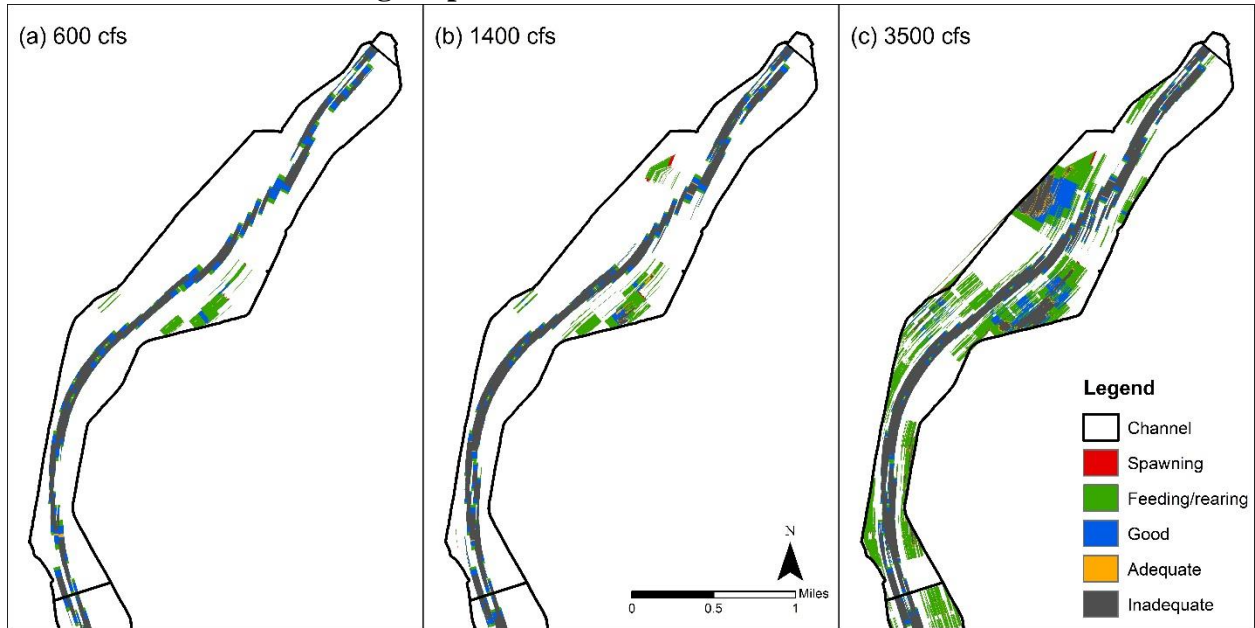


Figure D-1 HEC-RAS modeling map of subreach I1 from Yang et al. (2020)

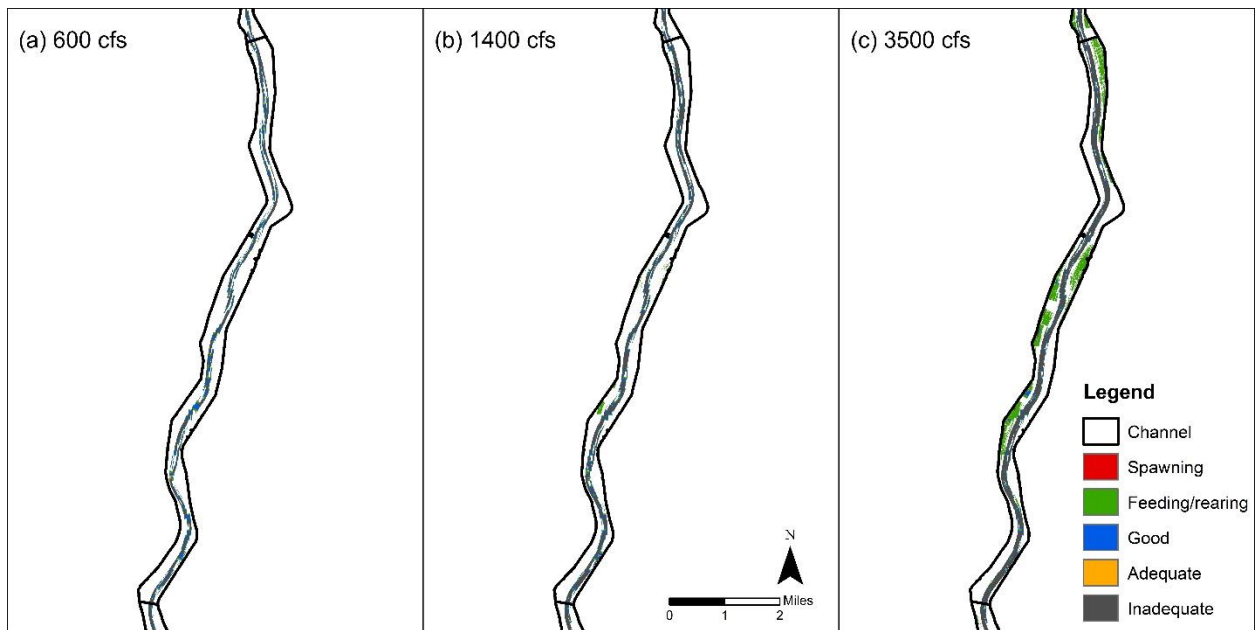


Figure D-2 HEC-RAS modeling map of subreach I2 from Yang et al. (2020)

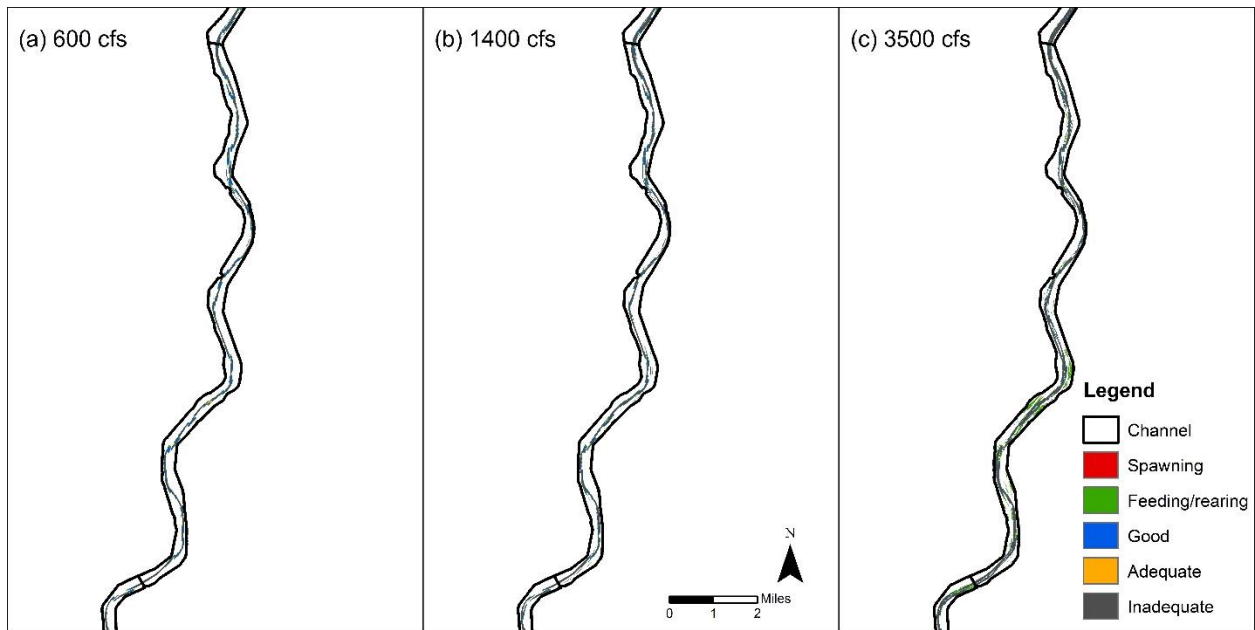


Figure D-3 HEC-RAS modeling map of subreach I3 from Yang et al. (2020)

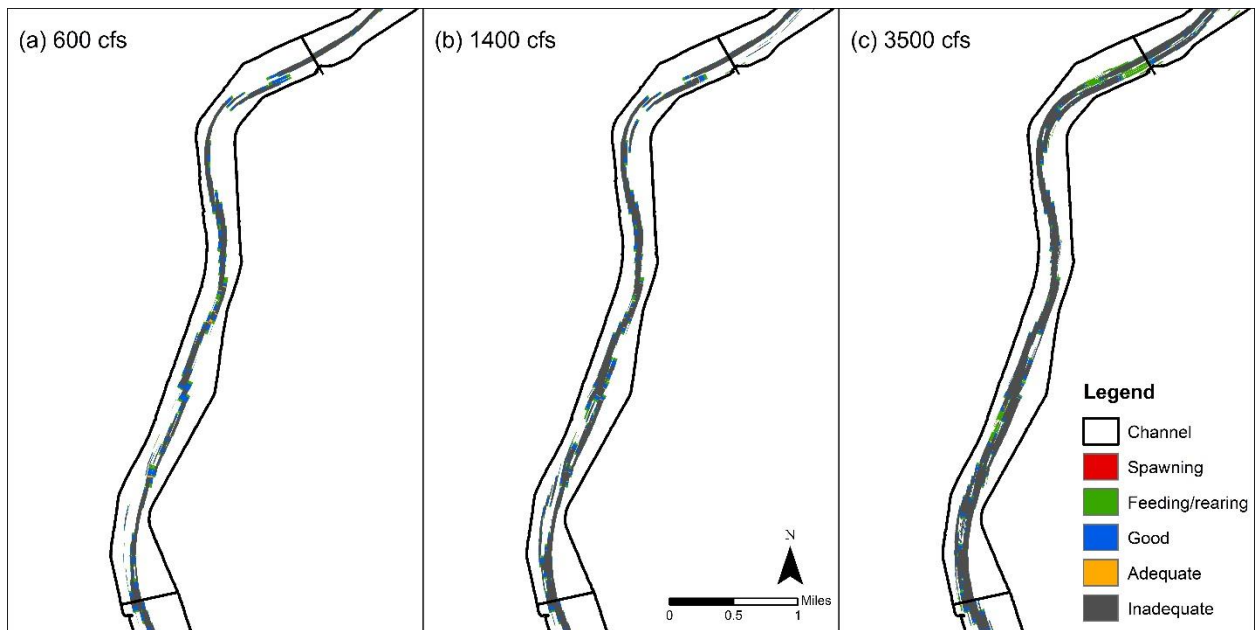


Figure D-4 HEC-RAS modeling map of subreach I4 from Yang et al. (2020)

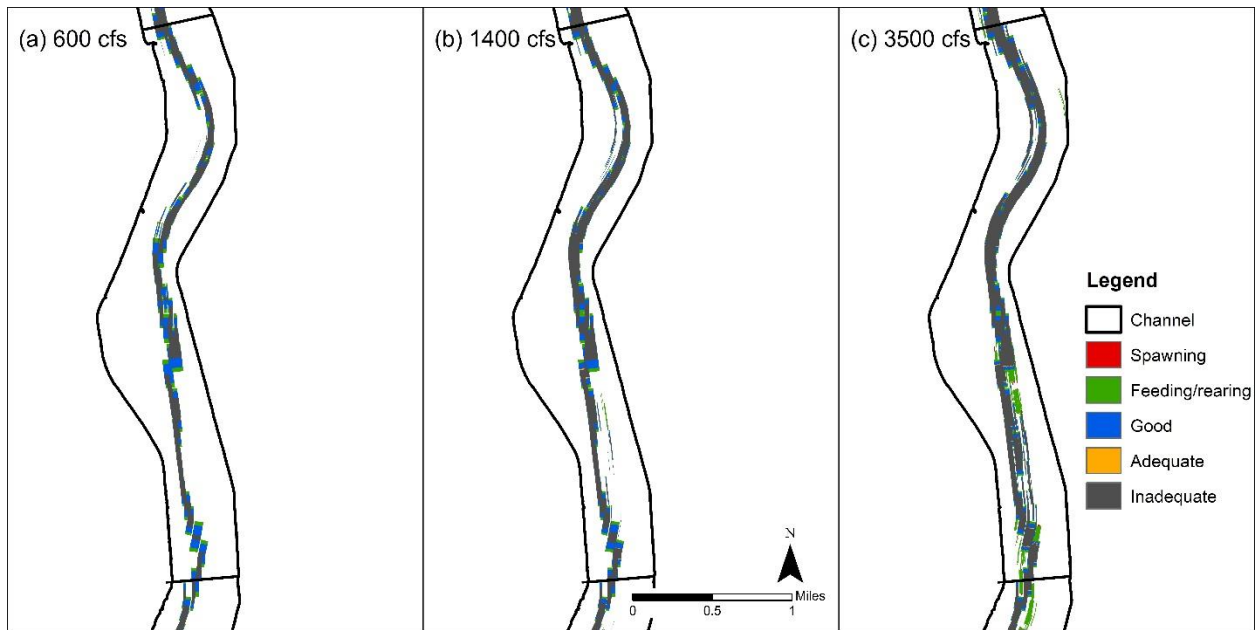


Figure D-5 HEC-RAS modeling map of subreach I5 from Yang et al. (2020)

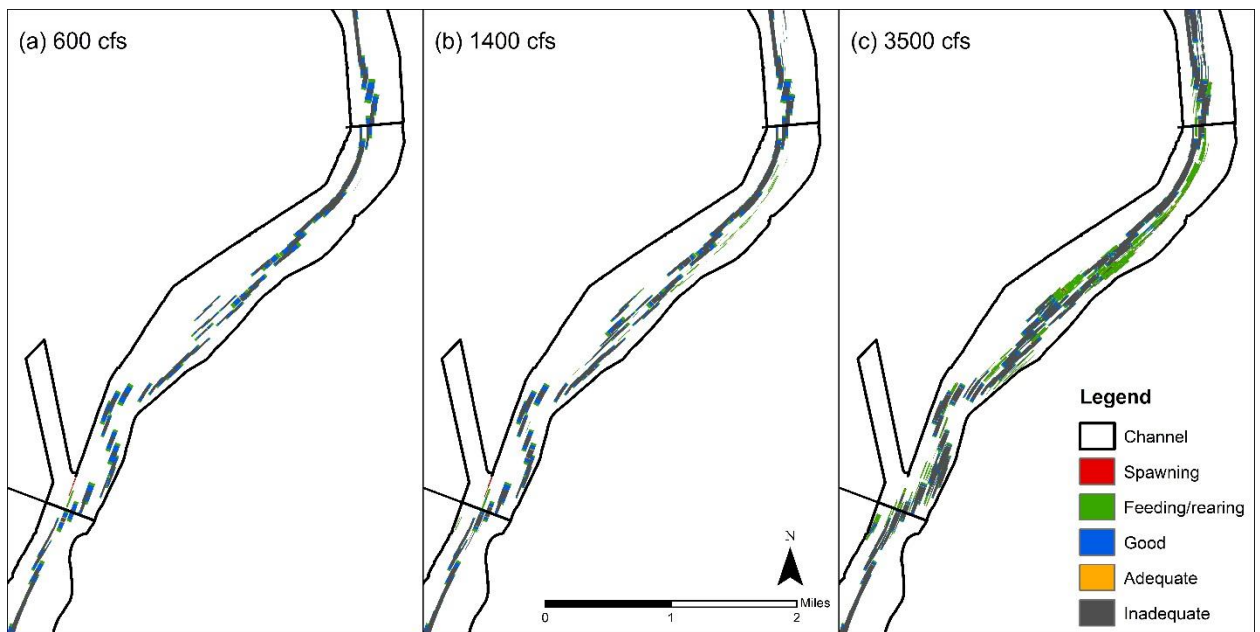


Figure D-6 HEC-RAS modeling map of subreach I6 from Yang et al. (2020)

## RGSM Habitat Scoring System

Table D-1 Habitat types and their respective alphanumeric categories (Yang et al., 2020)

Complex Shoreline	1a
Less Complex Shoreline	1b
Less Complex, Less Accessible Shoreline	1c
Main Channel Complexity (Large)	2a
Main Channel Complexity (Small)	2b
Large, Easily Accessible Dry Side Channel	3a
Medium, Easily Accessible Dry Side Channel	3b
Small, Less Accessible Dry Side Channel	3c
Non-Complex Wetted Side Channel	3d
Complex Wetted Side Channel	3f
Large Backwater	4a
Small Backwater	4b
Complex Bar	5a
Simple Vegetated Bar	5b
Simple Unvegetated Bar	5c
Large Unvegetated Island	6a
Small Unvegetated Island	6c
Large Vegetated Island	6b
Small Vegetated Island	6d
Large Complex Island	6e
Small Complex Island	6f
Active Confluence	7a
Inactive Confluence	7b

Table D-2 Habitat scoring criteria. A higher score indicates more habitat benefits (Yang et al., 2020)

<b>Score</b>	<b>Habitat Description</b>
1	Low chance of becoming inundated, in main channel, small features, and low complexity of topography.
2	Low chance of becoming inundated, in main channel or could be in margins, bigger features than 1 or smaller than 3, and low complexity of topography.
3	Medium chance of becoming inundated, in main channel or near shoreline, bigger features than 2 or smaller than 4, and medium complexity of topography.
4	High likelihood of becoming inundated on side channel or inundated but not very complex in main channel. Bigger features than 3 or smaller than 5.
5	Areas that are currently inundated with water and form complex flow with shallow areas and low velocities. Tend to be isolated from the main channel. Large features with high topographic complexity.

Table D-3 Physical features and their respective scores (Yang et al., 2020)

	Shoreline Complexity			Main Channel Complexity		Side Channels					Backwater		Bars			Islands						Confluences	
Criteria:	1a	1b	1c	2a	2b	3a	3b	3c	3d	3f	4a	4b	5a	5b	5c	6a	6b	6c	6d	6e	6f	7a	7b
Score:	4	3	2	4	3	4	3	2	3	5	5	4	5	2	1	3	2	1	1	4	3	4	3

Table D-4 Results from the habitat scoring system on the Isleta reach by Yang et al. (2020). Each year is given a total habitat score based on the number of habitat types that are present

Year	Month	Total Habitat Score	Flow (cfs)	Shoreline Complexity			Main Channel Complexity		Side Channels					Backwater		Bars			Islands						Confluences	
				1a	1b	1c	2a	2b	3a	3b	3c	3d	3f	4a	4b	5a	5b	5c	6a	6b	6c	6d	6e	6f	7a	7b
1992	February	4025	650 <sup>SA</sup>	23	6	7	85	88	0	3	1	211	184	9	7	42	103	58	3	0	11	2	180	147	0	1
2001	February	3300	687 <sup>A</sup>	26	6	0	125	103	0	0	3	111	111	1	1	45	26	8	5	6	26	8	216	83	1	1
2002	February	4335	800 <sup>SA</sup>	17	10	0	153	45	0	10	4	181	142	3	12	73	158	28	19	7	16	16	293	45	0	0
2005	April	3447	450 <sup>I</sup>	138	16	5	168	59	8	2	4	84	84	2	0	101	8	0	0	1	0	10	118	81	3	0
2005	June	4395	598 <sup>I</sup>	340	8	1	55	50	8	16	7	64	128	16	2	140	23	0	0	9	5	24	147	79	1	1
2006	January	3081	580 <sup>SA</sup>	45	33	2	42	76	8	75	3	124	65	21	14	24	140	33	6	2	16	7	156	56	2	1
2008	June	3050	499 <sup>I</sup>	81	9	0	30	22	0	0	1	193	39	8	1	143	16	1	0	33	0	33	148	82	2	0
2008	July	2905	163 <sup>I</sup>	38	35	11	7	35	7	31	24	165	123	12	8	17	40	13	3	109	9	54	128	45	1	1
2012	January	3301	740 <sup>SA</sup>	65	35	5	68	57	23	146	11	82	89	6	5	43	79	29	14	58	19	35	135	76	2	0
2016	October	719	40 <sup>SA</sup>	16	9	9	11	25	0	7	0	33	10	4	4	7	32	41	5	12	36	3	10	3	0	6

Note: Flows at different gages are given the following superscripts: <sup>I</sup> Isleta gage daily average discharge, <sup>SA</sup> San Acacia gage daily average discharge, <sup>A</sup> Albuquerque gage daily average discharge

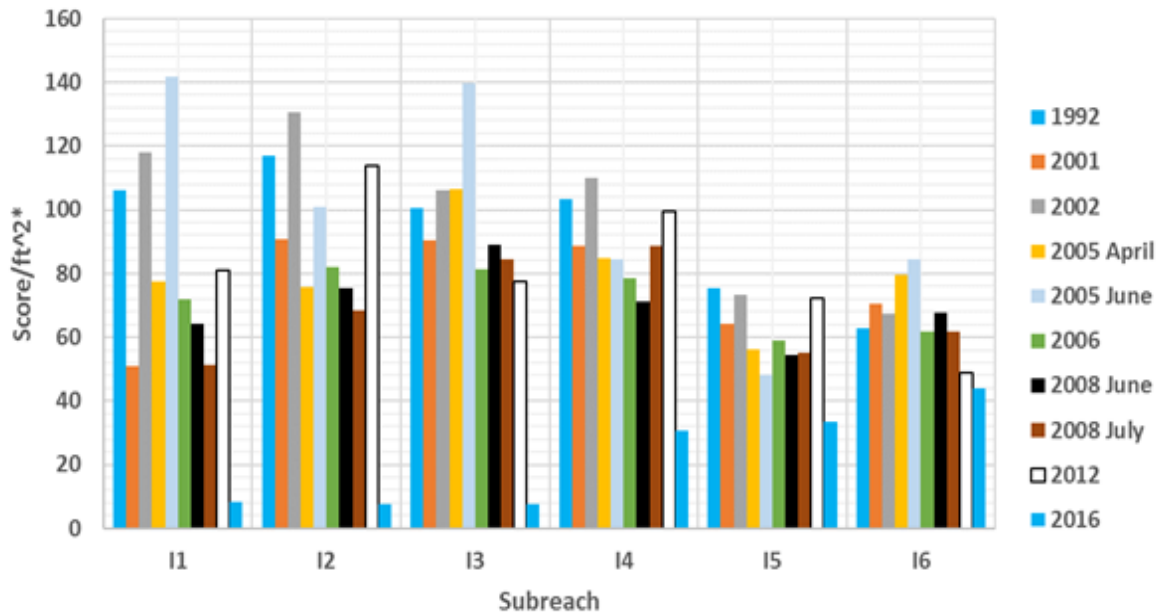


Figure D-7 Overall habitat scores by subreach in Isleta computed by Yang et al. (2020). Score is weighted per area of subreach

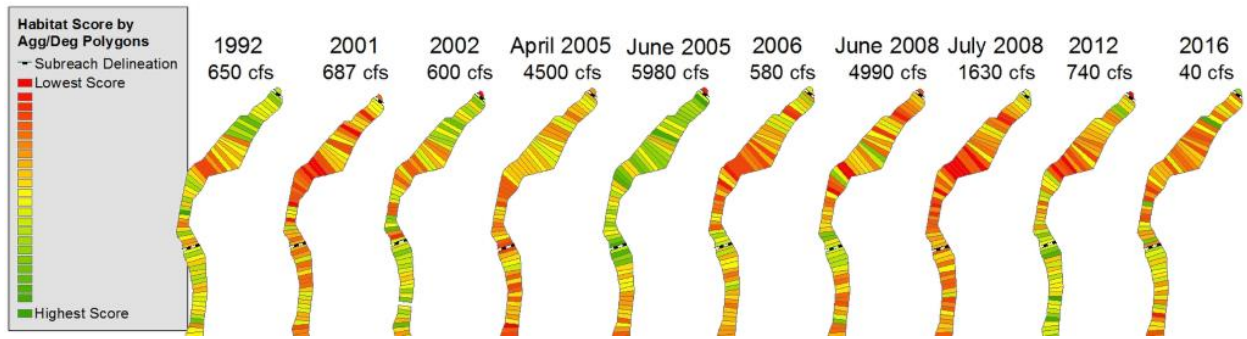


Figure D-8 Example of a habitat scoring map for subreach II from Yang et al. (2020)